



# Identification of novel drivers of collateral vessel remodelling in the chick embryo

---

Emily Clare Hoggar

**November 2014**

A thesis submitted for the degree of Doctor of Philosophy  
The University of Sheffield Department of Developmental and  
Biomedical Genetics

**MRC**

Centre for Developmental  
and Biomedical Genetics

## **Acknowledgements**

I would like to thank my supervisors Dr Tim Chico and Professor Marysia Placzek, whose continued guidance and support has allowed me to develop both personally and professionally as a scientist. Many thanks to my advisors Stephen Renshaw and Anne-Gaelle Borycki who offered both mentorship and advice along the way.

I would like to thank the members of both labs for their friendship, knowledge and support over the years. I would also like to acknowledge my parents and Rob who were always there to endure the hard times and celebrate the achievements; I couldn't have reached the end without you.

## **Statement of contribution**

The microarray was carried out by Dr Paul Heath in the University of Sheffield Microarray Core Facility. Raw data analysis and normalisation was provided by Dr Marta Milo at the University of Sheffield. Subsequent analysis and interpretation was carried out by myself. HUVECs were kindly acquired and prepared by Marwa Mahmoud and Professor Paul Evans at the Royal Hallamshire Hospital, Cardiovascular Science Department. I performed subsequent QRT-PCR and data analysis for these experiments. Particle Image Velocimetry was performed in the lab of Dr Christian Poelma with the help of Astrid Kloosterman at Delft University of Technology.

## **Publications**

Conference abstracts:

- Hoggar EC, Placzek M & Chico TJ (2012) FLOW INDUCED VESSEL REMODELLING IN THE CHICKEN EMBRYO IS ASSOCIATED WITH A SPECIFIC GENE EXPRESSION PROFILE. HEART, Vol. 98 (pp A4-A4)
- Hoggar EC, Placzek M & Chico TJ (2011) TRANSCRIPTIONAL PROFILING REVEALS A REQUIREMENT FOR PHOSPHODIESTERASE 10A DURING FLOW-INDUCED VESSEL REMODELLING IN THE CHICK EMBRYO. HEART, Vol. 97(20) (pp 15-15)

## Abstract

Arterial occlusion accounts for high rates of mortality in the western world. Strategies to bypass an occlusion by activating collateral vessels could reduce the consequences of arterial diseases. This thesis investigates the genes involved in collateral vessel remodelling in the chick embryo to gain insight into the process. Ligation of the right proximal vitelline artery of HH st 17 chick embryos occluded blood flow to the right hand side of the extra-embryonic tissue and vitelline vessel network. Collateral vessels were seen to develop from the pre-existing, left (unligated) vitelline artery and extended across the midline to carry arterial blood to the un-perfused side of the extra-embryonic tissue. The remodelling process was active over 48 hours and developed many small collateral vessels into a few, main conducting arteries. The number of collateral vessels peaked at 12 hours post tied-ligation and then decreased, whilst collateral vessel diameter continued to increase over the time period.

Analysis of the global transcriptional profile of collateral vessels in the chick embryo was assessed following ligation, during early stages of collateral vessel development (4 hours), at the point of pruning and remodelling of the collateral network (12 hours). Collateral vessel formation in the chick embryo was found to be associated with a unique and specific gene expression profile. Phosphodiesterase 10A (PDE10A), an cAMP hydrolysing enzyme, was upregulated in tied-ligated embryos at 4 hours post tied-ligation and hypothesised to play a role in the remodelling process. To study PDE10A papaverine hydrochloride was used to inhibit the enzyme. Papaverine had no effect on normal vessel development but significantly impaired collateral vessel diameter from 6 hours post-ligation. This effect was rescued by co-treatment with Protein Kinase A inhibitor, Rp-8-Br-cAMPS. To begin an assessment of the role of PDE10A in collateral vessel remodelling, proliferation was investigated, *in vivo*. However, a mechanism of action for PDE10A has yet to be elucidated.

## Table of contents

Acknowledgements.....	<b>Error! Bookmark not defined.</b>
Statement of contribution .....	<b>Error! Bookmark not defined.</b>
Abstract.....	2
Table of contents .....	3
Table of figures .....	7
Table of Tables .....	11
Abbreviations.....	12
Chapter 1.....	14
Introduction .....	14
1.1 Atherosclerosis and the clinical relevance of arterial occlusion.....	14
1.2 Arteriogenesis and the process of collateral vessel remodelling .....	15
1.2.1 Collateral vessel architecture.....	16
1.2.2 The timecourse of collateral vessel remodelling .....	16
1.3 Arteriogenesis vs angiogenesis .....	18
1.4 Cellular remodelling in arteriogenesis .....	23
1.5 Haemodynamic forces as a stimuli for collateral vessel formation .....	24
1.6 How do endothelial cells detect haemodynamic changes?.....	25
1.6.1 Signal transduction of fluid forces .....	28
1.6.2 How does stimulation of mechanotransduction pathways result in changes in gene expression? .....	29
1.7 Transcriptional changes induced by altered shear stress.....	30
1.8 Therapeutic promotion of arteriogenesis.....	33
1.9 Changes in haemodynamic flow can alter endothelial cell arterial/venous identity .....	38
1.10 Model systems of collateral vessel formation .....	40
1.11 The chicken embryo as a model system to study flow-induced remodelling .....	43
1.12 The development of the chicken embryo extra-embryonic vasculature.....	43
1.13 Chick embryo models to investigate the effects of changes in haemodynamic flow ...	49
1.14 The advantages of using the extra-embryonic vasculature of the chicken embryo to study blood vessels <i>in vivo</i> .....	51
1.15 Cyclic nucleotide phosphodiesterases.....	52
1.15.1 Cyclic nucleotides.....	53

1.15.2 Protein kinases.....	53
1.15.3 The phosphodiesterase family.....	54
1.16 Phosphodiesterase 10A .....	57
1.16.1 PDE10A function .....	57
1.16.2 PDE10A mechanism of action.....	58
1.17 Thesis aims.....	58
Chapter 2.....	60
Materials and methods.....	60
Materials .....	60
Kits/reagents.....	61
Antibodies .....	63
2.1 General chick embryo methods.....	64
2.1.1 Storage and incubation.....	64
2.1.2 Developmental stages of the chicken embryo .....	64
2.1.3 Windowing the egg.....	65
2.1.4 Embryo staging and inclusion criteria.....	65
2.2 Arterial ligation .....	65
2.3 Particle Image Velocimetry.....	67
2.3.1 Preparation of the embryo for imaging.....	67
2.3.2 PIV Recordings .....	67
2.3.3 Time-averaged velocity fields .....	69
2.4 Microarray methods .....	70
2.4.1 Tissue excision.....	70
2.4.2 RNA extraction .....	71
2.5 Spectrophotometry.....	72
2.6 Affymetrix microarray.....	72
2.6.1 Microarray data analysis.....	73
2.7 Gene ontology tools.....	76
2.8 Quantitative real-time PCR .....	76
2.8.1 Primer stocks.....	76
2.8.2 Heat Gradient PCR .....	78
2.8.3 Primer Concentration Optimisation for QRTPCR.....	79
2.8.4 cDNA dilution assay for standard curve analysis .....	80
2.8.5 ROTOR6000 Analysis.....	80

2.8.6 Creating standard curves .....	81
2.8.7 Running QRTPCR samples .....	83
2.8.8 Sample analysis .....	83
2.9 PDE10A response to changes in flow in cultured endothelial cells .....	84
2.9.1 HUVEC QRTPCR .....	86
2.10 cDNA synthesis.....	88
2.11 DNA Sequencing.....	89
2.12 Agarose gel electrophoresis.....	89
2.13 Molecular biology .....	90
2.13.1 Plasmid purification .....	90
2.13.2 Bacterial cell culture and DNA extraction.....	90
2.13.3 DNA linearisation .....	91
2.13.4 Riboprobe synthesis.....	91
2.14 Preparation of tissues for histology .....	92
2.15 Tissue sectioning.....	92
2.16 Immunohistochemistry .....	93
2.16.1 Haematoxylin and Eosin staining.....	93
2.16.2 Antibody immunolabelling.....	94
2.17 PDE10A immunohistochemistry optimisation.....	95
2.18 Whole-mount in situ hybridisation.....	96
2.19 Protein extraction .....	97
2.20 Western blotting.....	97
2.21 Pharmacological assays.....	98
2.22 Proliferation assays.....	101
2.22.1 <i>In vivo</i> proliferation assays.....	101
2.23 Microscopy.....	104
2.23.1 Fluorescence microscopy.....	104
2.23.2 <i>In vivo</i> microscopy.....	104
2.24 Image analysis .....	104
2.25 Statistical analysis .....	105
Chapter 3.....	107
Characterising the chick embryo as a model of flow-induced vessel remodelling.....	107
Summary .....	107
3.1 Occlusion of the right vitelline artery by surgical ligation .....	109

3.2 The effect of right vitelline artery ligation on the left proximal vitelline circulation ....	110
3.3 The collateral vessel response following unilateral vitelline artery ligation. ....	113
3.4 Flow-induced vessel remodelling requires pre-existing connections to form collateral vessels .....	120
3.5 Using Particle Image Velocimetry to measure blood flow in collateral vessels .....	122
3.6 Histological examination of the area of collateral vessel formation .....	128
3.6.1 Re-modelled collaterals express the endothelial cell marker, VE-cadherin .....	128
3.7 Collateral vessels change expression of arteriovenous markers during flow-induced remodelling .....	134
3.8 Is proliferation increased in areas undergoing collateral vessel remodelling? .....	139
3.9 Discussion.....	140
Chapter 4.....	155
Characterising the transcriptional profile during flow-induced vessel remodelling in the chicken embryo.....	155
Summary .....	155
4.1 <i>A priori</i> expectations of relevant gene expression changes .....	156
4.2 Assessment of the transcriptional changes during normal development and collateral vessel development in the chicken embryo .....	157
4.3 The transcriptional profile during collateral vessel development.....	159
4.5 Hierarchical clustering of genes differentially expressed during collateral development .....	161
4.6 Selection of candidate genes for quantitative analysis by QRT-PCR .....	165
4.8 Discussion.....	167
Chapter 5.....	184
Examining the role of phosphodiesterase 10A in collateral vessel development .....	184
Summary .....	184
5.1 The effect of altered flow on PDE10A expression in human endothelial cells.....	184
5.2 Temporal analysis of PDE10A protein expressed in the area of flow-induced vessel remodelling .....	187
5.3 Immunohistochemistry for PDE10A in proximal vitelline and developing collateral vessels .....	189
5.4 Investigating the effect of PDE10A inhibition on collateral vessel formation .....	193
5.5 The effect of papaverine on normal vitelline vessel development .....	193
5.6 Inhibition of PDE10A reduces collateral vessel diameter but does not affect collateral vessel number.....	195
5.7 PKA inhibition rescues the effect of PDE10A inhibition <i>in vivo</i> .....	200

5.8 Rp-8-Br-cAMPS does not affect normal vessel development, heart rate or collateral vessel development .....	201
5.9 Rp-8-Br-cAMPS is able to rescue the effect of papaverine on collateral vessel diameter .....	204
5.10 Investigating a functional role for PDE10A in collateral vessel remodelling .....	207
5.11 Discussion.....	210
Chapter 6.....	224
General discussion .....	224
References .....	238
Appendix .....	253

## Table of figures

Figure 1.1 A proposed timecourse of events during arteriogenesis in mammalian models.....	17
Figure 1.2 Angiogenesis and arteriogenesis are separate processes stimulated by different stimuli with different outcomes in vessel remodelling.....	19
Figure 1.3 Sprouting and intussusceptive angiogenesis form <i>de novo</i> vessels via different mechanisms.....	22
Figure 1.4 Endothelial cell mechanotransducers sense changes in flow and propagate the signal to the nucleus via various signalling pathways.....	26
Figure 1.5 The process of vasculogenesis in the extra-embryonic vasculature of the chicken embryo .....	43
Figure 1.6 Normal blood flow patterns through the extra-embryonic vitelline vessel network of a chick embryo at HH st 17 and HH st 20.....	45
Figure 1.7 The development of the extra-embryonic vasculature of the chicken embryo, from HH st 13-17.....	46
Figure 2.1. Micrograph images of a sham ligation and a tied ligation.....	64
Figure 2.2 Particle Image Velocimetry apparatus.....	66
Figure 2.3. Microarray RNA extraction was performed at 3 timepoints in sham and ligated embryos.....	71
Figure 2.4 Calculating primer efficiency using a standard curve.....	81
Figure 2.5 Filter paper discs were used as a method of drug delivery.....	99
Figure 2.6 Micrograph images to show how collateral vessels were identified.....	105

Figure 3.1 Representative micrograph images of the right vitelline vessel of a HH st 17 chick embryo showing a sham ligation and a tied ligation.....	109
Figure 3.2 Following right proximal vitelline artery ligation, the left vitelline artery increases in diameter significantly compared to sham controls.....	111
Figure 3.3 The vascular morphology of the vitelline network of a HH st 17 chick embryo immediately (T0) post-tied-ligation (right panel) or sham ligation (left panel).....	113
Figure 3.4 The vascular morphology over time following sham ligation of the vitelline network of a HH st 17 chick embryo.....	114
Figure 3.5 Unilateral vitelline artery tied-ligation induces a dynamic compensatory response to restore blood flow to the ligated territory.....	115
Figure 3.6 The sham and ligated chick embryo model at 24 hours post-ligation.....	116
Figure 3.7 Collateral vessels actively remodel to favour persistence of a small number of large vessels.....	118
Figure 3.8 Following right vitelline artery tied-ligation, the distal branches of the left vitelline artery remodelled in a flow-dependent manner.....	120
Figure 3.9 Particle Image Velocimetry recorded blood velocity in collateral vessels at 4 hour post-tied-ligation .....	123
Figure 3.10 Particle Image Velocimetry recorded blood velocity in collateral vessels at 7 hour post tied-ligation.....	124
Figure 3.11 Alignment of 4h and 7h images revealed an expansion of collateral network over time and increased velocity within collateral vessels.....	125
Figure 3.12 Blood velocity in collateral vessels measured by PIV 24 hours post-tied-ligation.....	126
Figure 3.13 Micrograph images to show the development of the extra-embryonic vascular network in the area of collateral vessel formation at the posterior of the chick embryo...	128
Figure 3.14 The vessel architecture of the proximal vitelline vessel of a HH st17 chick embryo.....	129
Figure 3.15 The vessel architecture of the extra-embryonic tissue of a HH st17 chick embryo.....	131
Figure 3.16 Immunohistochemistry with anti-VE-cadherin labelling was used to identify collateral vessels in wholemout tissue dissected from the area of collateral vessel formation 24 hours post tied-ligation.....	132
Figure 3.17 Neuropilin 1 expression can be seen in wholemout vitelline arteries of HH st 20 chick embryos. Neuropilin 2 venous marker labels the veins overlying the arteries...	135

Figure 3.18 Arterial neuropilin 1 is upregulated in collateral vessels.....	137
Figure 3.19 BrdU proliferation index in sham and ligated embryos 4 hours post-ligation.....	139
Figure 4.1 Schematic of microarray experimental protocol.....	157
Figure 4.2 Venn diagram showing number of differentially expressed genes at 4 h post-tied-ligation compared to 4h sham-ligation and 12h post tied-ligation compared to 12h sham-ligation.....	158
Figure 4.3 Hierarchically clustered heatmaps of the fold changes of the differentially expressed genes during flow-induced vessel remodelling.....	162
Figure 5.1 PDE10A gene expression in flow treated or static HUVECs.....	185
Figure 5.2 Western blot analysis of tissue dissected from the area of flow-induced remodelling at different timepoints following sham or ligation surgery shows up-regulation of PDE10A protein during early time-points in ligated embryos.....	187
Figure 5.3 PDE10A can be detected by immunohistochemistry in the collateral vessels 4 hours post tied-ligation.....	190
Figure 5.4 Higher magnification images revealed punctate staining patterns of PDE10A labelling.....	191
Figure 5.5 PDE10A inhibition was not toxic to HH st 15 embryos and did not affect the diameter of developing proximal vitelline vessels.....	193
Figure 5.6 PDE10A inhibition significantly impaired collateral vessel formation after 24 hours tied-ligation.....	195
Figure 5.7 Representative micrographs show that PDE10A inhibition impairs collateral vessel development after 24 hours at the anterior and posterior poles of the embryo...	196
Figure 5.8 Timecourse analysis of the effect of papaverine treatments showed PDE10A inhibition significantly impaired collateral vessel formation from 6 hours post tied-ligation.....	198
Figure 5.9 Rp8-Br-cAMP application to the vitelline vessels did not affect vessel diameter or heart rate.....	201
Figure 5.10 When applied to HH st17 ligated embryos, Rp-8-Br-cAMPS did not affect collateral vessel number, but at 30µM did increase mean diameter of collateral vessels compared to controls.....	202
Figure 5.11 30µM Rp-8-Br-cAMPS did not affect collateral vessel number, and had no effect on the mean diameter of collateral vessels when co-treated with papaverine for 24-28 hours post tied-ligation.....	204

Figure 5.12 100µM Rp-8-Br-cAMPS did not affect collateral vessel number, but did rescue the mean diameter of collateral vessels when applied to collateral vessels with papaverine for 24-28 hours post-ligation.....205

Figure 5.13 PDE10A inhibition does not affect proliferation in the area of collateral vessel formation at 6 hours and 8 hours post tied-ligation.....208

Figure 6.1 Proposed pathway occurring after proximal vitelline artery ligation in the collateral vessels undergoing flow-induced remodelling.....220

**Appendix figures**

Figure A1 Following tied-ligation, over an 8h timecourse collateral vessels could be seen to develop from a pre-existing distal branch of the unligated left vitelline artery.....252

Figure A2. A representative PIV image of the blood velocity in the left proximal vitelline vessel of a HHst 17 chick embryo .....253

Figure A3. The parabolic curves to show the blood flow was fastest at the centre of the vessel in collateral vessels recorded at 24h using PIV .....254

Figure A4. Venn diagram showing number of differentially expressed genes at 4 hours and 12 hours post-sham-ligation, compared to the baseline measurement.....255

Figure A5. Hierarchically clustered heatmaps of the fold changes of the differentially expressed genes during normal development.....256

Figure A6. Gene ontology was used to cluster differentially expressed genes by biological processes and molecular function from the data analysed at 4 hours after tied-ligation.....259

Figure A7. Gene ontology was used to cluster differentially expressed genes by biological processes and cellular components from the data analysed at 12 hours after tied-ligation.....300

Figure A8. Clustal alignment of the PDE10A antigen peptide sequence in human and chick.....301

Figure A9. PDE10A immunohistochemistry of a transverse section through embryonic mouse brain tissue.....302

Figure A10. PDE10A immunohistochemistry of a transverse section through chick embryo brain tissue (HH st 17).....303

Figure A11. Dye assays showed diffusion from the filter paper to the vitelline membrane.....304

## Table of Tables

Table 1. Annotations of some of the observed functions of vascular located PDEs reported in the literature.....	54
Table 2.1 Primers used for QRTPCR. Primer pairs selected for use are described for each gene in the table above.....	75
Table 2.2 A table to show the optimal concentration at which to use the primer sets in order for the primers to work most efficiently.....	80
Table 2.3 A list of enzymes used to extract the DNA from bacterial plasmids.....	90
Table 2.4 A list of antibodies used to detect proteins by immunofluorescence.....	93
Table 2.5 BrdU delivery to endothelial cells in the area of collateral vessel formation was optimised by testing a range of concentrations and volumes.....	101
Table 4.1; The 13 genes differentially expressed at both 4h and 12h after tied-ligation compared with sham-ligation.....	159
Table 4.2 Genes specifically expressed during collateral vessel development 4h or 12h post tied-ligation.....	163
Table 4.3 Relative gene expression in tied-ligated compared with sham-ligated embryos in the area of flow-induced vessel remodelling.....	165
Table 4.4 Comparison of the expression levels detected using microarray analysis and QRTPCR.....	166

## Appendix tables

Table A1. The shared differentially expressed genes which were expressed in both tied-ligated (L) and sham-ligated (sh) models (taken from the heatmap data).....	257
Table A2. The gene functions of the shared differentially expressed genes which were expressed in both tied-ligated (L) and sham-ligated (sh) models (as in Table A1).....	258

## Abbreviations

<b>ADAMTSL1</b>	A Disintegrin And Metalloproteinase with Thrombospondin Motif-like 1
<b>APO E</b>	Apolipoprotein E
<b>BrdU</b>	Bromodeoxyuridine
<b>CAM</b>	Chorio-allantoic membrane
<b>cAMP</b>	cyclic adenosine 3'5' monophosphate
<b>CC2D1B</b>	coil coil domain 1B
<b>cDNA</b>	Complementary Deoxyribonucleic acid
<b>cGMP</b>	cyclic guanosine 3'5' monophosphate
<b>Ct</b>	Cycle threshold
<b>CXCR4</b>	Chemokine receptor type 4
<b>Dll4</b>	Delta like 4
<b>Ect</b>	Ectoderm
<b>Egr-1</b>	Early growth response-1
<b>En</b>	Endoderm
<b>EC</b>	Endothelial cell
<b>E</b>	Erythrocytes
<b>ECM</b>	Extracellular matrix
<b>eNOS</b>	Endothelial nitric oxide
<b>FGF</b>	Fibroblast Growth Factor
<b>Fli-1</b>	Friend leukemia integration 1
<b>Flk-1</b>	Fetal liver kinase-1
<b>FSS</b>	Fluid shear stress
<b>Fps</b>	Frames per second
<b>GFP</b>	Green Fluorescent Protein
<b>H&amp;E</b>	Haematoxylin and eosin
<b>HH</b>	Hamburger and Hamilton
<b>HUVEC</b>	Human umbilical vein endothelial cells
<b>ICAM-1</b>	Intracellular adhesion molecule-1
<b>IRX4</b>	Iroquois-class homeodomain protein-4
<b>KLF2</b>	Kruppel like factor-2
<b>LED</b>	Light emitting diode
<b>MAPK</b>	Mitogen-activated protein kinase

<b>MCP-1</b>	Monocyte chemoattractant protein-1
<b>MIAME</b>	Minimum Information About a Microarray Experiment
<b>MMP</b>	Matrix metalloproteinase
<b>MRTFs</b>	Myocardin-related transcription factors
<b>NO</b>	Nitric oxide
<b>nrp1/nrp2</b>	Neuropilin-1
<b>PANTHER</b>	Protein ANalysis Through Evolutionary Relationships
<b>PDE</b>	Phosphodiesterase
<b>PDGF</b>	Platelet-derived growth factor
<b>PIV</b>	Particle Image Velocimetry
<b>PKA/PKG</b>	Protein kinase A/G
<b>PPLR</b>	Probability of Positive Log Ratio
<b>PSCA</b>	Prostate stem cell antigen
<b>PUMA</b>	Propagating Uncertainty in Microarray Analysis
<b>QRTPCR</b>	Quantitative real-time polymerase chain reaction
<b>RBC</b>	Red blood cell
<b>SMC</b>	Smooth muscle cell
<b>SRF</b>	Serum response factor
<b>SSRE</b>	Shear stress response element
<b>STC2</b>	Stanniocalcin-2
<b>TGFB1</b>	Transforming growth factor beta-1
<b>VCAM</b>	Vascular cell adhesion molecule
<b>VEGF</b>	Vascular endothelial growth factor
<b>VEGFR2</b>	Vascular endothelial growth factor receptor-2
<b>VL</b>	Vessel lumen

# Chapter 1

## Introduction

### 1.1 Atherosclerosis and the clinical relevance of arterial occlusion

Arterial occlusion accounts for high rates of morbidity and mortality in the Western world (Aschwanden *et al.*, 2014). Commonly, occlusion of the coronary or cerebral arteries results in myocardial infarction or stroke (Schaper., 1971, Helisch and Schaper., 2003). Arterial occlusion can also occur in the major conducting arteries or peripheral vasculature (Fung and Helisch, 2012). In most cases, arterial occlusion is caused by atherosclerosis, a disease of the arterial wall. Atherosclerosis is an inflammatory disease characterised by lipid deposition in the arterial wall and can be initiated when endothelial cells experience disturbed or low flow patterns (Ku *et al.*, 1985, Helderma *et al.*, 2007). This activates endothelial cells which up-regulate expression of adhesion molecules and recruit inflammatory cells (Libby *et al.*, 1996). In turn, the inflammatory response stimulates proliferation and migration of smooth muscle cells (van der Wal *et al.*, 1994). Consequently, the arterial wall thickens. Compensatory outward remodelling occurs in an attempt to maintain lumen diameter and constant flow. This was first observed by Glagov and colleagues in 1987 and referred to as 'Glagov's phenomenon' (Glagov *et al.*, 1987). As invasion of monocytes into the lesion occurs and plaque expansion continues, the lesion can ultimately reduce the vessel lumen. The mature plaque consists of a lipid core, surrounding necrotic tissue and a fibrous cap (Fuster *et al.*, 1990). When the plaque protrudes into the lumen and exceeds 40% of the vessel lumen area, Glagov's phenomenon ceases and stenosis of the vessel occurs. This remodelling is termed 'pathophysiological' remodelling and causes narrowing of the vessel lumen and restriction of blood flow (Glagov *et al.*, 1987). Stenosis of a vessel may also occur if a plaque becomes unstable due to reduced fibrous cap thickness, increased necrotic core and inflammation. Unstable plaque

rupture induces a thrombus to form due to mixing of lipid and blood, causing a thrombus to occlude the vessel (Fuster *et al.*, 1990). Vessel occlusion prevents downstream perfusion and results in tissue necrosis due to ischaemia.

Strategies to alleviate symptoms such as percutaneous coronary intervention (PCI) or bypass surgery are invasive (Kugler and Rudofsky., 2003). Statins are used to lower low-density lipoprotein (LDL) cholesterol which contributes to atherosclerosis progression (Vaughan *et al.*, 2000). There is increasing evidence from clinical trials to suggest that statins reduce ischaemic events, as well as regulating thrombotic tendency (Pourati *et al.*, 2003). High doses of statins reduce plaque volume by a small amount but there is currently no therapy that can significantly reverse atherosclerosis to reduce vessel obstruction (Nissen *et al.*, 2006).

There is a pressing need for novel therapies that could reduce the consequences of arterial diseases. One line of investigation is to encourage remodelling of small connecting blood vessels which exist between large conducting arteries that could naturally bypass the blockage and rescue/alleviate the symptoms and consequences of vessel occlusion. This process is known as arteriogenesis.

## **1.2 Arteriogenesis and the process of collateral vessel remodelling**

Flow-induced remodelling of collateral vessels has been studied for centuries. The term arteriogenesis was coined by Schaper and colleagues in 1976, to describe the adaptive response of pre-existing arterioles to remodel into collateral arteries (Schaper and Ito., 1996). Small vessel anastomoses (connecting arterioles which pre-exist between larger conducting arteries) divert blood flow around a blockage in a main conducting artery by remodelling into “collateral vessels” (Deindl and Schaper., 2005). These communications bridge the area proximal to the blockage with distal connections downstream (Schaper and Scholz., 2003). Following occlusion, a pressure gradient occurs which lowers pressure in

distal vessels, favouring an increase in flow in vessels proximal to the occlusion (Buschmann and Schaper., 2000). This increased flow and change in haemodynamics activates cells lining the blood vessels. This causes a cascade of events leading to expansion and enlargement of collateral vessels to accommodate the increase in blood flow. Although collateral vessels seldom if ever completely return flow levels to baseline, a sub-maximal amount of flow can compensate for the occlusion (Heil and Schaper., 2004), particularly at rest when basal blood flow requirements are low.

### **1.2.1 Collateral vessel architecture**

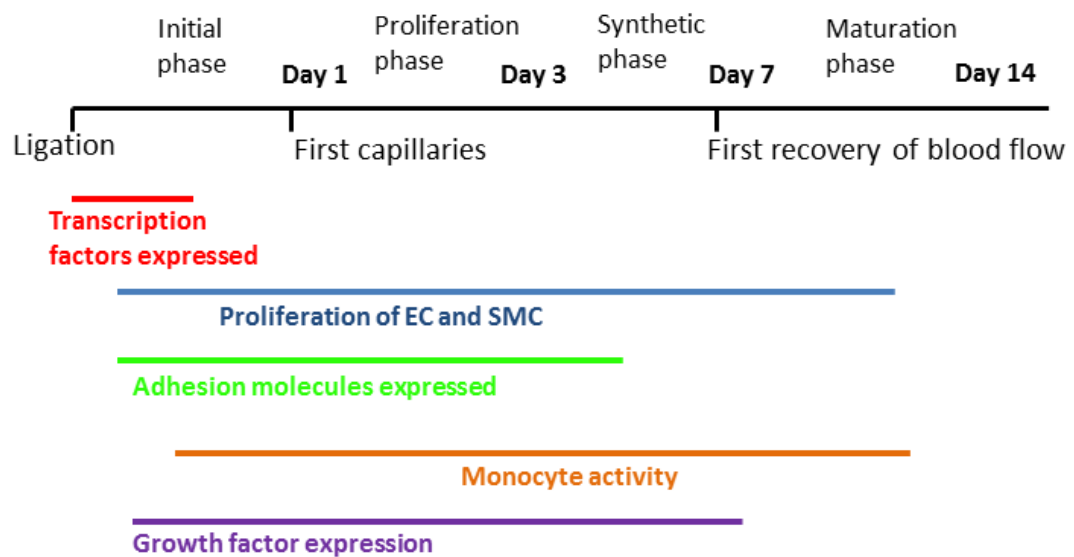
Collateral vessel remodelling has generally been examined in large vessels in mammalian systems. In these models, collateral vessels, like all vessels, consist of an inner endothelial cell layer (tunica intima) and an outer smooth muscle cell layer (tunica media) with a middle elastic layer (internal elastic lamina). An external elastic lamina lies between the tunica media and the tunica external (Schaper *et al.*, 1971).

### **1.2.2 The timecourse of collateral vessel remodelling**

Studies of collateral vessel development following arterial occlusion often observe that the process occurs in two distinct phases: an initial increase in collateral vessel number; followed by a “pruning” selection process, whereby the most efficient collateral vessels are selected for persistence (Duvall *et al.*, 2004). Vessels which do not carry enough blood flow do not remodel. Only 10% of initially expanding arterioles go on to become conducting collateral vessels (Scholz *et al.*, 2001). This reflects Poiseuille’s law, which states that it is more energy efficient to have fewer large conducting vessels than many small, high resistance vessels (Hoefler *et al.*, 2001).

Generally for all species arteriogenesis occurs in phases. Differences occur between species in the timecourse of arteriogenesis (reviewed by Heilmann *et al.*, 2002). Scholz *et al.*, (2000) described four main phases of arteriogenesis in rabbits following hind limb arterial

ligation. These were: initial changes in endothelial cell transcription; proliferation of endothelial and smooth muscle cells; a synthetic phase which involves other cell types such as monocytes and macrophages; and a maturation phase (Scholz *et al.*, 2000). This is summarised in Figure 1.1 and will be discussed in section 1.7.



Adapted from Heilmann et al review (2002)

**Figure 1.1 A proposed timecourse of events during arteriogenesis in mammalian models**

The timecourse begins at occlusion of the femoral artery. The initial phase lasts from ligation to day 1. During this time transcription factors are thought to be expressed. Other early events start to occur such as proliferation of endothelial (EC) and smooth muscle cells (SMC) and expression of adhesion molecules. Monocyte activation and growth factor expression are also initiated at this early event. From day 1 the first new capillaries start to appear. Day 1-3 is referred to as the ‘proliferation phase’ as it is the peak of EC and SMC proliferation. By day 3, adhesion molecule expression ends but monocyte activity reaches a peak. From day 3-7 the process reaches a ‘synthetic phase’. Although monocyte activity and EC/SMC proliferation continue, growth factors stop being expressed. Collateral vessels have begun to appear at day 7 and thus the first recovery of blood flow starts to occur. From day 7-14 collateral vessels become established, known as the ‘maturation phase’. This phase still requires proliferation and monocyte activity. By day 14 collateral vessels have restored flow and the process of arteriogenesis ceases.

### 1.3 Arteriogenesis vs angiogenesis

Following hind-limb arterial occlusion in mammalian models, two types of vessel growth are stimulated; angiogenesis and arteriogenesis (Hershey *et al.*, 2001, Hofer *et al.*, 2001). By occluding the femoral artery, the foot becomes ischemic thus creating a hypoxic environment that stimulates angiogenesis (Ito *et al.*, 1997). However, the small angiogenic vessels cannot facilitate re-perfusion of the foot as they do not carry substantial amounts of flow in the face of the occluded main artery. Proximal to the occlusion, in the upper leg, there is no hypoxia and pre-existing vessels are remodelled by arteriogenesis into collateral vessels to divert blood flow around the occlusion (Hofer *et al.*, 2001). Therefore, there is thought to be no direct correlation between ischaemia and collateral vessel development following arterial occlusion (Ito *et al.*, 1997). Arteriogenesis is instead thought to be driven by haemodynamic factors, including pressure, stretch, vasoactive chemicals in the blood and the frictional drag of blood over the endothelial cells, known as shear stress (Schaper and Ito., 1996). Arteriogenesis occurs in less time than formation of capillaries, due to the structural expansion of pre-existing vessels via proliferation of vascular cells instead of *de novo* vessel growth (Hershey *et al.*, 2001, Hofer *et al.*, 2001) .

The role of angiogenic stimuli in collateral vessel formation has previously been investigated. A study by Schierling *et al.*, (2009) created an arterio-venous (A-V) shunt between the distal femoral artery and vein following occlusion of a proximal femoral artery in a rabbit model (Schierling *et al.*, 2009). The reduction of distal pressure induced by the shunt created higher fluid shear stress in collateral vessels. Although the A/V shunt is used to investigate the relationship between shear stress and collateral vessels (as discussed in section 1.5; Pipp *et al.*, 2004), it has also been used to investigate if maximal levels of collateral conductance that occurred from increased shear stress, were in part due to angiogenic growth factors. Infusion of growth factors, vascular endothelial growth factor (VEGF), basic fibroblast growth factor (bFGF), platelet derived growth factor (PDGF) and

monocyte chemoattractant protein 1 (MCP1), separately or in combination, did not match the improved collateral conductance of increased shear stress from the shunt. The most effective stimuli at increasing collateral vessel conductance was MCP1, followed by bFGF, however, the authors suggested that increasing shear stress in the developing collaterals was the strongest stimulus to collateral vessel growth (Schierling *et al.*, 2009).

The processes of arteriogenesis and angiogenesis are different in terms of mechanism, stimuli and resulting remodelled blood vessels (Heil *et al.*, 2006) and these are summarised in Figure 1.2.

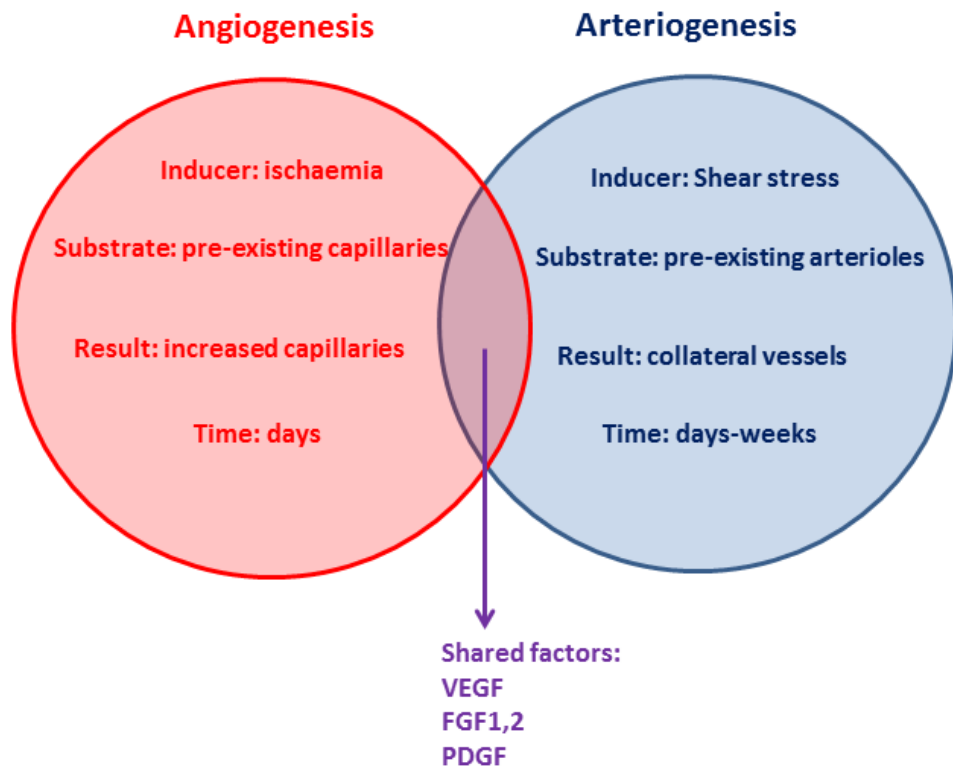


**Figure 1.2 Angiogenesis and arteriogenesis are separate processes stimulated by different stimuli with different outcomes in vessel remodelling**

The two circles describe, in brief, the processes of angiogenesis and arteriogenesis, highlighting the major differences between the two. The overlap at the centre demonstrates some shared factors exist in these two distinct processes. The circle in the left represents angiogenesis. Ischemia induces angiogenesis which causes pre-existing capillaries to sprout *de novo* endothelial cell connections to increase the number and density of capillaries. This process takes days to complete. Arteriogenesis is represented by the circle on the right. Shear stress is thought to induce arteriogenesis which causes remodelling of pre-existing connections into conducting collateral vessels. This process takes days to weeks. Both angiogenesis and arteriogenesis require some stimulation from growth factors such as VEGF, FGFs and PDGF.

Adapted from (Buschmann, Schaper *et al.*, 1999)

Angiogenic sprouting is induced by hypoxia in ischaemic tissue and involves *de novo* vessel formation from capillaries (Risau., 1997). *De novo* capillary tubes form by endothelial cell proliferation, coalescence, differentiation and directed growth, without any contribution from smooth muscle cells (Carmeliet., 2000). Directed angiogenic growth depends on endothelial cell fate controlled by Notch signalling (Lawson., 2001). Endothelial cells of angiogenic vessels can become tip cells at the leading edge or supporting stalk cells depending on the signals they receive (Hellstrom *et al.*, 2007).

Sprouting angiogenic vessels respond to gradients of signals in their environment. VEGF is a powerful mitogen and chemoattractant which stimulates directed growth. Tip cells respond to the ligand, VEGF-A, and further sprouting and branching is controlled by the interaction between the Notch receptor, delta-like-4 (Dll4), and Notch-1 signalling (Hellstrom *et al.*, 2007). Stalk cells receive the signal to proliferate and thus the vessel elongates in a manner that is also dependent on VEGF-A (Gerhardt *et al.*, 2003). Tip cells follow gradients of VEGF and other growth factors such as FGFs, or guidance cues such as ephrins, semaphorins, slits and netrins (Eichmann *et al.*, 2005).

The angiogenic response to occlusion usually happens within days. Hershey *et al.* (2001) used a rabbit model of ischaemia to show that angiogenesis and arteriogenesis were separate mechanisms of restoring blood flow (Hershey *et al.*, 2001). Angiogenesis was monitored in the foot of the animal. Collateral conductance in the hind-limb was measured at specific timepoints following femoral artery removal. Capillary density was measured as a marker of angiogenesis and an angiographic score was used to quantify arteriogenesis. Following removal of the femoral artery, capillaries that formed in the foot were counted histologically to determine an angiogenic score over 5, 10, 20 and 40 days. VEGF was also measured and corresponded to peaks in angiogenic growth which occurred at 5 days. Collateral vessel growth was detectable by angiography at 10 days and was not associated

with ischaemia, or VEGF levels, but did result in improvement of the functional blood flow capacity of the limb. The group concluded that although initial angiogenic sprouting following artery removal was induced by ischaemia, this response did not account for improved collateral flow, which was a result of increased collateral vessel growth (Hershey *et al.*, 2001).

Sprouting angiogenesis is not the only method of *de novo* capillary formation. Intussusceptive angiogenesis is a process of microvascular growth which requires less proliferation than sprouting angiogenesis and instead involves rearrangement of endothelial cell plates (Djonov *et al.*, 2000). Intussusceptive angiogenesis has been studied in the developing extra-embryonic vasculature of the chick embryo (Patan *et al.*, 1993) and will be discussed in subsequent chapters of this thesis.

In the developing extra-embryonic vasculature of the chick embryo, intussusceptive angiogenesis develops a mature vascular tree from a primitive vascular plexus (Nguyen., 2006) (section 1.12). It is hypothesised to occur in four stages: inter-endothelial bridges appear between capillary zones in the direction of flow; these 'bridges' become 'pillars' which fuse and create a narrow tissue septa; segregation, growth and maturation of the structure produces feed vessels which separate up from the capillary plexus mesh. The small, surplus connections between these structures are then pruned and septa dissociate the vessels from the underlying mesh network (Djonov *et al.*, 2000). The different mechanisms of sprouting angiogenesis and intussusceptive angiogenesis are summarised in Figure 1.3. In conclusion, experimental evidence from animal models suggests that therapeutic strategies for alleviating the consequences of arterial occlusive disease should be targeted to improving *arteriogenesis* rather than angiogenesis. Although an important feature of the response to vessel occlusion, angiogenesis alone is insufficient to reperfuse ischaemic tissue, whereas arteriogenesis has this capacity.

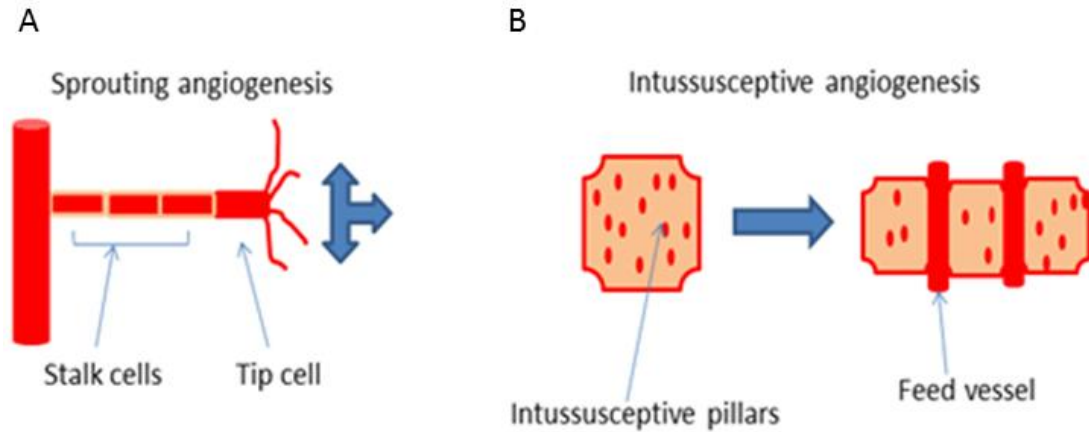


**Figure 1.3 Sprouting and intussusceptive angiogenesis form *de novo* vessels via different mechanisms**

**A** depicts the process of sprouting angiogenesis. A sprouting angiogenic vessel can be seen protruding from the main vessel. The sprouting vessel is made up of stalk cells and a leading tip cell. The vessel sprouts navigate and respond to VEGF through tip cell behaviours whilst stalk cells proliferate to elongate the vessel. **B** shows the process of intussusceptive angiogenesis. Intussusceptive angiogenesis occurs when intra-vascular pillars within a vascular mesh, fuse to produce larger feed vessels. These feed vessels protrude upwards and dissociate from the primitive mesh network to become independent lumenised capillaries.

Adapted from (Djonov *et al.*, 2000)

#### 1.4 Cellular remodelling in arteriogenesis

In contrast to the hypoxic stimulus in angiogenesis, collateral vessel formation is initiated when the endothelial cells lining connecting vessels experience changes in haemodynamic forces (Deindl and Schaper., 2005). The law of Histiomechanics proposed in 1893 suggests there is a relationship between the size of an artery and the blood velocity within it (Thoma., 1893). Fluid forces have therefore been studied in the context of collateral vessel formation for many years. In the cardiovascular system blood flow induces a range of physical forces on the vessel, including shear stress on the endothelial cells of the vessel lumen. The drag of blood flow over the cell surface creates shearing forces (Cunningham., 2005). Mechanotransducers on the cell surface detect shear stress and propagate this signal to the nucleus. These signals modulate the physiological changes exhibited by

endothelial cells exposed to changes in flow (Peters *et al.*, 2002). Genes involved in monocyte attraction, recruitment of inflammatory cells and cell proliferation, are upregulated to drive collateral vessel formation (Cai., 2008).

Endothelial cell activation is thought to lead to monocyte invasion into the vessel wall (Heil and Schaper., 2004). Monocyte recruitment involves the chemokine MCP1, released from activated endothelial cells (Hoefer *et al.*, 2001). Monocytes transmigrate through the vascular wall where upregulated adhesion molecules, Intercellular Adhesion Molecule 1 (ICAM1) and Vascular Cell Adhesion Molecule 1 (VCAM1), are thought to mediate attachment of monocytes to the endothelial surface (Schaper and Scholz., 2003). Monocytes differentiate into macrophages and produce cytokines which create an inflammatory environment for collateral vessel formation, and growth factors which stimulate proliferation (van Royen *et al.*, 2001). Endothelial and smooth muscle cell proliferation is required for outward remodelling which radially expands the vessel to accommodate the increased blood flow load (Scholz *et al.*, 2001). Monocytes also release proteases such as matrix metalloproteases (MMPs) to digest the surrounding matrix to increase the space available for collateral vessel expansion (Cai and Schaper., 2008).

### **1.5 Haemodynamic forces as a stimuli for collateral vessel formation**

Arterial occlusion induces a wide range of effects on the vasculature and the tissue deprived of perfusion, such as hypoxia and ischaemia/necrosis (Helisch and Schaper., 2003). It has been generally accepted that the driving force for collateral development is the alteration of local haemodynamic forces exerted on the nascent collateral vessel (Schaper., 1996). One theory is that occlusion of the main vessel leads to a pressure gradient and increased fluid shear stress in the developing collateral vessel, which remodels in response (Schaper., 1988). Schaper's group have attempted to define the relative contribution of fluid shear in collateral remodelling, although technically this is very

challenging to address. Another group created an A-V shunt between the distal femoral artery and vein following occlusion of a porcine proximal femoral artery (Pipp *et al.*, 2004). The collateral vessels remodelled due to the reduction of distal pressure, induced by the shunt, which exposed the developing collaterals to higher fluid shear stress. This change in blood flow was able to increase collateral vessel growth to a far greater size and improve the ability of collaterals to carry near baseline levels of blood flow. The authors concluded that this experiment confirmed the central role of fluid shear stress, as a driver of arteriogenesis (Pipp *et al.*, 2004). Although it remains difficult to exclude influences exerted by pressure, or even remote factors such as tissue ischaemia. Since distal ischaemia and angiogenesis may influence distal pressure, this could indirectly influence haemodynamics in the developing collateral vessels. The exact contribution of each influence initiated by arterial occlusion on arteriogenesis remains difficult to completely assess.

### **1.6 How do endothelial cells detect haemodynamic changes?**

The manner in which endothelial cells detect and respond to haemodynamic force is increasingly well understood. Davies (1995) suggested that transduction of mechanical stimuli occurred via specific mechanotransduction sites, by a local reorganisation of cell surface receptors and by transmission of the mechanical signal into the cell by cytoskeletal elements (Davies., 1995). A tensegrity model was proposed which further implied that, via integrins and cytoskeletal connections, mechanical stimuli could influence regulatory cell signalling, leading to changes in gene expression (Ingber., 2003). Other mechanosensors thought to detect changes in flow have been identified in endothelial cells, including: caveolae, ion channels, cilia, junctional proteins and signal cascades, G protein activation of mitogen-activated pathway kinase (MAPK) pathway to the cell nucleus (Davies., 1995, Noria *et al.*, 1999, Helmke and Davies, 2002, Osawa *et al.*, 2002, Helmke and Davies., 2002,

Weinbaum *et al.*, 2007). A summary of these flow-sensors can be seen in the cartoon in Figure 1.4.

If haemodynamic forces induce endothelial activation and initiate remodelling, these forces must be sensed by the endothelial cells. A primary flow sensor, responsible for mechanotransduction of a shear stress-related stimulus, has yet to be elucidated. Work in this field has been comprehensively reviewed and possible mechanisms advanced (Davies., 1995). However, there is no evidence to show that these mechanisms drive collateral vessel formation. Some of the pathways which have been suggested to be involved in mechanotransduction of changes in haemodynamic flow are summarised in Figure 1.4.

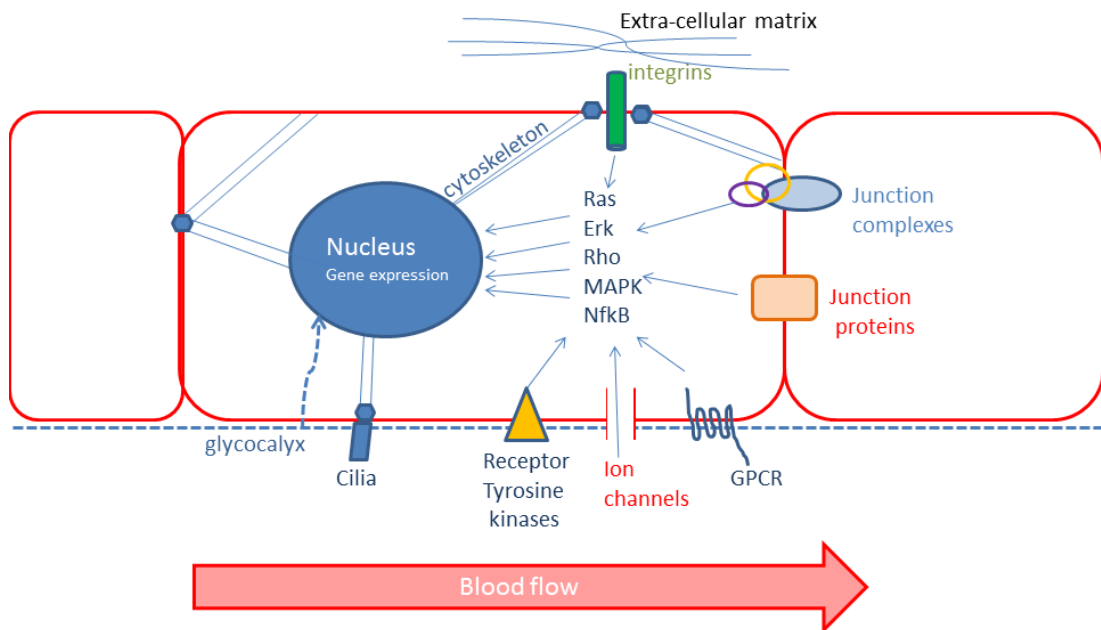


**Figure 1.4 Endothelial cell mechanosensors sense changes in flow and transduce the signal to the nucleus via various signalling pathways**

Changes in flow can be detected by primary cilia on the cell surface. Flow can also be detected by integrins which are involved in ECM-cell interactions. Junctional proteins and complexes between endothelial cells act as mechanotransducers which stimulate signalling pathways to the nucleus. Membrane structures at the cell surface such as the glycocalyx, ion channels, receptor tyrosine kinases and G protein receptors mediate shear stress signals to the nucleus by activating signalling cascades. The cytoskeleton not only senses flow-induced changes in cell shape, but ties together the mechanosensors to generate a shear stress response. Mechanotransducers stimulate signalling pathways by activating small GTPases such as Ras and Rho. Signalling pathways which propagate the signal to the nucleus include NfκB, MAPK and ERK. Shear stress signals cause a change in gene transcription in the nucleus to induce a remodelling response (Section 1.6.2).

Adapted from (Ngai, 2010)

### 1.6.1 Signal transduction of fluid forces

Eitenmuller *et al.*, (2006) identified three main pathways activated in endothelial cells exposed to changes in haemodynamic flow following arterial occlusion (Eitenmuller *et al.*, 2006). Rabbits were subjected to femoral artery occlusion and A/V shunts. Collateral arteries were identified and tissue was prepared for microarray and Western blot analysis, to assess gene and protein expression. The collateral vessels extracted from shunted legs showed increased protein expression of activated extracellular signal-regulated kinase (ERK) and the Ras-Erk pathway. This is a pathway known to be involved in growth factor-initiated cell proliferation. The Rho pathway was also upregulated in collateral vessels exposed to high shear stress. The Rho pathway is proposed to mediate cell motility by regulating the actin cytoskeleton. Nitric oxide (NO) pathways were also upregulated, however this pathway is extremely complex and no mechanism for upregulated NO was identified. The group deduced that changes in haemodynamic flow might cause deformation of endothelial cells and alter the cytoskeleton. This may initiate signals to the nucleus to up-regulate chemokines and adhesion molecules and Rho pathways. Attracted monocytes were hypothesised to release growth factors which induce cell proliferation via the RAS-ERK pathway.

Signalling pathways, RAS-ERK and Rho, were said to enable 'concerts of events' which contributed to the sustained growth of collateral vessels in shunt models with sustained shear stress. It has been proposed that development of collateral vessels, induced by changes in flow, may also be mediated by these same pathways (Eitenmuller *et al.*, 2006).

## 1.6.2 How does stimulation of mechanotransduction pathways result in changes in gene expression?

Many endothelial genes possess a shear stress response element (SSRE) in their promoter region. Shear stress signals transduced to the nucleus, result in activation of the SSRE in shear responsive genes, leading to alteration in gene transcription (Resnick and Gimbrone., 1995). The shear stress response element has been identified as a GAGACC sequence (GGTCTC complementary sequence) and has been found in the promoter region of shear responsive genes such as platelet derived growth factor (PDGF-B), Transforming growth factor  $\beta$ 1 (TGF $\beta$ 1), MCP1, endothelin1 (ET-1), ICAM1 (Resnick *et al.*, 1993, Miyakawa *et al.*, 2004). The SSRE binds transcription factors which both positively and negatively regulate gene expression. For example, transcription factor nuclear factor kappa- $\beta$  (NF $\kappa$ - $\beta$ ) has been shown to modulate expression of MCP1 (Resnick *et al.*, 1993). VCAM1 and ICAM1 have a repressive and active SSRE. In low shear stress VCAM1 is upregulated and ICAM1, downregulated, however, with increasing shear stress both molecules are upregulated (Walpola., 1995). Transcription factors such as early growth response protein-1 (Egr-1), sp1, NF $\kappa$ - $\beta$ , activator protein-1 (AP-1), c-myc, c-jun are induced early following exposure to shear stress and interact with the SSRE to mediate gene expression in the first few hours (Lan *et al.*, 1994, Khachigian *et al.*, 1997, Garcia-Cardena and Gimbrone., 2006). In cultured bovine aortic endothelial cells exposed to physiologic levels of laminar shear stress, this early expression of Egr-1 was investigated (Khachigian., 1997). Gel shift studies showed Egr-1 to bind the SSRE of PDGF-A, which was induced by shear stress. This was found to be specific and time-dependent. Egr-1 was upregulated 30 minutes-1 hour following increases in shear stress and is referred to as a 'master switch', controlling expression of other endothelial genes including PDGF-A, FGF2, VEGF and MCP1 and adhesion molecule ICAM1 (Khachigian., 1997).

## 1.7 Transcriptional changes induced by altered shear stress

There is increasing evidence that a number of genes are activated by shear stress following arterial occlusion, and modulated by different signalling pathways. Shear stress activated endothelial cells may modulate certain genes to regulate processes which contribute to vessel remodelling (Resnick and Gimbrone., 1995, Gimbrone *et al.*, 1997, Topper and Gimbrone., 1999) . Flow-induced changes in gene expression have been investigated in both *in vivo* and *in vitro* models, in a variety of species (as discussed below and in section 1.10). Different gene expression profiles are reported in these models, despite the detection of similar responses such as inflammation. This suggests that the transcriptional profile of the endothelial cell response to fluid mechanical forces is temporal, spatial and species-dependent. *In vivo* and *in vitro* experiments to investigate this shall next be described below.

*In vitro* experiments are often performed in cultured endothelial cells exposed to flow which can be exposed to physiologically similar levels of shear stress. DNA microarray analysis sheds light on the transcriptional changes which occur in shear stress activated endothelial cells. One such study found expression of 52 genes to be altered in response to changes in shear stress in cultured human umbilical cord endothelial cells (HUVECs) after 6 or 24 hours exposure to shear stress (25 dynes/cm<sup>2</sup>) (McCormick *et al.*, 2001). Genes, including MCP1, that were upregulated were involved in proliferation, vascular tone, cytoskeleton and inflammation. This study also documented up-regulation of genes with vasodilatory properties endothelial nitric oxide (eNOS) and down-regulation of vasoconstrictor genes (ET-1) (McCormick *et al.*, 2001). Expression of these genes was speculated to modulate vascular tone to normalise shear stress (Peters *et al.*, 2002, Hierck *et al.*, 2008).

Genes found to be upregulated in arteriogenesis *in vivo* have also been observed in *in vitro* studies. MCP1, which has been studied in a number of animal models of arteriogenesis (Ito *et al.*, 1997b, Scholz *et al.*, 2000, Pipp *et al.*, 2004), has been shown to be induced in response to increased shear stress in cultured HUVECs. Levels of MCP1 RNA increased 2-3 fold under shear stress, compared to static conditions. This was found to be an early, immediate gene activation response to increased shear stress (Shyy *et al.*, 1994). Further, Scholz *et al.*, (2000) conducted molecular histology on collateral vessels after femoral artery occlusion in rabbits, over a timecourse from 2 hours to 240 days after occlusion. The group first observed endothelial upregulation of ICAM1 and VCAM1 genes at early timepoints (12 hours) following occlusion. Infusion of MCP1 increased monocyte adhesion which improved collateral vessel formation. The authors then were able to reproduce the findings *in vitro* in cultured HUVECs following the onset of shear stress, where induction of ICAM1 and VCAM1 occurred early on following the onset of shear stress (Scholz *et al.*, 2000). Expression of ICAM1 and VCAM1 have been reported to not only be genes regulated by shear stress but also modulated by the presence of smooth muscle cells, *in vitro* (Chiu *et al.*, 2003). One investigation found that co-culturing endothelial cells with smooth muscle cells influenced the endothelial response to shear stress. In a parallel plate, flow system cells were separated by a porous membrane. Static co-cultured endothelial cells expressed upregulated genes ICAM1, VCAM1 and E selectin, however in the presence of shear stress, smooth muscle cells were inhibited from inducing adhesion molecule expression in endothelial cells. When endothelial cells were removed from co-culture or cultured next to fibroblasts, these genes were no longer expressed (Chiu *et al.*, 2003).

Low and high shear stress have been shown to modulate gene expression in cultured human coronary endothelial cells. Peters *et al.*, (2002) investigated cultured endothelial cells which were exposed to 0, 15 or 45 dynes/cm<sup>2</sup> of laminar shear stress for 1 hour and then the transcriptional profile was assessed by cDNA microarray (Peters *et al.*, 2002). Results

showed early upregulation of transcription factors, factors involved in signal transduction, antioxidants, vaso-reactivity, cell-cycle genes and genes regulating the cytoskeleton (Peters *et al.*, 2002). This data suggested that shear stress induced expression of transcription factors extensively re-programme the genes that coordinate an endothelial response to changes in flow. Another group investigated the genes expressed during oscillatory and laminar flow patterns of endothelial cells *in vitro* (White *et al.*, 2011). Kruppel-like factor 2 (KLF2) was found to be one gene that was upregulated under high shear conditions and said to play a role in the amplification of shear responsive signalling (White *et al.*, 2011). KLF2 is a shear responsive transcription factor which regulates expression of many genes and has been shown to be upregulated in response to prolonged shear stress *in vivo* and *in vitro* (Dekker *et al.*, 2002).

*In vivo*, low and high shear stress can also be investigated by analysing gene expression at different regions of the artery, such as bifurcations where shear stress is high and flow is disturbed. Egorova *et al.*, (2011), studied shear stress in a model observing embryonic endothelial cells of the chick heart and found KLF2 to be essential in coordinating the response of the endothelial cell to changes in flow (Egorova *et al.*, 2011). KLF2 is differentially activated in high shear and low shear environments and is athero-protective (Dekker *et al.*, 2002, Groenendijk *et al.*, 2004) . This gene may therefore also play a role in regulating changes in gene expression in endothelial cells of collateral vessels.

Temporal patterns of gene expression have been reported *in vivo* and *in vitro*. ‘Typical response patterns’ to continuous shear stress of a number of representative genes have been described in endothelial cells exposed to continuous laminar flow (Resnick, Gimbrone, 1995). Diamond *et al.*, (1990), were the first to show that fluid mechanical forces could directly alter gene expression (Diamond *et al.*, 1990).

In a comprehensive review of the subject by Resnick and Gimbrone (1995), mRNA encoding c-fos, a DNA binding protein, shows a rapid and immediate response to shear stress; PDGF-B mRNA shows a rapid upregulation and transcript levels remain high for a few hours after the onset of shear stress. MCP1, ICM1 and TGF-B genes also show this pattern. VCAM1 gene is downregulated in response to laminar flow (Resnick, Gimbrone, 1995).

Lee *et al.*, (2004), investigated temporal expression of flow-responsive genes using a DNA microarray in mice following tied-ligation or sham-ligation after 6 hours and 1,3,7 and 14 days. This group also found early upregulation of transcription factors and DNA binding proteins. This was followed by a mid-phase of upregulated inflammatory genes, along with cell cycle genes and cytoskeletal genes (Lee *et al.*, 2004a). Although a similar pattern of temporal gene expression was observed as the *in vitro* study by Diamond *et al.*,(1990) in the study by Lee *et al.*, (2004), the transcriptional profile of genes was not replicated between models: for example, adhesion molecules were not expressed, however, MCP1 was upregulated (Lee *et al.*, 2004a). This highlights the fact that some mechanisms may be universal to shear exposed endothelial cells, but that expression of key genes may differ due to differences in species, windows of expression, environment and flow patterns.

Understanding and characterising the expression patterns of 'shear-responsive' genes will provide a clearer overview of the transcriptional responses of endothelial cells to changes in haemodynamic flow. This information could then be used to further elucidate the pathology of vascular disease and endothelial dysfunction and suggest new therapeutic strategies.

### **1.8 Therapeutic promotion of arteriogenesis**

The above studies suggest potential mechanisms whereby haemodynamic alterations may influence arteriogenesis. Other studies provide more direct evidence of the mediators of

arteriogenesis. Transcription factors which control gene expression in response to changes in shear stress (discussed in section 1.6.3) have been shown to regulate expression of growth factors. *In vivo* experiments have gone on to explore whether exogenous infusion of growth factors, or manipulation of growth factor signalling, can affect arteriogenesis. A description of some of the investigations into the factors which might therapeutically promote collateral vessel growth are summarised below.

MCP1 has been shown to improve collateral vessels in rabbit and porcine models of arterial occlusion (Hofer *et al.*, 2001, Voskuil *et al.*, 2003). Infused MCP1, was given locally via a mini-pump for a 1 week period, either 3 weeks or immediately following ligation of the femoral artery in rabbits. MCP1 treatment caused a significant increase in collateral vessel density proximal to the ligation in the upper leg within the first week, compared to controls receiving saline only (Hofer *et al.*, 2001). A similar study showed the same results in rabbit models (Ito *et al.*, 1997). Femoral artery occlusion was performed in 12 rabbits which then received infusion of either MCP1 or saline via osmotic mini-pump for 7 days. Angiograms showed that rabbits that had received MCP1 had improved collateral vessel formation in the thigh (Ito *et al.*, 1997). These experiments suggest that stimulation of macrophages and monocytes could be a therapeutic tool to induce collateral vessel formation in mammals.

Granulocyte-Macrophage Colony Stimulating Factor (GM-CSF) is a cytokine that functions as a growth factor to stimulate production of macrophages. GM-CSF has been found to improve arteriogenesis in animal models such as the pig. Continuous infusion of GM-CSF by intra-arterial delivery for 1 week following femoral artery ligation increased collateral conductance in pigs when compared to saline infused controls (Grundmann *et al.*, 2006). However, clinical studies in patients with peripheral arterial disease (not eligible for bypass surgery) were not as successful. The patient study focussed on the effect of short term, local and systemic infusion of GM-CSF. Although some patients benefitted from the

treatment and showed improved collateral conductance, the study cohort was small and the results were variable and thus inconclusive (Seiler *et al.*, 2001).

In the 1990s experiments were performed to investigate the therapeutic potential of growth factors such as Vascular Endothelial Growth Factor (VEGF) and Fibroblast Growth Factor (FGF1 and FGF2) in stimulating collateral vessel growth (reviewed by Epstein *et al.*, 2001). Some of these shall next be described.

The effect of VEGF treatment on collateral vessel development was first observed in *in vivo* studies in which the coronary vessels of dogs were obstructed to cause ischaemia to the ventricle of the heart (Banai *et al.*, 1994, Unger *et al.*, 1994). Ten days after creating the vessel obstruction, intracoronary infusion of VEGF or saline were given daily for 28 days. Collateral blood flow was measured and quantified using microspheres, at regular intervals during treatment. VEGF administration significantly increased collateral vessel flow, showing a 40% increase in collateral flow. The treatment also increased the number of small vessels supplying the ischaemic tissue (Banai *et al.*, 1994, Unger *et al.*, 1994). Another group observed the effects of VEGF on endothelial and smooth muscle cell proliferation in collateral vessels (Takeshita *et al.*, 1995). Rabbits received femoral artery ligation and 10 days later a bolus injection of either VEGF or saline. Proliferation of endothelial and smooth muscle cells was assessed by Bromodeoxyuridine labelling at days 3, 5 and 7. VEGF did increase cell proliferation (maximal at 5 days) compared to untreated controls, but this response was returned to baseline by day 7. Further, collateral vessels in different areas of the upper leg were assessed and proliferation was confined to only mid-zone collateral vessels and was not observed at the stem or re-entry collaterals. However, the authors concluded that VEGF stimulated endothelial and smooth muscle cell proliferation was enough to improve collateral vessels and haemodynamic flow (Takeshita *et al.*, 1995).

One other mechanism for how weak arteriogenic effects of infused VEGFA might improve collateral vessel development was proposed by Breier *et al.*, (2002). The group investigated the monocyte attractant effect of VEGF A binding to VEGF receptor 1 on the surface of monocytes. Mice heterozygous for VEGFR1 were found to have impaired collateral vessels 21 days after femoral artery ligation leading the authors to conclude that VEGF and VEGFR1 are determinants of arteriogenesis (Breier *et al.*, 2002).

A role for up-regulation of endogenous FGFs in arteriogenesis remains unclear. In one study, FGF receptor 1 (FGFR1) mRNA, protein and kinase activity were upregulated briefly during femoral artery occlusion in rabbits (Deindl *et al.*, 2003). Increases in FGFR1 expression was thought to occur in response to monocyte release of FGF ligands, and not to FGFs produced by the endothelial cells of the collateral vessels. To investigate further, rabbits were treated with MCP1 to stimulate arteriogenesis and also received an FGF inhibitor. These animals showed reduced arteriogenesis, despite the increase in MCP1. This result suggested that FGFR1 is upregulated in vessels during arteriogenesis and FGF ligand is supplied by monocytes which produce and deliver growth factors to developing collateral vessels (Deindl *et al.*, 2003).

FGF2 has been shown to improve collateral vessels when delivered to mice by an osmotic mini-pump for seven days after hind-limb arterial occlusion (Scholz *et al.*, 2002). The mice receiving FGF2 showed enhanced speed of arteriogenesis. Morphometry analysis showed increases in collateral vessel diameter which was shown to be a result of increased endothelial and smooth muscle cell proliferation. Due to this improved collateral vessel conductance, less angiogenesis was observed distally as the limb was more efficiently re-perfused and therefore ischaemia was reduced (Scholz *et al.*, 2002).

PDGF has been found to act as a smooth muscle cell chemoattractant which induces smooth muscle cells to migrate (Dardik *et al.*, 2005b). RNA levels of PDGF do not appear to

change in the early stages of collateral vessel growth (reviewed by Schaper, 2003). The transmission of this growth factor from endothelial to smooth muscle cell is not thought to be important due to the presence of monocytes which fulfil this role (reviewed by Schaper and Scholz 2008). Protein levels of PDGF have also been assessed following insertion of an ameroid constrictor around the left circumflex artery of canine hearts, and in the femoral arteries of rabbits which had undergone hind limb artery ligation and arterial/venous shunt (Wu *et al.*, 2010). Immunohistochemistry revealed significant upregulation of PDGF in collateral vessels compared to control vessels which had not experienced changes in haemodynamic forces (Wu *et al.*, 2010).

Clinical evidence for the arteriogenic potential of growth factors remains contentious. However, one Phase 1 clinical trial in humans supported a case for VEGF in arteriogenesis but this trial did not progress to Phase II suggesting that more carefully monitored clinical investigations are needed (Epstein *et al.*, 2001). Naked DNA plasmids containing endothelial cells and an isoform of human VEGF were injected into the limbs of patients with peripheral arterial disease (Baumgartner *et al.*, 1998). Three patients, not suitable for invasive bypass surgery, received this treatment. Angiography and ability to exercise were measured. Two months after therapy, significantly more collateral vessels were observed by angiography which resulted in increased flow and limb salvage. Tissue samples from these patients showed increased endothelial proliferation. However, the study cohort was too small to draw conclusions from the data (Baumgartner *et al.*, 1998).

In conclusion, therapeutic factors can promote collateral vessel formation in animals which is promising for clinical application; however, more study into this field is required before an optimal approach to using growth factors as therapies for vascular diseases is identified.

## **1.9 Changes in haemodynamic flow can alter endothelial cell arterial/venous identity**

Changes in blood flow can directly alter molecular markers that specifically identify arterial or venous vessels (Othman-Hassan *et al.*, 2001, le Noble *et al.*, 2004). The studies described below provide an indication of the signalling pathways that govern arterial and venous identities. Research in this area could have implications in the clinic, for example, manipulating arterial/venous identity of endothelial cells in vessel biopsy surgery, to encourage graft patency, For my research however, an understanding of endothelial cell plasticity (i.e. regulation of arterial/venous marker expression) was important to understanding mechanisms involved in collateral vessel remodelling.

Identifying reliable endothelial arterial and venous markers allows investigation into how and when these markers are up or downregulated in response to haemodynamic forces. Two transmembrane receptors known to play a role in vascular development have been investigated in chimera studies (Moyon *et al.*, 2001). Arterially expressed neuropilin-1 (*nrp1*) and venous *tie-2* genes were analysed in sections of aorta, carotid artery and cardinal and jugular veins of quail embryo donors that were grafted onto the coelom of chick embryo hosts at different stages during development. From Embryonic day (E) 2-7 cells from arteries and veins did not maintain their original arterio-venous identities and were able to migrate from the donor graft to colonise the host vasculature. *Tie-2* expression did not persist when such cells colonised the chick host's artery. Grafted cells originally expressing *nrp1* did not maintain expression of the arterial marker when grafted into a vein. Eventually at later stages of development (E11) this plasticity was lost (Moyon *et al.*, 2001). The authors concluded that endothelial cell fate was plastic and arterial/venous marker expression was regulated by flow, until later stages of development.

le Noble *et al.*, (2004) investigated plasticity of endothelial cell arterial-venous fate by removing flow from the extra-embryonic vasculature of chick embryos (le Noble *et al.*, 2004). The group first observed flow-dependent development of the right vitelline artery by excising all 3 germ layers at HH st 10. Removing perfusion at this early stage of development resulted in the absence of the right vitelline artery which was replaced by a single vein. Flow in the vitelline vessels was further investigated in HH st 18 embryos by inducing a temporary arterial occlusion by elevating the right vitelline artery with tungsten wire for 24 hours. When arterial flow was obstructed to one side of the vitelline circulation, the arterial markers, ephrin B2 and *nrp1*, were downregulated after 10 minutes and undetectable after 4 hours. The venous markers, neuropilin-2 (*nrp2*) and *tie-2*, were upregulated, although expression was not strong until 12 hours post-ligation, suggesting that flow-regulation of arterial markers was more rapid than upregulation of venous markers. Aside from the expression of the molecular markers, vessel morphology showed the arterial bed on the tied-ligated side became venularised. Restoration of flow, by releasing the elevated wire, downregulated the venous markers and arterial markers were again expressed after 4 hours of re-perfusion (le Noble *et al.*, 2004). These findings provide evidence to suggest that endothelial cells remain plastic during early stages of development and can adapt their arterial/venous identity depending on the environment. Furthermore, the findings suggest that arterial identity is driven by flow.

Conversely, there is evidence that endothelial cell fate is pre-determined (Lawson *et al.*, 2001). In zebrafish a loss of Notch signalling results in a loss of arterial ephrinB2; over-expression of Notch inhibits venous fate. These changes in endothelial cell fate disrupted vessel patterning in developing embryos. This data suggested that Notch expression is required for determining arterial/venous fate and that a main role of Notch is to drive arterial expression and repress venous differentiation of endothelial cells (Lawson *et al.*, 2001). Evidence for arterial Notch signalling in arterial cells has also been investigated in

chick embryos where the Notch ligand, *dll4*, was identified, using *in situ* hybridisation, in the arterioles but not the venules of the yolk sac and could also be strongly detected in the proximal vitelline arteries of HH st 16 embryos (Nimmagadda *et al.*, 2007).

In conclusion it is likely that a balance of genetics and blood flow patterns vessel architecture. Although pre-determined cell fate is evident in endothelial cells of various model systems there is strong evidence for flow and mechanical forces altering gene expression and arteriovenous identity.

### **1.10 Model systems of collateral vessel formation**

Studying collateral vessel formation in humans is technically very difficult. It is not possible to induce this experimentally since this would require sustained arterial occlusion, which would be damaging. Although many patients present with occluded arteries, the timing of the occlusion is often unknown, the occlusion may be immediately or subsequently fatal, and the ability to visualise and quantify collateral vessels clinically is limited and often highly invasive. To understand the mechanisms of collateral vessel formation, researchers must therefore rely on animal models. Sir John Hunter first described collateral vessels in 1785 (reviewed in (Murley., 1984)). He ligated the external carotid artery in a stag preventing circulation to one antler. After ligation the antler became cool and the arterial pulse was impalpable. However, two weeks later, the antler was once again warm and a pulse could be felt. Dissection revealed small collateral vessel anastomoses which bypassed the ligation to restore blood flow. Since this experiment, many other animal models have been developed, both mammalian and non-mammalian: some of these are summarised below.

Mouse, rat and rabbit models have been widely used to investigate collateral formation (Scholz *et al.*, 2000, Herzog *et al.*, 2002, Stabile *et al.*, 2003, Terry *et al.*, 2011). The hind-

limb model involves invasive surgery under general anaesthesia to access the femoral artery, which is ligated, greatly reducing blood flow to the foot (Ito *et al.*, 1997a, Herzog *et al.*, 2002) . Laser Doppler or angiography is used to then quantify foot blood flow or to visualise collateral vessels (Limbourg *et al.*, 2009). These imaging methods do not allow for real-time observation of collateral development and are expensive and time-consuming. Nevertheless, many important discoveries concerning pro-arteriogenic factors have been identified using these models as described in section 1.8. A particular advantage of the mouse is the ability to study genetic knockouts. Athero-prone mice or those with other gene defects can be used to uncover more about the disease process and progression.

The canine and porcine models allow focus on the coronary vessels due to the larger cardiac size. These two models differ: Arteriogenesis in the canine heart depends on pre-existent vessels (Schaper *et al.*, 1990). The canine model facilitated much of Schaper's early work on arteriogenesis in the 1970s (Borgers *et al.*, 1971, Schaper *et al.*, 1971, Schaper and Pasyk, 1976) .

The pig can be used as a model for arteriogenesis research if using the hind limb model. It is not an ideal model as large inter-species differences exist (Voskuil *et al.*, 2003, Pipp *et al.*, 2004). Further, there are few pre-existing coronary collateral vessels which do not remodel in response to increased fluid shear stress. Instead large vessels devoid of smooth muscle resembling capillaries form to recompense for the lack of perfusion in the coronary arteries (van den Wijngaard *et al.*, 2011).

The zebrafish is a novel model of cardiovascular disease and has several advantages over mammalian models (Packham *et al.*, 2009). The optical clarity of the embryos allows for visualisation of the circulating blood within the vessels; further, transgenic fish can be created to enhance this visualisation. Endothelial-specific promoters can be used to drive expression of reporters such as green fluorescent protein (GFP) in blood vessels (Lawson

and Weinstein, 2002, Lyssenko *et al.*, 2007). Further to the use of fluorescent reporter lines to enhance vessel visualisation, mutants can be produced to model cardiovascular abnormalities. The *gridlock* mutant is a model of aortic occlusion and was characterised by Gray *et al.*, (2007) as a model of arteriogenesis (Gray *et al.*, 2007). Collateral vessels were observed to develop from pre-existing endothelial connections to restore aortic flow. However, the small size of these vessels, and absence of investing smooth muscle, mean that it cannot replace the use of mammalian models to understand human arteriogenesis.

In March 2004 the first draft of the chicken genome was completed (2004, Wallis *et al.*, 2004). This confirmed that many coding genes were homologous to human genes. We can thus use the chicken for comparative genomics and as a model of human disease and development. The chick embryo lends itself particularly to vascular biology and the study of haemodynamics (Hughes., 1935, Lee and Lee., 2010). Thoma discovered the effect of blood flow on vessel configuration and observed that in this system blood flow regulated vessel growth (Thoma., 1893). Before onset of blood flow there was a uniform pattern of vessels which became defined into arteries once circulation had begun (Hughes., 1937). Hughes continued Thoma's observations in the chick embryo; in an era predating advanced imaging techniques, he was able to document aspects of vascular development by simply drawing vascular structures injected with ink. Hughes also experimented with analysis of the extra-embryonic vasculature *in ovo* and *in vitro* (Hughes., 1937). This early work highlights the robustness of the chick embryo model system. The ability to observe vessel development over time without invasive or expensive procedures demonstrates attributes that the chick embryo can offer cardiovascular research.

*In vitro* analysis of endothelial cell responses can provide information on angiogenesis, wound healing, tumour biology, gene expression, cell proliferation and migration and endothelial dysfunction (Jaye *et al.*, 1985, Coomber and Gotlieb, 1990). Flow chambers can

model the effects of shear stress, and allow for external regulation of laminar and/or disturbed flow (Dewey *et al.*, 1981, Davies *et al.*, 1986). This technique allows for the monitoring of an exclusively endothelial cell response to a specified environment, but is less often applied to multi-cellular models. Although this is advantageous to an uncontrolled *in vivo* environment it is important to acknowledge that an *in vitro* cell response is limited; complex factors which may be present *in vivo* are eliminated in a controlled system. No significant *in vitro* models of collateral development have been so far developed, justifying the continued use of animal models.

### **1.11 The chicken embryo as a model system to study flow-induced remodelling**

There are many advantages in using the chick embryo over other model systems. Ethically it is preferable to use a non-mammalian model for clinical research; the chick embryo is cheap, husbandry is low maintenance and the embryo is robust. The vasculature is visible *in vivo* by light microscopy and real-time observation of vessel growth is neither invasive, nor time-consuming. The extra-embryonic vessels of the chick embryo are easily accessible *in ovo* after 66-68 hours of incubation, by making a small window in the shell. Manipulations of the extra-embryonic vasculature can be performed and then the chick can be covered and returned to the incubator to monitor flow-induced changes to the vasculature over time.

### **1.12 The development of the chicken embryo extra-embryonic vasculature**

In the chick embryo, as with other vertebrates, the majority of cells forming the cardiovascular system derive from ventral mesoderm or extra-embryonic endoderm. An early process, termed vasculogenesis, drives the earliest stages of development of the extra-embryonic vasculature. In this process, small blood islands in the extra-embryonic tissue begin to form (Gonzalez-Crussi., 1971). Haematopoietic cells form inside the blood islands, surrounded by angioblasts – endothelial precursors. As blood islands fuse,

endothelial cells differentiate and a primitive network of vessels form (Risau and Flamme, 1995). This is depicted in the schematic in Figure 1.5.

The orientation of this vessel network is thought to be genetically pre-determined; further remodelling of the vasculature is then under the influence of blood flow following the onset of perfusion (Jones *et al.*, 2006). Once vasculogenesis has completed and vascular precursor cells have formed lumenised tubes, angiogenesis continues to develop the vascular tree (as described in section 1.3).

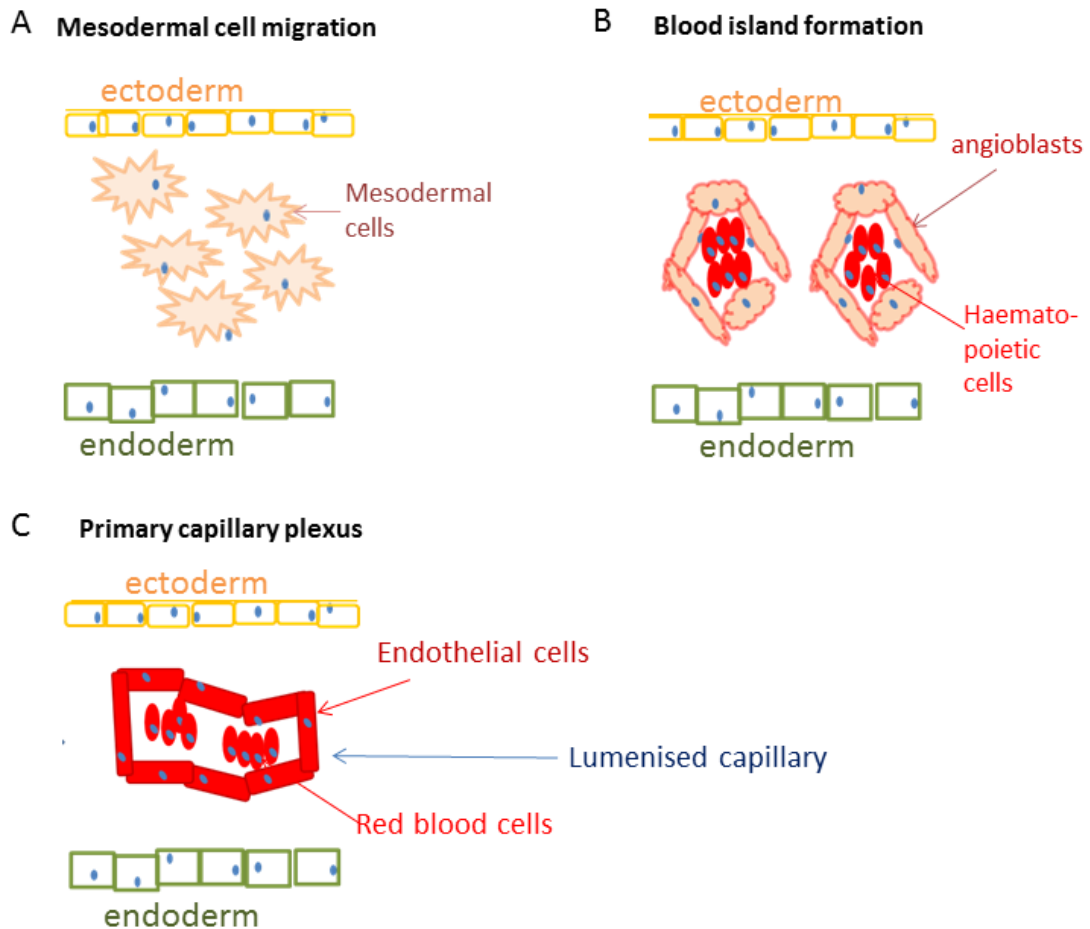


**Figure 1.5** The process of vasculogenesis in the extra-embryonic vasculature of the chicken embryo involves formation of blood islands from mesodermal cells which develop into capillaries with the onset of flow.

**A** Mesodermal cells committed to differentiate into endothelial cells initially give rise to angioblasts. Migrating mesodermal cells are bordered by ectoderm and endodermal cells in the primitive vascular primordial of the embryo. **B** Angioblasts fuse to create blood islands which are populated with haemopoietic cells derived from the yolk sac. **C** Blood islands fuse to form primitive capillaries and angioblasts differentiate into endothelial cells. Lumenised, functional capillaries mature and develop with the onset of circulation.

Adapted from (Risau and Flamme, 1995)

The development of the extra-embryonic vessels in the chick embryo has been studied in detail for many years (Hughes., 1935). In 1992, Viktor Hamburger and Howard Hamilton recorded a series of normal stages of chick embryo development, which has become the gold-standard for determining the age of chick embryos in research (Hamburger and Hamilton., 1992). The arteries are the first vessels to develop around HH st 15 (see section 2.1.4 for an explanation of Hamilton and Hamburger staging). The vitelline network is surrounded by a circular vein known as the sinus terminalis. This structure collects blood from peripheral capillaries and drains blood back to the heart via the posterior and anterior vitelline veins, which lie at the midline of the embryo. Before HH st 20, proximal vitelline vessels (lateral to the embryo body) are arterial (carry afferent flow out to the sinus vein). Proximal vitelline veins then develop to more efficiently return blood to the embryo as the extra-embryonic vasculature/tissue expands with the growing embryo (Hughes., 1935). These proximal vitelline vessels overlap one another, with the veins lying above the arteries in a cis-trans configuration carrying anti-parallel flow (Nguyen *et al.*, 2006). The veins in the extra-embryonic vascular network are said to develop from pre-existing arterial connections which dis-connect from the arterial tree and re-connect as veins (le Noble *et al.*, 2004). Figure 1.6 shows a diagrammatic figure of the extra-embryonic vasculature of a HH17 chick embryo and a later stage HH20 embryo to demonstrate the changes to the vascular tree as the embryo develops.

Figure 1.7 shows representative micrographs of the embryo and vasculature at different stages (HH st13-17) to show the change in extra-embryonic vascular morphology over time *in ovo*.

A Vitelline vessels of HH st17

B Vitelline vessels of HH st20

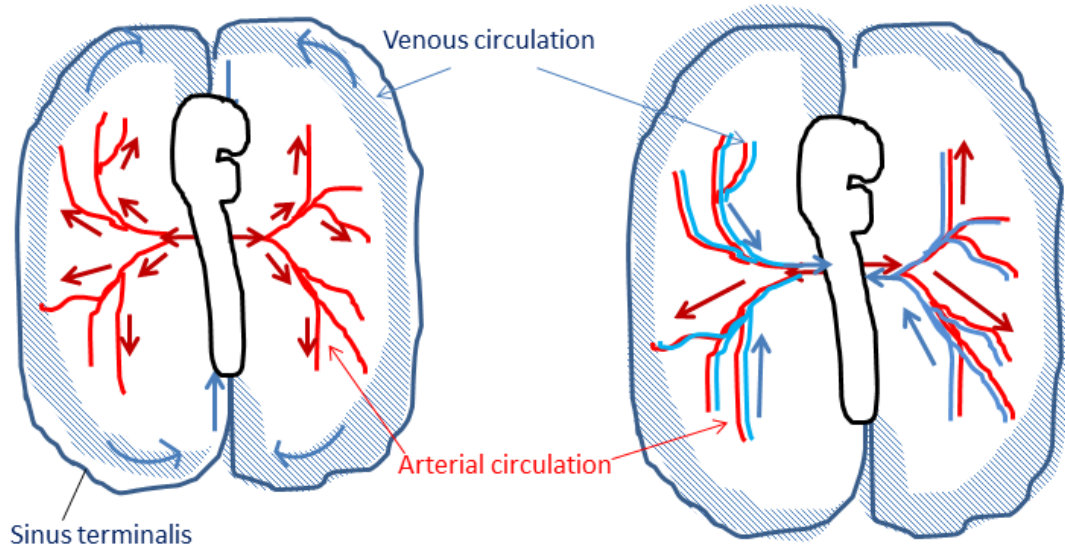


**Figure 1.6 Normal blood flow patterns through the extra-embryonic vitelline vessel network of a chick embryo at HH st 17 and HH st 20**

**A** shows a cartoon of the flow profiles in the vitelline vessel network of a HH st 17 chick embryo. Blue shading represents the area of small venules which drain blood back to the embryo via the main vein, known as the sinus terminalis which borders the vascular network. Red arrows represent arterial flow which enters the extra-embryonic network via vessels lateral to the body. Vessels become increasingly branched and smaller in size until capillaries reach the sinus terminalis and blood can be drained into the venous network and returned to the embryo. **B** shows the embryo at a later stage. The flow profile at HH st 20 is more complex. Anti-parallel blood flow now exists as veins proximal to the embryo have developed to overlie the proximal lateral arteries. This allows more efficient venous return to the embryo as the entire network has expanded in size to grow with the embryo.

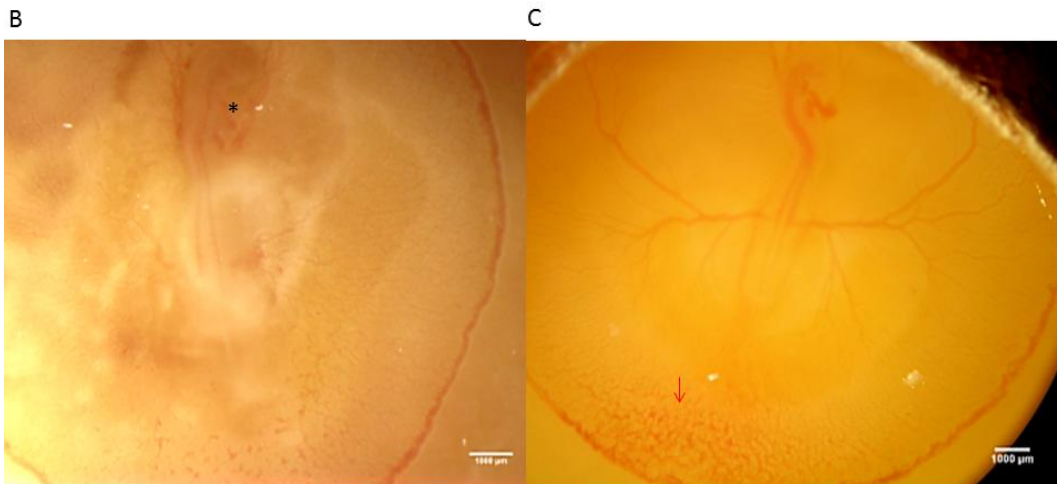
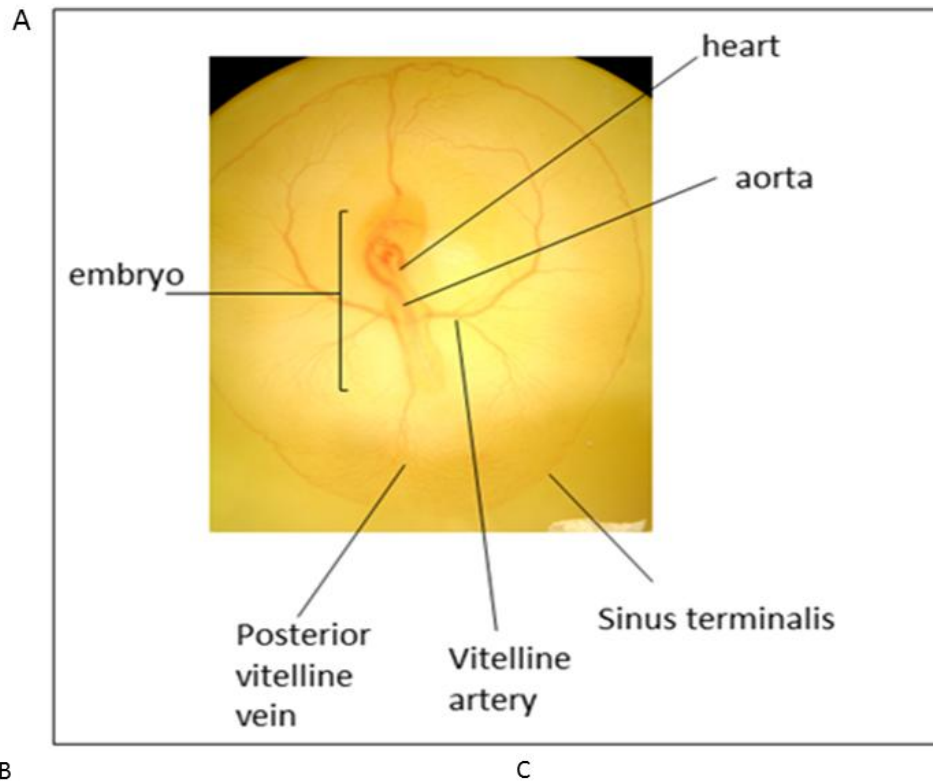


**Figure 1.7 The development of the extra-embryonic vasculature of the chicken embryo, from HH st 13-17**

**A** shows the labelled vasculature of a representative HH st17 embryo. Proximal vitelline arteries lateral to the chick embryo carry arterial flow at this stage. Posterior and anterior vitelline veins lie at the midline of the embryo/yolk sac and return blood to the embryo. The sinus terminalis vein creates a border around the extra-embryonic tissue and collects blood to be returned by the venous system. **B** At HH st 13 it is difficult to see the defined outline of the embryo by light microscopy (embryo indicated by star). Perfusion has not begun at this stage therefore the vasculature cannot be seen as it is not yet perfused and still primitive. The developing primitive vitelline network can be seen in **C**. **C** shows HH st 15 embryo, small capillary blood islands appear as spots of red at the posterior of the embryo and are indicated by the red arrow. Blood islands develop into the vitelline vein shown in **A**. These vascular orientations in these representative images were observed in all chicks at these stages (n=>100 embryos over the course of the project). Scale bar indicates 1000 µm.

### **1.13 Chick embryo models to investigate the effects of changes in haemodynamic flow**

Due to the accessibility of the vitelline vasculature, previous groups have been able to manipulate blood flow to observe morphological patterning and molecular changes which occur following induced vessel occlusion.

The previously mentioned study of flow regulation of endothelial identity by le Noble *et al.*, (2004) utilised tungsten wires, to elevate the vitelline vessel and prevent flow (le Noble *et al.*, 2004). This had the advantage of being easily removed to re-perfuse the vitelline vessel but le Noble also cauterised the vitelline artery prior to the onset of flow which prevented any further development of the right vitelline vessel. When 'ligation' of the right vitelline vessel was observed for 24 hours the group recorded '*venularisation*' of the right vitelline vessel and '*large arteries branching off the left vitelline artery were observed to project to the right side of the yolk sac, and crossed the midline*' (le Noble *et al.*, 2004). This was never observed in unligated control embryos. Although we identified these vessels as collateral vessels, the group did not further acknowledge or study the collateral vessels which developed after ligation. The group instead, used this flow manipulating technique to observe flow regulated endothelial markers and document the haemodynamically driven expression of arterial markers in reperfused vessels (discussed in section 1.9).

Groenendijk *et al.*, (2005) used HH st 17 embryos to investigate transcriptional changes in shear related genes after alterations of flow which is 'positively correlated with shear stress' (Groenendijk *et al.*, 2005). Flow and shear stress were altered by venous clipping of the right lateral vitelline vein which effected venous return to the heart. After 3 hours, analysis of mRNA levels from different areas of the cardiovascular system were analysed. This revealed that changes in blood flow through the heart and alterations in shear stress resulted in changes in gene expression. Following venous ligation, the aorta experienced

decreased shear stress, reduced expression of KLF2 and nitric oxide synthase 3 (NOS3) mRNA and up-regulation of ET1 mRNA. The opposite expression pattern was observed in the heart which experienced increased shear stress following ligation (Groenendijk *et al.*, 2005). This is one example of how the extra-embryonic vasculature of the chick embryo can be manipulated to alter flow and can be used to assess consequent transcriptional changes.

Flow manipulation of the vitelline network of HH st 17 chick embryos was also used by Buschmann *et al.*, (2010) during the course of my studies. Tungsten wire elevated the right vitelline vessel in order to occlude flow and induce morphological changes in vessel patterning, and the group then studies arterial expression of the connexin gene (*Gja5*) (Buschmann *et al.*, 2010). The group identified collateral vessels stemming from the left proximal vitelline vessel and crossing the midline to supply the tied-ligated territory with arterial flow. The group recorded the number of collateral vessels at a single 24 hour timepoint and used in situ hybridisation to detect *Gja5* expression. The group used vascular casts of the remodelled vessels post-ligation at the midline of the embryo and reported that 'splitting angiogenesis' or intussusceptive angiogenesis (as described in section 1.3) was involved in the process of remodelling. Small capillaries which fed into the main posterior vitelline vein pre-ligation were seen to disconnect from the venous network and contribute to the arterial territory which the collateral vessel extended into. This work is discussed further in chapter 3 in the context of my own work – our results taken together strongly suggest that the chick embryo is a good model to study collateral vessel formation at the endothelial level. Buschmann *et al.*, identified *Gja5* expression in the collateral vessels of the chick embryo at 24 hours and subsequently found that *Gja5* was involved in collateral vessel formation in mouse (Buschmann *et al.*, 2010).

In summary, the chicken extra-embryonic vasculature has been used to observe morphological patterning and molecular changes which occur following induced vessel occlusion. This model has enabled studies to investigate the effect of flow on expression of arterial and venous endothelial markers, shear stress regulated genes and alterations in morphology of the vascular network. These studies are examples of how the chick model can be used to investigate blood flow remodelling and facilitate discovery of mechanisms of arteriogenesis.

#### **1.14 The advantages of using the extra-embryonic vasculature of the chicken embryo to study blood vessels *in vivo***

As the chick embryo develops more oxygen is required, therefore from HH st 18 the allantois circulation develops and the chick depends on this, rather than the vitelline circulation (Deryugina and Quigley., 2008). The allantois is the embryo's connection to chorion which lines the egg shell and provides gas exchange. These structures fuse at around HH st 23, forming the chorio-allantois. The highly vascularised chorio-allantoic membrane (CAM) has been used for many decades to study angiogenesis (Ribatti *et al.*, 1997, Brooks *et al.*, 1999). The chick embryo has therefore been realised in recent years as an extremely good model for investigating the vasculature in terms of tumour growth (Deryugina and Quigley., 2008). This highly vascularised 3-D structure develops from the 2-D flat vitelline membrane, during embryo development to later stages. The vessels at this stage are fragile and not appropriate for ligation techniques or vessel clamping as they easily tear. I therefore used embryos at an earlier stage for my experiments and concentrated on the vitelline vessels. However, previous studies using the CAM have shown that pharmacological agents can be applied to the extra-embryonic tissue to investigate effects on the vasculature (Ribatti *et al.*, 1997, Deryugina and Quigley., 2008).

Pharmacological agents can be applied to the vitelline vessel on filter paper discs, matrigel plugs or gelatin sponges (Ribatti *et al.*, 1997). The advantage to these techniques as opposed to simply dropping the drug in solution into the egg is that a specific area of the vasculature can be targeted, although some diffusion is likely. A stimulator or inhibitor of vascular growth can be applied to filter paper and positioned over the area of interest on the surface of the CAM/vitelline membrane. The embryo can then be re-sealed and returned to the incubator to continue development. At intervals during development the effect of the substance can be monitored by simply removing the vehicle of drug delivery and observing the vessels beneath. The speed of vascular development and the accessibility of the treated vessels, not to mention the ease of the assay, highlight the advantages that the chick embryo model has over drug screens using mammalian counterparts (Brooks *et al.*, 1999).

### **1.15 Cyclic nucleotide phosphodiesterases**

During the course of my studies I found phosphodiesterase 10A (PDE10A) to be upregulated during collateral vessel formation in the chick embryo. In order to introduce findings in chapters 4 and 5 I will therefore now discuss some general background to phosphodiesterases and PDE10A in particular.

Phosphodiesterases (PDEs) are enzymes which perform phosphoric-diester hydrolytic cleavage of cAMP and cGMP. This cleavage inactivates the 5' monophosphate of the second messenger preventing any further signalling (Essayan., 2001). PDEs regulate a variety of cell functions, including cell proliferation, inflammation and gene transcription (Lugnier., 2006). PDEs have been documented to control physiological functions such as smooth muscle relaxation, fluid homeostasis, platelet aggregation, cardiac contractility and immune responses (Matsumoto *et al.*, 2003). PDEs themselves are regulated by

phosphorylation, sub-cellular localisation, protein interactions and small molecule association (Francis *et al.*, 2001).

### **1.15.1 Cyclic nucleotides**

Nucleotides have an aromatic base containing nitrogen, sugar (ribose/deoxyribose) and a phosphate group. Cyclic nucleotides have two phosphate groups linked to a ribose group in two different places making them 'cyclic' and allowing them to bind differently to proteins. Cyclic nucleotides act as intracellular second messengers to convey and amplify complex signals from outside to inside the cell (Essayan., 2001, Francis *et al.*, 2001). Their level must be strictly regulated in order for them to orchestrate complex signalling events and crosstalk between pathways (Beavo., 1995, Soderling and Beavo., 2000). Cyclic nucleotides regulate important mediators of cell signalling such as protein kinase A (PKA) and protein kinase G (PKG), exchange protein directly activated by cAMP (EPAC), gated ion channels and PDEs (Lugnie.r, 2006).

### **1.15.2 Protein kinases**

Protein kinases (PK) are cyclic nucleotide binding proteins consisting of two regulatory and two catalytic subunits (Seino and Shibasaki., 2005). Cyclic nucleotides stimulate their own degradation by binding to Protein kinases. For example, Protein kinase A (PKA) binds two cAMPs to its regulatory subunits which cause a conformational change to release two catalytic subunits. These catalytic subunits catalyse the phosphorylation of proteins such as PDEs (Christina., 2010). Protein kinases activate PDEs by transferring a terminal phosphate group from an ATP molecule to a hydroxyl group on the PDE (Christina., 2010). PDEs in turn inactivate cyclic nucleotides to reduce the cAMP/cGMP signal (Beavo., 1995).

In the vasculature, cAMP/PKA signalling has been shown to regulate endothelial cell differentiation by up-regulating VEGF-A receptors and nrp1. cAMP can also activate arterial fate and arterial gene expression by activating phosphatidylinositol-3 kinase (PIK3) which

activates Notch signalling (Chiu and Chien., 2011). cAMP/PKA activation has also been investigated in the context of vascular barrier integrity. cAMP/PKA signalling was found to regulate endothelial cell cytoskeletal reorganisation in cultured bovine endothelial artery cells. When the cells were treated with PKA antagonists, including RP-Br-cAMPs, Western blotting revealed increased ERK1/2 and MAPK signalling, and immunofluorescent studies showed that this lead to actin cytoskeleton rearrangement (Liu *et al.*, 2001).

Endothelial cell proliferation is mediated by complex interactions of multiple signalling pathways. In one study, cultured bovine brain endothelial cells were used to investigate cAMP/PKA signalling mitogen-activated proliferation (D'Angelo *et al.*, 1997). Mitogens, VEGF and bFGF stimulate cell proliferation and activate MAPK signalling pathways. Increased levels of cAMP/PKA signalling prevented activation of VEGF and bFGF-induced MAPK signalling and cell division (D'Angelo *et al.*, 1997). This finding suggested that cAMP/PKA signalling in endothelial cells could play a role in inhibiting mitogen-activated cell proliferation.

### **1.15.3 The phosphodiesterase family**

Eleven different PDEs have so far been described, categorised according to regulation, pharmacokinetics and sequence (Beavo., 1995). The different PDE isoforms also have different splice variants (Buschmann *et al.*, 2003, Bender and Beavo, 2006). The main classifying factor of the subgroups of PDEs depends upon the PDE substrate: cAMP, cGMP or both. All PDEs share a similar protein structure, with targeting and regulatory domains in the NH<sub>2</sub> terminal region and a conserved catalytic domain towards the COOH terminal end (Seino and Shibasaki., 2005).

Although PDEs are ubiquitously expressed in the cells of the body, PDE family members are distributed differently with higher expression in specific tissues (Lugnier., 2006).

In vascular smooth muscle PDEs 1-5 have been well characterised (summarised by Polson and Strada., 1996). Due to PDEs acting on cyclic nucleotides most investigations of PDEs in the vasculature have been related to control of vessel tone and therefore PDE function in vascular smooth muscle cells (Matsumoto *et al.*, 2003). For example, in the clinical setting, the PDE5 inhibitor, Sildenafil, has been widely used in vascular surgery as a tool to induce vasodilation. PDE5 degrades cGMP, therefore inhibition enables manipulation of vascular tone (Rybalkin *et al.*, 2003).

Table 1 shows the functions of some of the vascular located PDEs.

**Table 1. Annotations of some of the observed functions of vascular located PDEs reported in the literature.** The table lists the PDE, the observed location in the particular study and the observed effect of inhibition. This gives some clues as to the functional role of the PDE. PDEs 1-5 have been observed to play functional roles in endothelial and smooth muscle cells. Function is determined by cellular location.

PDE	Vascular location	Role of PDEs	Inhibition of PDEs	Ref
PDE1	Vascular smooth muscle cells	Lowers cGMP/cAMP to allow smooth muscle cell proliferation to occur	Inhibition results in reduction in DNA synthesis in smooth muscle cells	Rybalkin <i>et al.</i> , 2003
PDE2	Endothelial cells (HUVECs)	VEGF up-regulated PDE2 expression to increase cAMP hydrolysis  Regulatory effect on angiogenesis	Inhibitors prevented VEGF induced endothelial cell cycle progression	Favot <i>et al.</i> , 2004
PDE3	Vascular smooth muscle cells (Rat aorta)	Novel mediator of inflammation in vascular smooth muscle cells	Inhibition of PDE3 mediated the inhibitory effect of NO/cGMP in VSMC inflammatory responses.	Aizawa <i>et al.</i> 2003
PDE4	Vascular smooth muscle cells (Rat aorta)	Regulates cAMP mediated inhibition of vascular smooth muscle cells migration	PDE4 inhibitors increased effect of cAMP to reduce vascular smooth muscle cell migration	Palmer <i>et al</i> 1998
PDE5	Vascular smooth muscle cells	Respond to high levels of cGMP, activated by nitric oxide	PDE5 inhibitors are widely used as a vasodilator	Rybalkin <i>et al.</i> , 2003

## **1.16 Phosphodiesterase 10A**

Phosphodiesterase 10A (PDE10A) is cyclic nucleotide PDE which hydrolytically degrades dual substrates, both cAMP and cGMP (Lugnier., 2006). PDE10A protein expression has previously been investigated using immunohistochemistry in a variety of tissues taken from mouse, rat, dog, cynomolgus and human using an antibody against rat PDE10A (Coskran *et al.*, 2006). Coskran *et al.*, (2006) observed PDE10A to be strongly expressed in the brain in all of these mammals, in particular the striatum and substantia nigra. PDE10A expression was also found peripherally, including the heart and aorta but not in smooth muscle. Depending on the tissue, PDE10A protein could be detected in the cytoplasm or the nucleus of cells (Coskran *et al.*, 2006).

### **1.16.1 PDE10A function**

PDE10A has been widely studied in the brain and has been shown to contribute to neuronal function (Hebb *et al.*, 2004, Rodefer *et al.*, 2005, Nishi *et al.*, 2008). Anxiety, Huntington's disease and schizophrenia have all been related to PDE10A function (Hebb *et al.*, 2004, Rodefer *et al.*, 2005, Siuciak *et al.*, 2006a). In mice with Huntington's disease, treatment with the PDE10A inhibitor papaverine hydrochloride has suggested that PDE10A is a possible therapeutic target for improving the symptoms of schizophrenia, and to improve cognitive, motor and psychological function (Hebb *et al.*, 2004, Rodefer *et al.*, 2005). However, the role of PDE10A in brain function remains unclear.

During the course of my work, PDE10A was shown to play a role in pulmonary vascular remodelling in rats (Tian *et al.*, 2011). Pulmonary vessels that remodel due to proliferation of vascular smooth muscle cells, endothelial cells and fibroblasts, cause increased vascular resistance leading to pulmonary hypertension. Pulmonary hypertension can be induced in rats by injection of monocrotaline. PDE10A mRNA and protein levels were found to be upregulated in the nuclei of remodelling pulmonary vascular smooth muscle cells in

monocrotaline injected rats. When these rats were infused with the PDE10A inhibitor, papaverine hydrochloride for 14 days, this reduced proliferation and remodeling of vascular smooth muscle cells. Increased cAMP levels were measured in cultured pulmonary arterial smooth muscle cells and cAMP response binding protein (CREB transcription factor) phosphorylation levels were also found to be increased in these cells, in the presence of papaverine. Similarly to PDE10A inhibition with papaverine, siRNA knock down of PDE10A RNA reduced pulmonary artery proliferation and remodelling (Tian *et al.*, 2011).

### **1.16.2 PDE10A mechanism of action**

The anti-proliferative effect of PDE10A inhibition has been suggested to be due to PDEs counteracting pathways involved in smooth muscle cell proliferation by blocking cyclins and increasing anti-proliferative molecules (Hayashi *et al.*, 2000). Further evidence suggests that cAMP/PKA binding may block cell cycle progression by phosphorylating transcription factor CREB (Klemm *et al.*, 2001). One hypothesis is that as PDE10A can be found in different subcellular compartments (nucleus or cytoplasm) the effect of cAMP hydrolysis in different cellular locations will cause different effects (Zippin *et al.*, 2003). For example, PDE10A expression/inhibition in the nucleus may regulate cell proliferation by controlling cAMP/PKA levels and therefore CREB phosphorylation. It is likely that PDE10A expression/inhibition could induce a different effect if expressed elsewhere in the cell. PDE10A mechanism of action remains largely unknown and more work is required to further characterise the function of this enzyme in different cellular processes. The role of PDE10A in the endothelium has not previously been investigated.

### **1.17 Thesis aims**

Considering the clinical implications, research to understand arteriogenesis is extremely important. The chicken embryo appears to provide a good model system in which to investigate collateral vessel formation (discussed in section 1.14). I therefore set out to

characterise collateral vessel development in the chick embryos and identify genes involved in this process. Below I list the objectives for each of the three results chapters that follow.

### **Chapter 3**

Perform a longitudinal quantification of developing collateral/collateral number following unilateral vitelline artery ligation

Perform a longitudinal quantification of developing collateral/collateral diameter following unilateral vitelline artery ligation

Establish a system to assess blood flow in the vitelline vessels after unilateral vitelline artery ligation

Examine expression of various markers in developing collateral vessels histologically/histochemically

Examine proliferation in developing collateral vessels after unilateral vitelline artery ligation

### **Chapter 4**

Characterise transcriptional changes during different phases of flow-induced vessel remodelling

Identify candidate genes which may contribute to collateral development

### **Chapter 5**

To determine the temporal and spatial expression of PDE10A protein in the extra-embryonic vitelline vasculature during flow-induced remodelling

To establish the effect of pharmacological inhibition of PDE10A on flow-induced remodelling

To examine mechanisms whereby PDE10A may influence flow-induced remodelling

## Chapter 2

### Materials and methods

#### Materials

#### Equipment

Materials used	Purchased from
Forceps (#4, #5)	World Precision Instruments
25G/18G needle	Microlance
Plastic syringes (various sizes)	Plastipak, Sigma Aldrich
Suture	8/0 Prolene, Ethicon, Johnson & Johnson
Glass coverslip	Fisher scientific
Superfrost slides	Fisher Scientific
Spatula (5x7mm)	World Precision Instruments
Iris scissors	World Precision Instruments
Eppendorfs	Eppendorf UK
Filter	0.2um Filtopur
Filtertips/pipette tips	StarLabs
Pipettes	StarLabs
Pasteur pipettes	StarLabs
Filter paper	Whatman #1, Sigma Aldrich
Parafilm	Sigma Aldrich
Nitrocellulose membrane	Amersham, hyperbondC, Fisher Scientific
6-well plate (34mm diameter)	Sigma Aldrich
384-well plate	Anachem
Incubator	Sanyo
Waterbath	

Upright epi-fluorescent combi-microscope	Leica M216FA
Sensi-cam QE camera	PCO
Light emitting diode	LA GmbH
LaVision Davis 8.0	DaVis
Nanodrop	ND-1000, Labtech
Vortex	Cifton cyclone, MSE Sanyo
Microarray	Affymetrix chicken gene chip
QRTPCR	Rotor 6000, Corbett life science
Aspirator	Vacusafe, Integra
Orbital shaker	PSU 100, Grant instruments
Gel doc	Geni 2, Fisher Scientific
Ultra Centrifuge	Avanti J-25 Beckman Coulter Inc
Microtome	Leica RM2155, Leica 819 blade
Cryostat	Bright OFT
Spectrophotomer	Jenway
Apotome	Zeiss Imager Z1, AxioCam MRM 1.0X
Camera	Nikon Coolpix 5400
Stereomicroscope	Nikon SM21500
Spot cam	SPOT insight Colour 1.0X
Image J	National institute of health
Lightsource	Schott KL2500

### **Kits/reagents**

Reagent used	Purchased from
cDNA synthesis	Verso, Thermo scientific
ExoSAP IT	Affymetrix
Maxi prep	Quiagen
Ethanol/Methanol	Fisher Scientific

NaCl/KCL/CaCl <sub>2</sub>	SigmaAldrich
Isopropanol	Fisher Scientific
Super Optimal Broth (SOC)	Invitrogen
Luria Bertani (LB) broth	Sigma Aldrich
Luria Bertani (LB) agar	Sigma Aldrich
Ampicillin	Sigma Aldrich
Xylene	Fisher Scientific
Corazzi's Haemotoxylin	Gills #1, Sigma Aldrich
Eosin Y	Sigma Aldrich
Formamide	Fisher Scientific
NuPAGE 10X running/transefer buffer	NuPAGE, Novex
NuPAGE bis-tris pre-cast polyacrylamide gel	NuPAGE, Novex
NuPAGE antioxidant	NuPAGE, Novex
NuPAGE Reducing agent	NuPAGE, Novex
Tween	Sigma Aldrich
Triton X-100	Sigma Aldrich
Chaps	Sigma Aldrich
Papaverine hydrochloride	Sigma Aldrich
Dispase	Boehringer Mannheim
Sodium bicarbonate	Sigma Aldrich
DMEM	Sigma Aldrich
Paraformaldehyde	Sigma Aldrich
Sucrose	Sigma Aldrich
Chemiluminescence	Amersham, Fisher Scientific
Enzyme endonucleases	New England Biolabs
RNA polymerases	Promega
DNA buffer	Promega

DNase	Invitrogen
Nitro blue tetrazolium (NBT)	Roche
BCIP	Roche
Protease inhibitor	Roche
Lysis buffer	Qiagen
4',6-diamidino-2-phenylindole (DAPI) stain	Invitrogen
Heat Inactivated Goat Serum (HINGS)	Sigma Aldrich
Agarose	Invitrogen
SYBR green sensimix plus	Quantace
Primers	Sigma Aldrich
Phosphate buffered saline (PBS) 1X	Roche
Ethidium bromide	Life technologies
Hyperladder	Bioline
Loading buffer	Bioline
TRI reagent	Sigma Aldrich
Chloroform	Sigma Aldrich
Collagen (rat)	Sigma Aldrich
Vectorshield (with DAPI stain)	Vectorlabs
Glycergel mounting medium	Dako
OCT mounting media	VWR
Leibovitz-L15 media	Sigma Aldrich
BioRad protein assay	BioRad
Alpha competent cells	Invitrogen

### Antibodies

Antibody used	Concentration used	Purchased from
Rabbit polyclonal antibody to PDE10A	1:250	GeneTex

Rabbit polyclonal antibody to VE-cadherin	1:100	Abcam
Alexa Fluor 488/594 goat anti-rabbit IgG	1:500	Abcam
Rat monoclonal antibody to Bromodeoxyuridine	1:1000	Abcam
Alexa Fluor 488 donkey anti-rat IgG	1:500	Abcam

## 2.1 General chick embryo methods

### 2.1.1 Storage and incubation

Fertile White Leghorn (*Gallus gallus*) chicken eggs were purchased fresh from Henry Stuart & Co. Ltd, Louth, Lincolnshire. On delivery, eggs were stored blunt-end-up, in a controlled environment room at 18°C for up to five days before incubation. Eggs were incubated at 37°C in a humidified environment, for 60 to 68 hours prior to experimentation. For post-operative survival, opened eggs were sealed to avoid dehydration. Experiments extended no further than 48 hours following experimental manipulation.

### 2.1.2 Developmental stages of the chicken embryo

In 1951 Viktor Hamburger and Howard Hamilton developed a staging guide for embryologists using the chicken embryo as a model of development (Hamburger and Hamilton., 1951). The age of the chick is thus described in terms of Hamburger and Hamilton (HH) which describes the length of incubation and identifies the stage (st) of the embryo; at the stages used here, somite number and limb bud development provide highly accurate reference points. The guide itself provides a rigorously documented description of the embryo at each stage, followed by a series of images corresponding to each stage. I used embryos at HH st 17. At this stage the chick embryo has developed extra-embryonic blood vessels which connect the embryo proper to the yolk sac. The heart begins beating at

HH st 9 but circulation is not fully functional until HH st 15. Therefore at HH st 17 the extra-embryonic vessels are sufficiently mature and perfused.

### **2.1.3 Windowing the egg**

Eggs were positioned in a holder made of Styrofoam plastic to prevent movement. The blunt end was wiped with 70% ethanol to avoid infection. Instruments were sterilised with 70% ethanol. Blunt forceps (#4) were used to create a crack in the shell, into the air cell above the embryo. A small window was created by removing shell and first opaque membrane, with the forceps. Insertion of an 18G needle fitted with a 10ml syringe three-quarters of a way down the egg, removed 3-5ml albumin. This allowed the embryo to drop away from the window to avoid any harm or shearing of the embryo or extra-embryonic vessels. Further dissection of the overlying vitelline membrane with forceps (#5) revealed the embryo positioned on the yolk sac. To re-seal eggs after opening, sellotape or parafilm were used.

### **2.1.4 Embryo staging and inclusion criteria**

Incubation duration of 66-68 hours developed the chick embryo to HH st 17 (Hamburger and Hamilton, 1951). Morphological inclusion criteria were implemented to standardise the experimental model due to variation between embryos in a batch. Embryos were required to have circulation in the yolk sac vasculature (blood flow through right and left vitelline arteries, with venous return through single anterior and posterior veins). The vitelline veins were used as markers of the midline (the boundary between the left and right vitelline artery perfusion territories). The vitelline arteries needed to be of an adequate size (diameter of approximately 200-250 $\mu$ m) to allow successful ligation.

## **2.2 Arterial ligation**

Microsurgical ligation was performed on the right vitelline artery using straight-tipped forceps, surgical spring scissor and a length of suture (8-0 sized prolene suture). Ligations

were created before the first bifurcation of the artery, most proximal to the embryo. A windowed egg was placed under a stereo-microscope with an overhead light source. A magnified view of the embryo allowed the suture needle to be guided under the artery and tied. The knot was pulled tight, taking care not to tear the blood vessel. Excess suture length was cut off (example shown in Figure 2.1). Control (sham-ligated) embryos underwent the same procedure as tied-ligated embryos however the suture was left untied beneath the right vitelline artery in a manner that did not interrupt blood flow. In the results chapters for clarity I refer to embryos where the suture was tied off to induce vessel occlusion as “tied-ligation” and embryos where the suture was left untied as “sham-ligation”.

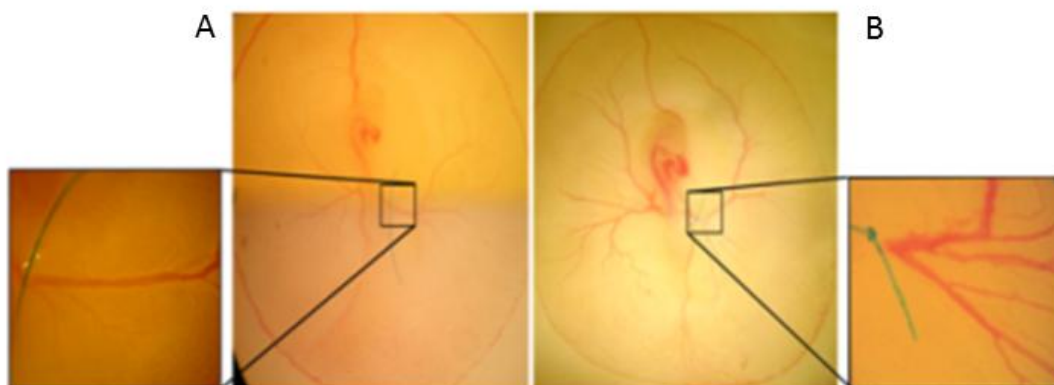


**Figure 2.1. Micrograph images of a sham ligation and a tied ligation**

Low power and high power views of examples of chicks after sham (A) or tied (B) ligation. The black box around the right vitelline vessel indicates the location of the suture, shown at higher magnification. **A** shows the suture beneath the vessel. The suture is left un-tied to leave blood flow un-disturbed. Sham ligations do not occlude flow. **B** shows a knot around the vessel. Blood appears darker in image B due to stagnant blood distal to the occlusion.

## **2.3 Particle Image Velocimetry**

Particle Image Velocimetry (PIV) was performed in the lab of Dr Christian Poelma (University of Technology, Delft). Protocols for imaging were carried out in line with the protocol of the Poelma lab (described in 2.3.2). PIV measurements were performed at the anterior and posterior poles of the embryo, to record flow within developing collateral vessels. I acquired data from collateral vessels at 4 hours post tied-ligation and followed these collaterals to a later stage (7 hours post tied-ligation). I had hoped to obtain data up to 24 hours, but embryos died before reaching this stage (discussed in Chapter 3). Unfortunately due to the limited length of time that I was visiting the Poelma lab I was unable to optimise this to improve survival. I therefore recorded a separate group of embryos which had been ligated for 24 hours to assess the velocity of blood flow in mature collateral vessels.

### **2.3.1 Preparation of the embryo for imaging**

To elevate the embryo within the egg, and prevent dehydration during imaging, drops of Locke's solution (0.94% NaCl, 0.0045% KCl, 0.004% CaCl<sub>2</sub>) were added. A small circular glass coverslip was then placed over the surface of the vitelline membrane, creating a seal around the edge of the windowed shell. This kept the embryo hydrated and prevented movement but also ensured completely flat 2D imaging – important for data acquisition. The eggs were then placed in a water bath (38°C) which allowed constant and prolonged recordings of up to 20 minutes without observing a reduction in chick heart rate. After imaging eggs were removed from the water bath, 1-2ml albumin extracted using a 18G needle and 1ml syringe, in order to reseal the window, and then returned to the incubator.

### **2.3.2 PIV Recordings**

Eggs were placed under an upright epifluorescent combi-microscope with zoom (Leica MZ 16 FA). Magnifications of 5x and 10x were achieved with a Leica FluoCombi III objective. A

PCO Sensicam QEcamera (1376 x 1040 pixels) was used for recordings with binning to improve signal-noise ratio. A high-powered pulsed light emitting diode (LED) was used to illuminate and capture images (pulse-rate=200us). Pulsed light is used in order to acquire consecutive images milliseconds after each other. This is necessary because the interval between light pulses needs to be sufficient to capture the largest displacements in the selected area of measurement. For all measurements 1000 images were recorded for each vessel at 5x and 10x magnifications, 5000 $\mu$ s time delay between frames. When embryos required a ligation during the recording process this was done whilst the embryo remained in the water bath. Figure 2.2 shows the equipment set-up used for PIV experiments.

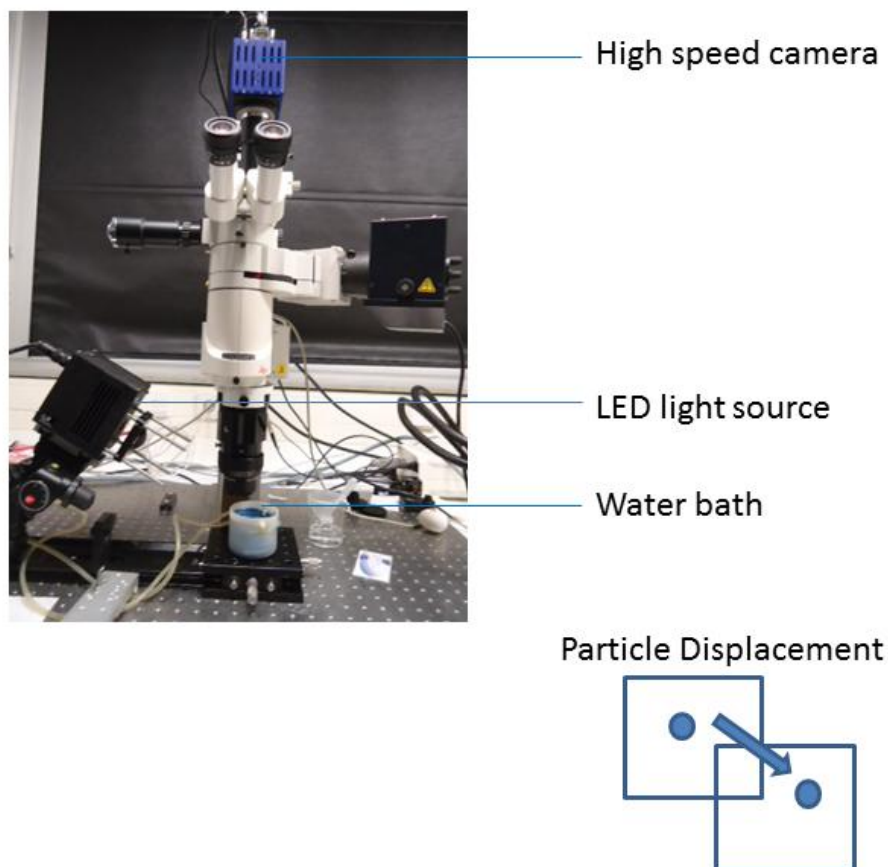


**Figure 2.2 Particle Image Velocimetry apparatus**

Embryos were imaged in ovo. Eggs were kept warm in a water bath maintained at 38°C. Recordings were made using a pulsing light source and high speed camera. From one frame to the next the particle (red blood cell) is tracked and recorded and the particle displacement is then calculated to measure the velocity of blood flow.

### 2.3.3 Time-averaged velocity fields

PIV quantifies blood flow within blood vessels by using red blood cells as tracers (Poelma, 2012). Individual red blood cells can be followed by taking a series of images with a high-speed camera. From this, the distance individual red blood cells travel between two frames can be calculated - this is known as the particle displacement (Lee *et al.*, 2007, Poelma *et al.*, 2012). The area of measurement in an image can be sub-divided into smaller windows of view, known as interrogation windows. The displacement of a red blood cell from one window to the next, over these consecutive measurements, can then be statistically analysed using a cross-correlation algorithm. The local velocity of the blood flow can be calculated by dividing the displacement of the red blood cell by the time difference between the two frames (interrogation windows) (Vennemann *et al.*, 2006).

For large collateral vessels the velocity of the flow was slow enough to record with a single frame. However in most cases the blood velocity (and therefore pixel displacement) was slightly faster than anticipated and required a double frame recording. Images were therefore recorded in pairs. The time difference ( $\Delta t$ ) between frames was specified to ensure pixel displacement did not exceed 10-15 pixels during a cardiac cycle. For double frame recordings we used  $500\mu s$   $\Delta t$ . Displacement is calculated from one frame to the next by cross-correlation. Each correlation of a single pair of interrogation windows leads to a single displacement vector. Overlap of interrogation windows can be specified which then determines the size of the grid of computed velocity vectors. Multi-pass PIV evaluation uses vectors in the first image as a reference for the vector field of the second image. This shifts the interrogation window accordingly to determine the particle image shift and correlate the correct particles. Finally, vectors are combined to get a complete 2D vector field of the vessel of interest.

LaVision DaVis 8.0 software was used to correlate images and further processed the recordings to acquire time averaged blood velocity field profiles for each vessel. PIV analysis was performed using version 7.2.

The processing of each image involved: shift correcting for any movement of the embryo during recording; calculating an average for this shift corrected image; subtracting the averaged image from shift corrected image; calibrating the image to display velocity as  $\mu\text{m/s}$ ; calculating the vector field of the calculated 'difference'; cross correlating this result (constant multi-pass; 50% overlap of consecutive images (interrogation windows); 32x32 pixels, interrogation window size).

Image J was used to measure the diameters of the vessels in Figure 3.7 by calibrating the scale of the image and using the line tool to measure the length of the line drawn across the diameter of the vessel (section 2.24).

For vessels recorded at 24 hours LaVision processing software also produced parabolic curves from the data which showed blood velocity was highest at the centre of the vessel and these can be found in the Appendix (Figure A3).

## **2.4 Microarray methods**

I performed all surgical procedures, tissue sampling and RNA extraction. Sample labelling, array hybridisation and scanning of the array was performed by Dr Paul Heath of the University of Sheffield Microarray Core Facility. The raw .CEL data files were analysed by my bioinformatician colleague Dr Marta Milo to generate fold-change data and the probability of a positive log ratio (PPLR) for each gene (section 2.6.1). I performed all further analysis.

### **2.4.1 Tissue excision**

Embryos were prepared with either a sham or tied-ligation (Figure 2.1). For microarray analysis of gene expression, tissue was excised from the area of collateral vessel growth at

T0, 4 hours and 12 hours post tied-ligation. Control samples were collected at the same timepoints after sham-ligation. A sterilised spatula with angled tip (5x7mm) and Iris scissors (~2cm straight blade) were used. A vertical incision was made from the sinus terminalis up to the tail of the embryo, along the midline. The spatula tip was slid under the yolk sac membrane, to the left of the first incision. Scissors were then used to cut around the tip of the spatula, leaving a rectangular area of the membrane. Figure 2.3 shows the area dissected for microarray.

#### **2.4.2 RNA extraction**

For microarray analysis, three replicates were used per timepoint and each replicate contained pooled RNA from three embryos. RNA was pooled to provide sufficient RNA and to reduce variability while three replicates were performed to assess array variability and to allow statistical comparison.

Dissected tissue was placed in a 1.5ml Eppendorf containing 200µl TRI reagent for immediate RNA extraction. The tissue was homogenised through a 25G needle and 1ml syringe five times. Excised tissue was pooled from three embryos for each time point. This was because 1 individual embryo did not provide enough tissue for analysis but also, use of pooled embryos reduces the influence of variability between individual embryos. When all tissue samples had been collected and homogenised the Trizol method of RNA extraction was used as it provides a greater and more accurate RNA yield than commercially available column assays (Nolan *et al.*, 2006). All pipette tips were single use sterile filter pipette tips and sterile conditions were maintained during the experiment. 300µl of TRI reagent was first added to the tissue sample. The solution was mixed, and 100µl of chloroform added. The solution was mixed using a vortex and centrifuged at 13,000rpm for 15 minutes at 4°C. Centrifugation and aqueous solutions separated out RNA and removed protein. The colourless upper aqueous phase was transferred to a new RNase-free Eppendorf and 250µl

isopropanol was added. The solution was mixed and centrifuged at 13,000rpm for 20 minutes at 4°C. A pellet was identified at the bottom of the solution. The solution was removed without disturbing the pellet. 0.5ml 75% ethanol was added and the Eppendorf vortexed to free the pellet from the side. The Eppendorf was centrifuged at 8,000rpm for 15 minutes at 4°C. All ethanol was removed and the pellet re-suspended in 15µl RNase-free water. Volumes were measured and dispensed using laboratory pipettes.

## **2.5 Spectrophotometry**

The quality and quantity of RNA samples was quantified using a NanoDrop spectrophotometer (ND-1000, Labtech). Spectrophotometers measure absorbance of light through a sample to calculate the concentration of RNA based on the optical density. 2µl of each RNA sample was tested. Purity of RNA was assessed by the ratio of absorbance at 260nm and 280nm.

## **2.6 Affymetrix microarray**

An Affymetrix chicken gene chip was used which assessed expression of 32,773 transcripts. Affymetrix chips are a synthesised oligonucleotide array which claim high sensitivity, specificity, standardisation and reproducibility (Jayapal and Melendez, 2006). Affymetrix microarray protocols involve RNA extraction and single labelling and hybridisation of each sample to a different chip. Hybridisation occurs between sequence-specific binding of target sequences and probe sequences. Fluorescent labelling enables detection of probe bound transcripts. The intensity of the fluorescence relates to the amount of bound probe and in turn acts as a measure of the target RNA sequence (Liu *et al.*, 2005). Affymetrix system uses a 'perfect match/mismatch' hybridisation (Liu *et al.*, 2005). A perfect match probe is complimentary to the target sequence. The mismatch probe acts as a control for hybridisation specificity: 1 base is mismatched in an otherwise complimentary sequence (Lee., 2004). Standardised methods of reporting microarray studies are available for the

scientific community on databases such as MIAME (The Minimum Information About a Microarray Experiment) (Jayapal and Melendez, 2006).

Microarrays were performed on the 3 best quality RNA samples (determined by purity and concentration from spectrophotometry) for each timepoint; pre-ligation, 4 hours post tied-ligation, 12 hours post tied-ligation, 4 hours and 12 hours after sham-ligation (Figure 2.3) and selected from a total of 5 samples at each timepoint. Microarrays were performed using Affymetrix GeneChip arrays (Affymetrix) by Paul Heath (University of Sheffield Microarray Core Facility) at the Royal Hallamshire Hospital, Sheffield.

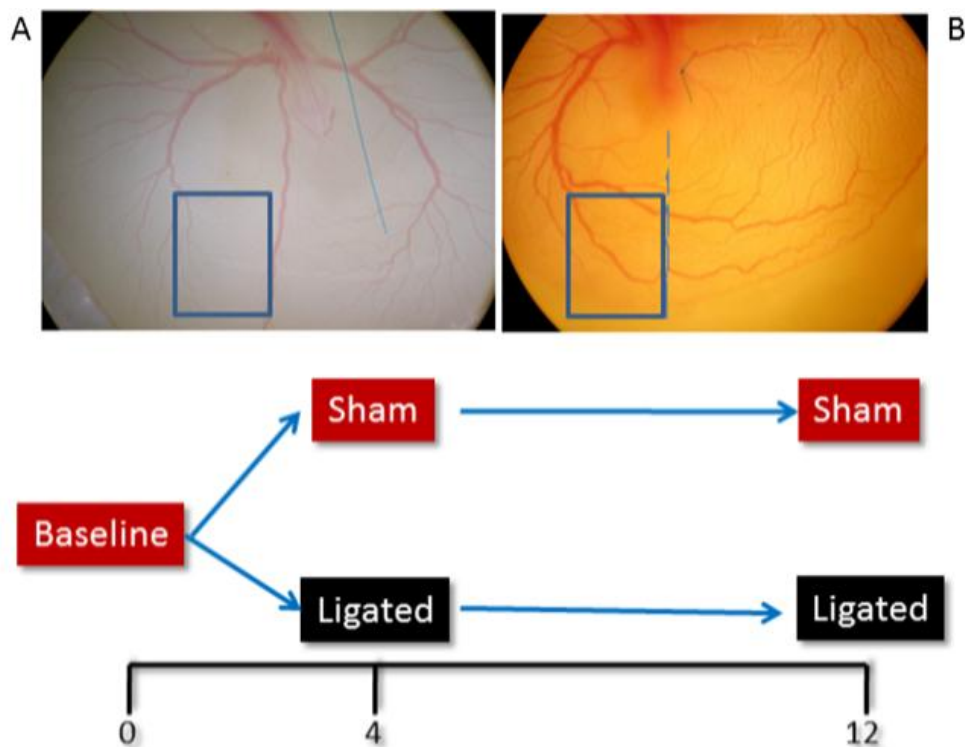


**Figure 2.3. Microarray RNA extraction was performed at 3 timepoints in sham and tied-ligated embryos**

Tissue was excised from the posterior midline area in sham and ligated embryos (indicated by the blue box; midline indicated by dashed line). Dissections of uniform sizes of tissue were performed at T0, 4h and 12h post-ligation or post-sham in HH st 17 embryos.

### 2.6.1 Microarray data analysis

Raw microarray data files (.CEL files) were analysed to generate levels of gene expression.

This is based on an algorithm which compares the difference in signal between perfect

match and mismatch hybridised probes (Milo *et al.*, 2003). The signal intensity and quality of the average difference is then also calculated by an algorithm. For data analysis, hypothetical genes and non-annotated genes were excluded. These refer to genes which have not yet been experimentally characterised and whose function cannot be elucidated on sequence comparisons alone (Kolker *et al.*, 2004). Cut-offs for the Probability of Positive Log Ratio (PPLR) and fold-change were used to identify the most significantly differentially expressed genes. The PPLR takes into account variations between samples and variations between chips by working out uncertainty measurements from replicate experiments to calculate standard errors and estimations of expression levels. This makes it more stringent than a P value when assigning significance to an observation (i.e. the likelihood of that observation occurring by chance) (Pearson *et al.*, 2009). A PPLR close to 1 indicates a high probability of upregulation and a PPLR close to 0 implies a high probability of down regulation. For this study transcripts were selected for further analysis based on a PPLR of  $>0.8$  or  $<0.2$ .

The microarray data was normalised to give the signal of each array the same distribution and arrays were scaled to have the same mean values. Normalisation takes into account the variation from each microarray chip to make the numbers from one chip mean the same as the numbers from another chip. Variation between signal from different arrays may come from experimental conditions or slight differences in RNA concentration for example. Reducing the variability of the signal for each individual probe set increases the likelihood of detecting true differences in differential gene expression between groups. The signal of the array was normalised over all 15 chips. Normalisation of the microarray data was performed by Dr Marta Milo, a bioinformatician. Dr Milo also performed statistical analysis on normalised microarray data for this project using open source software Propagating Uncertainty in Microarray Analysis (PUMA) (Pearson *et al.*, 2009). This method of probe level analysis extracts a level of uncertainty associated with each probe set to

estimate gene expression with a credibility interval (similar to a confidence interval) (Milo *et al.*, 2003). This model has been shown to be more effective than traditional statistical models as it increases reproducibility of fold-change observed, by more accurately identifying differential gene expression (Milo *et al.*, 2003).

To calculate the significance of changes in expression ratios the following formula was used:  $E_g = T_g/C_g$ , where  $g$  represents gene,  $T$  is the test sample and  $C$  is the control sample. When the level of  $g$  is the same in both the test and control samples the ratio equals 1. If  $g$  is upregulated in the test sample the ratio will be greater than 1. If  $g$  is downregulated the ratio will be between 1 and 0. Fold change is then calculated by multiplying the reciprocal of the downregulated gene by -1. In order to identify differentially expressed genes in my microarray data I decided to use a cut off of a fold change of greater than 1.5 or -1.5.

The key comparison was between the sham and tied-ligated groups at each timepoint. For comparisons between 4 hours sham and tied-ligated, and 12 hours sham-ligated and tied-ligated, I clustered expression of these genes by their **relative change from baseline**. Normalisation for baseline expression allowed assessment of changes over time in each group as well as assessment of differential expression between sham and tied-ligated tissue.

TreeView analysis was by software designed by Michael Eisen (Stanford University). Data was uploaded into the programme and was automatically clustered hierarchically. Cluster currently performs three types of binary, agglomerative, hierarchical clustering. The basic principle of TreeView is to assemble a set of items (genes or arrays) into a tree, where items are joined by very short branches if they are very similar to each other, and by increasingly longer branches as their similarity decreases (Eisen *et al.*, 1998).

## 2.7 Gene ontology tools

Gene ontology Protein ANalysis THrough Evolutionary Relationships (PANTHER) can be used as a tool to predict the pathways and processes of genes in microarray data. Differentially expressed genes were compared to a reference list and sorted into biological processes. The results give an estimation of the number of genes observed in the process (from the microarray data) and the number of genes expected to be in the process (from the reference list). A fold change representation was calculated by dividing the number of genes observed by the number of genes expected in the reference list (fractional difference). A positive fractional difference implies an overrepresentation of a gene in the process. PANTHER analysis also assigns a P value to the genes in the list. A p value <0.05 was considered statistically significant. PANTHER analysis of biological pathways and cellular components can be found in the Appendix (Figure A6, A7).

## 2.8 Quantitative real-time PCR

### 2.8.1 Primer stocks

Ensembl was used to detect cDNA sequences for the candidate genes (<http://www.ensembl.org/>). Primers were then selected from sequences ~250 base pairs long using Primer3Plus (<http://www.bioinformatics.nl>). The primer size parameters were based on the optimum number of base pairs for successful DNA binding. The melting temperature (TM) was based on the optimum range of temperature for annealing. This is important as GC bases share triple hydrogen bonds instead of normal double hydrogen bonds, therefore more heat is required to break the bonds (Nolan *et al.*, 2006). The primer GC% relates to the number of GC base repeats in the primer sequence; more GC bases in a sequence results in less successful DNA amplification (Nolan *et al.*, 2006).

The parameters used were as follows;

Primer Size = minimum 18 base pairs long ; maximum 24 base pairs long

Primer TM = minimum annealing temperature 58°C ; maximum temperature 60°C

Primer GC% = minimum GC content 50% ; maximum GC content 60%

Candidate genes to validate by QRT-PCR were selected based on fold change, and a list of specific genes as described in Chapter 4. Housekeeping genes were essential to use as a reference gene to compare expression fold changes. Housekeeping genes were selected from the microarray data and were picked based on a constant expression level across all timepoints and experimental conditions.

**Table 2.1 Primers used for QRT-PCR. Primer pairs selected for use are described for each gene in the table above.**

Forward and reverse sequences are shown. Those in red highlight the primer sets that had to be designed numerous times (MMP9 re-designed on 3 occasions, CC2D1B re-designed on 3 occasions, IRX4 re-designed on 4 occasions).

Gene name	Primer	Sequence
Prostate stem cell antigen	PSCA (forward)	CTTCAGCATCATCAGCAAGG
	PSCA (reverse)	GGTCATGGGAGCTCTGTTTC
Stanniocalcin 2	STC2 (forward)	AGCTGCATCAGCCGTAAGT
	STC2 (reverse)	CATCTCCACAATGACCTGGA
A Disintegrin And Metalloproteinase with Thrombospondin Motif(ADAMTS)-like 1	ADAMTSL1 (forward)	CATCTGTGGTGTGCACTGG
	ADAMTSL1 (reverse)	AGGCTTGTTGGTACGGATGT
Phosphodiesterase 10A	PDE10A (forward)	AGCCATCCCATGTTACACC
	PDE10A (reverse)	TTCCAGGAGCAACGGACT
FAT tumour suppressor homolog 4	FAT4 (forward)	CCAAGCATTACGCCTGTATC
	FAT4 (reverse)	TTGGGTTGACACCTGTTCTG
Matrix metalloproteinase	MMP9(forward)	CGTGATAGATGATGCCTTCC
	MMP9 (reverse)	CTAAGCCGGTCCAGAGT
Iroquois homeobox 4	IRX4 (forward)	CTGAAGACGTGGCTGTACGA

	IRX4 (reverse)	TTGGGAGACCAGGTCATCTT
Coil-coilC2domain containing 1B	CC2D1B (forward)	GCGGTACAGGGAGCAATCT
	CC2D1B (reverse)	CTCTTCTGGAAGGCAGCATC
RPL4(housekeeping gene)	RPL4 (forward)	TGAACAAGCTGAACCTGCTG
	RPL4 (reverse)	TGGATCTCCTGGCTTCTCAG
U1 (housekeeping gene)	U1 (forward)	GTGTGACTGGTGGCATGAAG
	U1 (reverse)	CCCGGAGTCTTGGTCCTATT

Filtered lab water (MilliQ) was used to dissolve primers to a concentration of 100µM. From this a working stock of 10µM was made for heat gradient PCR tests. For all other QRT-PCR runs, 5µM concentrations were used. Table 2.1 shows a list of the primers used, obtained from Primer 3 Plus based on the parameters above. Primers were tested with cDNA synthesised from chick embryo RNA collected as described above (Section 2.4) using the Thermo scientific verso cDNA synthesis kit. A justification of the primers selected for analysis can be found in Chapter 4.

### 2.8.2 Heat Gradient PCR

A gradient PCR of varying temperatures was performed on each primer pair using chick embryo cDNA. This was to test for an optimum temperature at which the primer binds to the product without primer dimers or extra product. Each row of the machine corresponded to a set temperature along the gradient. A master-mix was calculated for the required number of tubes using the following measurements:

#### Gradient PCR master-mix solution

2x Biomix	10µl
reverse primer	2µl OF 10µM
forward primer	2µl OF 10µM
cDNA	1µl

Nuclease free Water      5 $\mu$ l

20 $\mu$ l was pipetted into small PCR tubes and run on a gradient PCR machine with heated lid on the following program: 96 well plate; [gradient] HS5 grad with heated lid: 3 minutes at 95°C , 40 cycles at 75°C for 30 seconds (primer binding), range of temperatures (50-65°C ) 30 seconds (to find optimal annealing temperature), 72°C extension step for 1min (amplification of DNA product), 40 cycles at 72°C for 5 minutes.

The lowest temperature tested was 50°C , highest 65°C . At the end of the programme, 1-2 $\mu$ l of product was run on an Agarose gel as described (section 2.12) and run at 150v for 15mins. Optimal temperatures for further QRTPCR were selected based on bright bands with no primer dimers and no extra product.

### **2.8.3 Primer Concentration Optimisation for QRTPCR**

A range of forward and reverse primer concentration (nM) combinations were tested with standardised cDNA: 50/50, 100/100, 150/150, 150/300, 300/150, 300/300, 300/600, 600/300, 600/600, 900/600, 600/900, 900/900 (i.e. 50nM forward primer/50nM reverse primer)

Master-mixes were made up to the required primer concentration for the combination tested. Each volume was calculated for 3 replicates (x3.5) strip tubes. Sensimix plus SYBR kit was purchased from Quantace. SYBR green allows detection of PCR products as it fluoresces when it binds to double stranded DNA. During the PCR reaction, the dye binds to each new copy of double stranded DNA (generated at the annealing/extension stage following primer binding) (<http://www.lifetechnologies.com/uk/en/home/life-science/pcr/real-time-pcr/qpcr-education/taqman-assays-vs-sybr-green-dye-for-qpcr.html>). For all QRTPCR work sterile conditions were maintained and filter tips (Starlab) used.

### **An example of a master-mix for testing primers at 50/50nM concentrations**

	Per tube( $\mu$ l)	master-mix( $\mu$ l)
SYBR (sensimix)	10	35
Forward primer	0.2	0.7
Reverse primer	0.2	0.7
MiliQ water	7.6	30.1
cDNA	1	3.5

### **2.8.4 cDNA dilution assay for standard curve analysis**

A NanoDrop was used to test cDNA yield and purity (260/280). cDNA was then serially diluted to obtain a range of concentrations as follows: dilution factors: 1,  $\frac{1}{2}$ ,  $\frac{1}{5}$ ,  $\frac{1}{10}$ ,  $\frac{1}{20}$ ,  $\frac{1}{50}$ ,  $\frac{1}{100}$ ,  $\frac{1}{200}$ ,  $\frac{1}{500}$ ,  $\frac{1}{1000}$ . cDNA was run with the selected primer concentration as decided from the primer test. 19 $\mu$ l of master-mix was run with 1 $\mu$ l cDNA (2-3 replicates) at each concentration.

### **2.8.5 ROTOR6000 Analysis**

cDNA was prepared using a Thermo Scientific kit and extracted RNA (section 2.4). 1 $\mu$ l was pipetted with 9 $\mu$ l of master-mix into strip tubes with caps on ice in triplicate. Tubes were labelled and loaded into the Rotor 6000 machine. For ROTOR6000 a 3-step program with melt was used for a total of 45 cycles; the temperature was altered to be primer specific.

To assess specific binding melt curve analysis was performed by slowly raising the temperature of the reaction and monitoring fluorescence. From a melt curve graph the melting temperature of the created product can be identified. The peak that this related to allowed me to observe if there was a clean amplification of a single product. Melt curve analysis was used to check for primer dimers (left of curve) and extra product (right of curve), one peak was deemed optimal and indicated an optimal primer concentration. If

melt curves showed extra peaks and concentration alteration did not improve the result, primer sets were re-designed to a more specific sequence.

### **2.8.6 Creating standard curves**

To measure the efficiency of my assay I ran template dilution curves in real time and from the resulting slope of the curve I was able to calculate the efficiency. A slope value of -3.3 suggested that primers were amplifying at close to 100% efficiency. If the value was more negative this suggested that primers were not amplifying efficiently at this concentration.

The efficiency calculation (E) was as followed:

$$E = \text{Gradient of the line (R}^2\text{)} / -3.3 \times 100$$

**If primers are >110% = hyper efficient                      <100%= under efficient.**

Serial dilutions were prepared using 1 $\mu$ l template cDNA and run in triplicate with a minimum of 5 dilution points. Data was extracted from cycle threshold (Ct) values. Log of concentration was plotted against ct value. Fewer Ct values indicate high gene expression as each Ct value relates to a doubling of the target product (Nolan *et al.*, 2006).

Hyper/hypo efficient primers (i.e. those that were not in the accepted range between 100%-110% efficiency) were not used, to avoid false positive/false negative results. Primers that could not be optimised were re-designed. If re-designed primers could not be optimised it was assumed the level of gene expression was too low to identify. These genes were therefore not studied further. Figure 2.4 shows a typical melt curve. Figure 2.4 also shows how the gradient is calculated from the plotted standard curves.

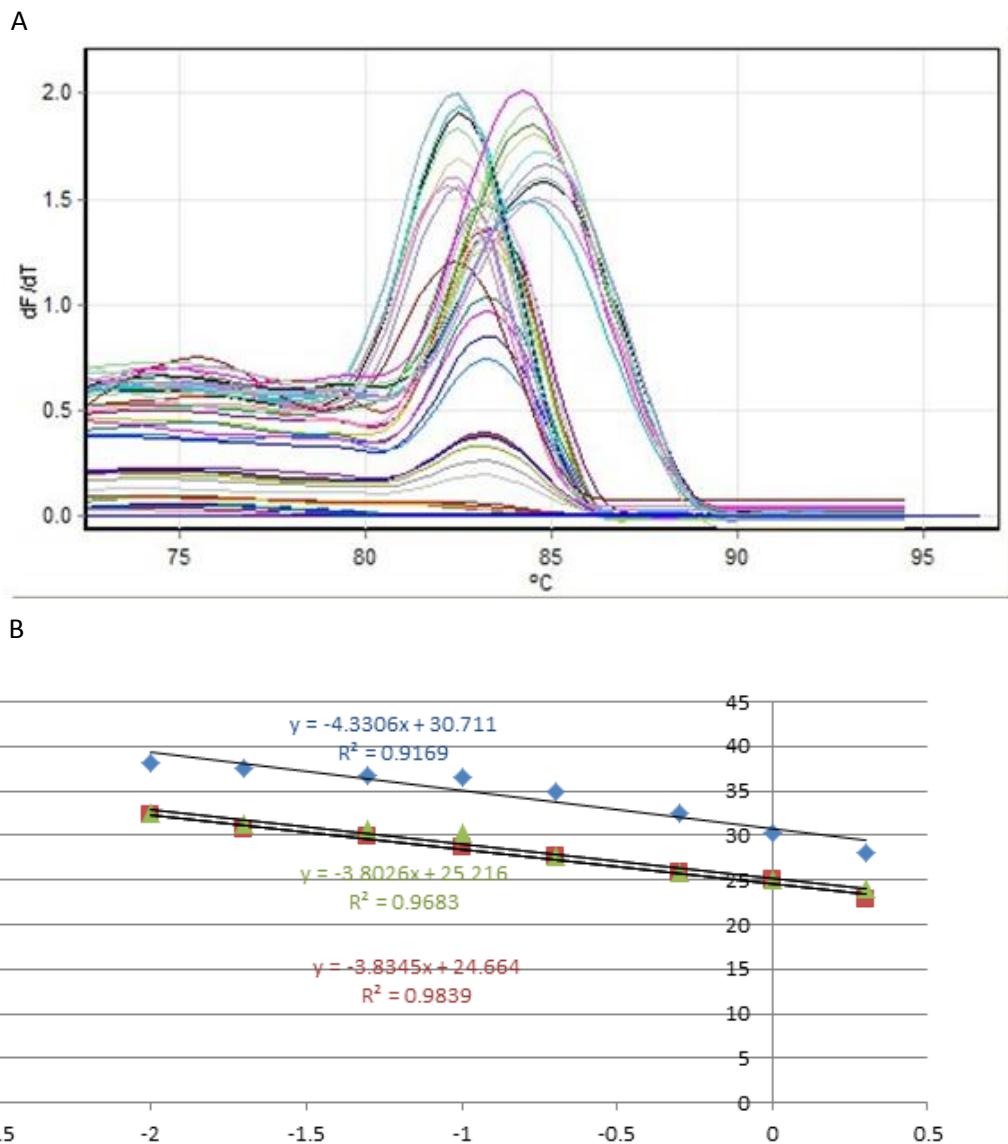


**Figure 2.4 Successful primer binding was indicated by a lack of primer dimers, appropriate cycle threshold (ct value) and primer efficiency, calculated from a standard curve**

**A** shows a representative plot from a QRT-PCR run. Each curve represents an individual sample. Samples run at a variety of concentrations/temperatures and each was run with a technical repeat. Primer dimers indicated non-specific binding and can be seen as small bumps prior to the large curve which indicates the cycle threshold at which the gene could be amplified successfully. **B** shows the plot of log of concentration against ct value for a representative sample. From the gradient of the line the efficiency of the primer can be calculated.

**Table 2.2 A table to show the optimal concentration at which to use the primer sets in order for the primers to work most efficiently.**

Primer set	Optimal concentration (μl)	Optimal temperature (°C)	Primer efficiency
ADAMTSL1	150/150	60	105%
PDE10A	150/300	60	107%
PSCA	300/300	59	110%
STC2	150/300	58	105%
RPL4	300/150	60	101%
U1	150/300	60	107%

### 2.8.7 Running QRTPCR samples

Samples were diluted with purified (milliQ) water to a constant concentration of ~200ng/μl. For each run, 3 biological samples at 3 different time-points were pipetted with 2 technical repeats for the gene of interest and the housekeeping gene. Housekeeping genes, U1 (RNA splicing) and RL4 (ribosomal protein) were selected based on their consistent expression levels to maintain cell function. These genes were not affected by experimental conditions (as observed in the microarray in sham and tied-ligated embryos at T0, 4 hours, 12 hours) and therefore could be used as reference genes.

### 2.8.8 Sample analysis

Cycle threshold (Ct) values (as a mean of the 2 technical reps) were recorded for each timepoint. A low Ct value indicated high gene expression. From this data, the relative fold change could be calculated using the delta Ct formula ( $2^{-\Delta\Delta Ct}$ ) (Nolan *et al.*, 2006). mRNA fold change greater than 1 indicated an increase in gene expression compared to the experimental control, values less than 1 were indicative of a decrease in expression.

### The delta delta ct formula:

Gi = gene of interest      G ref = reference gene

$$G_{i_{ct}} - G_{ref_{ct}} = \text{change in ct}$$

$$\text{Change in ct}_{\text{Ligated}} - \text{change in ct}_{\text{sham}} = \Delta\Delta\text{ct}$$

$$2^{-\Delta\Delta\text{ct}} = \text{Fold change relative to control}$$

(1 = no change in expression)

## 2.9 PDE10A response to changes in flow in cultured endothelial cells

Human Umbilical cord Vein Endothelial Cells (HUVECs) were collected from post-natal mothers who gave consent to donate this tissue. Ethical approval was obtained from the Multicentre Research Ethics Committee (MREC 05/Q2308/17) and the study is on the National Institute for Health Research Portfolio (ID3635). HUVEC RNA samples were prepared by Marwa Mahmoud, a colleague at the University of Sheffield (Evans laboratory).

HUVEC were isolated from 7 umbilical cord veins. The cords were cleaned with Azowipe™ tissue (70% v/v Isopropyl Alcohol) to remove blood. Using a 20ml syringe 10ml-15ml of serum-free M199 media was flushed through the veins. 10-15ml per cord of 1mg/ml collagenase from Clostridium histolyticum (sterile filtered using a 0.2µm Filtropur™ filter) was injected into the vein. The flow-through containing the extracted HUVECs in collagenase was flushed into a 50ml tube, and was centrifuged at 1200rpm (210g) for 5 minutes. The cell pellet was resuspended in 5ml of complete M199 growth medium and was seeded onto a pre-gelatinised (1% gelatin from bovine skin); the media was made up to 12ml in each flask. The cells were maintained at 37°C in M199 growth medium for 24 hrs, then rinsed in phosphate buffered saline (PBS) (warmed at 37 °C for 10 minutes), before adding fresh M199 media. The cells were then maintained in growth medium,

changed every 2-3 days. Once isolated HUVEC (passage 0) reached 80-90% confluence, they were passaged. The cells were washed with HBSS and detached by adding 1ml of pre-warmed (in 37 °C incubator) TrpLe™ Trypsin and incubation at 37 °C for 1-2 minutes then neutralised with serum and M199 media. Trypsinised cells were centrifuged at 1200rpm for 5 minutes. The pellet was resuspended in growth medium and divided accordingly into pre-gelatinised T75 flasks. For all experiments the cells were used at passage 2-4.

The 6-well orbiting plate *in vitro* method was used to expose HUVECs to physiological levels of shear stress to attempt to simulate an *in vivo* environment (Warboys *et al.*, 2010). HUVECs at 90% confluency growing in a T75 flask were seeded into 1% gelatin-coated 6-well plates at a cell density of 400,000 cells, and maintained at 37 °C for 24 hours in order to allow cells to reach confluence. The media was removed by aspiration using a Vacusafe aspirator and the cells were washed with HBSS (pre-warmed at 37 °C). 3ml of growth media was added to each well. The cells plated on the 6-well plates were placed on a PSU-10i orbital shaker for 72 hours at a speed of 210rpm (5g), which was kept in a 37 °C incubator. HUVECs at the periphery of the orbiting well of a six-well plate are subjected to non-disturbed flow, while those at the centre of the well experience disturbed flow patterns (De Luca, Warboys and Evans, unpublished). Static cells were placed in the incubator for 72 hours and experienced no changes in flow or shear forces.

Following orbiting, media was aspirated using the Vacusafe aspirator and cells washed twice with ice cold PBS. Cells were isolated from the periphery and centre of the well in PBS using the rubber end of a 1ml syringe. The cells were then added to a 15ml tube. Cell scrapes were centrifuged to a pellet at 1200rpm for 5 minutes. The pellet was resuspended in lysis buffer and homogenised by passing through a 21G needle and a 1ml syringe 5-7 times. 70% ethanol was added to the cell lysate to precipitate the nucleic acid. Total RNA was extracted using the RNeasy kit. RNA concentration and purity was assessed by nanodrop.

### 2.9.1 HUVEC QRTPCR

PDE10A expression in flow treated HUVECs was assessed by QRTPCR. 200ng RNA was converted to cDNA using the iScript cDNA synthesis kit™.

#### An example of a master-mix solution for cDNA synthesis

	Volume (µl)
5X iScript reaction mix	5
iScript reverse transcriptase	1
Nuclease free Water	variable
Template RNA(200ng)	variable
Total volume	25

Thermal profile used: 5minutes at 25°C , 42°C for 30 minutes, 85°C for 5 minutes, 4°C for 10 minutes.

For the QRTPCR 5µl of cDNA (2ng) and 15µl of QRTPCR mastermix was aliquoted in triplicate into a 384 well plate. KAPA SYBR green detection system was used.

#### Gradient PCR master-mix solution

1x KAPA SYBR FAST qPCR kit master mix	10µl
reverse primer	0.4µl of 200nM
forward primer	0.4µl of 200nM
cDNA(2ng)	5µl
Nuclease free Water	4.2µl

Thermal profile used: 3 minutes at 95°C , 95°C for 5 seconds, 60°C for 45 seconds (x40 cycles), 95°C for 5 minutes with gradual temperature increase by 0.5°C increments. Melting curves were used to assess primer specificity as before.

QRT-PCR analysis was carried out using Bio-Rad CFX manager 3.0 software. Samples were run alongside a housekeeping gene, Hypoxanthine-guanine phosphoribosyltransferase (HPRT) involved in nucleotide synthesis and PDE10A primers (sequences shown below) were used at a concentration of 5 $\mu$ M. The data was analysed using the previously described delta delta Ct formula ( $2^{-\Delta\Delta Ct}$ ) (Nolan *et al.*, 2006). The Ct value of each sample was normalised to the Ct value of a non-flow responsive housekeeper gene (delta Ct) and the relative mRNA fold change between samples was calculated using the delta comparative Ct ( $2^{-\Delta\Delta Ct}$ ) equation. The  $\Delta\Delta Ct$  was calculated by subtracting the average  $\Delta Ct$  value of sample 1 (e.g. disturbed flow/static flow sample) from sample 2 (e.g. non-disturbed flow sample) and then subtracting the average  $\Delta Ct$  value of sample 2 from itself. As before, an mRNA fold change greater than 1 indicated an increase in gene expression compared to the experimental control, values less than 1 were indicative of a decrease in expression. An un-paired t-test was used to look for statistical differences in the data. This was more stringent than a paired t-test, which could have been performed as disturbed/non-disturbed flow treated cells were from the same cord, it also accounted for the fact that HUVECs experienced different experimental conditions.

**PDE10A Primer sequences for QRT-PCR on HUVECs:**

Primer	Set 1: Amplicon Size = 127	length	TM
L1	AGCAATGCTGTCCTCACTTG	20	59.04
R1	CCCTGTGTGCCATTGATTAG	20	59.00
P1	ACGGCTTTGCAAGCCCTGCT	20	68.59
Primer	Set 2: Amplicon Size = 97	length	TM
L1	TCTCTGCTTATGTGGCCAAG	20	59.02
R1	GTCCCTGATTCCAGTCCAGT	20	58.95
P1	CATCCTTGGAGATGAACGATTTCCAA	26	68.06

## 2.10 cDNA synthesis

cDNA was synthesised using a Thermo Scientific kit.

### An example of a master-mix solution for cDNA synthesis

	Volume ( $\mu$ l)
5X cDNA buffer	4
DNTP mix	2
Random hexamer Primer (Bioline)	1
Verso enzyme mix	1
Water	variable
Template RNA( $\mu$ g/ $\mu$ l)*	1-5
Total volume	20

\*RNA volume based on NanoDrop reading (ng/ $\mu$ l)

A reverse transcription cycling program was used: 30 minutes at 42°C for 1 cycle; 2 minutes at 95°C for 1 cycle.

Exonuclease 1 and Shrimp Alkaline Phosphatase (ExoSAP) in buffer reduced unconsumed dNTPs and primers in PCR product prior to DNA sequencing. ExoSAP-IT kit and ExoSAP PCR program (45minutes at 37°C, 10 minutes at 98°C) were used to recover as much PCR product as possible and to clean-up the product for sequencing. The brightness of the product band on the Agarose gel corresponded to the amount of product (ng). For sequencing, PCR products were diluted to 10 $\mu$ l of 50ng concentration. Primers were made to 1 $\mu$ M concentration.

## 2.11 DNA Sequencing

Sequencing of purified PCR products was performed by the Core Genomic Facility (University of Sheffield), using Applied Biosystems 3730 DNA Analyser. I then analysed the chromatogram data. I then analysed the chromatogram ABI file data using FinchTV (<http://www.geospiza.com/Products/finchtv.shtml>). Wherever possible, ambiguous sites along the sequence ('N' bases) were re-annotated using the software. Data was then exported and BLAST searches were performed using Ensembl, supported by the National Centre for Biotechnology information (NCBI). This gave a probability score that the sequence was correct for the gene of interest. It also allowed alignment of the sequence to other published sources.

## 2.12 Agarose gel electrophoresis

To determine the size of DNA product, agarose gel electrophoresis was performed. In this technique, an electric current causes the negatively-charged sugar phosphate backbone of the DNA to be attracted to the positively-charged anode. DNA products are separated by size and detected using a fluorescent DNA binding dye. 1g agarose was dissolved in 100ml TAE buffer (40mM Tris, 20mM acetic acid, 1mM EDTA) using a microwave. 50ml of the solution was left to cool before adding 2 drops of the DNA binding dye, ethidium bromide (~0.5µg/µl). The solution was poured into a gel mould and a comb inserted to form loading wells for samples. Once cool and solid, the comb was removed from the set gel. 2µl hyperladder IV (0.1-1kb) was used to run alongside samples as a marker of DNA molecular weight. PCR product was added to DNA loading buffer. Gel electrophoresis was performed for 15 minutes at 150volts. Bands on the gel (corresponding to sample size) were visualised and photographed using a GENi2 gel documentation system with in-built trans-illuminator and camera.

## **2.13 Molecular biology**

### **2.13.1 Plasmid purification**

Neuropillin 1 (nrp1) and neuropillin 2 (nrp2) probes were kindly sent from Ofra Kessler of Professor Neufeld's laboratory, Israel Institute of Technology. Gene sequences of interest were ligated in bacterial DNA plasmids. These were salvaged from blotting paper by immersion and gentle mixing in TE buffer (TRIS, EDTA). To amplify the DNA plasmids and gene of interest, 2µl DNA plasmid and TE solution were added to *E.Coli* DH5 alpha competent cells (Invitrogen), which had been thawed on ice. DNA was introduced into the cells by a process of first combining plasmids and cells in an Eppendorf tube and gently mixing (so as not to shear DNA), incubating tubes on ice (30 minutes) and then inducing an increased temperature heat shock reaction by placing tubes in a water bath at 42°C for 2 minutes. Sudden increases in temperature create pores in the cell membrane of the bacteria to allow plasmids to enter the cell ([www.Jove.com](http://www.Jove.com)). Following heat shock reaction the cells were returned to ice for 2 minutes. 250µl Super Optimal broth with Carbolite repression (SOC) was added to the tubes in a sterile manner. The tubes were incubated for 1 hour at 37°C on a lab shaker (225 rpm). 50µl and 150µl of transformation mix were spread onto pre-warmed agar plates using a sterile protocol and sterile filter tips.

### **2.13.2 Bacterial cell culture and DNA extraction**

Bacterial colonies were grown on static Luria Bertani (LB) agar plates containing the appropriate antibiotic at 37°C. A single colony of cells was grown first in LB broth and antibiotic (ampicillin, 50µg/ml) on a shaker at 225rpm for 8 hours at 37°C. 2 ml of the culture was then transferred to 200ml of LB broth containing ampicillin and cultured overnight on the shaker (37°C, 225rpm). The next day the culture was spun at 6000g for 15 minutes at 4°C (Beckman centrifuge, Avanti J-25). DNA was extracted from the pellet and purified using HiSpeed Plasmid Maxi kit according to manufacturer's instructions.

### 2.13.3 DNA linearisation

To linearise the bacterial plasmid, specific restriction enzyme endonucleases were used to obtain sense and anti-sense cDNA (see Table 2.3). Digests were left at 37°C for 4 hours in total to ensure the DNA was efficiently linearised. 1µg of un-cut plasmid DNA was run alongside 1µg of linearised DNA on a 1% Agarose gel to check for successful linearisation. DNA was purified by ethanol precipitation. Purified DNA was reconstituted in Milli Q water.

### 2.13.4 Riboprobe synthesis

To transcribe riboprobes from the linearised DNA, RNA polymerase enzymes (and supplied buffer) were added to a reaction with 1µg of linearised DNA, Digoxigenin (DIG) RNA labelling mix (containing antigen labelled bases for immunohistochemical reaction) and RNASE inhibitor. Table 2.3 lists the restriction enzymes used to linearise the DNA and the polymerase enzymes used to transcribe from the linearised DNA to make anti-sense and sense riboprobes for the nrp genes of interest.

The reaction was left at 37°C for 2 hours. In this reaction, any remaining DNA was degraded by DNase. RNA was purified by ethanol and lithium chloride precipitation. RNA was reconstituted in ice cold TE buffer. RNA probes were run on a 1% agarose gel and RNA concentration and quality was recorded using a NanoDrop spectrophotometer. Probes were stored at minus 20°C.

**Table 2.3 A list of enzymes used to extract the DNA from bacterial plasmids**

Plasmid	Linearised	Transcribed	Source
NRP1	Sense: Sal I	T7	Proemga
	Anti sense: SacII	SP6	
NRP2	Sense: Hba I	SP6	Promega
	Antisense: Hind III	T7	

## 2.14 Preparation of tissues for histology

Tissues were fixed in 4% paraformaldehyde (PFA) at 4°C. For whole mount *in situ* hybridisation, embryos were fixed overnight. For whole mount immunofluorescence and cryo-sectioning of frozen tissue and paraffin wax embedded tissue, embryos were fixed for 2 hours. For cryo-sectioning of extra-embryonic vessels, 30% sucrose solution (overnight) preceded mounting in mounting medium (OCT).

For immunohistochemistry the area dissected was either the proximal vitelline vessel or the area of collateral vessel development in the extra-embryonic area vasculosa (see Figure 3.14-3.15). For all histological protocols which required fine dissection, the embryo and surrounding extra-embryonic tissue was dissected out of the egg into ice-cold Leibovitz (L-15) medium. The fine membrane covering the extra-embryonic vessels was removed using fine forceps (#5). Further dissection of the tissue was performed using sterile tungsten wire dissecting needles. Vitelline vessels were relatively easy to isolate from surrounding tissue, however collateral vessels were more challenging due to nature of their development (i.e. from pre-existing connections (section 3.4)) and could not be isolated. Collateral vessels were therefore sectioned within a dissected area of tissue.

For paraffin embedded sections wholemount tissue was dehydrated through increasing concentrations of ethanol (70%, 90%, 100%, 30 minutes each), ethanol was then cleared with Xylene (mixed isomers) (immersing in solution twice for 10 minutes each). Paraffin wax was heated to 60°C. Tissue was placed in an embedding cage and placed into the molten paraffin wax in an oven over night. Once tissue and wax had hardened, the wax blocks were mounted onto a chuck for sectioning by microtome.

## 2.15 Tissue sectioning

Microtome sectioning, for immunohistochemistry, was performed using a Leica (Model RM2155) with Leica 819 brand blade. The water bath was warmed to 42°C and filled with

filtered Milli Q lab water. 7µm thick sections were cut (as advised by colleague Janet Chamberlain's protocol for tissue sectioning with microtome) and paraffin wax sections collected using a SuperFrost/Plus slide. Slides were stored in a rack to dry at 40°C overnight.

Cryosectioning, for immunohistochemistry, was performed using a Bright OTF cryostat, in a temperature controlled environment (specimen -23°C). Tissue was mounted onto metal chucks on dry ice using OCT and sectioned at 12- 15µm thickness. Sections were thaw mounted on to slides and air-dried for 1 hour.

## **2.16 Immunohistochemistry**

### **2.16.1 Haematoxylin and Eosin staining**

Haematoxylin and Eosin (H&E) staining allows a distinction within a sample of tissue structure and nuclei. As wholemount labelling was prone to high background, due to the overlying vitelline membranes and ectoderm obscuring the intricate vasculature, cross sections through tissue were acquired by sectioning paraffin-wax embedded tissue samples.

For paraffin wax-embedded tissue, wax was removed from slides by placing the rack in a bath of xylene (twice for 10 minutes each) followed by graded reduced concentrations of ethanol (100%-50%) for 2 minutes each. For Haematoxylin and Eosin staining, the slides were immersed in Haematoxylin (Gills #1) for 2-3 minutes. Slides of sectioned tissue were immersed in 1% acid alcohol for 30 seconds then washed in tap water for 2 minutes. Slides were then dipped 10 times in 95% alcohol. This was followed by counter-labelling with Eosin Y solution for 20 seconds. Tissue was then dehydrated (95%, 5 minutes each), followed by two immersions in xylene for 5 minutes each. Tissue was mounted in xylene-based mounting medium.

### 2.16.2 Antibody immunolabelling

Slides were placed in a humid environment and washed with PBS before blocking for 1 hour with PBS supplemented with 1% heat inactivated goat serum, 1% Triton 10X in PBS. Sectioned tissue was incubated with primary antibody overnight at 4°C. Tissue was then incubated in secondary antibodies (Invitrogen goat anti-rabbit IgG; Alexa 488 or Alexa 594, 1:500) for 1 hour at room temperature. Tissue was washed in PBS and mounted for microscopy in Vectashield with DAPI.

For whole-mount immunohistochemistry embryos were blocked using PBS supplemented with 1% Triton 10X, 1% heat inactivated goat serum overnight at 4°C. Tissue was incubated with primary antibody solution was incubated overnight at 4°C. PBS washes were performed throughout the following day on a gentle rocker at room temperature. Tissue was then incubated in secondary antibody solution was incubated overnight at 4°C and all samples were kept in the dark. Extensive washing was performed before staining with DAPI nucleic acid stain for 1 hour and mounting embryos in a depressed slide with Vectashield and coverslip.

For negative controls, separate slides with adjacent sections were incubated with secondary antibody only. Positive tissue was difficult to acquire, although for PDE10A antibody optimisation, mouse cerebellum and chick cerebellum were used (Appendix A9).

**Table 2.4 A list of antibodies used to detect proteins by immunofluorescence.**

The table lists the antibodies and where they were purchased as well as the species they were raised in and the optimal concentration which was used.

Antibody	Source	Species	Optimal concentration
PDE10A (polyclonal)	Genetex	Rabbit anti-human	1:250
VE-cadherin (polyclonal)	Abcam	Rabbit anti-human	1:100

<b>BrdU (monoclonal)</b>	<b>Abcam</b>	<b>Rat anti-BrdU</b>	<b>1:1000</b>
--------------------------	--------------	----------------------	---------------

### **2.17 PDE10A immunohistochemistry optimisation**

To initially predict if the PDE10A antibody would react against chick PDE10A protein I used clustal alignment to check that the peptide sequence the antibody binds to in human was present in the chick PDE10A protein. Clustal alignment showed a good match between sequences (Appendix, Figure A8), however this was not sufficient to confirm specific binding I therefore sought to test the antibody in tissue positive for PDE10A (positive control).

In the literature PDE10A is reported to be expressed in the mouse brain and testis tissue, further the manufacturers of the antibody reported reactivity in mouse tissue. I therefore attempted to find an optimum concentration to use the antibody at using embryonic mouse brain tissue by testing a range of concentrations (1:500, 1:1000, 1:1500) (Appendix, Figure A9) and by altering blocking steps (duration of time tissue was incubated with PBS supplemented with 10% heat inactivated goat serum). After acquiring preliminary results, I tested the antibody in embryonic chick brain tissue. I tested the same range of concentrations but found the optimal concentration to be 1:250 in the chick brain tissue (Appendix, Figure A10). I therefore performed subsequent analysis on extra-embryonic/vascular tissue using a concentration of 1:250 (as shown in Chapter 5, Figures 5.3, 5.4). Despite my efforts to find an optimal concentration at which to achieve specific binding, PDE10A antibody remained difficult to use. Due to lack of funds, a second antibody could not be purchased, I therefore had to settle on the concentration which appeared to give sufficient results (Table 2.4) (further discussed in chapter 5) and validate PDE10A expression with the same antibody but a secondary technique (Western blotting). Optimisation steps took many months and an estimated n=50 chicks.

## 2.18 Whole-mount in situ hybridisation

To detect RNA/gene expression in whole mount tissue preparations, whole embryos were carefully dissected using a similar method as described in section 2.4.1. Iris scissors were used to cut around the sinus vein border to dissect the whole embryos along with all the extra-embryonic tissue/vessels and placed into ice cold Lebovitz (L-15). Any yolk was washed from the membrane. Embryos were transferred carefully with the aid of spatula and laid flat in separate wells of a 6-well plate in PBS. Following washes, embryos were fixed in ice cold 4% PFA overnight at 4°C to fix transcripts in place. Embryos were then dehydrated in a series of graded methanol/PBT concentrations (25%, 50%, 75%, 100%). Liquid was pipetted on and removed from the wells using a Pasteur pipette being careful not to contact the embryo. Embryos were stored in 100% methanol overnight at minus 20°C. Embryos were rehydrated (100%, 75%, 50%, 25% methanol/PBT) and washed in PBT (PBS and 1% Tween) before incubating for 18 minutes on ice in Proteinase K solution (10µg/µl). Embryos were washed and fixed with ice cold 4% PFA on ice for 20 minutes. Pre-warmed prehybridisation solution (50% formamide, 5X saline-sodium citrate (SSC) pH 7, 0.1% Triton x100, 0.5% CHAPS (Sigma) 1mg/ml YEAST RNA, 5mM EthyleneDiamineTetraAcetic acid, 50 µg/ml heparin) was pipetted into each well, submerging each embryo adequately and incubated with embryos at 65 °C for 90 minutes. DIG-labelled RNA probes were added (1 µl in 10ml prehybridisation solution) overnight to allow hybridisation to occur between the probe to the target sequence. The following day embryos were washed in buffer 1 (50% Formamide, 5X SSC pH4.5, 1% Sodium Dodecyl Sulfate) and buffer 2 (50% Formamide, 2XSSC pH4.5, 1% Tween); each wash was performed twice for 30 minutes at 65°C. Embryos were washed in Tris-buffered saline and Tween (TBST) and left at 4°C overnight. Embryos were washed in an alkaline phosphatase buffer (NTMT) solution (5M NaCl, 2M Tris pH9.5, 1M MgCl<sub>2</sub>, Tween 20, water) three times for 30 minutes in total; the salt and detergent concentrations were optimised to help specific binding and remove non-specific elements. Antibody

phosphatase binding was performed with nitro-blue-tetrazolium (NBT) and 5-bromo-4-chloro 3'-indolyphosphate p-toluidine salt (BCIP) enzymes in NTMT solution. These were added to each embryo until a colour change was observed, indicating a complete reaction and gene expression.

### **2.19 Protein extraction**

Tissue was collected, from the area of flow-induced vessel remodelling (as indicated in Figure 2.3), in sham and tied-ligated chick embryos at T0, 4 hours, 8 hours, 12 hours and 24 hours post tied-ligation/sham-ligation (as described in Section 2.2). Eight embryos were used, per group. Tissue was added to lysate buffer (150mM NaCl, 50mM Tris, 0.1%SDS, 0.5% Sodium deoxycholate, 1%NP-40, PBS) and homogenised by passing it through an 18G needle and 1ml syringe 5-7 times. 1 tablet per 10ml of protease inhibitors were added to homogenised tissue samples to prevent protein degradation. Following centrifugation (13,000 rpm), lysate supernatant was kept for protein quantification by Bradford assay (Biorad assay). Bovine Serum Albumin (BSA) (1mg/ml) and tissue lysate was serially diluted to create a standard curve using a spectrophotometer. Optical density was measured at an absorbance of 595nm. This data was used to calculate the optimum concentration of each protein sample to use in the Western blot procedure.

### **2.20 Western blotting**

Tissue lysates were first heated to denature the protein and allow SDS binding. Lysates were then added to loading buffer and reducing agent before loading 12µl into a polyacrylamide NuPAGE, Bis-Tris gel (4-12%). A pre-stained protein ladder was loaded at either end of the gel and 500µl of anti-oxidant was added to the SDS NuPAGE running buffer. Protein was resolved by electrophoresis at 160v for 1 hour.

Electro-blotting (90v, 1.5hours) transferred proteins to nitrocellulose membranes (Amersham Hybond C) in NuPAGE transfer buffer with 20% Methanol. To prevent non-specific binding,

membranes were blocked with 5% milk, 0.1% Tween, TBS for 1h at room temperature in a Falcon tube and experienced gentle rotation. Anti-rabbit PDE10A polyclonal antibody was added to 5% milk (1:3000) overnight at 4°C. Membranes were washed in a solution of tris-buffered saline and tween (TBST) 5 times and incubated for 1 hour at room temperature with secondary antibody and reporter enzyme (Jackson labs, anti-rabbit HRP 1:6000). Membranes were again washed 5 times in TBST and then wrapped in clingfilm. Blots were developed with Enhanced Chemi-luminescence which provided a substrate for the horseradish peroxidase (HRP) enzyme. Blots were exposed onto hyperfilm and labelled with protein sizes as was indicated by the protein ladder used initially to identify the correct band of interest.

Unfortunately, extra bands on my blots did limit the results and therefore the conclusions. I therefore attempted to improve this by optimising blocking steps using both milk solutions and bovine serum albumen (BSA). Blocking steps were optimised by trialling different concentrations of blocking reagents and length of time of blocking. I also tested whether the blots could be improved by altering antibody concentration. In case the antibody was binding non-specifically I reduced the concentration from 1:250 to 1:500 and 1:1000 but this had no effect.

## **2.21 Pharmacological assays**

I conducted pharmacological assays to attempt to elucidate a role for PDE10A in flow-induced vessel remodelling.

At HH st17, embryos were prepared as described in sections 2.1.3-2.2 (depending on the experiment). At T0 (post tied-ligation/sham-ligation) embryos received drug treatments or PBS by a drug delivery mechanism of Whatman #1 filter paper discs which had been previously prepared. Filter paper discs were cut uniformly with a 5mm diameter hole punch and put into a beaker which was covered and sterilised by autoclaving and drying. The sterilised discs of filter paper were soaked in 5µl of drug or PBS and placed over the vitelline membrane (the thin layer of membrane) covering the extra-embryonic vasculature

area of interest (See Figure 2.5). Most filter paper assays were assessed after a single timepoint (24h), however, this is described as 24-28 hours as for practical reasons analysis at the exact time was not physically possible. I therefore describe results as 24-28 hours to include the time taken to conduct operate on and analyse each individual embryo during these experiments.

For studies investigating an initial toxic effect of the drug, discs were placed lateral to the embryo body over the proximal vitelline vessels. For studies affecting the effect of the drug on collateral vessel formation discs were placed at the anterior and posterior poles of the embryo (Figure 2.5). Heart rate was measured by counting heart beats *in ovo* of each embryo for 15 seconds.

Filter paper was the ideal method of drug delivery for this model as it was inexpensive, easy to use and remove from the membrane and preliminary experiments showed that it was able to deliver solvents such as food colouring to the extra-embryonic membrane (Appendix, Figure A11). When administered systemically to humans, papaverine is renally excreted with a half-life of 1.5-2 hours (Ritschel and Hammer., 1977). These are therefore effectively slow-release reservoirs of drug and the half-lives are therefore anticipated to be longer than those following single systemic administration.

Although the discs were applied topically to the area of interest, since the drug is expected to diffuse from the filter paper, there is a likelihood of drug effects both outside the area of application of the drug, and also systemically. These potentially confounding effects are discussed in the relevant results chapter (Chapter 5 discussion).

I first used a PDE10A inhibitor, papaverine hydrochloride. To investigate the effect of PDE10A inhibition on vessel remodelling I used the cAMP analogue (PKA inhibitor), Rp-8-Br-cAMPS.

Papaverine hydrochloride is an opium alkaloid used clinically for its ability to induce relaxation of smooth muscle at high concentrations. Although its pharmacology is not entirely clear, papaverine has been shown to be an antagonist of PDEs. Papaverine has been shown to be most specific against PDE10A, with an IC<sub>50</sub> of 0.036Mm, thirty six-fold lower than the IC<sub>50</sub> for PDE3A and over 270 times lower than for PDE5 (the PDE present in smooth muscle) (Ritschel and Hammer., 1977). In my studies papaverine hydrochloride was diluted to the specific concentrations specified in Chapter 5 (5µm, 10µm, 20µm) using PBS, with gentle heat and constant stirring until the powder had dissolved. The vial was protected from light as the drug is light-sensitive.

Rp-8-Br-cAMPS is a cAMP analogue which competitively binds to PKA. By occupying cAMP binding sites, Rp-8-Br-cAMPS prevents PKA from dissociation and therefore activation. In this study, Rp-8-Br-cAMPS stock solution was a gift from Dr Stephen Renshaw's laboratory (The University of Sheffield). Rp-8-Br-cAMPS was diluted into PBS to achieve the required concentrations as described in Chapter 5 (30µM, 50µM, 100µM, 200µM, 500µM). The assays were performed according to the same protocol as for papaverine assays. Control chicks were also treated in the same way as in the papaverine assays and received PBS alone.

For assays which examined the effect of more than one drug, 5µl of each (papaverine and Rp-8-Br-cAMPS) was pipetted onto the same disc but the concentration was doubled (200µM Rp-8-Br-cAMPS; 40µM papaverine).

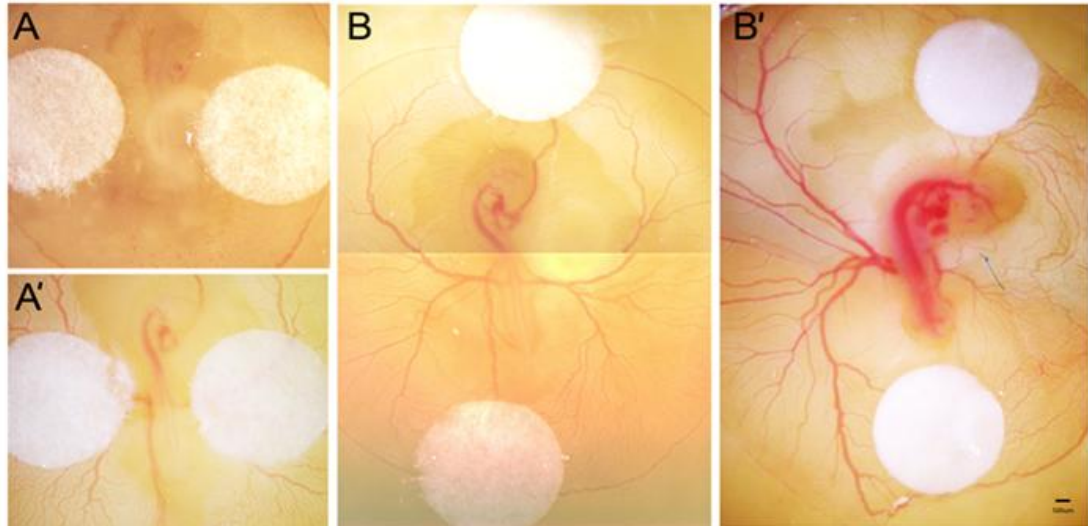


**Figure 2.5 Filter paper discs were used as a method of drug delivery**

Discs were placed over the vitelline vessels of early stage chicks (**A**) or later stages (**A'**) to assess the effect of the drug on normal vessel development. Discs were placed over the midlines of either sham (**B**) or tied-ligated chicks (**B'**) to assess the effect on remodeling.

## 2.22 Proliferation assays

### 2.22.1 *In vivo* proliferation assays

To assess proliferating cells in the area of flow-induced remodelling I assessed Bromodeoxyuridine (BrdU) incorporation into the DNA of cells in this area. The disadvantage to using BrdU is the antigen retrieval step, which requires damage of the nucleus to reveal the epitope in the DNA. Quantification of DNA positive labelling therefore had to be conducted by calculating DAPI area and positive BrdU area.

Immediately following *in ovo* ligation, BrdU was pipetted onto the vitelline membrane in the area of flow-induced vessel remodelling (area indicated in Figure 2.3). Optimisation of this technique was required as it was questionable as to whether BrdU sufficiently reached the endothelial cells and was incorporated into the DNA (see Table 2.5) therefore a range of concentrations and volumes and were tested. I also tried injecting the BrdU underneath and over the top of the vitelline membrane to test whether this made a difference. I further validated positive labelling by sectioning tissue from the neural tube of the same developing

embryos that vessels were taken from. The neural tube in a growing embryo contains proliferating cells, therefore acting as a positive control. I used 25 $\mu$ l of 1mM BrdU injected over the vitelline membrane for my experiments as this was found to give optimal results.

For each analysis of collateral vessel tissue, 6-8 sections were taken and mounted onto slides. Once each section on each slide was imaged using the Apotome fluorescent microscope, Image J was used to assess the positive BrdU labelling. Each section was divided into 4-6 fields of view and fluorescent micrograph images were taken. Using ImageJ the colour channels of each image was split to more specifically calculate positive DAPI or BrdU labelling. Blue and green channels were analysed separately for individual quantification which could then be used to calculate proliferation index. The extent of positive labelling, was measured automatically by ImageJ. To do this the threshold tool was used as adjusting the threshold intensity of an image which picked up the positive labelling. Once the threshold parameters were set, this remained the same for each image analysed. Image J then calculated the area of positive labelling. When all fields of view had been analysed the data was added together to give the result of BrdU staining over the whole section. The average was then calculated from the individual sections to give a single data reading for one piece of tissue.

For proliferation assays investigating pharmacological effects, 5mm sterilised filter paper discs containing 20 $\mu$ M papaverine were applied to the anterior and posterior poles of the embryo over the midline (Figure 2.5) . Embryos were re-sealed and returned to the incubator for the required length of time. After this time, if filter paper had been applied discs were removed using forceps, then using spring scissors and fine forceps the area of collateral vessel remodelling was excised and dissected (as described in Section 2.4). Tissue was fixed in 4% PFA for 2 hours and incubated in 30% sucrose overnight then mounted in OCT on dry ice for cryosectioning (as described Section 2.15). Sections were cut at 15 $\mu$ m and processed for immunohistochemistry (as

described in Section 2.16) and assessed for anti-BrdU (1:200) and anti- VE Cadherin (1:100) labelling.

**Table 2.5 BrdU delivery to endothelial cells in the area of collateral vessel formation was optimised by testing a range of concentrations and volumes.**

Concentration of BrdU ( $\mu\text{M}/\text{mM}$ )	Volume pipetted ( $\mu\text{l}$ )	Number of embryos (location of injection on/over vitelline membrane)
100 $\mu\text{M}$	25	3 injected under 3 injected over
100 $\mu\text{M}$	100	3 injected under 3 injected over
1mM	25	3 injected over 3 injected under
1mM	100	3 injected over 3 injected under

For analysis of proliferating cells, Apotome images were split into red, green, blue channels. For DAPI analysis threshold was altered to optimise visualisation of labelled cells. This threshold was then set and was kept constant for all DAPI image analysis. This was repeated to assess the positive labelling of the proliferation marker and again, threshold, once set, remained consistent for each image. Threshold analysis (ImageJ) removed any bias and measured the density of the labelling in the image. To acquire a proliferation index the area of DAPI staining was divided by the area of positive proliferation marker labelling (+ve BrdU area/+ve DAPI area x100). All analysis was performed blinded from knowledge of which sample was from which condition.

## **2.23 Microscopy**

### **2.23.1 Fluorescence microscopy**

Slides were analysed and photographed using a Zeiss Apotome (Imager z1 + Apotome) with an AxioCam (MRM 1.0X). Data was collected using AxioVision version 4.6.3. For Alexa 488 visualisation, a laser with an excitation wavelength of 488nm was used; Alexa 594 was observed at 594nm; DAPI was visualised at 405nm. For Apotome Z stack images, stacks were compounded to a flat, single picture using image J software (National Institutes of Health). Channels were split into red, green and blue using Image J, to visualise individual staining patterns before merging.

### **2.23.2 *In vivo* microscopy**

For time-course experiments, a digital camera was mounted onto the camera mount of a stereomicroscope and an overhead light source positioned over the platform of the microscope. Photomicrographs for drug assay analysis were performed on a Leica microscope (M2125, 10x/21b) connected to a Spot camera and software (SpotCam). Photography was performed at room temperature (around 24°C). Eggs were prepared as described in Section 2.1.2-2.1.4 and positioned in the Styrofoam holder. Photographs were taken of the midline superior and inferior to the embryo. The embryo was then re-sealed using parafilm and returned to the incubator (38°C).

## **2.24 Image analysis**

Images of the yolk sac vasculature were used to assess collateral vessel growth across the midline (the original location of the vitelline veins). Micrographs were analysed using ImageJ software (version 1.35p)(National Institutes of Health). The image scale was calibrated to 0.213 pixels/ $\mu\text{m}$  for time-course images and 0.310 pixels/ $\mu\text{m}$  for drug assays. Image analysis was performed blinded; each of the image folders containing the different

groups to be analysed were temporarily re-named by a colleague so that the true identity of images were unknown until post-analysis. Images were viewed at high magnification (200-600% original image size). Using a line draw tool and automatic measurement (ImageJ), the diameter of all arteries crossing the midline was recorded. Collateral vessel number and diameter were noted for each image and was limited only by the resolution of the micrographs. Pixel intensity was not appropriate to use for analysis of these images as the albumen over the surface of the vitelline membrane blurred vessel boundaries which would have caused anomalies and given false results. The light source was also difficult to keep constant for all eggs analyse between different experiments and so would have also hampered this type of analysis. These limitations are discussed further in chapter 5.

## **2.25 Statistical analysis**

Statistical analysis was performed using GraphPad Prism software. For each graph presented, data is shown as mean  $\pm$  standard error of the mean (SEM). For data with two groups, Student's t-test was used to examine whether statistically significant differences between groups were present. For data with more than two groups a one-way ANOVA was performed with an appropriate post-test. Post-tests were selected based on the comparisons performed; to compare a mean to every other mean a Tukey post test was used; to compare every mean to the control mean a Dunnett post test was used; To compare selected means a Bonferroni post test was used.

For data which analysed two nominal variables and one measurable variable a 2-way ANOVA was performed. In all these statistical comparisons, a p value <0.05 was considered statistically significant. A record of the n numbers used in each experiment is presented in the figure legends of each of the results. On average, experiments were repeated on a minimum of 2 separate occasions.

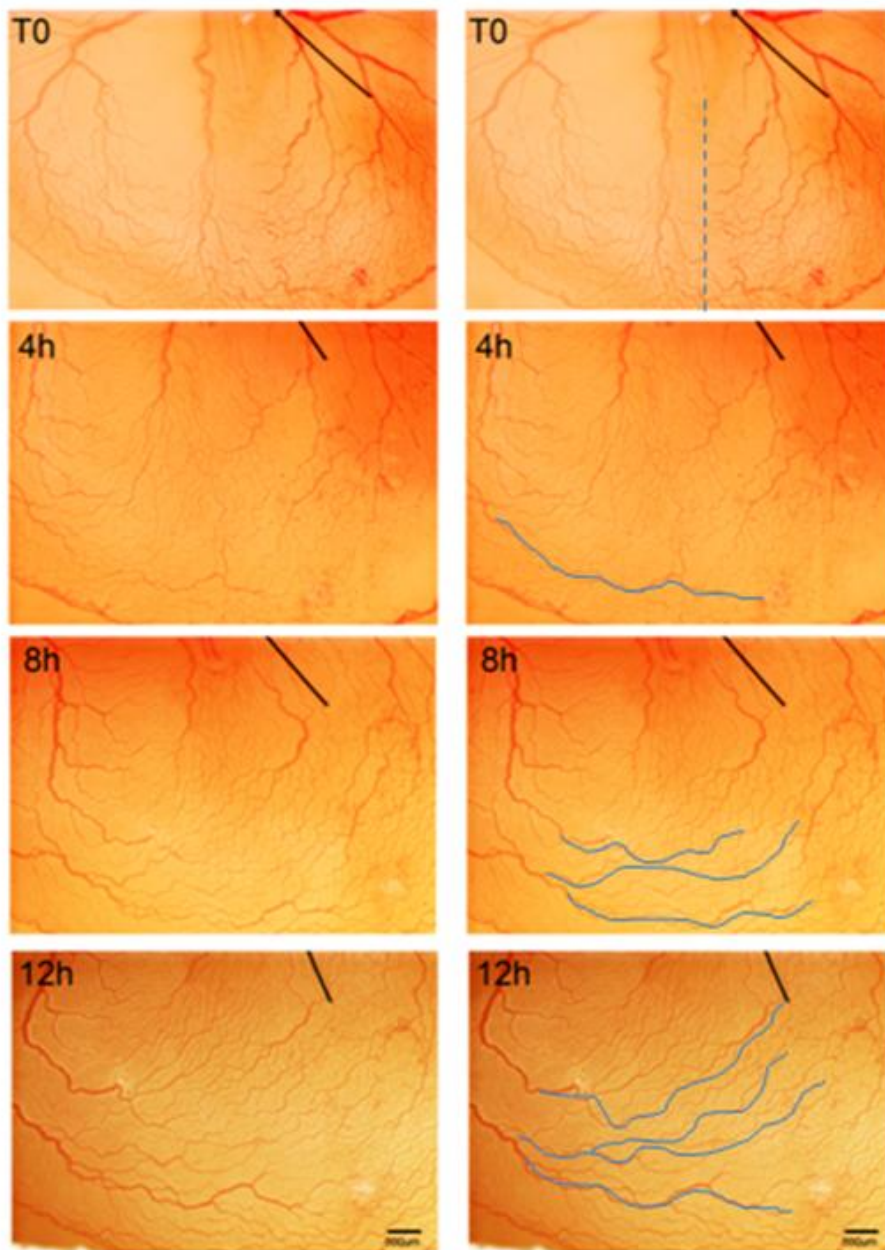


**Figure 2.6 Micrograph images to show how collateral vessels were identified.**

The panel shows representative images of developing collateral vessels in one embryo over a 12h timecourse. Collateral vessels can be seen crossing from left to right across the midline. The midline is defined by a dashed line at T0. Blue lines in the images on the right trace examples of collateral vessels seen in the images on the left. The midline can be seen to retract as collateral vessels extend over 12h. (scale bar = 1000 $\mu$ m)

## Chapter 3

### Characterising the chick embryo as a model of flow-induced vessel remodelling

#### Summary

In this chapter I describe my studies that extend and further characterise the chicken embryonic model of flow-induced remodelling first described by le Noble *et al.* (2004). As outlined in section 1.13, Le Noble's description of this model was in a study that attempted to define the contribution of blood flow to arterio-venous identity of the extra-embryonic vasculature. They induced unilateral vitelline artery occlusion and demonstrated that this downregulated arterial identity in the ligated circulation, an effect reversed with restoration of blood flow (le Noble *et al.*, 2004). The focus of their study was the effect of removal of blood flow on the ligated/reperfused vitelline vessels, not the unligated vasculature. Although the authors described remodelled vessels extending from the unligated territory at the poles of the embryo, these were not quantified or characterised nor termed 'collateral' vessels. My intention therefore was to study the effects of unilateral vessel ligation upon the **unligated** territory in the expectation this might provide insight into flow-induced remodelling and **collateral vessel formation**.

During the course of my studies, le Noble's group published a second paper (Buschmann *et al.*, 2010) that, in fact, confirmed that following obstruction of the right proximal vitelline vitelline artery, the unligated vessels of the left vitelline circulation remodelled. The authors termed such vessels that extended across the midline, carried arterial flow and connected to the left proximal vitelline vessel, "collateral vessels" and showed that these supplied the tied-ligated territory. The number of collateral vessels was quantified, **but only at a single timepoint (24h after ligation)**. Finally, this study identified an arterial gene,

Gja5, which was upregulated in collateral vessels in the chick embryo and required for collateral development in a mouse model (Buschmann *et al.*, 2010).

Despite the fact that this second paper described the model that I had been working to establish, a number of outstanding questions remained. In particular, the group did not perform a detailed time-course of collateral vessel development, nor did they quantify collateral vessel number over time. Further, they did not analyse collateral vessel diameter, nor the cellular/molecular profile of collateral vessels. Finally, this study did not investigate mechanisms of collateral development in the chick. I wished to address these issues in order to better characterise collateral vessel remodelling in the chick, and inform subsequent analyses (chapters 4 and 5).

I therefore set out to:

- Perform a longitudinal quantification of developing collateral/collateral number and diameter following unilateral vitelline artery ligation
- Establish a system to assess blood flow after unilateral vitelline artery ligation
- Examine expression of various markers in developing collateral vessels histologically/histochemically
- Examine proliferation in developing collateral vessels after unilateral vitelline artery ligation

### **3.1 Occlusion of the right vitelline artery by surgical ligation**

I adapted the model of le Noble *et al.*, (2004) but instead of using tungsten needles to elevate the artery and occlude flow (le Noble *et al.*, 2004), I developed a surgical suture method (see Materials and Methods section 2.2).

Microsurgical ligation of the right proximal vitelline artery was performed. Ligations were performed proximal to the first bifurcation of the artery, i.e. immediately distal to the embryo. Control embryos underwent the same surgical procedure leaving the suture untied beneath artery (referred to as 'sham-ligated'). Such sham-ligations left blood flow undisturbed (Figure 3.1A) as evidenced by moving red blood cells observed by light microscopy. By contrast, in a tied-ligated embryo, 30 seconds after occlusion, the vessel distal to the suture site darkened, as flow was abolished and blood stagnated (Figure 3.1B). In these vessels, I observed that red blood cells were not moving, indicating flow cessation. In all experiments, successful occlusion was judged by observation of cessation of blood flow and stagnation.

Having induced right vitelline artery occlusion, I examined the effect on the architecture of the left vitelline circulation. Tied-ligated embryos were compared with sham-ligated embryos to control for any non-specific effects of the surgery.

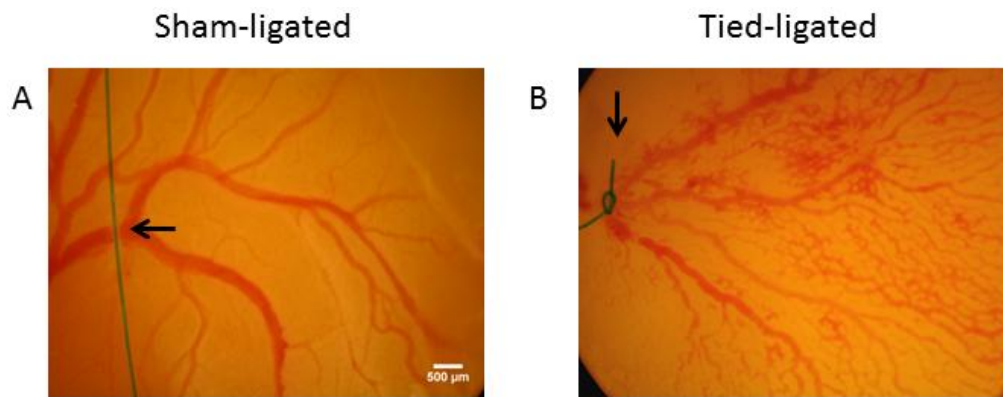


**Figure 3.1 Representative micrograph images of the right vitelline vessel of a HH st 17 chick embryo showing a sham ligation and a tied ligation**

**A** shows a sham suture beneath the right vitelline vessel (arrow). Sham ligations do not occlude flow. The suture is left un-tied to leave blood flow un-disturbed **B** shows a vitelline vessel which has been tied and ligated. The suture (arrow) was tied into a knot around the vessel. This image was taken 1-2 minutes after surgery.  $n \sim >100$  embryos over the course of the project

### **3.2 The effect of right vitelline artery ligation on the left proximal vitelline circulation**

Since unilateral vitelline artery ligation abolishes blood flow to one side of the vitelline vasculature, it is highly likely this alters the haemodynamics in the unligated territory. The exact nature of this disturbance will be determined by a range of complex factors, including effects on cardiac output, alterations in pressure, vaso-regulation and passive vessel expansion. To examine evidence for such events I examined whether the diameter of the unligated proximal vitelline artery alters following ligation of the contralateral proximal vitelline artery.

I measured the diameter of the left proximal vitelline artery immediately pre- and post-tied-ligation of the right vitelline artery, and 10 minutes following tied-ligation. The change in vessel diameter from baseline (pre-ligation) is shown in Figure 3.2A, expressed as percentage change from baseline diameter, to account for variability in vessel diameter prior to ligation.

In embryos undergoing sham-ligation of the right vitelline artery, there was a small reduction in the diameter of the left vitelline artery, particularly 10 minutes post-surgery (Figure 3.2A). By contrast, in embryos in which the right vitelline artery was ligated, there was a significant increase in the diameter of the left vitelline artery both immediately and 10 minutes post tied-ligation (Figure 3.2A). Although this suggests a change in the haemodynamic forces exerted in the unligated territory, it is not possible to conclude what is driving the increase in diameter. Further measurements of pressure, cardiac output, vasoregulation, and shear stress would be necessary to elucidate the exact mechanism.

Heart rate was not significantly different between sham and tied-ligated embryos (Figure 3.2B). Analyses of embryonic development over the entire timecourse of the experiment showed that ligation does not adversely affect the embryo or the rate of embryonic development, relative to control.

In the course of my studies, Buschmann *et al.*, (2010) showed an increased diameter, mean velocity and mean shear in the unligated vitelline artery at a later, single (5 hour) timepoint (Buschmann *et al.*, 2010). My findings are therefore consistent with theirs and taken together; suggest that blood flow is increased to the unligated territory in response to the tied-ligation.

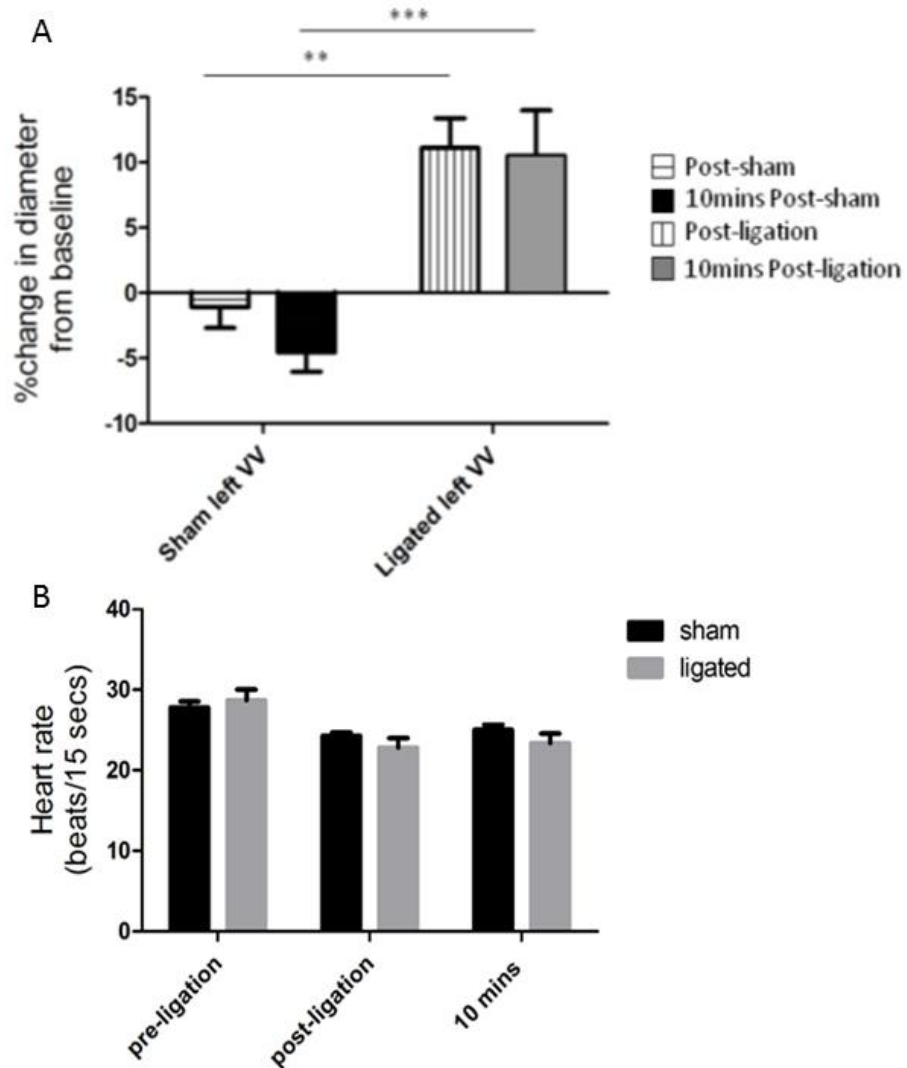


**Figure 3.2 Following right proximal vitelline artery ligation, the left vitelline artery increases in diameter significantly compared to sham controls**

**A** shows right proximal vitelline artery diameter (%) change from baseline (pre-ligation). Measurements were taken post-ligation, and a further 10 minute follow-up. The left vitelline artery expands after ligation and this persists to 10 minutes following the procedure. The difference in size is significant compared to the sham-ligated vessel, immediately after and 10minutes after ligation. ( $p < 0.005$ ,  $p < 0.0005$ ;  $n = 20$  embryos) **B** Neither ligation nor sham ligation affects heart rate ( $n = 20$ ). Data was analysed with 2-way ANOVA and Bonferroni multiple comparison post-test.

### **3.3 The collateral vessel response following unilateral vitelline artery ligation.**

I next examined the effect of unilateral vitelline artery tied-ligation on development of the unligated posterior medial vitelline territory. As detailed above, Buschmann *et al.*, (2010) identified collateral vessels in a chick embryo model of occlusion but only quantified collateral vessel number at 24 hours after tied-ligation (Buschmann *et al.*, 2010). I wished to extend these studies to attempt to identify key phases of the remodelling process. I performed right proximal vitelline artery tied-ligation or sham-ligation as before and quantified number and diameter of “collateral vessels”. In keeping with the Buschmann study, collateral vessels were defined as those crossing the embryo/yolk sac midline from the unligated to the ligated territory, carrying blood flow (from left to right across the midline – termed ‘arterial flow’) and stemming from an identifiable source (left proximal vitelline vessel) (Buschmann *et al.*, 2010). Following ligation, micrographs of each embryo were acquired every 4 hours until 48 hours. The number and diameter of collateral vessels extending from left to right towards or across the midline were quantified for each embryo. Immediately post tied-ligation, the vitelline vasculature in the posterior-medial extra embryonic tissue was identical in sham-ligated and tied-ligated embryo: no collateral vessels were apparent (Figure 3.3). As expected, the vitelline vasculature of sham-ligated embryos maintained a normal symmetrical orientation over the 48 hour timecourse, with no collateral vessels crossing the midline (Figure 3.4). No vessels crossing the midline were ever observed at any timepoint in sham-ligated embryos.

In contrast, tied-ligated embryos showed evidence of collateral vessel remodelling at the earliest time-point examined (4 hours post tied-ligation). Even at this early time-point, I could detect vessels that carried blood across the midline (left to right), not seen in sham-ligated embryos.

Over the next 4 hours, the posterior vein gradually regressed to be replaced by a collateral network delivering blood across the midline to supply the tied-ligated side of the chick (Figure 3.5). Although only the posterior of the embryo is depicted in Figure 3.5, a similar though less pronounced process occurred at the anterior pole with 1 or 2 collaterals extending from left to right (Figure 3.6 shows a representative image of the whole embryo at 24 hours post tied-ligation).

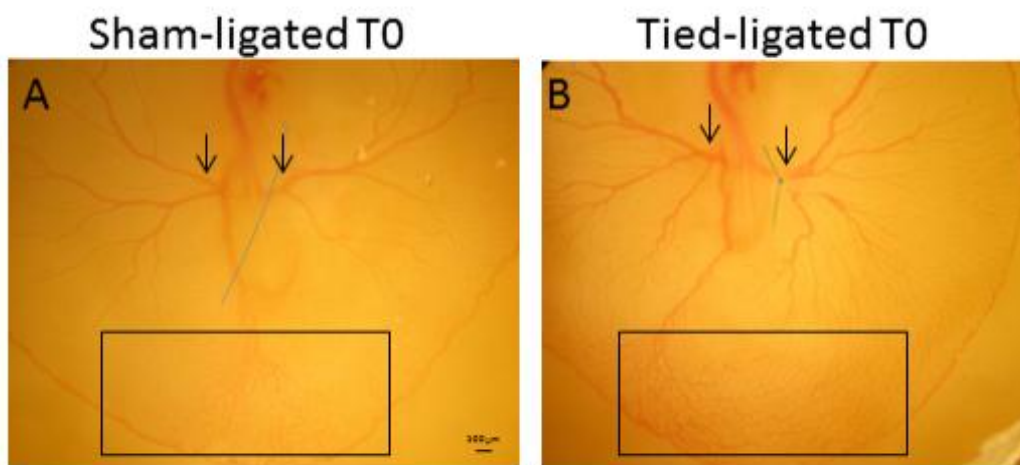


**Figure 3.3** The vascular morphology of the vitelline network of a HH st 17 chick embryo immediately (T0) post-tied-ligation (right panel) or sham ligation (left panel)

**A** Shows a representative sham-ligated HH st 17 chick embryo. The embryo body is in the centre of the image. Vitelline arteries (indicated by arrows) protrude from the embryo body in branches. The suture (blue thread) can be seen to lie under the right vitelline artery. The box indicates the posterior medial region of the embryo. Small capillaries in this area can be seen to join to the posterior vitelline vein. **B** Shows a representative image of a tied-ligated embryo at T0. The suture in this image was tied in a knot around the right vitelline artery. The back boxed area highlights the area at the posterior of the embryo which also contains many small capillaries (n=18 but ~>100 embryos over the course of the project showed this same morphology) (scale bar = 500µm)

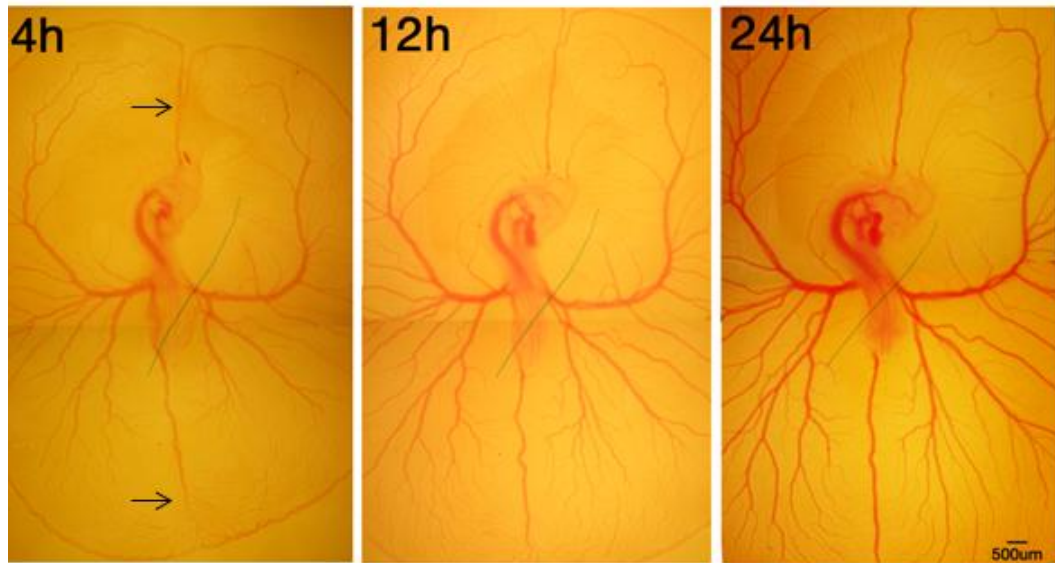


**Figure 3.4 The vascular morphology over time following sham ligation of the vitelline network of a HH st 17 chick embryo**

As in Figure 3.3A, the suture is passed beneath the right vitelline artery and left untied (blue thread). At 4h post-ligation the orientation of the vitelline vascular network has not changed. Anterior and posterior midlines remain in a central position (arrows). Capillaries at the posterior of the embryo join to the posterior vitelline vein. The branched network of arteries remains symmetrical. At 12h although the network has increased in size over time it remains in the same orientation. At 24h the network has again expanded, the embryo has also grown in size, but the orientation of vessel morphology remains much as it was at earlier timepoints. (n=18 but ~>100 embryos over the course of the project showed this morphology) (scale bar = 500µm)

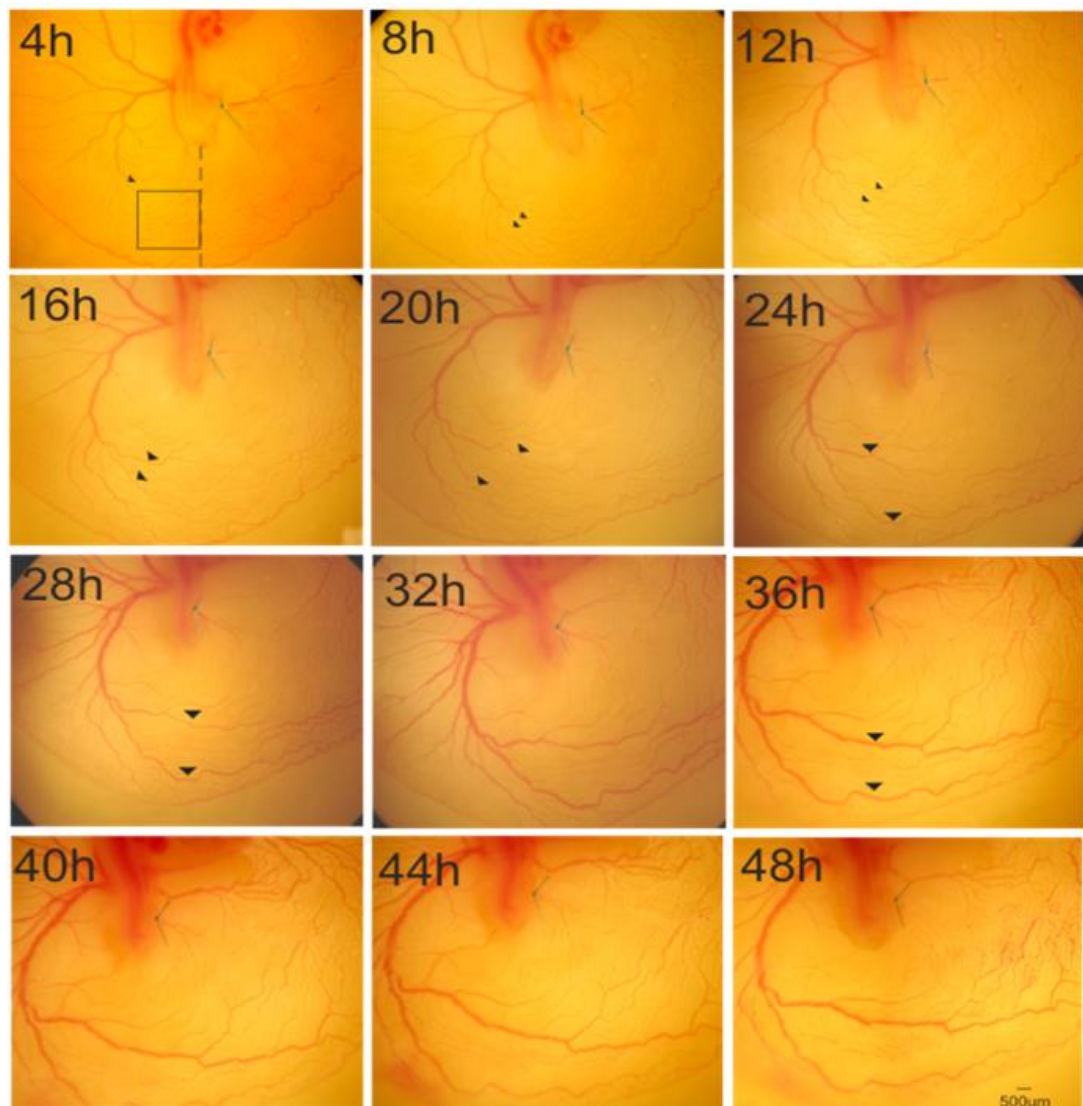


**Figure 3.5 Unilateral vitelline artery ligation induces a dynamic compensatory response to restore blood flow to the tied- ligated territory**

The time-course of collateral development after right vitelline artery tied-ligation in a single chicken embryo. The blue suture can be seen to be tied around the right proximal vitelline artery. The chick body is in upper middle of the image. The anterior vitelline vessels are not shown (see Figure 3.6). At 4 hours post tied-ligation developing collateral vessels extended from the distal branches of the left vitelline artery and cross the midline (indicated by the dashed line) by making small connections with pre-existing capillaries in the area. The arrows in the images indicate examples of collateral vessels. (n=18)

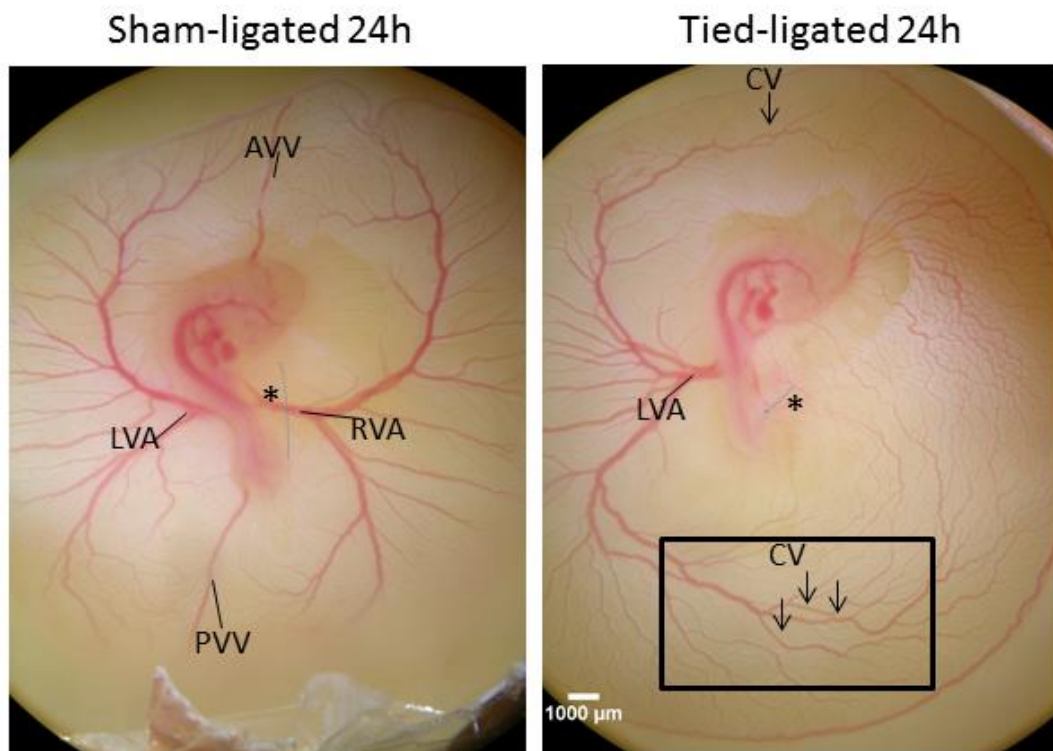


**Figure 3.6 The sham and tied-ligated chick embryo model at 24 hours post-ligation**

**A** Micrograph of a sham-ligated chick embryo 24h post-surgery. The suture can be seen untied underneath the proximal right vitelline artery (RVA) (indicated by star). The midline vitelline vein at the anterior (AVV) and posterior (PVV) remains in the same location as at T0, Figure 3.3). The right vitelline artery (RVA) and left vitelline artery (LVA) maintain a symmetrical orientation. **B** shows a tied-ligated embryo at 24h (ligated suture indicated by star). Collateral vessels (CV) indicated with arrows and can be seen at the anterior and posterior poles. The proximal right vitelline artery regressed and was replaced by small venules which extended from the distal branches of the collateral vessels crossing the midline. Compared to the embryo in A, the embryo in B clearly shows the remodelled vitelline vascular network which no longer maintains a symmetrical distribution either side of midline veins. (n=18)

I next quantified collateral vessel number and diameter in tied-ligated embryos over a 48 hour timecourse at 4 hour intervals (Figure 3.7). Following ligation, number of collateral vessels crossing the midline rapidly increased, with a peak around 12 hours post-ligation (mean  $8 \pm 2$ ). After this, the number of collaterals gradually fell (mean:  $4 \pm 1$  at 48h post-ligation, Figure 3.7A). Statistical analysis revealed a significant increase in collateral number from immediately post-tied ligation (T0) to 12 hours ( $p < 0.0001$ ). Between 12 hours and 36 hours collateral vessel number decreased significantly ( $p < 0.05$ ).

Collateral vessel diameter progressively increased over time until a plateau around 36 hours post tied-ligation (Figure 3.7B). Over time the diameter of the collateral vessels significantly increased between T0 and 12 hours ( $p < 0.0005$ ), 12 hours and 32 hours ( $p < 0.05$ ) and 24 and 36 hours ( $p < 0.005$ ).

I sought to infer the haemodynamic properties of the collateral vessels indirectly from the anatomical measurements acquired. If a circular lumen is assumed, the cross sectional area (CSA) of each collateral vessel is  $\pi * \text{radius}^2$ . The sum of the CSA of all collateral vessels is likely to reflect total conductance or capacity. I therefore calculated the sum total CSA of all collateral vessels at each timepoint. This showed that despite the reduction in collateral vessel number after 12 hours post tied-ligation, there was a steady increase in total CSA until at least 36 hours post tied-ligation (Figure 3.7C). CSA significantly increased between T0 and 32 hours ( $p < 0.005$ ), 12 to 36 hours ( $p < 0.0005$ ) and 24 to 36 hours ( $p < 0.005$ ).

This data supports the premise that some collateral vessels are selected for persistence and increasing diameter, while others regress. This is haemodynamically more efficient according to Poiseuille's law, and thus a favourable response. A similar response has been described in rabbits and other rodents (Scholz *et al.*, 2002, Eitenmuller *et al.*, 2006). Although the mechanisms behind these processes have not been elucidated, my studies suggest that the chick model of collateral vessel development parallels mammalian species.

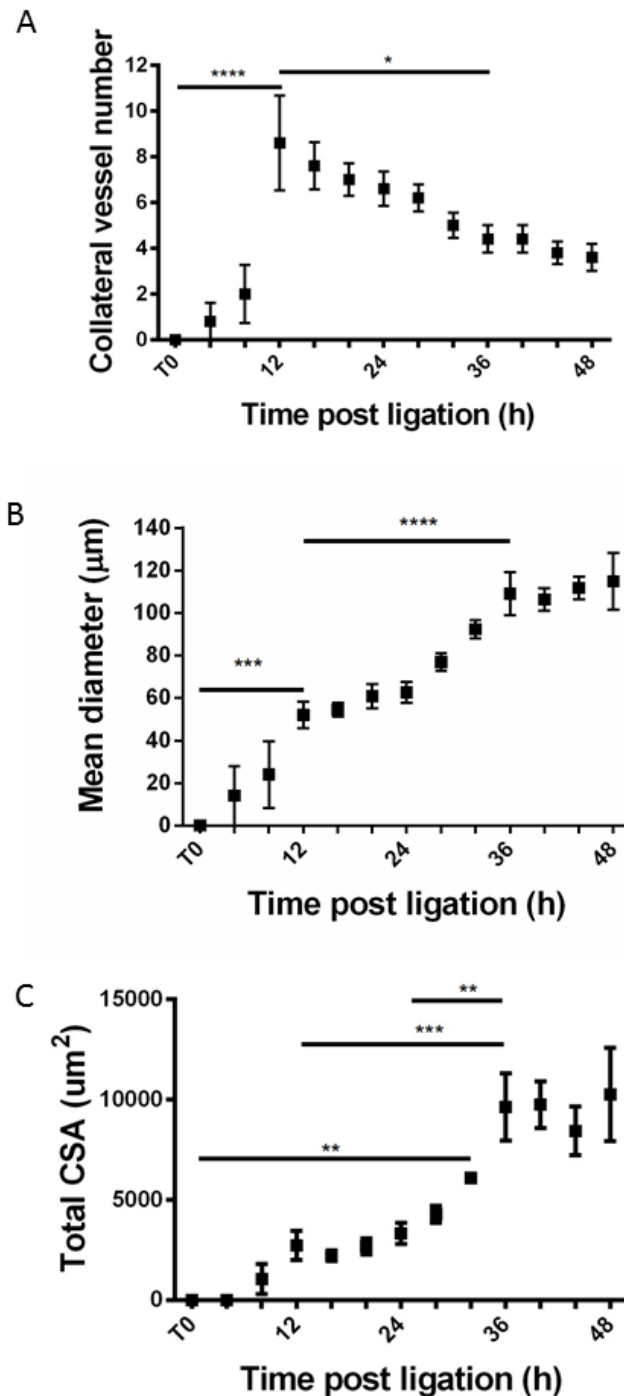


**Figure 3.7 Collateral vessels actively remodel to favour persistence of a small number of large vessels**

**A** The mean number of collateral vessels over time from T0 to 48h. There was a statistically significant increase in the number of collateral vessels between T0 and 12h ( $p < 0.0001$ ). Between 12h and 36h collateral vessel number decreased significantly ( $p < 0.05$ ). **B** The mean diameter of these persisting collaterals at each timepoint. Mean diameter significantly increased between T0 and 12h ( $p < 0.0005$ ), 12h and 32h ( $p < 0.05$ ), 24 and 36h ( $p < 0.005$ ) **C** The mean total cross sectional area of all persisting collaterals at each timepoint. CSA was significantly increased between T0 and 32h ( $p < 0.005$ ), 12 and 36h ( $p < 0.0005$ ), 24 and 36h ( $p < 0.005$ ). 2 way ANOVA with multiple comparisons ( $n = 18$  embryos)

### **3.4 Flow-induced vessel remodelling requires pre-existing connections to form collateral vessels**

Although in mammalian systems collateral vessels form from a pre-existing source (Heil *et al.*, 2006) it was important to establish that the collaterals in the chick model also developed from pre-existing vessels (i.e. mimicking the situation in mammals). I performed high-power analysis of the distal branches of the left vitelline vessels at hourly intervals over the first 8 hours following right proximal vitelline artery ligation (Figure 3.8). Vessels extended by recruiting previously apparent, but smaller, vessels. From numerous distal vitelline vessel branches, one or two became dominant. These vessels were termed 'developing collateral vessels' as they eventually carried arterial flow across the midline but at this early timepoint did not extend across the midline. Figure 3.8 shows a panel of representative micrographs of distal vitelline branches. For example, at 2 hours following ligation vessels labelled **c** and **d** appeared of equal size. By 3 hours post-ligation, vessel **c** has a greater diameter. From 4 hours onwards branch **d** regresses whilst **c** persists.

These studies suggest that in the chick, collateral vessels develop by recruitment of pre-existing vessels and that some form of selection must take place, such that some collateral vessels continue to enlarge while others regress. Figure 3.8 gives a static picture of collateral vessel development at individual timepoints. To investigate a role for haemodynamic forces in the process of 'selection' in this model more research would be required.

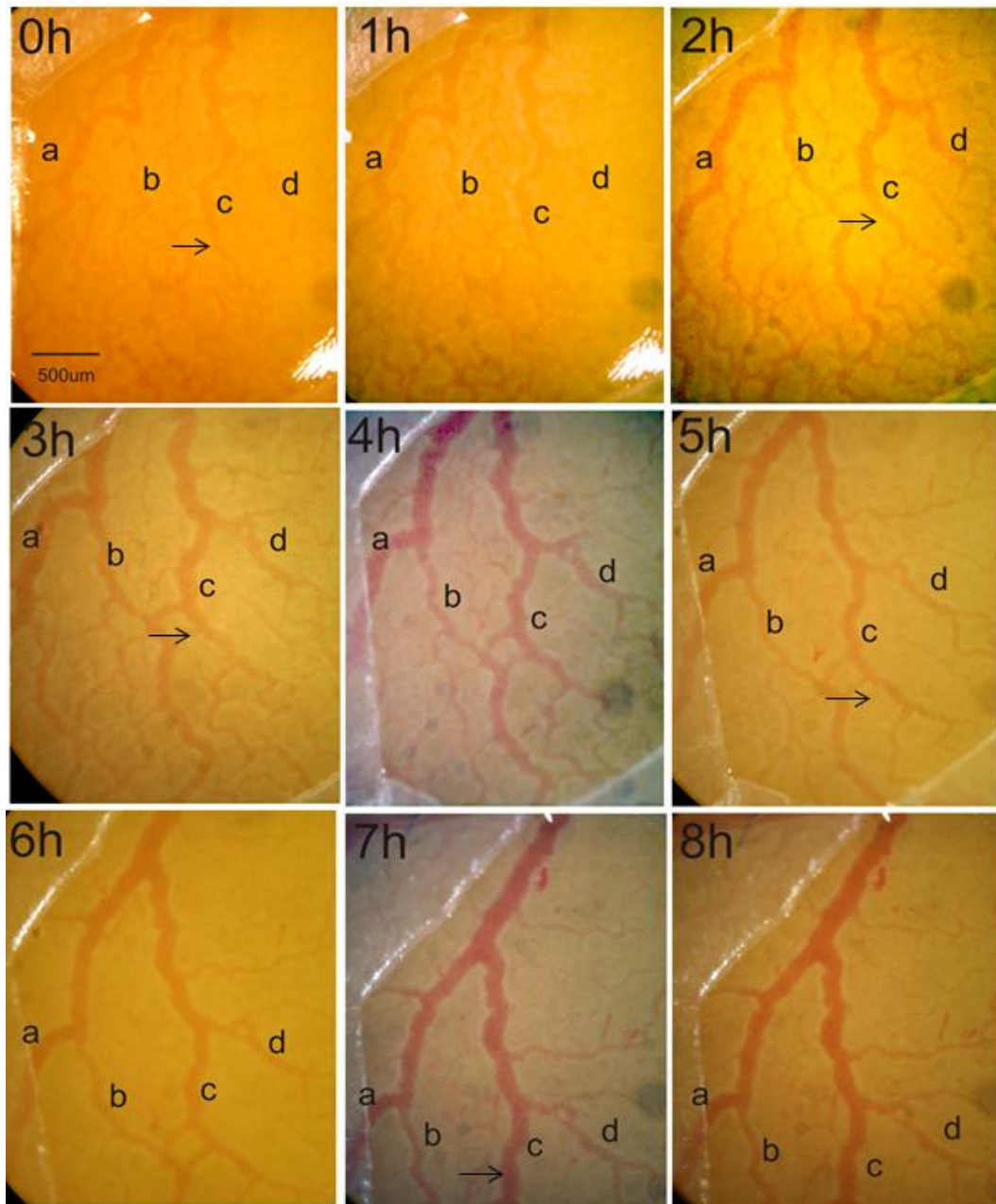


**Figure 3.8** Following right vitelline artery tied-ligation, the distal branches of the left vitelline artery remodelled in a flow-dependent manner

Representative micrographs of the distal branches of the left vitelline artery over a time-course from T0 post tied-ligation to 8h. At 2h post tied-ligation vessels labelled **c** and **d** appeared of equal size. By 3h vessel **c** appears to have a wider diameter. From 4h onwards branch **d** regresses whilst vessel **c** persists to become a forming collateral vessel. Arrows point to developing collateral vessel **c** (n=12 embryos). The same process occurring in the same embryo can be seen at a lower magnification in the Appendix (Figure A1).

### 3.5 Using Particle Image Velocimetry to measure blood flow in collateral vessels

A technique to measure blood flow, in real-time, in developing collateral vessels could determine if flow is involved in driving a selection process. I therefore investigated one such technique to measure flow within developing collateral vessels, Particle Image Velocimetry (PIV). Previous studies have characterised flow profiles within chick extra-embryonic vascular network (Lee and Lee, 2010, Poelma *et al.*, 2010) or investigated the effects of venous clip obstruction and shear stress responsive genes (Groenendijk *et al.*, 2005). However, no previous work has measured blood flow or velocity in collateral vessels in chick embryos. These vessels are smaller than assessed in previous studies, and their peripheral site, and highly dynamic remodelling, presents significant technical challenges. I therefore attempted to establish whether it is possible to use PIV to quantify blood velocity in collateral vessels in the chick embryo. These studies were performed in the lab of Dr Christian Poelma, Delft, The Netherlands (section 2.3).

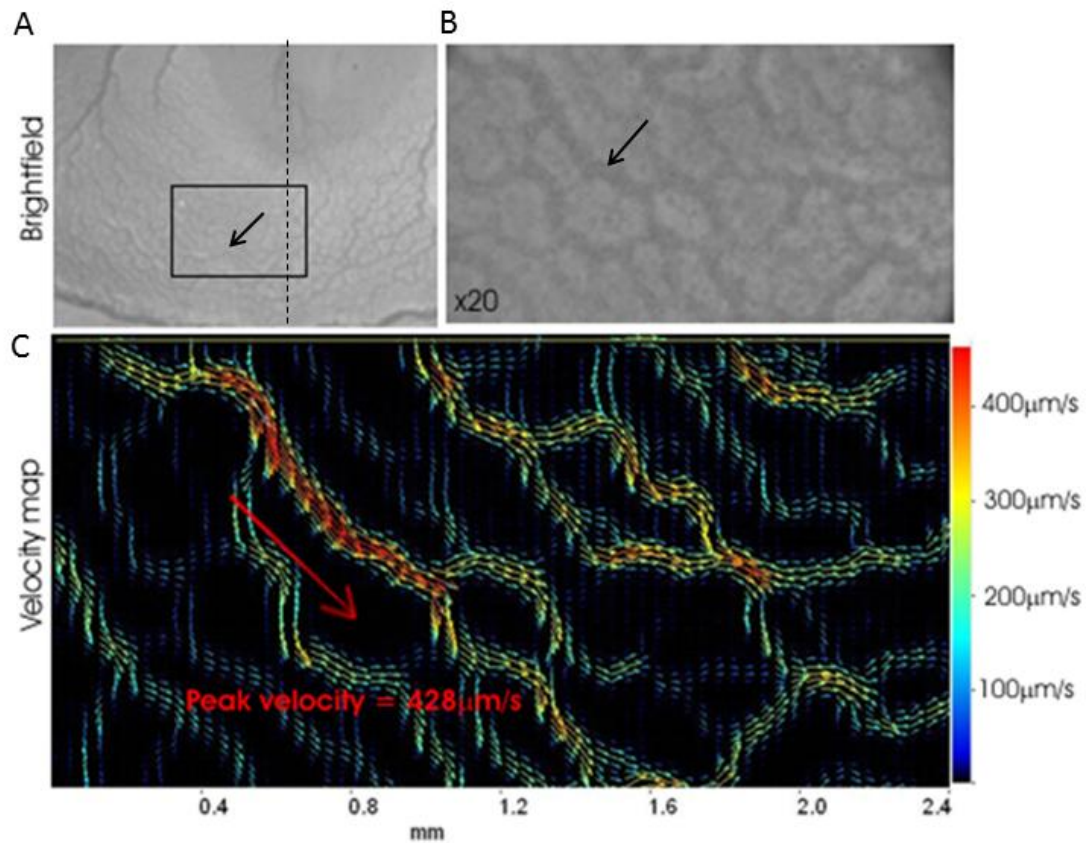
I measured blood velocity in developing collateral vessels, 4 hours after tied-ligation - a point at which these are only just apparent on static micrographs (see Figure 3.5). Figures 3.9-3.11 show PIV velocity maps, false coloured to indicate velocity, in an area of collateral vessel development. I annotated velocity on a single vessel for illustration; the dataset allows extraction of velocity at any point in the image acquired, which is a significant improvement over techniques such as Doppler which only allow single point assessment.

Figure 3.9 shows the brightfield image of the embryo assessed at a low magnification to demonstrate the area of focus and developing collateral vessels. The velocity map shows the coloured vectors in the direction of flow. The fastest blood velocity detected in Figure 3.9 was 428  $\mu\text{m}/\text{second}$ . At a later timepoint (7 hours post-ligation) the highest velocity in a collateral vessel was 488  $\mu\text{m}/\text{second}$  (Figure 3.10).

Figure 3.11 shows images acquired 4 hours and 7 hours post-ligation in an individual embryo, aligned to allow comparison of size and velocity of the same vessel (blue arrow)(i.e. not just focussing on the vessel carrying the fastest velocity). The image at 4 hours (Figure 3.9) was rotated and cropped to orient to the appearance in the 7 hour velocity map. These images show that the collateral network in this individual chick increased both in diameter and velocity between 4 and 7 hours post-ligation. Figure 3.10 shows that at 4 hours the vessel indicated by the arrow measures  $69\ \mu\text{m}$  in diameter and flow is  $300\ \mu\text{m}/\text{second}$ , but at 7 hours this same vessel had increased in size to measure  $100\ \mu\text{m}$  and velocity has increased to  $488\ \mu\text{m}/\text{second}$ .

I next attempted to determine whether it was possible to assess velocity serially in the same embryo at later timepoints. This was technically challenging, as many embryos died (discussed further in the conclusions at the end of this chapter), and identification of the same region of interest in an area undergoing both embryonic growth and collateral development was difficult. I was able to assess collaterals at 24 hours after ligation. At this timepoint collaterals are larger and somewhat easier to image. Figure 3.12 shows a single embryo where I have quantified blood velocity and diameter of 4 separate collateral vessels.

These results are the first demonstration that PIV is able to characterise haemodynamics in developing collateral vessels in the chick embryo over time. I did not use these data to calculate shear stress as I felt that from the limited repeats (n numbers), the data was not sufficient to draw conclusions about shear stress in these collateral vessels. Although preliminary (as I was only able to spend a small amount of time in Delft performing these studies) these results show promise in allowing a more comprehensive assessment of the alterations occurring during vessel remodelling.



**Figure 3.9 Particle Image Velocimetry recorded blood velocity in collateral vessels at 4 hour post-tied-ligation**

**A** Brightfield image of a representative HH st 17 embryo, to show the area of the vitelline vasculature recorded at 4 hours post tied-ligation. Dotted line indicates midline. Box indicates area of B. Arrow indicates developing collateral vessel recorded with PIV at 4h  
**B** Brightfield image of boxed area in **A** at higher magnification to show the developing collateral vessel recorded (arrow).  
**C** PIV velocity map shows developing collateral vessel at 4 hours post tied-ligation. Arterial flow is indicated by direction of vectors (small coloured arrows) which pointed from left to right. The blood velocity in the main collateral vessel in the centre of the image (red vectors) was  $428 \mu\text{m}/\text{second}$ . Flow was towards the midline of the embryo/yolk sac (representative image from  $n=3$ )

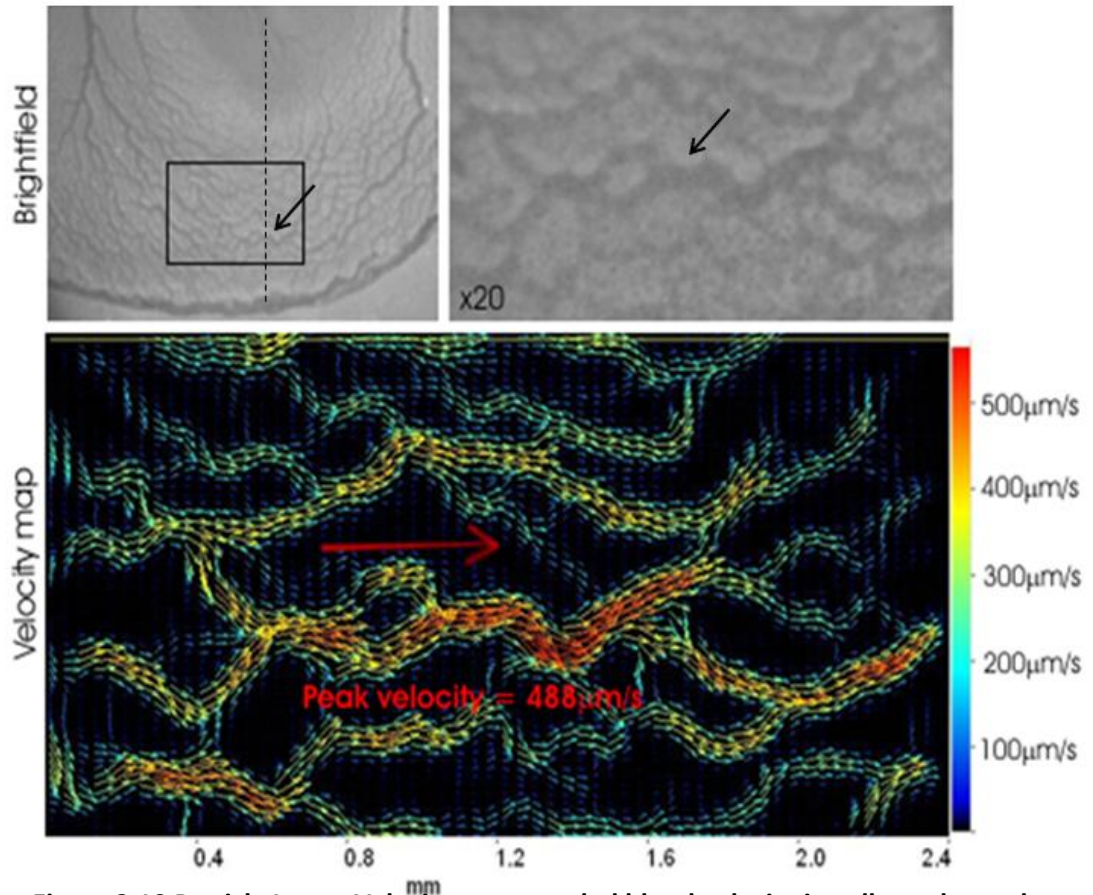


**Figure 3.10 Particle Image Velocimetry recorded blood velocity in collateral vessels at 7 hour post tied-ligation**

**A** Brightfield image of same embryo as Fig 3.9, 7h post tied-ligation. Dotted line shows midline. Box indicates area containing collateral vessels that crossed the midline. Arrow indicates collateral vessel recorded with PIV at 4h and 7h **B** Brightfield image of boxed area in **A** at higher magnification to show the 7h collateral vessels recorded in **C** (arrow). **C** PIV velocity map shows 7h collateral vessel. The vessel with the highest blood velocity was recorded to be  $488\mu\text{m/s}$  (representative image from  $n=3$ )

A

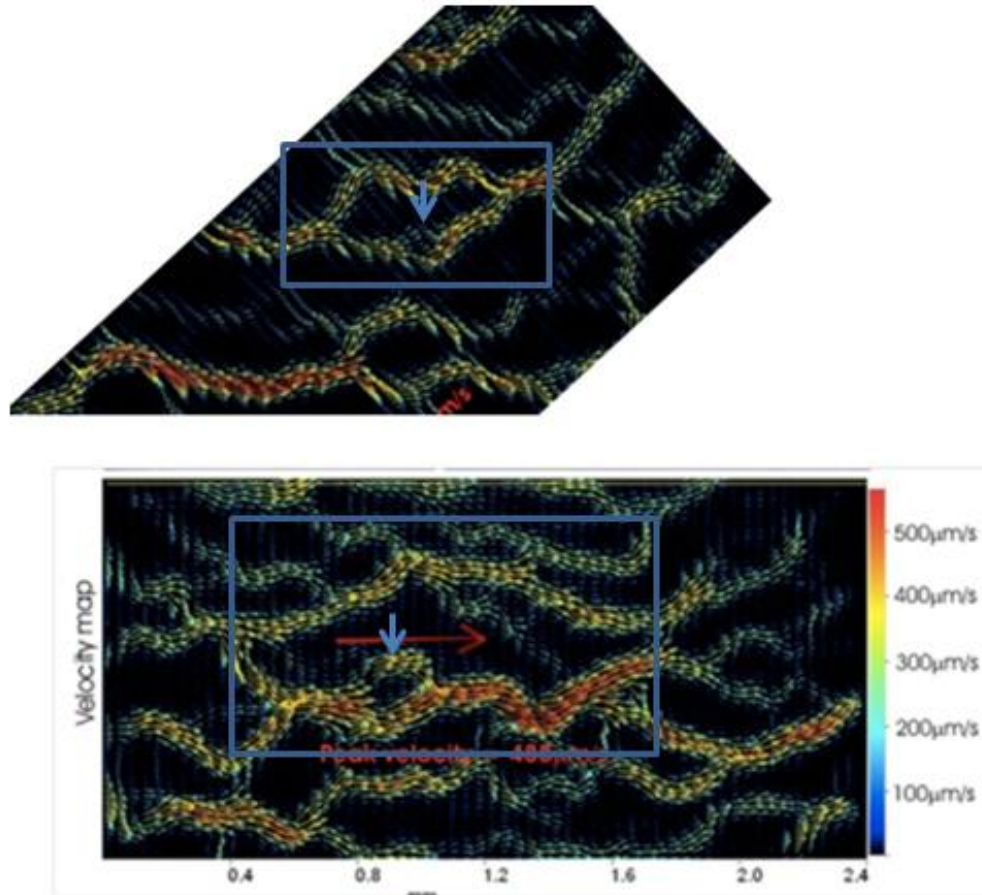


**Figure 3.11** Alignment of 4h and 7h images revealed an expansion of collateral network over time and increased velocity within collateral vessels

**A** Individual velocity maps from vessels recorded at 4h and 7h post tied-ligation (Figures 3.9,3.10). Vessels can be aligned by identifying the large loop in the vasculature (indicated by blue box) and the smaller loop inside this (indicated by blue arrow). This allows the same vessel to be followed over time points to assess changes in size and blood velocity. At 4 hours the vessel indicated by the arrow measures  $25\mu\text{m}$  in diameter and flow is  $300\mu\text{m}/\text{second}$ . At 7 hours this vessel had increased in diameter to  $55\mu\text{m}$  and velocity to  $488\mu\text{m}/\text{second}$  ( $n=1$ )

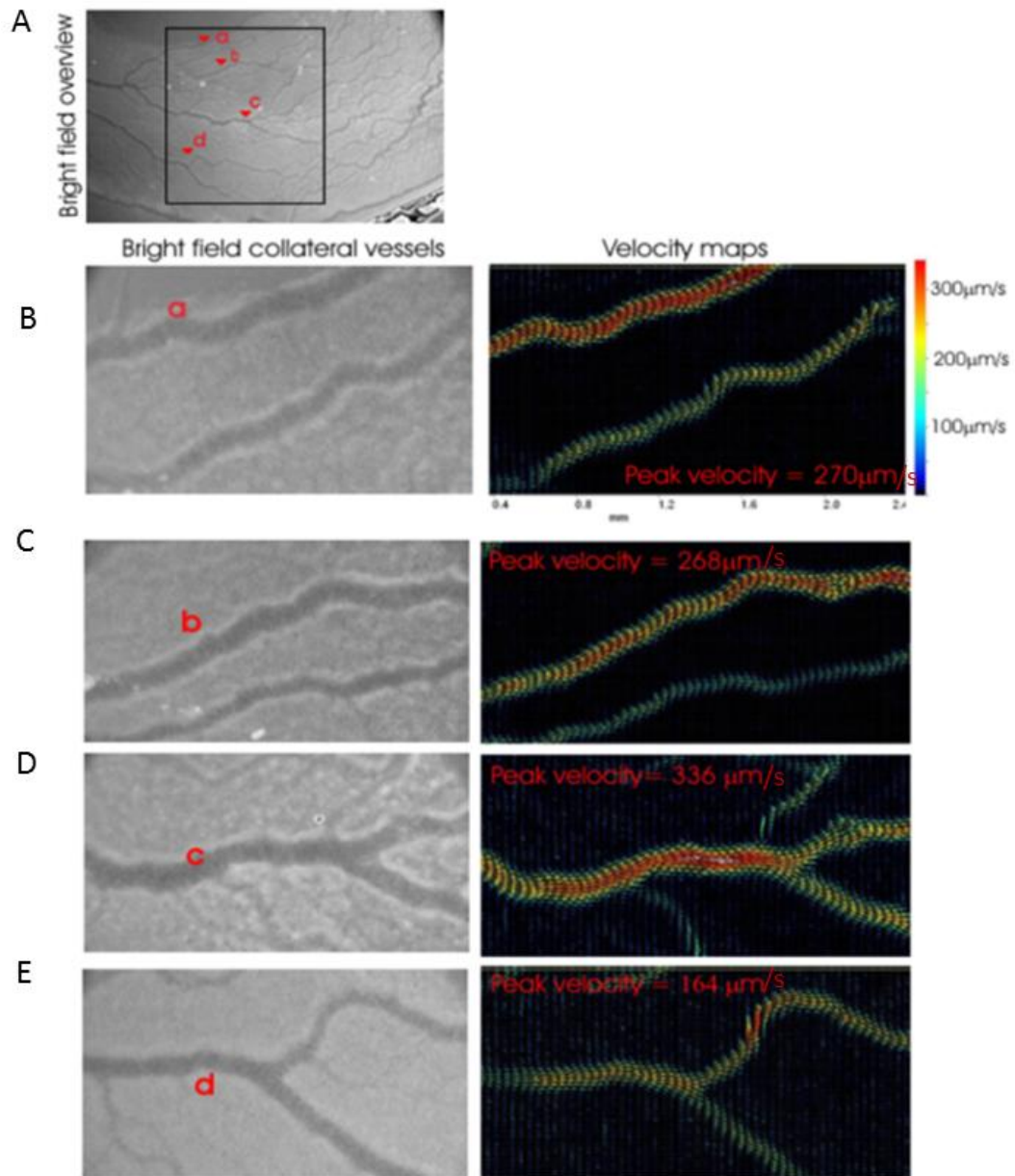


**Figure 3.12 Blood velocity in collateral vessels measured by PIV 24 hours post-tied-ligation**

**A** Brightfield image of the area containing collateral vessels at 24h post tied-ligation. Labelled vessels (a-d) were assessed using PIV. **B-E** Collateral vessels (a-d) were recorded and are shown as a brightfield image (left panels) and as a velocity map (right panels). Vessel c had the fastest velocity ( $336\mu\text{m/s}$ ) High velocity is represented by red colour (vectors) and can be correlated to the colour map in B. (Representative recordings of collateral vessels from 3 embryos)

### **3.6 Histological examination of the area of collateral vessel formation**

I first established that I could identify vessels in the un-instrumented extra-embryonic tissue. Previous studies have shown that capillaries form from the mesoderm, and can first be detected shortly after HH st 13 (Flamme, 1989). Figure 3.13 shows brightfield images which were taken over time in one representative embryo from HH st 13-st 17. As depicted in Figure 3.13, my observations concurred with earlier reports (Flamme, 1989), showing that capillaries are readily detected in the extra-embryonic mesoderm by HH st 15. I next performed histological/histochemical analyses of the extra-embryonic vasculature, to determine the cellular composition of developing collateral vessels.

#### **3.6.1 Re-modelled collaterals express the endothelial cell marker, VE-cadherin**

To observe the structure of the extra-embryonic tissue to determine whether I could successfully visualise vascular structures in cross-sections, I first dissected easily accessible proximal vitelline vessels. These vessels could be isolated from surrounding tissue and cross-sectioned to show endothelial cells of the vessel wall, when labelled with an endothelial specific antibody. Anti-vascular endothelial-cadherin (VE-cadherin) was found to successfully label endothelial cells in the chick specifically (Section 2.16.2), I therefore chose to use this antibody to orientate vascular structures in my immunohistochemical studies. Figure 3.14 shows immunohistochemical labelling of HH st 17 proximal vitelline vessels with anti VE-cadherin.

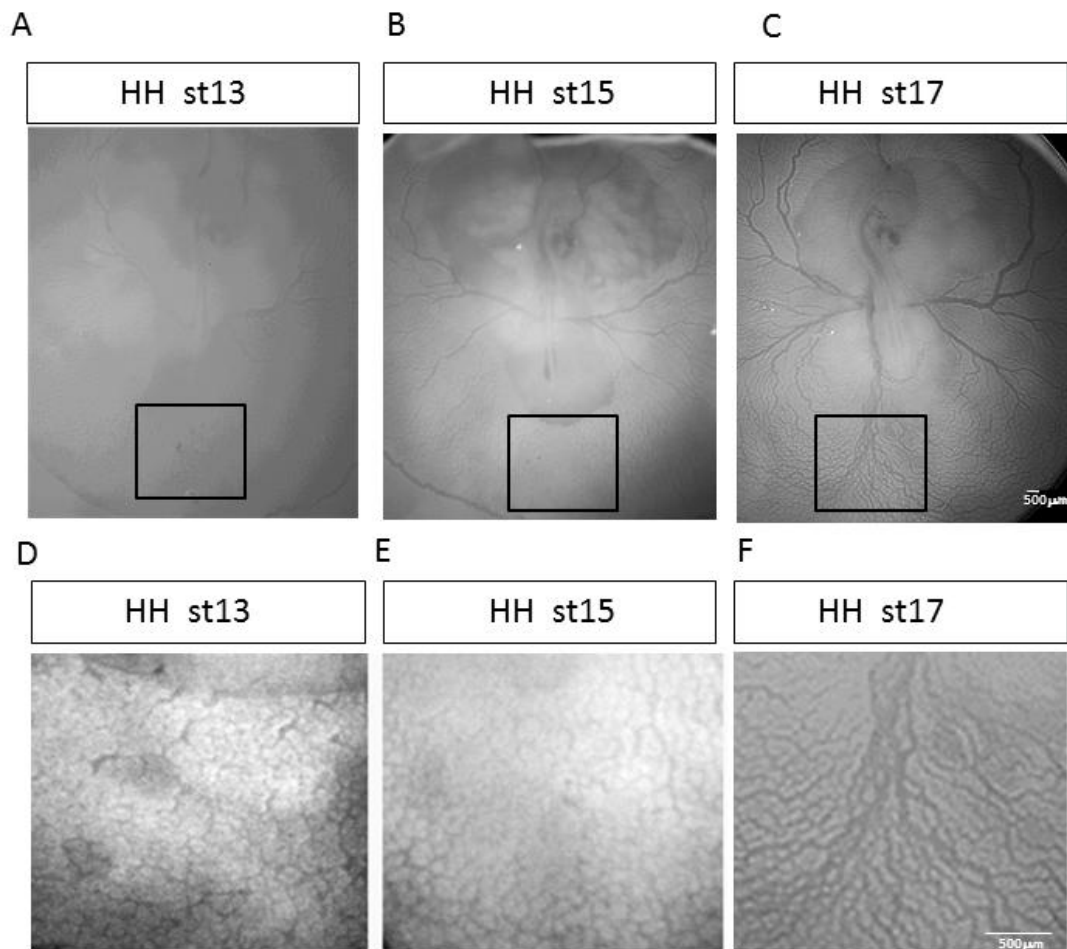


**Figure 3.13** Micrograph images to show the development of the extra-embryonic vascular network in the area of collateral vessel formation at the posterior of the chick embryo

The panels show representative images of developing extra-embryonic vessels in one embryo from stage HH st 13-17. **A-C** shows whole developing embryos from HH st13-17 at a lower magnification. Black boxes indicate areas of focus of D-F. **D** At HH st13 small connecting capillaries can be seen in the posterior-medial vitelline territory. **E** By HH st15 these small capillaries were more structured and resembled a primitive vascular network **F** By HH st17 the small capillary network remodelled into a vitelline vein at the centre line of the tail of the embryo. Venules either side of the vein can be seen to connect to a main vessel, delivering blood back to the embryo. (Representative embryos/images n>100 embryos over the course of the project)

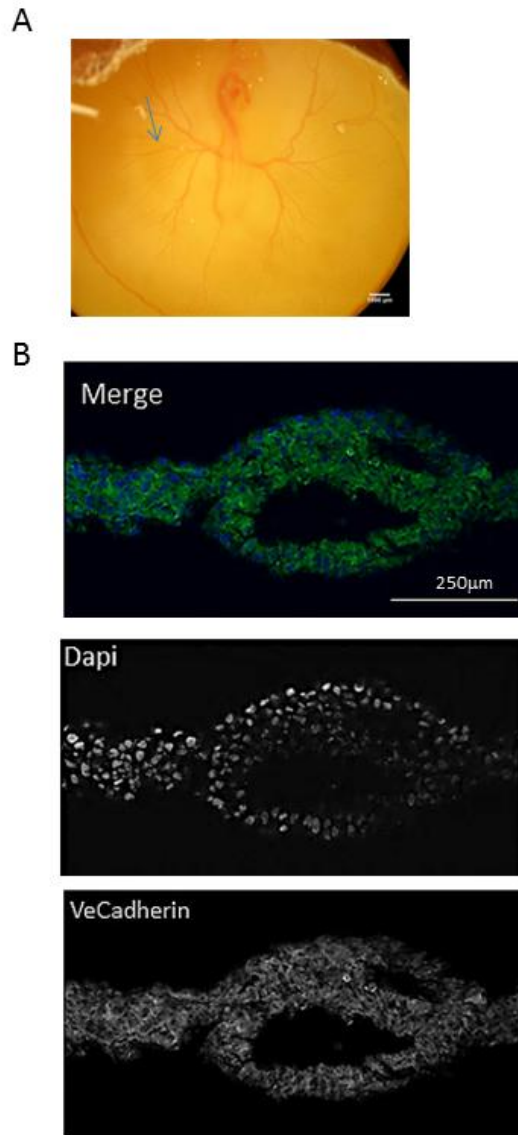


**Figure 3.14 The vessel architecture of the proximal vitelline vessel of a HH st17 chick embryo**

**A** Micrograph of a HH st 17 chick embryo. Blue arrow indicates the proximal vitelline vessel sectioned and stained histologically **B** a transverse section through cryo-sectioned vitelline vessel. The vessel lumen can be seen surrounded by endothelial cells. DAPI staining labelled cell nuclei, VE-cadherin can be seen to border the edges of endothelial cells. The merged image shows VE-cadherin labelling in green. Representative examples from 6 embryos.

I next sought to elucidate the structural architecture of the collateral vessels. I performed Haematoxylin and Eosin (H&E) staining on transverse sections through the extra-embryonic tissue in the area of collateral vessel formation in HH st 17 chick embryos. Figure 3.15B shows a representative section showing lumenised vessels with the appearance of a single-layered capillary. As suggested in previous reports, there is no evidence of vascular smooth muscle investment of the vitelline vessels until at least HH st 27 (Lucitti *et al.*, 2005) and even at this stage there is only a thin layer of smooth muscle which does not contain proteins such as elastin and therefore is unlikely to be capable of regulating vascular tone.

H&E staining only showed cellular composition of the vessels and could not confirm that the collateral vessels were comprised of endothelial cells without a smooth muscle coat. I therefore next attempted to confirm their endothelial identity. VE-cadherin immunostaining labelled vessels in frozen cryosectioned extra-embryonic tissue, confirming their endothelial composition (Figure 3.15C).

Having ascertained that collateral vessels express VE-cadherin, I asked whether VE-cadherin could be detected on collateral vessels in whole mount preparations. Tied-ligated embryos were examined 24 hours post-surgery in wholemount preparations which showed VE-cadherin immunolabelling was readily detectable in collateral vessels (Figure 3.16).

The data did confirm my expectation that collateral vessels are composed of VE-cadherin expressing endothelial cells. However, this experiment highlighted the limitations of whole mount immunolabelling in the chick embryos in the area of collateral vessel formation and suggested that cross-sectioned tissue provided more valuable data. I therefore chose to use cross-sections of tissue for future immunohistochemical assays.

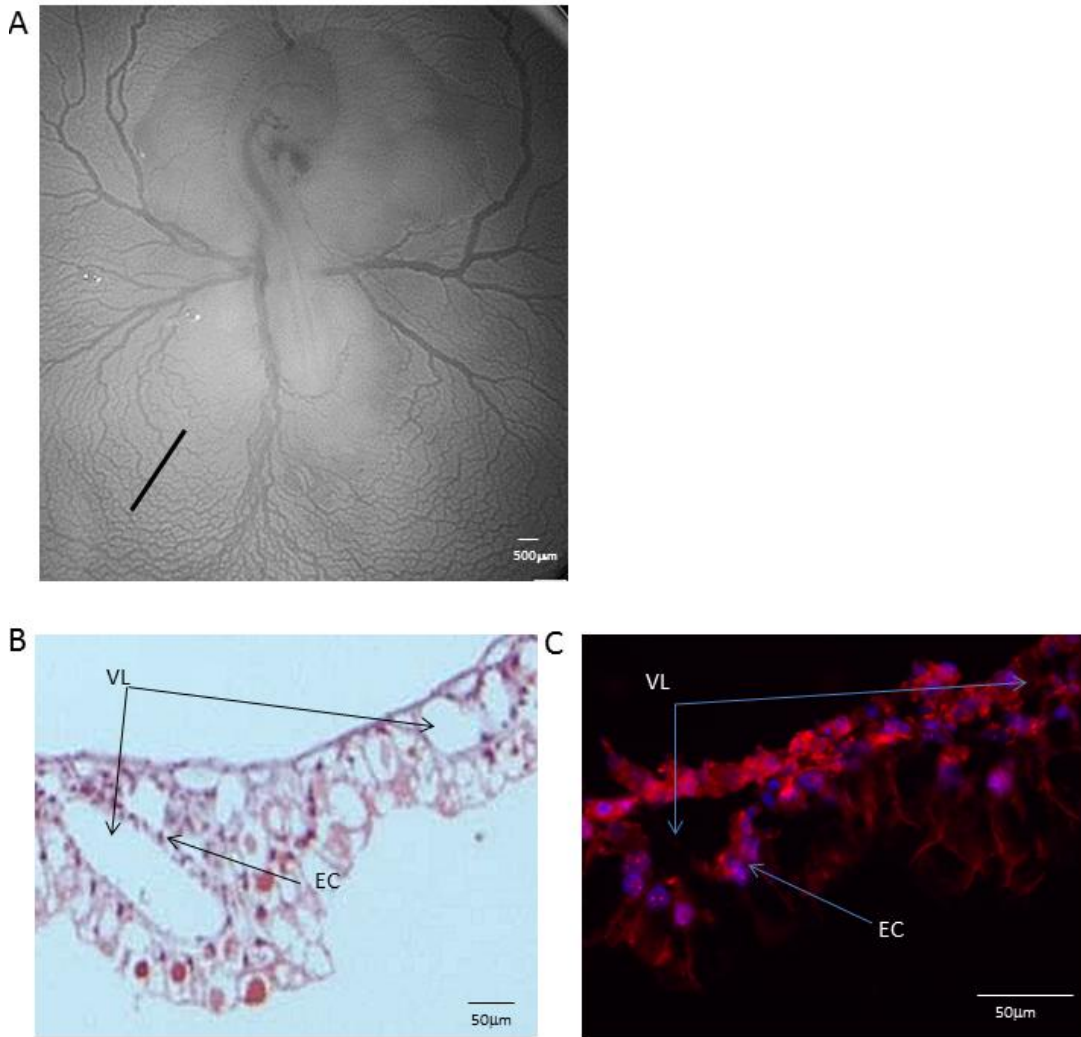


**Figure 3.15 The vessel architecture of the extra-embryonic tissue of a HH st17 chick embryo**

**A** Micrograph of a HH st17 chick embryo. Black line indicates the area of extra-embryonic tissue sectioned and stained histologically **B** H&E staining of a transverse section through the extra-embryonic tissue. Vessel lumen can be seen (VL) surrounded by a single layer of cells (EC). **C** shows a similar transverse section through cryo-sectioned extra-embryonic tissue from the same area, from a different embryo. Immunofluorescent anti-VE-cadherin labelling shows positively labelled endothelial cells (EC) surrounding a vessel lumen (VL). Representative examples from 6 embryos.

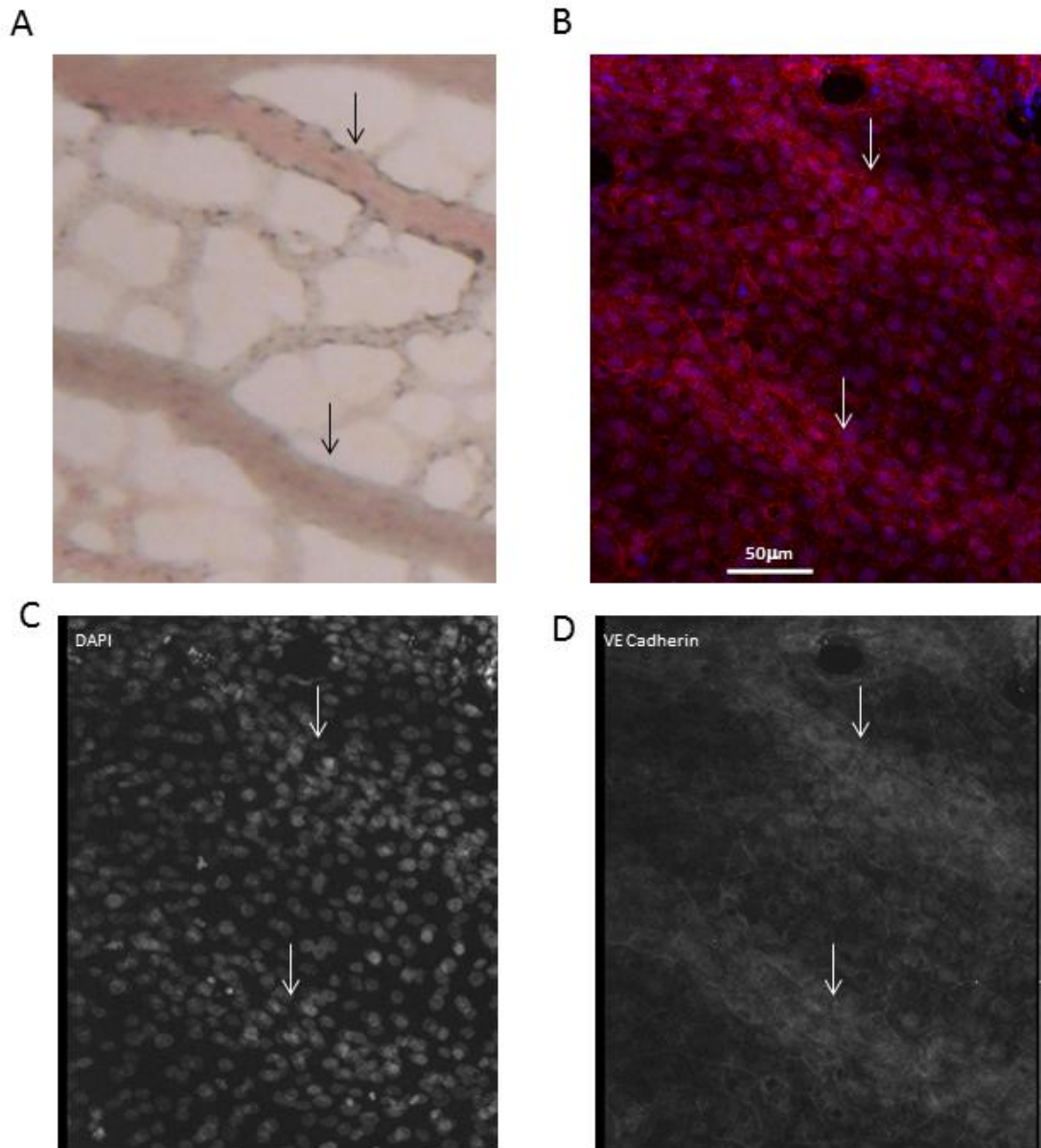


**Figure 3.16** Immunohistochemistry with anti-VE-cadherin labelling was used to identify collateral vessels in wholemount tissue dissected from the area of collateral vessel formation 24 hours post tied-ligation.

**A** shows two collateral vessels in a brightfield image (black arrows). **B** shows collateral vessels (white arrows) labelled with VE-cadherin antibody. The borders of the endothelial cells could be seen. **C** shows the DAPI labelling of the endothelial nuclei in the blue channel. **D** shows the VE-cadherin labelling in the red channel. Representative image from 4 embryos.

### 3.7 Collateral vessels change expression of arteriovenous markers during flow-induced remodelling

Previous research has found that endothelial cells of the vitelline network are plastic in their vascular identity and endothelial cells express arterial/venous markers depending on their haemodynamic environment (le Noble *et al.*, 2004). They investigated arterial/venous plasticity in the chick model using *in situ* hybridisation to assess mRNA expression of endothelial cell markers neuropilin 1 (*nrp1*), ephrin B2, EphB4 and neuropilin 2 (*nrp2*) after occlusion of the right proximal vitelline vessel. The focus of the le Noble study (2004) was on the proximal vitelline vessels, in particular the occluded artery which became venularised after 24 hours of vessel occlusion. The group observed expression of these arterial/venous markers in the proximal vitelline vessels at different timepoints following vessel occlusion. Flow was found to up-regulate arterial markers and in the occluded vessels without flow, venous markers were expressed (le Noble *et al.*, 2004).

Buschmann and colleagues (2010) also observed that gene expression could be altered by changes in flow. The group used *in situ* hybridisation in ligated embryos, to study expression of the connexin gene *Gja5*. This was upregulated in collateral vessels at 20 hour after ligation. The group concluded *Gja5* expression was therefore driven by arterial flow (Buschmann *et al.*, 2010).

As yet, no study has studied different timepoints following ligation to address if **collateral vessels** alter their arterial/venous identity over time, in a manner that correlates with altered haemodynamic environment. I therefore wanted to characterise the arterial/venous identity of collateral vessels in the chick model and test the hypotheses that collateral vessels acquire arterial identity over time. I did this by observing *nrp1* and *nrp2* expression in collateral vessels.

I performed *in situ* hybridisation following ligation to track the changes in endothelial vascular markers during collateral vessel development. The timepoints I selected reflected two key phases of collateral vessel formation observed in the timecourse experiment (Figures 3.5, 3.7): at 4 hours post-ligation collateral vessels were developing and beginning to extend across the midline; at 12 hours post-ligation the number of collateral vessels has ceased to increase and vessels subsequently either persisted or regressed (Figure 3.7).

I first sought to optimise riboprobes directed against an arterial marker, *nrp1* (Moyon, 2001) and a venous marker, *nrp2* (le Noble, 2004) in unligated embryos. I used HH st 20 embryos as at this stage the venous network has developed and overlies the arterial vitelline vessels giving me an opportunity to compare expression patterns. Figure 3.17A shows a representative schematic of the blood flow direction and arterial/venous patterning in a HH st 17 chick embryo. Figure 3.17B and C show wholemount *in situ* hybridisation preparations of the proximal vitelline vessel branches. Arteries expressed *nrp1*. Veins overlying the arteries appear clear as they do not express *nrp1*. Figure 3.17C in contrast showed expression of *nrp2*. Cells in the venous network expressed *nrp2* whereas the vitelline artery beneath the vein showed no expression.

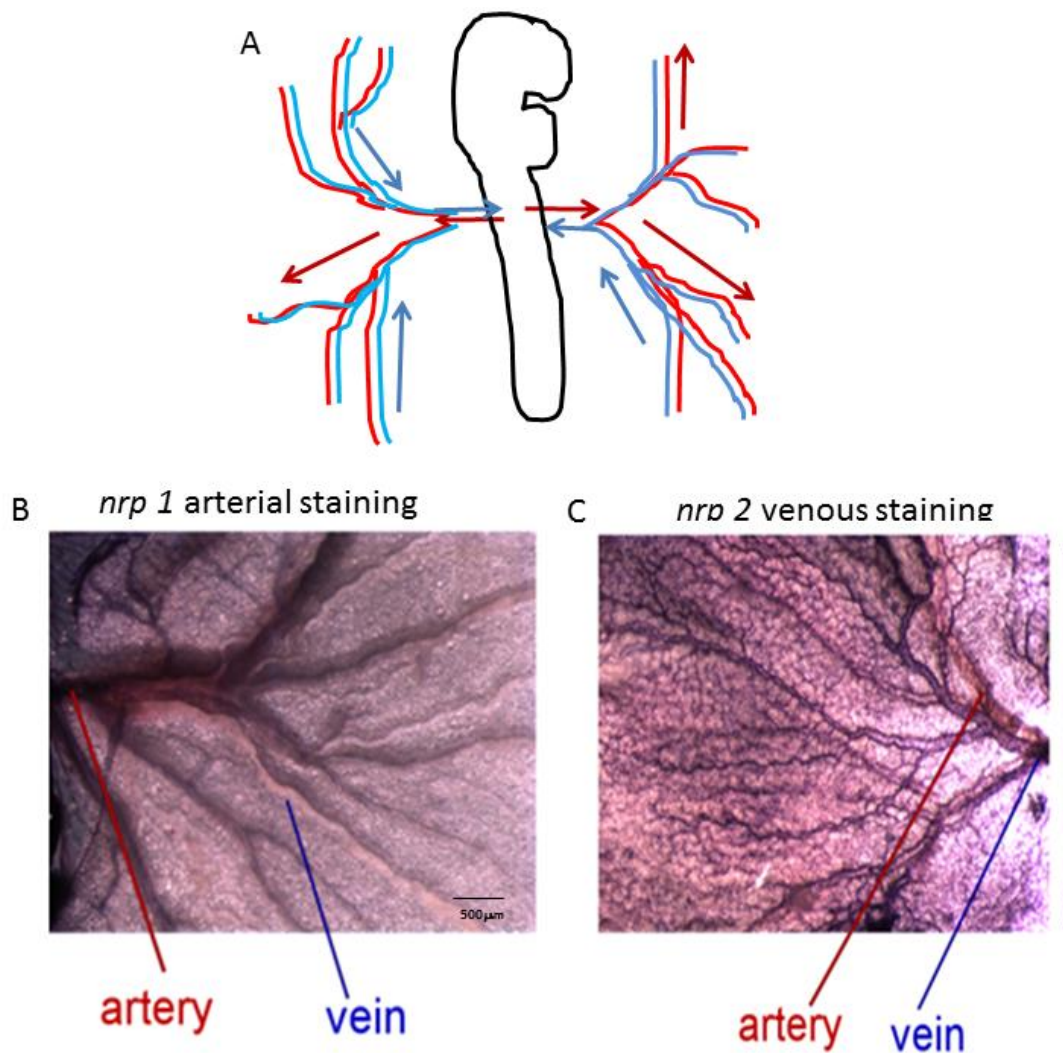


**Figure 3.17** Neuropilin 1 expression can be seen in wholemount vitelline arteries of HH st 20 chick embryos. Neuropilin 2 venous marker labels the veins overlying the arteries.

**A** At HH st20 veins overlie arteries in the vitelline vasculature. This schematic shows direction of blood flow in this cis-trans network. Red arrows indicate arterial flow away from the embryo body. Blue arrows represent venous blood flow returning to the embryo **B and C** wholemount views of *in situ* hybridisation for *nrp1* and *nrp2*. **B** shows dark blue staining in the arterial branches of the right proximal vitelline artery indicating neuropilin1 (*nrp1*) expression. Veins are clear in comparison and show no *nrp1* expression **B** shows the opposite staining pattern. Venous branches were superimposed over the arterial branches of the left vitelline artery and stained dark blue indicating *nrp2* expression. (n=6)

I next examined expression of these genes during collateral vessel formation. Figure 3.18 shows *nrp1* and *nrp2* in situ hybridisation after ligation. Four hours after tied-ligation the unligated side of the chick showed increased *nrp1* expression, compared to the ligated side. The area of collateral development (indicated by the box, Figure 3.18 A-B) showed high *nrp1* expression (Panels A and C). At the same time, expression of *nrp2* was downregulated in this region (Panels B and D). This suggests that venous capillaries become arterial as they are recruited into the expanding arterial collateral network. By 12 hours post-ligation, collateral vessels expressed *nrp1* but not *nrp2*, suggesting that they adopt an arterial identity over time.

Together these experiments suggest that increasing flow, i.e. altering haemodynamics, within the remodelling collateral vessels provokes a down-regulation of venous markers on endothelial cells and an up-regulation of arterial markers. *Nrp1* expression increases over time, was in keeping with the observation that as collateral vessels develop and become established, they carry arterial flow (direction of flow from left to right) across the midline to the unperfused tissue (Figure 3.5).

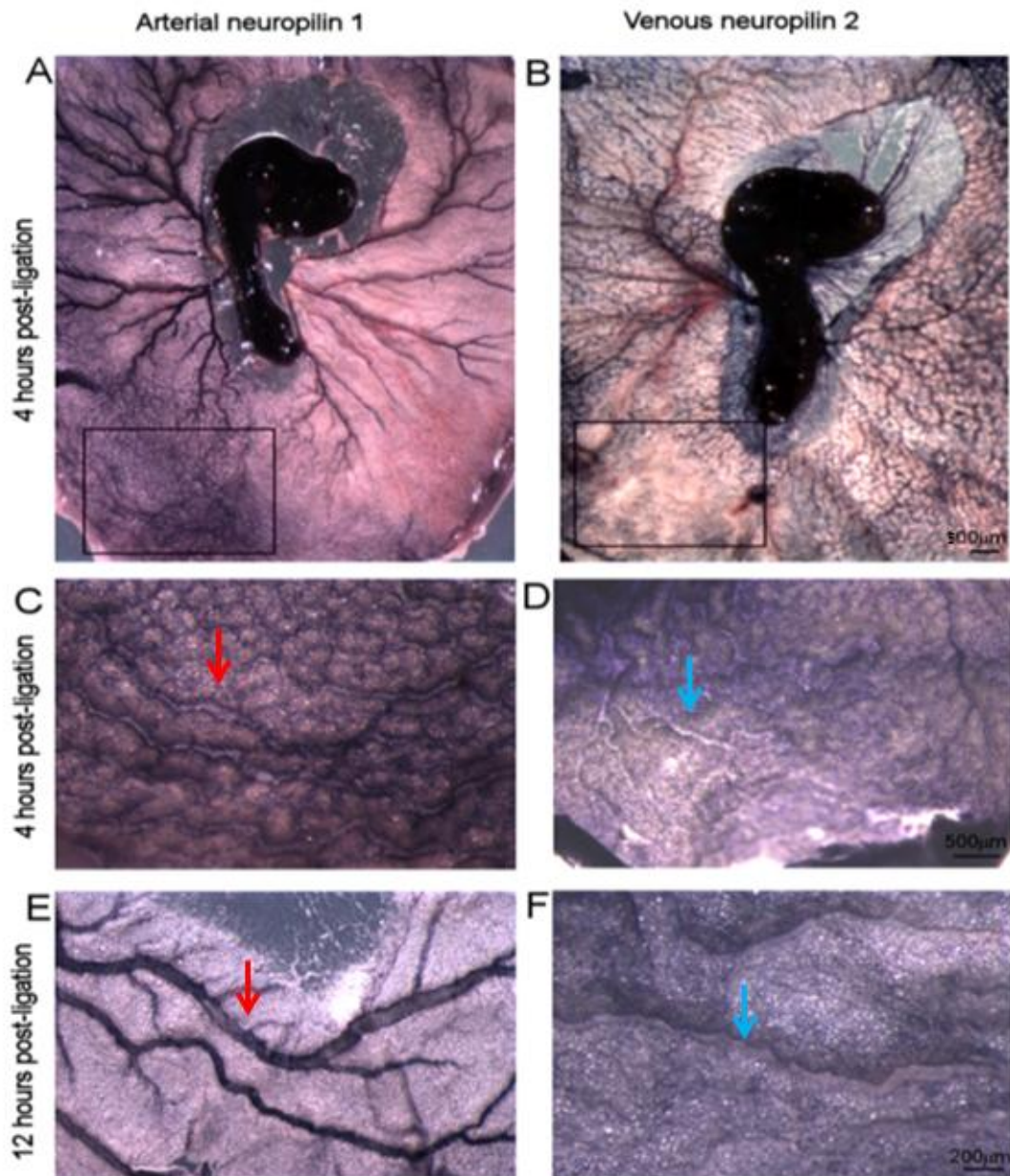


**Figure 3.18 Arterial neuropilin 1 is upregulated in collateral vessels**

**A** Shows up-regulation of nrp1 expression in the area of collateral vessel development (boxed area) 4h after tied-ligation. The right side of the embryo shows less expression. **B** Shows down-regulation of nrp2 expression in the area of collateral vessel development indicated by less staining **C** Higher magnification images of **A** showing nrp1 positive collateral vessels at 4h post tied-ligation (red arrow) **D** shows that there no nrp2 staining was detected in the collateral vessels at the same time-point (blue arrow points to clear vessel). **E** By 12 h post tied-ligation nrp1 is expressed by endothelial cells of collateral vessels (red arrow). Collateral vessels appear dark blue. **F** No expression of nrp2 was detected in collateral vessels at this time-point (blue arrow points to comparatively clear vessel). (n=6 embryos per group)

### **3.8 Is proliferation increased in areas undergoing collateral vessel remodelling?**

Collateral vessels are already apparent 4 hours post-ligation and their number increases rapidly (Figures 3.5, 3.7). As outlined in Chapter 1, little is understood of the mechanisms that govern collateral vessel formation. However, a number of studies suggest that in mammals, collateral vessel formation is accompanied by proliferation of endothelial and smooth muscle cells (Schaper *et al.*, 1971, Hofer *et al.*, 2001). I therefore wanted to assess whether I could detect an increase in proliferation during collateral vessel remodelling in the chick, in a system in which vessels appear composed only of endothelial cells.

I applied BrdU, topically to sham or tied-ligated embryos immediately after ligation to assess proliferating cells. Embryos were sacrificed after 4 hours, sectioned, and immunolabelled with anti-BrdU antibodies in the area of collateral vessel formation (section 2.22.1). Each embryo produced around 6 sections. For each section, BrdU positive cells were analysed (section 2.22.1) and the average proliferation index calculated for each embryo (Figure 3.19). Proliferation index was calculated by dividing the total area of BrdU positive nuclei by the total area of DAPI positive nuclei. These percentage area measurements were necessary as antigen retrieval damaged nuclei making it less accurate to count these individually. I found that the proliferation index was not significantly increased in tied-ligated embryos compared to sham-ligated controls (sham-ligated embryos  $10\pm 3\%$ ; tied-ligated embryos  $15\pm 3\%$ ) although there was a trend towards increased proliferation in tied-ligated embryos. I cannot conclude that proliferation does not play a role in the remodelling process, but no significant differences in proliferation were detected between sham and tied-ligated embryos.

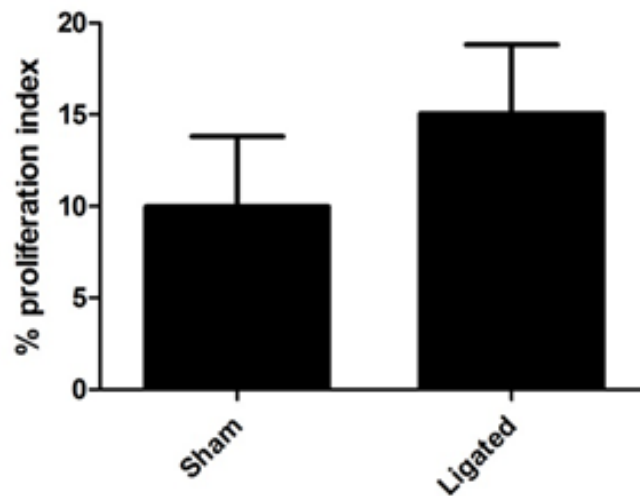


**Figure 3.19 BrdU proliferation index in sham and tied-ligated embryos 4 hours post-ligation**

Proliferation index was calculated based on area of positive staining for DAPI and BrdU. There was no statistically significant difference in proliferation index between sham and tied-ligated groups at 4 hours post-ligation (n=6. Student's t-test = n.s)

### 3.9 Discussion

In this chapter I set out to characterise collateral vessels that form in the extra-embryonic vasculature of the chick embryo following unilateral vitelline vessel occlusion. My data showed that following unilateral proximal vitelline vessel ligation, downstream distal branches in the unligated territory developed into collateral vessels. These collateral vessels increased in number until a plateau around 12 hours after ligation, before declining in number, with continued expansion of the persisting collateral vessels. This appears to involve selection of more efficient collateral vessels which persist over time but it was not possible to confirm what drives this selection. Collateral vessels were shown however to remodel from pre-existing vessels to carry arterial (afferent) blood across a previously venous territory. Histological examination showed that collateral vessels are predominantly endothelial and that this process involves a change in endothelial cell arterio/venous

identity (small venules become arterial as they are incorporated into the collateral vessel network).

I first set out to address whether I could successfully manipulate flow in this system without harming the embryo, and secondly, whether I could measure any changes in diameter of the left, (unligated) proximal vitelline artery, following occlusion of the right proximal vitelline artery. The unligated artery did indeed increase in vessel diameter, immediately post tied-ligation, and 10 minutes after ligation. This data suggested that the ligation neither caused the embryo harm nor lead to a marked reduction in cardiac output. My findings were also consistent with those of Buschmann *et al.*, (2010) published during the course of my work who showed similar effects on the unligated artery diameter 5 hours after ligation (Buschmann *et al.*, 2010). Early observations to monitor immediate effect of ligation on the size of the unligated vessel had not previously been investigated.

The response to arterial occlusion in mammalian models is well documented and it is widely accepted that, following vessel occlusion, local changes in haemodynamics are the main driving force to remodelling. It also widely accepted that arteriogenesis is not due to contributions from angiogenic or ischaemic factors (section 1.3). A large proportion of this work derives from Wolfgang Schaper who refers to shear stress as the driving force of collateral vessel formation (Schaper, Scholz 2003). Following extensive conversations with experts in the field of biomechanics (Professor Rod Hose, Professor Pat Lawford, Medical Physics, University of Sheffield) I conclude that my data reflected a complex system whereby it is likely that a combination of factors, including pressure, flow, shear stress, vaso-regulation and cardiac output influence the remodelling response observed in my model. From my data alone, I cannot conclude which of these individual or combination of factors are driving collateral vessel formation in my model, although the literature suggests local shear stress may play a driving role.

Heart rate measurement following ligation showed no adverse effect of the arterial occlusion compared to sham-ligated controls (Figure 3.2B). Heart rate was around 120 beats/min. This rate is slightly lower than chick embryos at the same stage in other studies, such as Lee *et al.*, (2007) who described a mean heart rate of  $146 \pm 2$  beats/min (Lee *et al.*, 2007). This slight reduction in heart rate could be due to a cooling of the egg during experimental periods. The speed of my ligations was initially slow (4-5 minutes) but it is worth noting that this was not the case with later experiments as the speed of my ligations improved over the course of my project (1min-30 seconds). Temperature can induce vasoconstriction (Nakazawa *et al.*, 1985), although this was also unlikely to have affected results in my model due to the lack of smooth muscle in the vitelline vessels of the embryo at this stage and therefore a lack of vascular tone (Lucitti *et al.*, 2005). I therefore do not consider it likely that this adversely influenced my findings. However, to remove any concerns a heated lamp could be used to keep a constant temperature during experimental procedure.

I acknowledged that in this study, measurements of collateral vessels from the micrograph images were subjective (section 2.24). I therefore attempted to reduce error/bias in the following ways. I made repeated observations and measuring vessels with the same tools and protocol each time. This was controlled for with repeated experiments and biological replicates which made the data more reliable. I was blinded in my analysis and when measuring proximal vitelline vessels at high magnifications I was not aware if these were from tied-ligated or sham-ligated embryos. Future studies could explore automation of vessel analysis, such as by pixel intensity of photomicrograph images. Comparing red pixels (blood vessels) to background pixels might have allowed for automated and objective measurements of vessel size. However, the albumin over the surface of the vitelline membrane blurs the defined vessel boundaries and makes even illumination of

micrographs challenging. This would make it difficult to automate detection of blood vessels accurately against the background.

Further findings from my initial ligation experiments showed that unilateral vitelline vessel ligation of the right proximal vitelline artery resulted in distal remodelling of the vitelline network. ‘Collateral vessels’ were observed to cross the posterior and anterior medial territories to re-perfuse tissue with arterial blood (Section 3.3). I investigated this remodelling process further by serially quantifying collateral vessel remodelling by vessel number and size. I used the same definition of collateral vessels as Buschmann *et al.*, (2010) (i.e. vessels which cross venous territories from left to right across the midline, carrying arterial flow) (Buschmann *et al.*, 2010).

My analysis of collateral vessel development following unilateral arterial ligation revealed a feature not previously described in this model; an initial “expansion” phase, which began around 4 hours post tied-ligation with a rapid increase in collateral number to a peak around 12 hours, followed by a “remodelling” phase, during which some collaterals regressed to favour persistence and continued expansion of a remaining smaller number (Figure 3.5, 3.7). Despite the reduction in vessel number after 12 hours, the mean diameter of the persisting vessels (and hence the likely flow carrying capacity) of the collateral vessels continued to increase over 48 hours. This process of selection of persistent collaterals allows development of a more haemodynamically favourable configuration. The mechanism behind such selection remains unclear, but it seems likely to be driven by local haemodynamic forces within the vessels based on mammalian studies (Pipp *et al.*, 2004, Eitenmuller *et al.*, 2006).

My data showed a biphasic remodelling response similar to that observed in mammals (Hoefler *et al.*, 2001, Herzog *et al.*, 2002); both systems exhibit an initial rapid rise in collateral vessel number that then is refined to achieve a more haemodynamically efficient

configuration. This is described in a rabbit model of femoral artery occlusion where a timecourse identified an initial peak in collateral vessels (Hoefer *et al.*, 2001). This 'expansion' phase was then followed by selective growth of large vessels and 'pruning' of less efficient vessels. The chick embryo thus appears to display parallels to mammalian arteriogenesis.

As discussed, it is widely accepted that arteriogenesis involves pre-existing vessels (as reviewed by Schaper, Scholz., 2003). However, there was a possibility that as I was studying collateral vessel formation in a developmental, embryonic model, the process may have involved *de novo* vessel formation. I therefore set out to show that collateral vessels in the chick stemmed from pre-existing vessels. My data showed that in the chick embryo (as in mammals) collateral vessels do not form from *de novo* sprouting of capillaries. Section 3.4 describes 8 hour timecourse observations post-ligation and confirmed that pre-existing connections form collateral vessels. Collateral vessels were shown to extend from branches of the left, unligated vitelline artery. Further, small vascular connections downstream of 'developing' collaterals could be seen to contribute to the remodelling vessel (Figure 3.8).

The molecular mechanisms required to sense changes in haemodynamic forces, and then induce such selective remodelling, are unknown (although my later work sheds some light on this). However, in the literature, there is strong evidence to suggest that selection of persisting vessels is driven by haemodynamic force (Hoefer *et al.*, 2001). Measurements of blood flow (and other parameters) are capable of examining this in detail in the context of fluid forces, but the micrographs appeared to suggest that bigger vessels were favoured over smaller vessels (Figure 3.8).

To support the argument that collateral vessel formation in my model is not an angiogenic response, other characteristics of angiogenesis, not present in arteriogenesis could be investigated as described below:

Tests for hypoxia, the driving force of angiogenesis, could be investigated using embryos incubated in a hypoxic environment (~15% oxygen levels) (Ruijtenbeek *et al.*, 2000) to see if this increased the number/diameter of remodelled vessels post-ligation. Previous literature however, has shown that this area of the extra-embryonic vasculature in the chick embryo is normoxic (Buschmann *et al.*, 2010) supporting the idea that angiogenesis is not forming collateral vessels and is not required for this process. It is likely also that hypoxic conditions would reduce cardiac output and confound any results.

VEGF levels could have been analysed by immunoassays (Jelkmann, 2001), as this is a strong signal for angiogenic growth (Gerhardt *et al.*, 2003). However, growth factors such as VEGF may also play a role in arteriogenesis (Lanahan *et al.*, 2013)(section 1.8). Therefore, this analysis would not have provided conclusive results about whether collateral vessel formation in the chick occurs by angiogenesis or not.

Other indications the collateral vessel formation in the chick embryo occurs by an arteriogenic rather than angiogenic process could have come from studies into the presence of arteriogenic factors such as MMPs, macrophages or arteriogenic genes such as MCP1 (Hofer *et al.*, 2001) (as discussed in section 1.4). Later work shed more light on the genetic profile of the area of collateral vessel formation in the embryo and will be discussed in the next chapter (Chapter 4). The data from this chapter taken together provided good evidence to suggest that collateral vessels do not form *de novo* in this model, and that the driving force was haemodynamic force rather than an angiogenic stimulus.

PIV measurements of the distal vitelline branches, at early timepoints following ligation (T0 and 2 hour intervals) could have helped to assess whether the vessels carrying more flow were the ones that persisted to become established collateral vessels. I had not yet discovered PIV at the time of this study and future work could utilise this method. I did

however go on to generate proof-of-principle that PIV represents a viable tool to examine blood velocity in chick collateral vessels. Although preliminary data, PIV analysis did show that even at early timepoints, collateral vessels carried arterial flow across the midline to unperfused tissue (Figure 3.9, 3.10). It is important to note that time matched observations could not be made in the sham-ligated embryo. In the area of collateral vessel remodelling the sham-ligated model maintains its symmetrical distribution of vitelline branches either side of the vitelline vein (midline). The flow profiles of the vitelline vein are physiologically different to the arterial profiles of collateral vessels and cannot therefore be compared.

From my PIV experiments I have shown that serial PIV is possible in chick embryo collateral vessels at two timepoints. I have also shown that blood velocity can be measured in both developing and established collateral vessels. Technical limitations (which could not be optimised in the length of visit to our collaborators in Delft) prevented me from acquiring sufficient data to draw any firm conclusions about haemodynamics in my model. Some of these shall next be discussed:

A short window of time existed at which PIV analysis was optimal in my model; at early developmental stages, vessel boundaries were difficult to visualise, at later stages veins obscured arteries. Flow at high velocities in proximal vessels, was difficult to record with the camera and light source available. Occasionally due to movement of the embryo or debris on the yolk sac, images could not be processed. Processing took ~6 hours for each dataset, which also limited my ability to generate replicate datasets. One significant limitation was that embryos did not tolerate repeated imaging. Kloosterman (2014) had previously performed PIV on chick embryos at two points: HH st 13 and HH st 17 (a gap of 4 hours) (Kloosterman *et al.*, 2014), however, it is worth noting that these embryos had not undergone surgery prior to imaging and had not been subjected to more than two observations. Due to the limited amount of time I had working in Delft (7 working days) I

was not able to investigate why the embryos were perishing where usually they would survive (e.g. Timecourse analysis over 48 hours Figures 3.5, 3.7).

I next went on to examine vitelline and collateral vessel architecture. The vitelline vessels were found to be composed of endothelial cells and VE-cadherin successfully labelled endothelial cells in these vessels (Figure 3.14). Smooth muscle has been investigated by other groups previously and has not been found in these vessels at this development stage in the chick embryo (Taber *et al.*, 2001, Lucitti *et al.*, 2005). There is little requirement for vitelline vessels to regulate vascular tone as the entire network is maximally expanded to increase the surface area to the yolk sac (le Noble *et al.*, 2004) allowing oxygen and nutrient uptake.

VE-cadherin immunolabelling of endothelial cells of the extra-embryonic vasculature represented a marker which could be used for examination of the area of collateral development, to distinguish endothelial cells from non-vascular structures. Immunohistochemistry can be technically challenging in this model (see later studies in chapter 5). Lectins have been used by other groups to label the vasculature of chick embryos and have benefits over immunohistochemical antibodies as they bind to specific glycoproteins on the luminal surface of blood vessels. Jilani *et al.*, (2003) investigated 9 different lectins to find the most selective option for vessel visualisation and found *Lens culinaris* agglutinin, concanavalin A to bind most successfully to endothelial cells (Jilani *et al.*, 2003). The drawback to using lectins in my model is the intra-vascular delivery required. My attempts at microvascular injection often ended in death of the embryo due to haemorrhaging. This was why I opted to use immunohistochemical techniques instead.

My finding that collateral vessels in the chick embryo are mainly endothelial in structure can be seen as an advantage or a potential limitation of the model when compared to mammalian models. Arguably, the initiation of arteriogenesis in mammals appears to

derive from activated endothelial cells and given that the chick extra-embryonic vessels appear endothelial in nature; this suggests that the chick could provide a means to examine the role of the endothelium in isolation. However, native collateral vessels in higher species classically have a tunica intima of endothelial lining; a tunica media composed of smooth muscle cells; and elastic tissue and a tunica adventitia of collagen and elastic lamina (Cai *et al.*, 2003). Following occlusion and elevated shear stress in these models, the activated endothelial cells release factors which initiate remodelling (Arras *et al.*, 1998, Heil and Schaper., 2005). The internal elastic lamina ruptures, which separates the smooth muscle layers (Heil and Schaper., 2007). The intima and adventitia thicken as smooth muscle cells proliferate (Buschmann and Schaper, 2000). Therefore the process of collateral remodelling in the chick embryo is not comparable from an architectural viewpoint.

Conversely, the chick model could provide valuable insights into an exclusive endothelial response to changes in flow, *in vivo*, not possible in mammalian models. Further, it could be argued that this *in vivo* system provides information about the endothelial cell response to changes in flow which are difficult to reproduce *in vitro*. *In vitro* assays have benefits in that they produce rapid, reproducible and quantifiable results. External stimuli can be strictly controlled. However, physiological *in vivo* conditions are difficult to replicate accurately *in vitro*; endothelial cells behave differently in static vs. flow conditions. Isolation of cells *in vitro*, may give the benefit of studying an isolated reaction to a drug. Further, indirect effects from surrounding cells, such as endodermal or ectodermal cells in the extra-embryonic tissue *in vivo*, which may influence the response to a drug, would not be captured in *in vitro* assays. It has also been shown that endothelial cells in culture change their active state, chromosome number, cell surface antigens and growth properties (Jackson and Nguyen., 1997). *In vitro* experiments must therefore be interpreted with caution and validated with multiple tests with either more than one cell type, tested on different matrices with different compounds (Staton *et al.*, 2004).

There is also evidence to suggest that endothelial cells differ, for example HUVECs and endothelial cells from the microvasculature (Jackson & Nguyen 1997). These differences (phenotypic or structural) may affect behaviour (Jackson & Nguyen., 1997). It is therefore difficult to know which cell line best recapitulates the *in vivo* situation. Although a valid method, these *in vitro* limitations support the utility of the chick embryo as a model to investigate flow-induced remodelling. The chick allows analysis of an *in vivo* endothelial system, with further benefits of real-time vessel observation, easy access for vascular manipulation and pharmacological assays.

Further characterisation of the endothelial behaviours of remodelling collateral vessels in my model came from *in situ* hybridisation studies of arterial/venous markers, post-ligation. This data revealed that endothelial cells appeared to adopt an arterial identity as the expanding collateral network extended across the midline into venous territory. This was a time-dependent process as *nrp1* expression increased over time, not previously reported by other groups. Arterial markers were upregulated from at least 4 hours post-ligation and were more strongly expressed at 12 hours in the collateral vessels (Figure 3.18).

My data was predominantly concerned with **flow-induced** arterial expression patterns. In the literature, there is debate about whether arterial expression is pre-determined genetically and determined by Notch signalling (Lawson *et al.*, 2001) or if expression is plastic and can be altered by flow (le Noble *et al.*, 2004). Although our findings agreed with those of le Noble *et al.*, (2004) as flow appeared to drive *nrp1* expression, I could investigate some of the findings of Lawson *et al.*, (2001) to validate these results.

Notch has been found to be required for arterial/venous patterning (Lawson *et al.*, 2001). This group investigated expression of ephrinB2 (arterial marker) and ephB4 (venous marker) in the blood vessels of zebrafish embryos. They disrupted Notch signalling by inhibiting DNA binding proteins of downstream Notch targets and created mutants

defective in Notch signalling. In both of these models vessel architecture did not develop normally and expression of ephrinB2 and ephB4 was affected. The group concluded that activation of Notch represses venous differentiation in developing arteries which leads to changes in vessel patterning (Lawson *et al.*, 2001).

My data gave an indication that changes in haemodynamic force were driving expression of arterial markers and the resulting pattern of vessel networks post-ligation. This implies that a) collateral vessels can respond to changes in altered demand by modulating gene expression – a hypothesis I later investigate in Chapter 4, and b) that changes in haemodynamic force may be the stimulus driving collateral vessel remodelling.

Final experiments in this chapter attempted to determine if endothelial proliferation was required for collateral vessel remodelling. Proliferation was investigated because studies have shown that in mammalian models outward remodelling of collateral vessels involves smooth muscle cell and endothelial cell proliferation (Scholz *et al.*, 2002). The literature suggests that proliferation might be required for flow-induced vessel remodelling (Schaper *et al.*, 1971) but there are currently no investigations in the chick model into proliferation and collateral vessel growth.

I hypothesised that developing collateral vessels would require more proliferation early on at a time when the process is dynamic. However, at an early 4 hour timepoint following ligation there was no significant difference in the number of proliferating cells in the area of collateral vessel development between sham and tied-ligated embryos (Figure 3.19). VE-cadherin double staining was performed alongside BrdU labelling to aid analysis of proliferating endothelial cells. The sham-ligated control allowed for an estimation of any differences in proliferation due to collateral vessel formation, but none were observed. Although the n numbers were not sufficiently high to be entirely confident, this data supports the hypothesis that collateral vessels do not form *de novo* by a sprouting

angiogenic process, which would require proliferation (Gerhardt *et al.*, 2003). Further, Buschmann *et al.*, (2010) reported that intussusceptive angiogenesis, which was likely to play a role in collateral vessel formation in the chick embryo, was a process requiring little proliferation (Djonov *et al.*, 2000, Buschmann *et al.*, 2010). My data does not provide sufficient evidence to draw conclusions as to whether proliferation is or is not required for collateral vessel remodelling as it could be argued that there is a trend towards tied-ligated chick embryos showing more proliferation in this area. Increasing the n number would increase the statistical power which could help to detect significant differences. It is possible that since the entire chick is growing rapidly, the baseline level of proliferation is high enough to mask the effect of collateral remodelling, which will only represent a proportion of proliferation in the area assessed.

The evidence for increased proliferation in collateral vessel formation comes from early studies in canine models (Schaper *et al.*, 1971). The group found that following constriction of the left circumflex coronary artery, consequent collateral vessels showed increased proliferation. Radioactively labelled thymidine was titrated into the vessels and DNA synthesis and mitosis in coronary collateral vessels was measured. The tunica media and tunica intima of collateral vessels showed most proliferation. They could not distinguish if proliferation was occurring in endothelial or smooth muscle cells so did not draw conclusions about the contribution of endothelial cell proliferation to collateral vessel remodelling (Schaper *et al.*, 1971). However, Odori *et al.*, (1983) showed increased proliferation of endothelial cells after renal artery stenosis was induced by clipping the artery in rats. The proliferative response was assessed by coded reading of images showing positive labelled nuclei of endothelial cells following titration of thymidine, 5 days after the stenosis. Compared to sham-ligated models which showed no change in proliferation, 12 out of 18 rats showed a significant proliferative response. The group concluded that

increased proliferation led to increased number of collateral vessels during remodelling (Odori *et al.*, 1983).

Other studies have shown that peaks in proliferation of endothelial/smooth cells occurs at different timepoints following vessel occlusion, in different species: Scholz *et al.*, (2000) showed mitosis of smooth muscle and endothelial cells was present 24 hours after femoral artery occlusion in rabbits (Scholz *et al.*, 2000). One study found a peak to occur at 3 weeks in dogs (Schaper *et al.*, 1971) whilst another group found the peak at 1-4 days in rats (Ilich *et al.*, 1979). Similarly the number of proliferating cells that contributes to collateral vessels may be species dependent. In collateral vessels of the canine model it ranges from 2.6-3.5% (Schaper *et al.*, 1971), 5-6% in rodents (Ilich *et al.*, 1979) and <1% in porcine models (White *et al.*, 1992). My results showed a general level of proliferation which was higher (~10%). This difference could be species dependent or reflective of the fact that a developing chick embryo may require increased proliferation for growth.

BrdU labelling and assessment requires an antigen retrieval step. This procedure often damaged tissue and made identification of specific cellular staining of VE-cadherin/BrdU difficult. A second proliferation marker could validate the result acquired with BrdU labelling. This would also further validate that BrdU was successfully incorporated into cells during the remodeling period *in vivo* – an especially technically challenging procedure (section 2.22.1). For example, Ki67 would be a good antibody to test as it can be detected at all phases of the cell cycle and would provide a more stringent analysis of all the proliferating cells. It is possible that increases in proliferation may occur after 4 hours. In later studies I therefore investigated proliferation during later timepoints (chapter 5).

In summary, the data in this chapter suggests the following:

- Unilateral arterial ligation causes changes in haemodynamics which remodel the pre-existing vitelline vessel network into collateral vessels
- Collateral vessel number rises and falls, implying active selection of a favourable configuration via an unknown mechanism
- Collateral vessels are endothelial in nature and adopt an arterial identity as they remodel to perfuse a venous territory
- Proliferation is limited in collateral vessels at early timepoints

### **Future work**

The PIV technique could be developed to be used in future studies to enhance and support data from static images (for example, in Figure 3.5). When optimised, PIV would allow comprehensive blood velocity mapping in the collateral vessels of this model. Future work could investigate whether Notch signalling increases in ‘developing’ collateral vessels as they adopt an arterial fate when crossing the venous territory at the midline. Immunohistochemistry could be used to analyse Notch receptor (Notch 1, 3, 4) or ligand expression (delta-like4, jagged 1, 2) in collateral vessels. These results could be compared to my previous *nrp1* findings (Figure 3.18). Inhibition of Notch signalling with a gamma secretase inhibitor could confirm a role for Notch in collateral vessel formation. Inhibition of ephrinB2 could be tested to see if this resulted in impairment of the patterning of the collateral vessel architecture.

In conclusion, the vitelline network remodels after occlusion in a similar way to mammalian models. The chick model has technical advantages over higher model systems: easy accessibility of the vessels; simple visualisation methods; ease of manipulation. Although

the vessel architecture between species differs, the chick embryo model provides mechanistic similarities to collateral vessel formation in mammals. The chick embryo provides a unique platform from which to identify novel endothelial cell responses to changes in haemodynamic alteration. I exploited these advantages in the next chapter to characterise the gene expression profile during collateral remodelling.

## Chapter 4

# Characterising the transcriptional profile during flow-induced vessel remodelling in the chicken embryo

### Summary

In this chapter I used microarrays to assess the transcriptional response at two timepoints during collateral development in the chicken embryo.

My aims were to:

- characterise transcriptional changes during different phases of flow-induced vessel remodelling
- identify candidate genes which may contribute to collateral development

Figure 4.1 shows a flowchart of the experimental groups and timepoints. In addition to the sham-ligated and tied-ligated groups, I included a 'baseline' group of uninstrumented HH st 17 embryos (the stage at which other groups underwent tied-ligation/sham-ligation) (section 2.6.1).

To examine the gene expression changes detected, I undertook the following analysis pipeline. Using PUMA, I identified genes that were differentially expressed in the following comparisons;

4 hours post tied-ligation vs. 4 hours post sham-ligation

12 hours post tied-ligated vs. 12 hours post sham-ligation

Data from each array was normalised before being analysed, to make sure signals between different array chips were distributed evenly and any variations due to technical issues were removed to make the data comparable (section 2.6.1). This data was then used for clustering.

It is important to understand the 'normal developmental' programme in chick embryos as it develops from HH st 17 to the timepoints observed for the tied-ligated embryos. This gives an idea of the genes which are required for growth and which may be expressed as a result of experimental conditions. I therefore also performed comparisons between baseline vs. 4 hours post sham-ligation and baseline vs. 12 hours post sham-ligation. These data are included in the appendix due to space considerations (Figure A4 and A5). Further, despite needing knowledge of normal development, these genes are biologically less relevant as my focus is a comparison of differentially expressed genes in tied-ligated and sham-ligated embryos.

#### **4.1 *A priori* expectations of relevant gene expression changes**

Microarrays generate a large amount of data that often require *a priori* assumptions about what gene expression changes might be relevant. As I showed in the previous chapter, the tissue at the site of collateral vessel remodelling is complex. Even in sham-ligated embryos, there is ongoing development of the vitelline vasculature over the timepoints assessed (Appendix figures A4, A5). During collateral vessel remodelling, there are highly dynamic changes in vessel morphology (Figure 3.5) that would be predicted to correlate with significant alteration in transcription. I therefore chose to focus my efforts on identifying two key groups of genes (that encode known proteins with homologues in mammalian species).

The first group were **genes that are differentially expressed both 4 hours and 12 hours after tied-ligation**. These genes showed more or less expression in the area of collateral

vessel formation compared to sham-ligated embryos, but expression was also detected in the sham-ligated embryos. These genes might be expected to include genes that are generally required for collateral development (or at least vascular remodelling). The second group were **genes that were expressed *only* in tissue undergoing collateral vessel remodelling** (at either 4 or 12 hours after tied-ligation). These genes showed little to no expression in sham tissue or at baseline, but appeared specific to the area of collateral vessel remodelling. These genes could therefore be specific to vessels undergoing remodelling and might represent mediators of collateral vessel transcriptional response, rather than more general vascular remodelling or growth. Focusing on these genes would exclude those whose expression was simply delayed or accelerated by ligation, or whose expression was simply a function of the amount of vascular tissue at the site of remodelling (which appears to be greater during collateral remodelling).

#### **4.2 Assessment of the transcriptional changes during normal development and collateral vessel development in the chicken embryo**

As discussed in the previous chapter, collateral development following unilateral vitelline artery ligation proceeds over at least 48 hours. I chose to study gene expression at 4 hours and 12 hours post-ligation. I chose these timepoints because at 4 hours the vessels have been exposed to altered blood flow for sufficient time to induce a biological response but collateral vessel development is in an early stage. Figure 3.7 showed numbers of collateral vessels and their diameter remained low at 4 hours and at 12 hours collateral vessel number had peaked and a process of selection of the most favourable configuration seemed to have commenced. Examining these timepoints might therefore identify drivers of the initial expansion of collateral number (at 4 hours) and genes that contribute to the selection of persisting collateral vessels (at 12 hours).

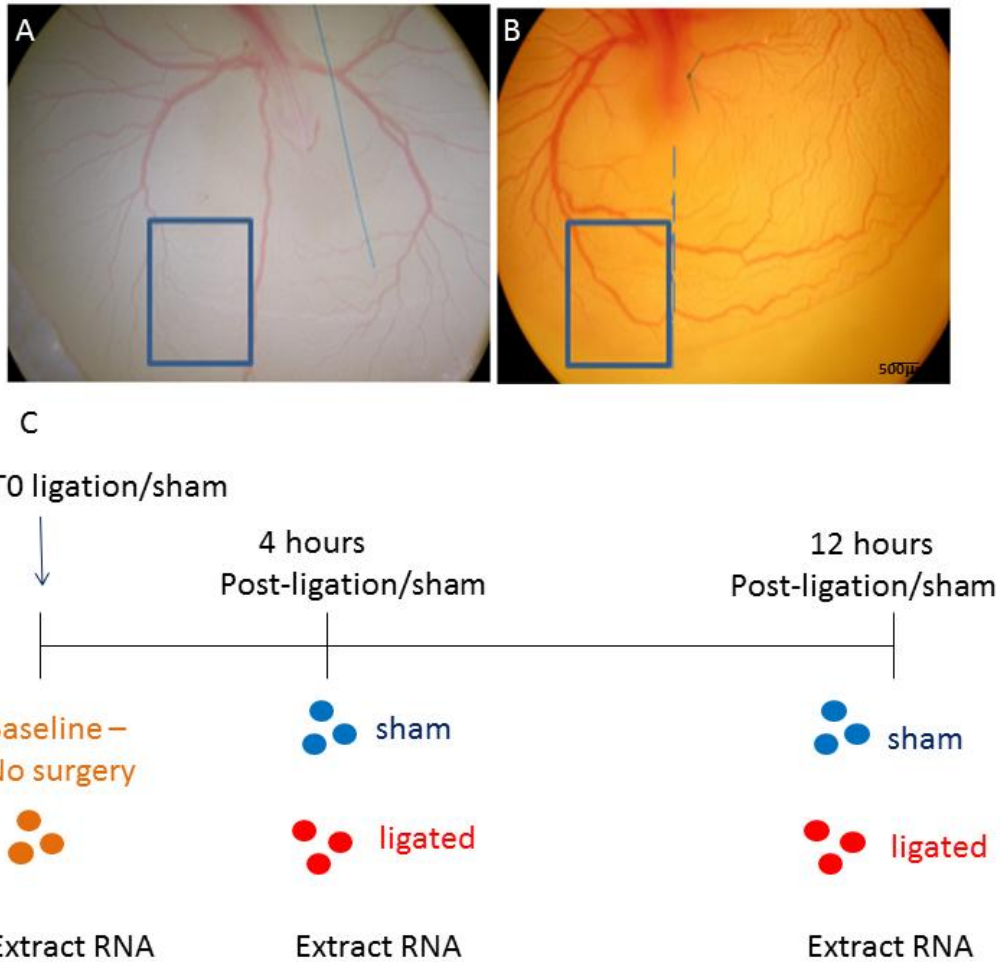


**Figure 4.1 Schematic of microarray experimental protocol**

Tissue was excised from the same medial posterior area in sham and tied-ligated embryos (represented by box). **A** indicates the excised area in a sham-ligated embryo. **B** indicates excised area in a tied-ligated embryo. **C** The timeline shows the timepoints selected for microarray analysis. Tissue was taken from embryos pre-surgery for a baseline measurement (HH st17). At T0 either a tied-ligation or a sham-ligation was performed. Tissue was then removed from groups of 3 embryos at 4h and 12h post-ligation/sham. RNA from each group was pooled. Each experiment was repeated 3 times (i.e. 9 embryos per timepoint per group, n=3 arrays per timepoint per group).

### 4.3 The transcriptional profile during collateral vessel development

My key aim was to compare gene expression at the site of collateral vessel development in tied-ligated embryos compared with sham-ligated embryos. I therefore next compared the transcriptional profile at both 4 hours and 12 hours post tied-ligation. At 4 hours post tied-ligation, 158 transcripts were differentially expressed between sham-ligated and tied-ligated embryos by more than 1.5 fold with a PPLR of  $>0.8$  or  $<0.2$  (see Materials and Methods). At 12 hours post tied-ligation, 187 transcripts were differentially expressed between sham-ligated and tied-ligated embryos by more than 1.5 fold with a PPLR of  $>0.8$  or  $<0.2$  (Figure 4.2).

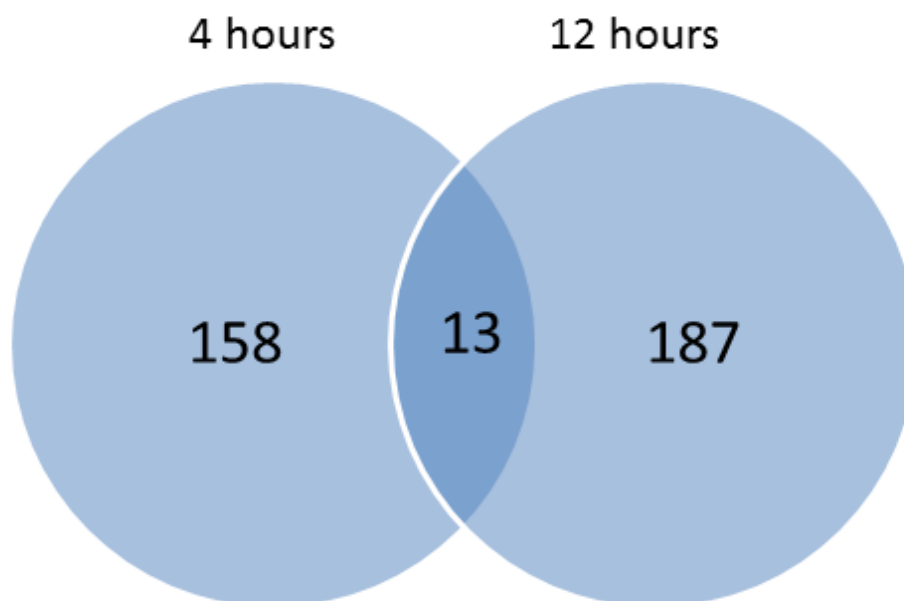


**Figure 4.2 Venn diagram showing number of differentially expressed genes at 4 h post-tied-ligation compared to 4h sham-ligation and 12h post tied-ligation compared to 12h sham-ligation.**

The circle on the left represents 158 differentially expressed genes at 4 hours post tied-ligation compared to 4 hours post sham-ligation. The circle on the right represents 187 differentially expressed genes at 12 hours post tied-ligation compared to 12 hours post sham-ligation. The overlapping section of the circles represents 13 shared genes differentially expressed at both timepoints compared to the sham operated embryos.

After excluding 81 hypothetical genes at 4 hours post tied-ligation, this left 77 differentially expressed genes: 33 upregulated and 44 downregulated in tissue undergoing collateral vessel development. After excluding 100 hypothetical genes at 12 hours post tied-ligation, this left 87 differentially expressed genes: 61 upregulated, 26 downregulated in tissue undergoing collateral vessel development. Only 13 genes were differentially expressed at both 4 and 12 hours after tied-ligation. These are listed in table 4.1. Although potentially playing a role in general vascular remodelling, I chose not to focus on most of these genes as I ultimately would focus my efforts on genes that were more specifically altered as a result of tied-ligation (i.e. only showed differential expression in the area of collateral vessel remodelling). However, the genes in table 4.1 are discussed at the end of this chapter.

**Table 4.1; The 13 genes differentially expressed at both 4h and 12h after tied-ligation compared with sham-ligation.** Blue shows genes downregulated at both timepoints. Red indicates genes upregulated at both timepoints.

Gene Symbol	Gene Name	Function
CC2D1B	Coil coil and C2 domain containing 1b	Transcriptional repressor
DPP6	Dipeptidyl peptidase 6	Change expression of voltage gated K <sup>+</sup> channels
TTN	Titn	Structural protein
SELE	Selectin E	Shear responsive monocyte chemoattractant
RGS7	Regulator of Gprotein signalling	Inhibition of signal transduction
ZFPM2	Zinc finger protein	Transcriptional regulator, acts with GATA genes
FH0D3	Formin homolog 2 domain 3	Actin organisation – causes stress fibre formation and regulates cytoskeleton
GAS2	Growth arrest specific 2	Regulates cell shape change in apoptosis
COL8A1	Collagen protein	Component of endothelial cells, maintains vessel wall structure
IRX4	Iroquois homeobox 4	DNA binding transcription factor activator
SPECC1L	Sperm antigen with calponin homology	Cytokinesis and spindle organisation, involved in cell adhesion and migration
SLC35B3	Solute carrier family	Solute carrier
JPH1	Juntophilin 1	Junctional membrane complex

(Gene information from Gene cards [www.genecards.org](http://www.genecards.org) and Ensembl [www.ensembl.org](http://www.ensembl.org))

## 4.5 Hierarchical clustering of genes differentially expressed during collateral development

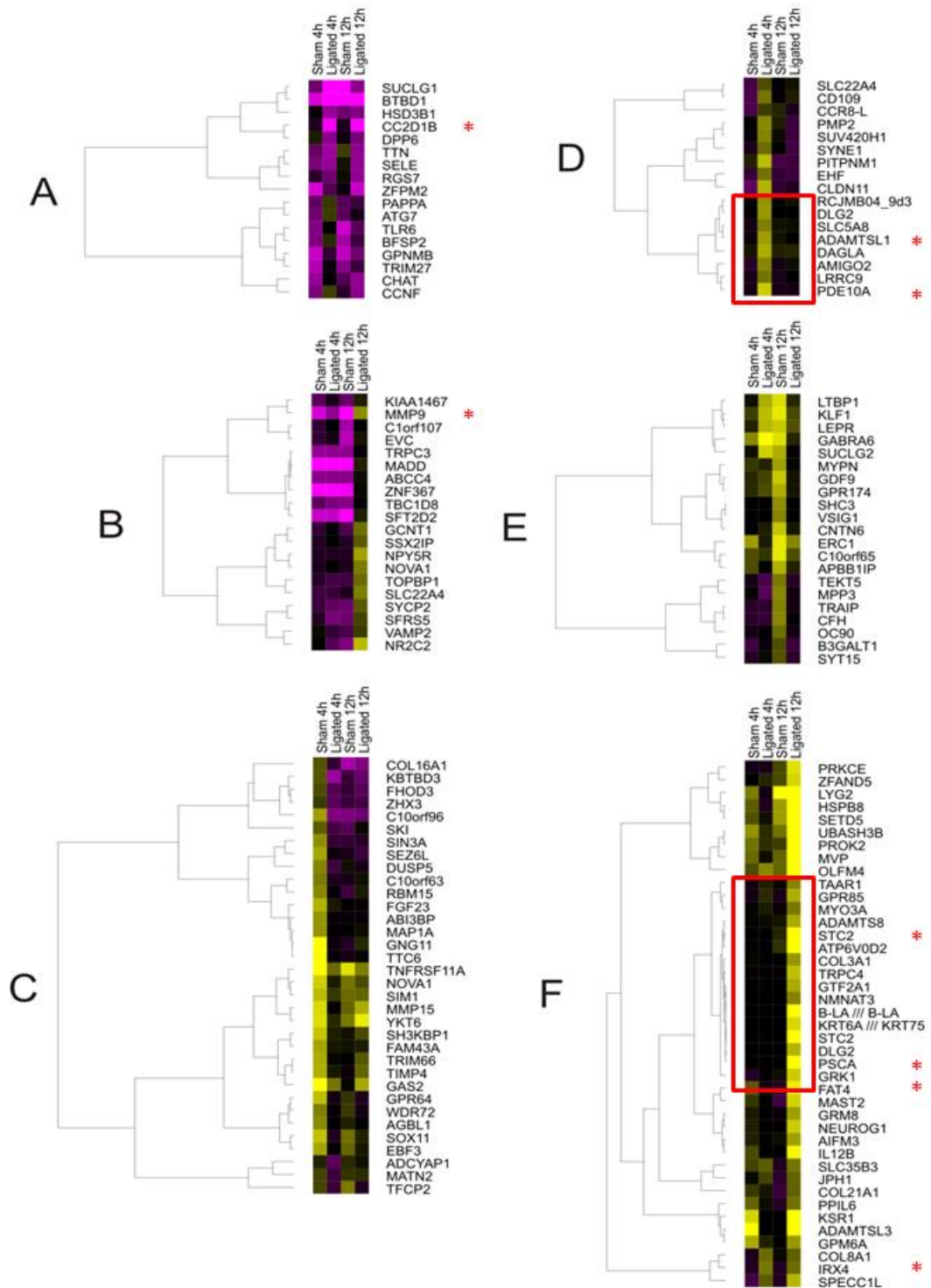
Large sets of microarray data can be organised into hierarchical clusters using programmes such as TreeView (<http://taxonomy.zoology.gla.ac.uk/rod/treeview.html>). Data sets are assembled into a tree which indicates the mean expression of the different groups. Branches of the dendrogram connect clusters of genes with similar expression changes. I used TreeView to cluster genes that were differentially expressed between tied-ligated and sham-ligated embryos at 4 hours or 12 hours post-ligation. Data is expressed as expression level relative to baseline (unligated, HH st 17). Figure 4.3 shows a dendrogram with genes coloured purple if downregulated compared with baseline, or yellow if upregulated (intensity proportional to expression). The four columns allow a direct comparison of the expression profiles between the four different groups (4 hours sham-ligated, 4 hours tied-ligated, 12 hours sham-ligated, 12 hours tied-ligated).

Figure 4.3 A-F show individual clusters of genes with similar expression profiles, separated into related nodes. Node A shows genes downregulated during collateral development at both 4 hours and 12 hours post-ligation. Node B shows genes whose expression falls after sham-ligation but either does not fall as much or is upregulated at 12 hours in tied-ligated embryos. Node C shows genes upregulated in sham-ligated embryos at 4 hours. Node D genes upregulated at 4 hours post-ligation with very little expression in any other group. Genes in node E are generally upregulated in the sham-ligated group at 12 hours, while node F shows genes that are upregulated in tied-ligated embryos at 12 hours post tied-ligation, with little or no expression in other groups.

To observe the genes that were only expressed at the sites of collateral vessel development (with little or no expression in the sham-ligated group) I focussed on genes in nodes D and F, and those with most specificity to tied-ligated tissue (little or no expression in baseline or

sham-ligated groups). These are indicated by red boxes on Figure 4.3. The known functions of these genes are described in table 4.2.

To confirm differential gene expression, of selected candidate genes identified by the microarray, I then went on to perform quantitative real-time polymerase chain reaction (QRTPCR).



**Figure 4.3 Hierarchically clustered heatmaps of the fold changes of the differentially expressed genes during flow-induced vessel remodeling**

Data is expressed as fold change from baseline (yellow indicates an increase in expression, purple is a down-regulation from baseline). Genes were clustered to describe related expression profiles of up or down-regulation at each time-point. Red boxes indicate genes specifically expressed at 4h or 12h post tied-ligation. Red stars indicate genes selected for QRT-PCR analysis (section 4.6).

**Table 4.2 Genes specifically expressed during collateral vessel development 4h or 12h post tied-ligation**

These genes were differentially expressed in embryos remodelling the vitelline vasculature in response to changes in haemodynamic forces, with little or no expression in baseline or sham-ligated embryos at either timepoint.

4h Gene Symbol	Gene name	Function
RCJMB04	Membrane bound O-acetyltransferase domain 04	Guanine nuclear exchange factor for Ras and Raf1. GPCR signalling to MAPK
DLG2	Discs large homolog 2	Interact at postsynaptic sites to form a multi-meric scaffold for the clustering of receptors, ion channels, and associated signaling proteins
SLC5A8	Solute carrier 5	Sodium/monocarboxylate co-transporter. Cell activation/signal transduction
ADAMTSL1	A disintegrin and metalloproteinase with thrombospondin motif-like 1	This protein may have important functions in the extracellular matrix. Cell-cell/cell-matrix interactions to regulate ECM proteases
DAGLA	Diacylglycerol lipase, alpha	Lipase enzyme. Esterases that can hydrolyze long-chain acyl-triglycerides into di- and monoglycerides, glycerol, and free fatty acids at a water/lipid interface.
AMIGO2	adhesion molecule with Ig-like domain 2	May contribute to signal transduction through its intracellular domain
LRRC9	Leucine rich repeat containing 9	Formation of protein-protein interactions
PDE10A	Phosphodiesterase 10A	Signal transduction. regulates the intracellular concentration of cyclic nucleotides. hydrolyse both cAMP and cGMP to the corresponding nucleoside 5' monophosphate, but has higher affinity for cAMP,

12h Gene symbol	Gene name	Function
TAAR1	Trace amine associated receptor	G protein-coupled receptor activated by trace amines. Receptor expression is concomitant with lymphocyte immune activation, suggesting a possible role for TAAR1 in the generation or regulation of an immune response
GPCR 85	G protein-coupled receptor 85	Induces an intracellular signaling cascade mediated by heterotrimeric GTP-binding proteins, or G proteins
MYO3A	Myosin IIIA	Actin-dependent motor proteins . Cellular transporter and actin cross-linker
ADAMTS8	ADAM metalloproteinase with thrombospondin type 1 motif, 8	The enzyme encoded by this gene contains two C-terminal TS motifs, and disrupts angiogenesis in vivo.
STC2	Stanniocalcin 2	This gene encodes a secreted, homodimeric glycoprotein, may have autocrine or paracrine functions. May play a role in the regulation of calcium and phosphate transport, cell metabolism, or cellular calcium/phosphate homeostasis.
ATP6V0D2	ATPase, H+ transporting, lysosomal	Specialised proton pump. Essential for acidification of diverse intracellular compartments
COL3A	Collagen type III a	May contribute to collagen deposition into the ECM. Mutations can cause arterial ruptures
TRPC4	Transient receptor potential cation channel	Non-selective calcium-permeable cation channel, activated by Gq-coupled receptors and tyrosine kinases, plays a role in endothelial permeability, vasodilation, neurotransmitter release and cell proliferation.

GTF2A1	General transcription factor	Transcription initiation on TATA-containing class II genes involves the ordered assembly of RNA polymerase II
NMNAT3	Nicotinamide nucleotide adenylyltransferase 3	These enzymes use ATP to catalyze the synthesis of nicotinamide adenine dinucleotide or nicotinic acid adenine dinucleotide from nicotinamide mononucleotide or nicotinic acid mononucleotide,
B-LA	MHC class II alpha chain	Class II molecules are expressed in antigen presenting cells (B lymphocytes, dendritic cells, macrophages) and are used to present antigenic peptides on the cell surface to be recognized by CD4 T-cells
KRT6A	Keratin 6A	Expressed during differentiation of simple and stratified epithelial tissues
PSCA	Prostate stem cell antigen	Encodes a glycosylphosphatidylinositol-anchored cell membrane glycoprotein. Member of the Ly-6 neurotoxin-like family in the nervous system, and is likely to play a role as a modulator of alpha7 signaling-induced cell death during development
GRK1	G protein-coupled receptor kinase 1	Encodes a member of the guanine nucleotide-binding protein (G protein)-coupled receptor kinase subfamily of the Ser/Thr protein kinase family. Phosphorylated by PKA when cAMP levels are elevated
FAT4	Protocadherin FAT4	Associated with the HIPPO signalling pathway, involved in cell proliferation and apoptosis

#### 4.6 Selection of candidate genes for quantitative analysis by QRTPCR

From the heatmap clusters (Figure 4.3), 151 genes were identified which were differentially expressed in tissue from chicks undergoing collateral vessel development (tied-ligated). To select a realistic number of genes with which to perform validation of expression using QRTPCR, I chose to examine expression the sub-set of selected genes (boxed region of nodes D and F in figure 4.3). These genes were most highly differentially expressed between sham-ligated and tied-ligated and therefore I hypothesised that expression was likely to be specific to vessels undergoing remodelling. I also investigated genes whose known functions made their involvement in collateral vessel development plausible and genes that only showed expression either exclusively in tied-ligated or sham-ligated embryos.

To validate the expression profiles observed in the microarray I used QRTPCR to assess transcription of the following genes: ADAMTSL1 (node D, boxed region), PDE10A (node D, boxed region), MMP9 (node B), STC2 (node F, boxed region), PSCA (node F, boxed region), FAT4 (node F, unboxed), IRX4 (node F, unboxed), and CC2D1B (node A). Table 4.3 lists the differential expression detected by the microarray and some of the known functions of

each gene. However, only 4 primer sets were successfully optimised (section 2.8.3 and discussed at the end of this chapter); ADAMTSL1, PDE10A, STC2 and PSCA. Table 4.4 shows the QRTPCR results for the four genes whose primers were successfully optimised. The QRTPCR results showed similar (though not identical) patterns of differential expression to the microarray.

Of the four candidate genes whose differential expression was confirmed by QRTPCR, PDE10A seemed most suitable for further assessment (discussed at the end of this chapter). This selection was based on the criteria above, the roles of other PDE family members in the vascular system (section 1.15.3) and the availability of reagents that allow manipulation of pathways influenced by PDE10A. The next chapter of this thesis focuses on the regulation of PDE10A expression and its role during collateral vessel development.

**Table 4.3 Relative gene expression in tied-ligated compared with sham-ligated embryos in the area of flow-induced vessel remodelling** (Red indicates genes whose differential expression was confirmed using QRTPCR (primer sets for others could not be optimised))

Gene Symbol	Gene name	Relative gene expression compared to sham-ligated	Gene function
ADAMTSL1	ADAMTS like 1	2.46 ↑	May play a role in the extra-cellular matrix and is related to the matrix metalloproteinases
PDE10A	Phosphodiesterase 10A	3.48 ↑	Enzyme that degrades c AMP and c GMP
PSCA	Prostate stem cell antigen	5.72 ↑	May regulate cell proliferation
STC2	Stanniocalcin2	5.28 ↑	Regulates calcium and phosphate homeostasis
FAT4	Protocadherin FAT4	2.2 ↑	Regulates planar cell polarity in drosophila; Cell-cell interactions; plays a role in proliferation and apoptosis
MMP9	Matrix metalloproteinase 9	3.7 ↑	Degradation of ECM
CC2D1B	Coiled-coil and C2 domain containing 1B	Only expressed in sham-ligated tissue	Regulates Notch receptor trafficking
IRX4	Iroquois- class homeodomain	Only expressed in tied-ligated tissue	Regulator of ventricular differentiation during cardiac development

**Table 4.4 Comparison of the expression levels detected using microarray analysis and QRTPCR.**

Gene name	Microarray gene expression levels (fold change relative to controls)	QRTPCR gene expression levels (fold change relative to controls)
ADAMTSL1	2.46	3.01
PDE10A	3.48	6.90
PSCA	5.72	2.91
STC2	5.28	3.09

#### **4.8 Discussion**

In this chapter I used microarrays to assess the transcriptional response at two timepoints during collateral development in the chicken embryo (Figure 4.1). I clustered the data into heatmaps which helped to analyse groups of genes with similar expression profiles (Figure 4.3). I used the data to identify candidate genes with which to validate expression profiles using QRTPCR (Table 4.1).

My more general aim was to identify genes that were differentially expressed in tissue from tied-ligated compared with sham-ligated embryos (section 4.5). The ultimate aim was to finally select a gene which was appropriate and relevant for further investigations using functional assays in my model, which could be used for assessing a role in flow-induced collateral vessel remodelling (section 4.6).

There were three options to clustering my microarray data into heatmaps. Option 1 would be to compare sham and tied-ligated differentially expressed genes in a direct 2-way comparison; however, this does not give an idea of expression relative to baseline. Option 2 would be to compare tied-ligated data from 4 and 12 hours post-ligation directly with the baseline measurement; however, this would not reveal information about the gene in the

sham-ligated model. These 2 methods have merits but I wished to answer the specific question about the differentially expressed genes between sham and tied-ligated models. I therefore analysed expression of the genes which were differentially expressed over time between sham and tied-ligated models, in terms of relative expression to baseline (Figure 4.3).

Before analysing the transcriptional profile of tied-ligated embryos undergoing vessel remodelling, it was necessary to first assess the 'normal developmental' gene expression profile. I therefore first identified genes that were differentially expressed between a baseline, uninstrumented measurement (genes expressed at T0), and 4 hours after sham-ligation. This was repeated for data at 12 hours after sham-ligation. A heatmap of the 'normal developmental' programme can be found in the appendix (Figure A5). This allowed me to better interpret and put into context data from the tied-ligated embryos and allowed me to confirm that the differentially expressed genes in tissue from these embryos were not simply an amplification, delay, or acceleration of the normal developmental transcriptional response.

Comparisons of the heatmaps from the sham and tied-ligated microarrays showed that a large number of genes were shared between these two groups (Appendix, table A1 and table A2). Some had similar expression profiles, suggesting that these genes were required for normal development of the tissue. Some had contrasting expression profiles which suggested a need to alter normal developmental signals and react to the tied-ligation and a change in flow. These shared genes hold less interest for this study as they may be either a result of a delayed expression due to the ligation or an amplification of a normal developmental process. I therefore focussed on the genes in the heatmap of the tied-ligated microarray data which was separated into nodes of genes with most similar expression profiles (as had been performed in the heatmap of the sham-ligated data).

Although differential expression is neither necessary nor sufficient to confirm a functional role in collateral vessel formation, some of these differentially expressed genes may be involved in the process. Below are some speculations about how the differentially expressed genes I identified in these studies may be related to the process of collateral vessel remodelling. However, at this point in my studies I took no position as to whether they truly play such a role, particularly as the array data does not allow identification of genes specifically expressed in the vasculature. Discussed below are the 13 genes differentially expressed at both 4 hours and 12 hours after tied-ligation compared with sham-ligation. Some of these 13 genes were expressed in the sham-ligated model and therefore, although interesting, did not show a specific response to ligation and may have just been an amplification of the normal developmental signal. However, of the three transcription factors identified in the table (CC2D1B, ZFPM2, IRX4), two of these were expressed specifically in the tied-ligated embryos (CC2D1B and IRX4), indicating that they may play specific roles during collateral vessel remodelling. Given what is known about collateral vessel development, it is possible to hypothesise what broad mechanisms and pathways might be reflected in transcriptional changes. These would include mechanotransduction, cytoskeletal rearrangement, vasoregulation, inflammation, migration, proliferation, and increased transcriptional activity. Some of these are discussed below.

It could be expected that transcriptional activity would be a common activity to cells undergoing remodelling at both 4 and 12 hours post-ligation. For example, Coiled-coil and C2 domain containing 1B (CC2D1B) is a transcriptional repressor. In my microarray this gene was downregulated in tied-ligated compared with sham ligated embryos at both 4 and 12 hours post tied-ligation. Little is known of the targets of CC2D1B although it is known to negatively regulate expression of the serotonin 1A receptor in brain (Hadjighassem *et al.*, 2009). Serotonin exerts a range of vascular effects mediated by the

family of serotonin receptors. The serotonin 1, but not the serotonin 2 receptor, has been shown to mediate migration of endothelial cells (Matsusaka and Wakabayashi, 2005). Although I did not detect upregulation of the serotonin 1A receptor in my array data, it is possible that down regulation of CC2D1B enhances vascular sensitivity to serotonin activity via effects on receptor expression. Since serotonin positive cells have been shown to be present at sites of coronary collateral vessel development in canine models, it would be interesting to pursue the effects of serotonin signalling in collateral vessel development, especially given the availability of reagents that can block serotonin receptors experimentally (Wolf *et al.*, 1998). However, it is possible CC2D1B is a transcriptional regulator of other genes within the chick vasculature, including those that influence arterial/venous identity or other processes involved in collateral development. Chromatin immunoprecipitation of CC2D1B, or microarray comparisons of endothelial cells with and without siRNA knockdown of CC2D1B might identify genes that are regulated by this repressor and reveal unexpected roles for CC2D1B in vascular development.

Dipeptidyl peptidase-6 (DPP6) was downregulated at both 4 hours and 12 hours in tissue from chicks undergoing collateral vessel development (tied-ligated) compared with sham-ligated embryos. DPP6 is a peptidase which changes expression of voltage gated potassium channels (Xiao *et al.*, 2013). It has been recorded that potassium channels may play a role in the endothelial cell mechanotransduction of signals, following changes in blood flow (Davies, 1995). It is possible that DPP6 is downregulated during collateral vessel formation to allow potassium channels to transduce flow-induced signals inside the cell. To further analyse a role for potassium channels in my model of collateral vessel formation, patch clamp recordings could be used to measure activity during changes in flow following ligation or potassium channel blockers could be used to test if this inhibited collateral formation.

Titin (TITIN), was also downregulated in tissue from chicks undergoing collateral vessel development (tied-ligated) compared with sham-ligated at 4 and 12 hours post-ligation. This protein is involved in the structural integrity of cells, including the alignment and shape of cardiomyocytes (May *et al.*, 2004). There is evidence from the *shrunk-head* phenotype in mice, which results from a *Titin* mutation, that suggests this gene also helps endothelial cells to maintain their cell shape (May *et al.*, 2004). A downregulation of this structural protein may be required for endothelial cells to morphologically adapt to the change in flow conditions.

More specific functions to the process of collateral vessel formation may explain the regulation of genes at both timepoints following ligation. For example, E-selectin (SELE) was downregulated at both timepoints. SELE is a receptor expressed on activated endothelium and plays a role in monocyte adhesion, essential for arteriogenesis (Hofer *et al.*, 2004). This gene may therefore be expected to be upregulated in my model, however collateral vessel formation can be selectin independent (Hofer *et al.*, 2004). It is also possible that this gene was initially upregulated at earlier timepoints but was then downregulated to modulate a response and was therefore missed by my timepoints. This early response is supported by studies which show a narrow time window for endothelial responsiveness to attraction of monocytes during arteriogenesis (Hofer *et al.*, 2001). Further, flow-sensitised HUVECs *in vitro* show early induction of MCP1 followed by swift downregulation and do not show upregulation of SELE at any timepoint (Diamond *et al.*, 1990).

Increased signalling may also be expected in an activated cell. Regulator of G protein signalling (RGS7), was downregulated at both timepoints. The reason for this may be that RGS7 inhibits signal transduction via G proteins. For example, RGS7 may be downregulated to relieve its inhibitory effect on signalling pathways or transcription factors which have

been stimulated by external factors such as inflammation (Winsauer and de Martin., 2007) or changes in flow. We can speculate that RGS7 may usually prevent signals which determine cell fate, such as an endothelial cell adopting an arterial fate. Its downregulation may therefore lead to cells becoming arterial during collateral vessel formation.

Formin homology protein (FHOD3) was downregulated at both 4 and 12 hours in the tied-ligated model. FHOD3 has been found to be involved in actin organisation. This was observed in cardiomyocytes of the heart (Taniguchi *et al.*, 2009). Growth-arrest specific 2 (GAS2) was upregulated at both timepoints post-ligation. Phosphorylation of GAS2 has been shown to result in the reorganisation of the actin cytoskeleton in mouse fibroblasts. It is possible that this gene may have a similar role in organising the cytoskeleton in activated endothelial cells (Brancolini and Schneider., 1994). Considering the strong implications that the cytoskeleton is important to mechanotransduction of flow-induced signals in activated endothelial cells of collateral vessels (Helmke and Davies., 2002), it would be interesting to further investigate genes related to the cytoskeleton and actin organisation in my model.

Another cellular function which may be required at both timepoints following ligation and changes in flow is increased cell communication to allow endothelial cells to coordinate a response to changes in flow. Collagen type VIII, type 1 (COL8A1) was also upregulated at both timepoints and is thought to be involved in forming gap junctions and maintaining the structure of the endothelial cell (May *et al.*, 2004). Gap junction proteins have been implicated in endothelial responses to flow. Connexin 40 (Gja5) has been identified in chick and mice collateral vessels and found to be involved in flow-induced arterial remodelling (Buschmann *et al.*, 2010).

It is possible that some genes which showed similar expression profiles at both timepoints may determine endothelial cell characteristics important to the formation of collateral vessels such as regulating an arterio/venous identity. Iroquois homeobox gene (IRX4) was

upregulated at 4 and 12 hours post ligation. IRX4 is a transcription factor which activates gene transcription and may regulate other key genes (Hatcher and Basson, 2009). Conversely, zinc finger protein (ZFPM2) was downregulated at both timepoints and acts with GATA genes to also regulate gene expression. IRX4 has been found to be involved in patterning chambers of the heart in development (Bruneau *et al.*, 2000). ZFPM2 has been shown to be involved in patterning the valves of the developing heart (Tan *et al.*, 2012). Although there is little other information in the literature about these two genes and their roles in an endothelial context, it is possible that due to their involvement with gene transcription, they may be involved with regulating endothelial cell change of fate during collateral vessel formation. For example IRX4 may promote arterial fate and is therefore upregulated, whilst ZFPM2 may work to inhibit an arterial fate and is downregulated.

Sperm antigen with calponin homology and coiled-coil domains 1-like, (SPECC1L) was upregulated at both timepoints. This cytoskeletal, structural protein is involved in actin cytoskeleton re-organisation (Saadi *et al.*, 2011). This gene has been suggested to also play a role in cell migration and adhesion which may have implications for endothelial cells in contributing to collateral vessel formation in my model and could be further analysed with *in vitro* studies.

It is likely that some genes were expressed at both timepoints to carry out generic functions required by an activated endothelial cell, for example, Solute carrier (SLC35B3) which was upregulated at 4 and 12 hours post-ligation. It is likely that increased solutes, including amino acids, glucose and signalling molecules would be required for the increased metabolic needs of the activated cell, and for functions such as phosphorylation of proteins or cross-talk between signalling pathways (Mann *et al.*, 2003).

Junctophilin 1 (JPH1) was upregulated at both 4 and 12 hours in the tied-ligated model. Junctional proteins may be involved in mechanotransduction (Davies, 1995). Junctophilins

are important components of junctional complexes which mediate cross-talk between the cell surface and intracellular ion channels (Takeshima *et al.*, 2000). Junctional complexes allow direct exchange between neighbouring cells of signalling molecules or electrical signals to allow cells to communicate and adapt to changes such as alterations in haemodynamic forces (Haefliger *et al.*, 2004, Wagner., 2008).

Although genes differentially expressed at both timepoints are interesting, data from Chapter 3 showed that the processes occurring post-ligation are complex. There are regressing vessels as well as remodelling vessels in the tissue of interest which rely on complex signalling. I therefore needed a stringent selection process to identify genes most likely to be relevant and only expressed in collateral vessels. The most relevant portion of the heatmap was therefore a sub section of genes exclusively expressed at 4 or 12 hours post-ligation (boxed regions in Figure 4.3). These genes were either not expressed or expressed at very low levels in sham-ligated embryos. Clearly, these stringent requirements exclude many genes that may be relevant to collateral development but the number of genes differentially expressed in embryos undergoing flow-induced vascular remodelling (Figure 4.3) prevented investigation and discussion of all of these individually.

Some of the genes which showed more specific upregulation at 4 hours (node D) or 12 hours (node F) in the microarray shall now be discussed in an attempt to interpret expression profiles in the context of collateral vessel remodelling; they are discussed speculatively and would require further experiments to determine their actual role in the process.

In node D, genes of interest within this node (i.e. upregulated in tied-ligated at 4hours only), could play a role in activated endothelial cell signalling. Claudin 11 (CLDN11) is involved in tight junctions (Morita *et al.*, 1999) which have been reported to be involved in endothelial cell response to changes in flow (Davies, 1995). Discs-large homolog 2 (DLG2) is

a variant of discs-large protein which plays a role in cell proliferation and cell polarity of smooth muscle cells (Mahoney *et al.*, 2006). DLG2 may play a role in endothelial cell orientation during changes in flow. Interestingly FAT4, another polarity molecule (Saburi *et al.*, 2008) was upregulated in the microarray at 4 hours post tied-ligation (node F). A Disintegrin And Metalloproteinase with Thrombospondin Motif-like1 (ADAMTSL1) was upregulated. Other studies have shown that ADAMTSL1 may facilitate cell-matrix interactions (Hirohata *et al.*, 2002). Upregulation of Adhesion Molecule with Ig-like domain 2 (AMIGO2) may also suggest a role in collateral vessel formation; as discussed previously, adhesion molecules are known to play a role in arteriogenesis (Hofer *et al.*, 2004, Hofer *et al.*, 2001). Finally, PDE10A was also upregulated. PDE10A is known to degrade cAMP and cGMP and has been shown to play a role in pulmonary vascular remodelling (Tian *et al.*, 2011). As a note of interest, Adenylate cyclase activating polypeptide 1 (ADCYAP1) was downregulated in group C. This polypeptide increases levels of cAMP which is a molecule involved in signal transduction. cAMP is discussed later in the context of vessel remodelling in my model in chapter 5.

Node F shows the genes which are upregulated at 12 hours post-ligation. A Disintegrin And Metalloproteinase with Thrombospondin Motif 8 (ADAMTS8) disrupts angiogenesis (Campbell *et al.*, 2010) and may be necessary for arteriogenesis to occur. Interleukin 12B (IL12B) is a cytokine that has been studied in tumour biology and has been found to inhibit angiogenesis (Lee *et al.*, 2002). A Disintegrin And Metalloproteinase with Thrombospondin Motif like-3 (ADAMTSL3) is involved in MMP activity (Porter *et al.*, 2005); as discussed before, ECM breakdown is an important feature of collateral vessel formation. Sperm Antigen with Calponin homology and Coiled-coil domains (SPECC1L) regulates actin cytoskeleton rearrangement (Saadi *et al.*, 2011) and may therefore be important in endothelial mechanotransduction of a flow-induced signal or a change in cell shape due to changes in flow.

Known flow responsive regulator of endothelial gene expression, Klf2, (Dekker *et al.*, 2006) was a gene which I expected to see differentially expressed in tied-ligated compared to sham-ligated tissue, but was not detected. I had also previously detected nrp 1 and nrp2 RNA transcripts in the area of flow-induced remodelling using whole mount *in situ* hybridisation in Chapter 3 (Figure 3.18). In the microarray data nrp1 and nrp2 are expressed, but show uniform levels of expression across timepoints in tied and sham-ligated embryos. I suggest that these genes might be highly dynamically regulated and that expression of these genes is exquisitely sensitive to haemodynamic forces. In this model it is possible that sustained haemodynamic forces are required to reveal or maintain expression profiles. In the time taken to dissect the tissue for the microarray, this exquisite regulation could be lost. Future experiments could be designed to test this. By excising small pieces of tissue from the area of collateral vessel formation at the two timepoints and performing whole mount *in situ* hybridisation expression of these two genes could be compared to the results in Figure 3.18. In support of this idea, ongoing studies in the lab of Professor Marysia Placzek show that cell cycle regulated genes are dynamically regulated. Unless the tissue being investigated is fixed within one minute, expression patterns of cell cycle genes are lost (Placzek *et al.* data unpublished). Such dynamic maintenance could explain why other markers I expected to see in the microarray did not appear, but clearly more experiments are needed to test this theory.

Dynamic regulation does not account for all examples where flow-sensitive genes were not detected and could be explained instead by the timepoints selected. It was obvious that between 4 and 12 hours many temporal changes in gene expression occurred. Shear stress responsive genes have a small window of expression (Resnick and Gimbrone, 1995). Previous microarray data has shown that certain shear stress responsive genes are expressed with an early elevation which quickly returns to baseline. This includes genes such as c-jun, PDGF-B, MCP1, TGF-B, bFGF and ICAM1. Genes such as endothelin 1 and

thrombomodulin have been seen to briefly increase expression, then become significantly downregulated during the shear stress response (Resnick and Gimbrone, 1995). Other studies in mice have shown distinct phases of gene expression during collateral development which have been divided into early induction, mid-phase induction and late-phase induction (Lee *et al.*, 2004b). Early induced genes include transcription factors, followed by genes involved in angiogenesis and inflammation as well as stress-related genes. Mid-phase includes genes involved in cell cycle and cytoskeleton regulation and inflammation genes. Late-phase includes genes associated with anti-inflammatory and extracellular matrix effects (Lee *et al.*, 2004a). This data suggests that one reason I did not see differential expression of these predicted genes is that my timepoints may have missed temporally expressed 'shear stress' genes (including Klf2). To test this earlier timepoints could have been analysed or endothelial tissue extracted from the proximal vitelline vessels where shear stress is highest. Despite this, my data did show evidence of key genes such as ECM remodelling MMPs, inflammatory genes, certain adhesion molecules and genes involved in cytoskeletal rearrangement, all known to be involved in arteriogenesis in mammalian models (Lee *et al.*, 2004a). This suggests that certain processes involved in flow-induced remodelling are universal to species and a requisite for successful remodelling.

Another reason for the lack of shear stress responsive genes observed in the microarray data could be due to species as it cannot be ignored that the chick has a different vessel architecture to that of mammals (as discussed in Chapter 3). Further, this relates to the different flow profiles the chick embryo extra-embryonic collateral vessels experience compared to that in mammalian models. Different flow profiles are known to activate different genes (Chiu *et al.*, 2009). It has also been shown that the surrounding cellular environment can effect gene transcription in flow-treated cells. For example, Chiu *et al.*, (2009) showed the different expression profiles of flow treated endothelial cells when

cultured next to either smooth muscle cells or fibroblasts. The cells were separated by a porous membrane in a parallel flow chamber and received either shear stress induced levels of flow or remained static. In the shear stress environment, smooth muscle cells were found to inhibit endothelial expression of adhesion molecules such as ICAM1, VCAM1 and E selectin. The authors concluded that smooth muscle cells regulate shear stress induced genes in endothelial cells (Chiu *et al.*, 2009). As the chick embryo collateral vessels do not contain smooth muscle at this stage, endothelial cells would not be regulated in this way and therefore may express different genes.

The microarray was performed using heterogeneous tissue from the chick model, containing ectoderm and endoderm as well as blood vessels. Sham-ligated tissue was extracted from the same region to correct for any changes in gene expression which were not driven by, or not effected by, flow. However it is possible that gene expression profiles may not have been exclusively endothelial and may therefore have masked endothelial shear stress responses.

Although some of the 'expected' arteriogenic genes were not detected in my array, I believed that the results of the transcriptional analysis could provide a useful platform to discover novel genes involved in collateral vessel formation. To select candidate genes for validation of the microarray I prioritised analysis of genes based on the following criteria: only expressed in the area of collateral vessel remodelling (boxed regions of nodes D and F); a known function related to vessel remodelling in the literature; easily investigated pharmacologically with *in vivo* study; those with high enough expression that they could be detected by QRTPCR. Based on these criteria, genes were selected to take forward to the validation stage using a second, QRTPCR technique, to confirm the expression profiles observed in the microarray and identify a gene to investigate *in vivo*.

Four genes were successfully optimised for QRT-PCR and which reflected expression profiles observed in the microarray. A disintegrin and metalloproteinase with thrombospondin motif (ADAMTSL1), phosphodiesterase 10A (PDE10A), stanniocalcin 2 (STC2) and prostate stem cell antigen (PSCA). ADAMTSL1 and PDE10A could be found in the boxed region of node D, suggesting specific upregulation in collateral vessel tissue at 4 hours post tied-ligation. STC2 and PSCA were found in the boxed region of node F, suggesting a specific upregulation in collateral vessel tissue at 12 hours post tied-ligation. I selected a gene to take forward into functional analyses which were necessary to further validate gene expression in the context of collateral vessel formation.

I chose not to pursue studies into ADAMTSL1 expression as this gene had already been investigated for an involvement in vessel remodelling due to its role in the extra-cellular matrix (Jonsson-Rylander *et al.*, 2005). Therefore it was a likely possibility that ADAMTSL1 was enabling collateral vessel development in my model and so did not offer an opportunity to identify a novel contribution to the field.

PDE10A had not previously been investigated in the remodelling vasculature. Since beginning my studies on PDE10A Tian *et al.*, (2011) published a role for PDE10A in pulmonary vascular remodelling and linked levels of cAMP to vascular smooth muscle cell proliferation (Tian *et al.*, 2011). However, this did not explain the up-regulation of PDE10A in the chick model during the early phase of collateral vessel growth in the area of extra-embryonic vasculature, which lack smooth muscle and apparently show little need for cell proliferation. An interesting possible interaction between PDE10A's degradation of cAMP and flow-induced remodelling is implied by White (White *et al.*, 2011). This group used transcriptomics and functional assays to compare HUVECs exposed to laminar shear stress (15dynes/cm<sup>2</sup>) with elevated shear stress (75dynes/cm<sup>2</sup>). Both flow profiles regulated different gene expression profiles. In this study ATF transcription factors, which are highly

enriched in shear responsive genes, were regulated by levels of cAMP which fluctuated as a result of shear stress. Further, shear induced changes reduced cAMP levels. cAMP activity (and PKA activation) usually causes ATF4 (which can be an activator or a repressor of transcription) to repress gene transcription. Reduced cAMP (and PKA activity) increased ATF4 gene activation. Interestingly, ATF4 binding sites are enriched in genes upregulated in elevated shear stress (White *et al.*, 2011). This study provides an intriguing link to PDE10A's up regulation and function (to reduce levels of cAMP), to the role PDE10A may play in flow-induced vessel remodelling in the chick embryo.

STC2 was another interesting gene. STC2 has recently been investigated in vascular biology in the cancer field (Chang *et al.*, 2003, Buckanovich *et al.*, 2007). STC2 transduction by lentiviruses into HUVECs showed increases in cell cycle regulators, MMPs and junctional proteins like Ve-cadherin. STC2 was also found to mediate VEGF pathways. Once again, for functional validation of expression and investigative experiments, lentiviral transfections and *in vivo* studies in the chick would have been difficult. It was therefore logical to begin with investigations into PDE10A, as this was an enzyme with inhibitors readily available.

Other technical considerations directed my choice of focus on particular candidate genes . PSCA encodes a glycoprotein and has never been associated with the remodelling vasculature. To investigate its functional role in my model, agents which would block PSCA function such as blocking antibodies would have to be designed or genetic studies to silence the gene would be required which were not possible at the time.

I chose to pursue functional studies to investigate a role for PDE10A expression in collateral vessel formation. This was a gene that was highly expressed at 4 hours post-ligation. Pharmacological inhibitors were readily available to investigate the effect of PDE10A inhibition on collateral vessel formation

Microarrays provide a powerful tool for the analysis of a whole genome transcriptome. This approach can be used to examine the transcriptional profile induced by a treatment or disease state (Duggan *et al.*, 1999). However, although microarrays have provided a means to identify novel mechanisms of disease or potential therapies, limitations of using this genetic profiling technique cannot be ignored.

In both microarray and QRTPCR technology, technical limitations exist however, these can be diminished by a number of factors: template quality and variability; flaws in protocol/assay design and optimisation steps; ineffective data normalisation, which all effect results (Dallas *et al.*, 2005, Morey *et al.*, 2006). Control parameters correct for these factors and are now widely used as standard procedure: biological and technical replicates; use of probabilistic or statistical approaches (Liu *et al.*, 2005); standardised calculations such as  $2^{-\Delta\Delta ct}$  (Nolan *et al.*, 2006) and careful selection of a non-fluctuating housekeeping gene.

Although the validation of my candidate genes did support the expression profiles in the microarray, there were differences in the relative amounts of gene expression. This may be partly explained by cross hybridisation of microarray probes binding to related sequences, which mask true expression levels (Rajeevan *et al.*, 2001). Sample quality at the time of QRTPCR analysis may have degraded compared to when the microarray was conducted. Other contributing factors may be amplification errors and mis-priming, which leads to primer dimers affecting QRTPCR results (Rajeevan *et al.*, 2001). I attempted to check and decrease the amount of error. The samples were checked for quality first by nanodrop and then by the RNA Integrity Number (RIN) which is assessed by a computer algorithm. I chose to have 3 biological replicates per sample and ensured that each sample was of a similar quality and yield. The microarray itself consisted of a chip with many copies of the same PM/MM probes which reduced error. PUMA analysis also increased integrity of results by

using computer algorithms and normalisation to increase accuracy of probe level data. QRT-PCR was performed with primers optimised for temperature, cDNA concentration and primer concentration. 3 biological replicates were run to increase accuracy of results and reduce pipetting error. Technical runs were repeated to ensure reproducibility. To extract fold change data from the results a well characterised formula was applied to the ct value data (delta delta ct method (Nolan *et al.*, 2006). Despite differences in gene expression levels, the gene expression profiles observed in the microarray were reproducible with QRT-PCR at both 4 hour and 12 hour timepoints for PDE10A, ADAMTSL1, STC2, PSCA. This gives me confidence that these genes are regulated by flow in the chick embryo model.

It is important to recognise that important mediators of collateral vessel development may not be transcriptionally altered, or that the complex nature of the tissue and processes involved could mask real changes in gene expression (Kerr *et al.*, 2000). There are different approaches to extracting relevant data from the large datasets (Duggan *et al.*, 1999). There is some discrepancy over the best method of estimating probe level data to select differentially expressed genes, which include: implementing fold change limits (Duggan *et al.*, 1999); cut offs determined by P-values (O'Donovan *et al.*, 2008) or probabilistic approaches which assess PPLR (Milo *et al.*, 2003). Analysis of our microarray data was conducted using PUMA to identify the PPLR value for each gene. This probabilistic approach accounts for variance between chips and samples and error at the probe level and has been found to improve detection of differentially expressed genes (Liu *et al.*, 2005).

### **Future work**

Future work could include performing the microarray on the collateral vessel tissue at a wider range of timepoints. Collateral vessels could attempt to be isolated from surrounding tissue with a Dispase enzyme that might make the results more specific. A microarray could

be performed more proximally to the chick. For example, a microarray on tissue extracted from the unligated proximal vitelline artery immediately following contralateral artery ligation might show regulation of more specifically flow-responsive genes.

In conclusion, my study revealed a number of interesting, novel differentially expressed genes, some of which appeared to be both temporally regulated and/or flow-regulated. A number of the genes which differentially expressed between sham and tied-ligated embryos at both 4 and 12 hour timepoints included those involved in the structure of the cell or the cytoskeleton. There were also many shared genes involved in cell communication and signalling, which could be expected due to the complicated coordination of events involved in the endothelial response to changes in flow.

The next chapter focuses on the functional role of PDE10A, to attempt to uncover a functional role for this gene in flow-induced vessel remodelling

## Chapter 5

### Examining the role of phosphodiesterase 10A in collateral vessel development

#### Summary

In this chapter I examined the transcriptional regulation of PDE10A in flow-treated HUVECs *in vitro* and confirmed expression of PDE10A protein in the area of collateral vessel formation in the chick embryo. I used pharmacological assays to show that PDE10A is required for flow-induced vessel remodelling. This effect could be rescued by blocking the downstream effects of PDE10A inhibition.

The aims of this chapter were;

- To confirm expression of PDE10A in endothelial cells *in vitro* and to determine whether this is affected by altered fluid forces
- To determine the temporal and spatial expression of PDE10A protein in the extra-embryonic vitelline vasculature during flow-induced remodelling in the chick
- To establish the effect of pharmacological inhibition of PDE10A on flow-induced remodelling
- To examine mechanisms whereby PDE10A may influence flow-induced remodelling

#### 5.1 The effect of altered flow on PDE10A expression in human endothelial cells

My microarray data suggested PDE10A is upregulated at the site of collateral vessel development, an upregulation which I considered most likely to be in endothelial cells in response to altered blood flow. I therefore wished to confirm that endothelial cells express PDE10A and that this expression changes under conditions of altered flow.

I therefore examined PDE10A expression in human umbilical vein endothelial cells (HUVEC, the endothelial cell line most commonly used and available in my department). PDE10A expression was quantified by QRT-PCR on RNA from HUVECs extracted from 7 different umbilical cords (Section 2.9). HUVECs were either cultured in static conditions or on an orbital shaker. In the plates on the orbital shaker, cells in the centre of the well are exposed to disturbed flow, while those at the periphery are exposed to non-disturbed flow (Dardik, 2005). The cells in the centre display a 'cobblestone' appearance with high levels of proliferation whereas cells at the periphery have an elongated shape and align with the direction of flow with little proliferation (Dardik, 2005). Endothelial cells exposed to different flow patterns have been shown to express different genes based on an atheroprotective or atheroprone requirement (Partridge *et al.*, 2007).

I detected PDE10A mRNA in all HUVEC samples, confirming my hypothesis that endothelial cells express this gene. PDE10A mRNA expression was significantly higher in cells at the periphery of wells exposed to orbital shaking compared with either cells exposed to static conditions ( $p=0.02$ ) or cells in the centre of the same wells (disturbed flow) ( $p=0.03$ ) (Figure 5.1). This data suggested that PDE10A expression in HUVECs is regulated by altered flow.

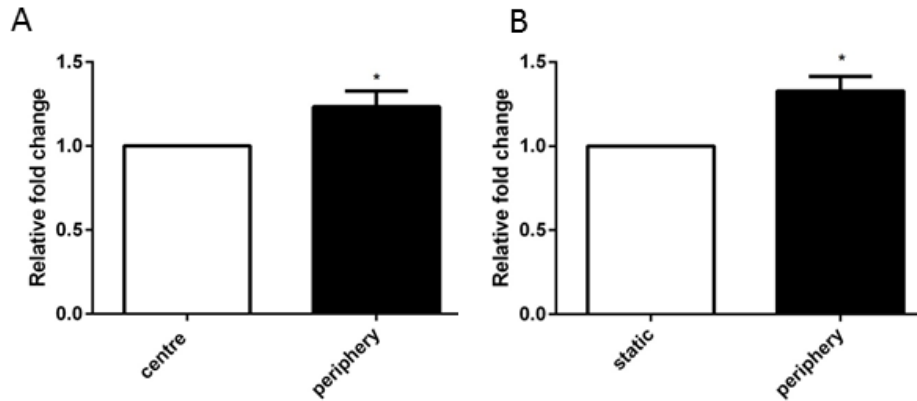


**Figure 5.1 PDE10A gene expression in flow treated or static HUVECs**

HUVECs extracted from 7 different umbilical cord veins were cultured in 6 well plates to ~400,000 cell density. Following orbiting QRT-PCR was performed on extracted RNA. (n=6) Relative fold change was calculated using the delta Ct equation. Ct of each sample was normalised to a non-flow responsive housekeeping gene **A.** shows QRT-PCR results from HUVECs exposed to disturbed (centre) or non-disturbed (periphery) flow for 72 hours in culture. PDE10A mRNA was upregulated in cells exposed to non-disturbed flow at the periphery compared to cells at the centre. QRT-PCR was performed on 2 occasions, Unpaired Student's t-test  $p=0.03$  **B.** Expression of PDE10A in HUVEC cultured under static conditions or at the periphery of wells on orbital shaker. QRT-PCR was performed on 2 separate occasions) Unpaired Student's t-test  $p=0.02$  ( $\Delta\Delta Ct$  calculated as described in Section 2.8.8)

## 5.2 Temporal analysis of PDE10A protein expressed in the area of flow-induced vessel remodelling

In the previous chapter I showed by microarray and QRT-PCR that PDE10A mRNA is upregulated during collateral vessel development 4 hours after ligation. This did not confirm whether PDE10A protein was upregulated, as some mRNA transcripts are not translated into proteins (Jayapal and Melendez, 2006). I therefore performed Western blots on protein lysates extracted from the area of collateral vessel formation in ligated and sham-ligated chicks (Section 2.20), to analyse PDE10A protein expression in groups of pooled embryos, across different timepoints, including those used in the microarray.

Figure 5.2 shows a representative blot (n=3) of PDE10A protein expression at the site of collateral development at 4, 8, 12 and 24 hours in sham or tied-ligated embryos. Although PDE10A is expressed in the testis and brain it is also expressed in the heart (Bender and Beavo, 2006). I therefore used chick embryo heart tissue from the same stage (HH st 17) as a positive control to confirm PDE10A protein expression.

The blot shows a number of different bands. This is most likely to be due to the non-specific nature of a polyclonal antibody and unfortunately, due to cost it was not possible to purchase a second, more specific antibody. PDE10A has a molecular weight of 95kDa. There were two bands at the correct protein size for PDE10A, one of which was also detected in the positive control tissue. The top band was the band of interest (as shown in the positive heart tissue, indicated by the arrow at 95 kDa). The presence of two bands may be due to post-translational modification such as phosphorylation or glycosylation. It is possible that there are more than one isoform of PDE10A although there is only 1 predicted splice variant of the gene in the *Gallus gallus* species, according to Ensembl

([http://www.ensembl.org/Gallus\\_gallus/Gene/Evidence?db=core;g=ENSGALG00000011537;r=3:42463951-42626252;t=ENSGALT00000018810](http://www.ensembl.org/Gallus_gallus/Gene/Evidence?db=core;g=ENSGALG00000011537;r=3:42463951-42626252;t=ENSGALT00000018810)).

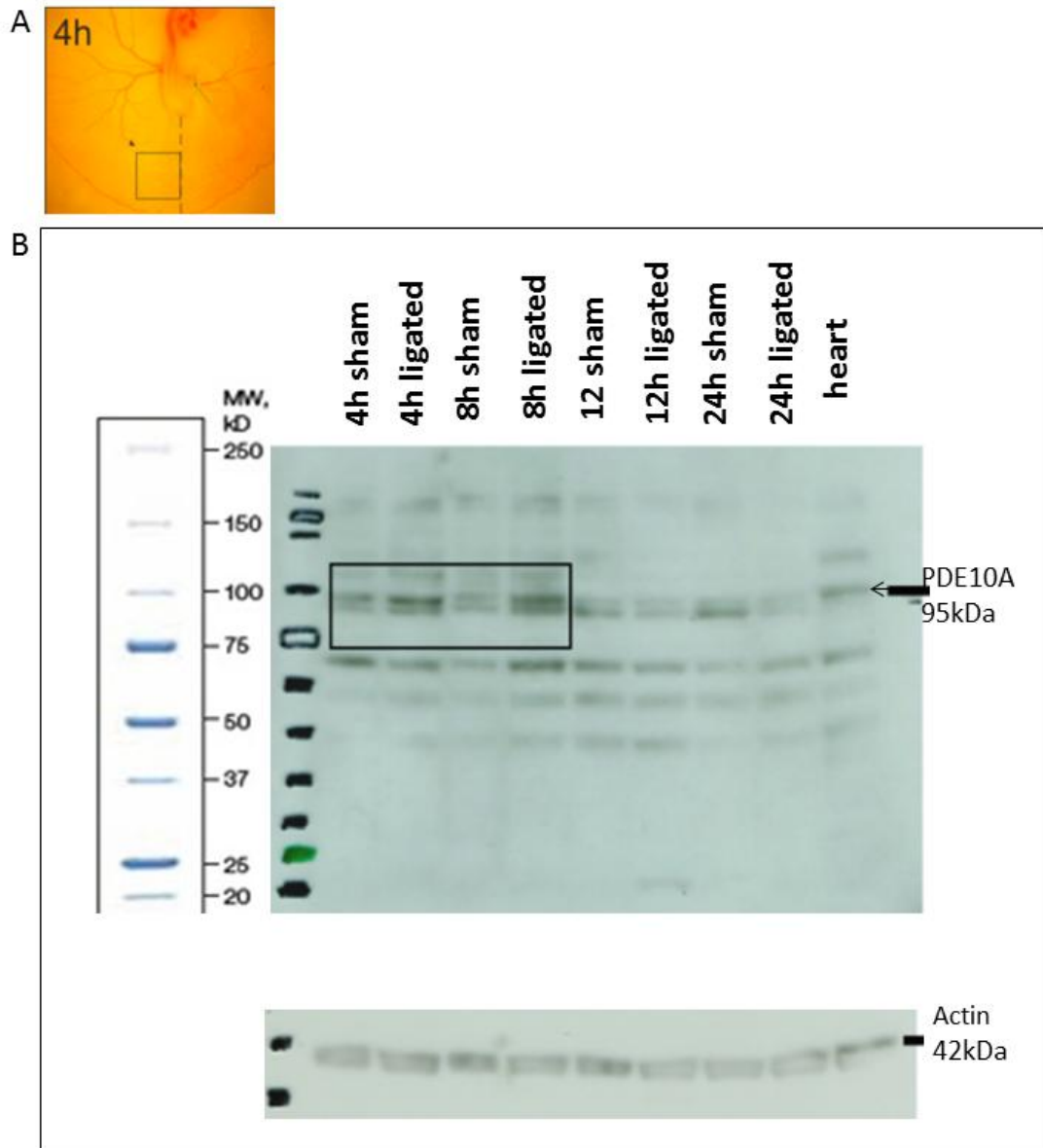


**Figure 5.2** Western blot analysis of tissue dissected from the area of flow-induced remodelling at different timepoints following sham or ligation surgery shows up-regulation of PDE10A protein during early time-points in tied-ligated embryos

**A** HH st 17 embryo. The black box at the posterior midline of the embryo shows the area from which protein lysates were extracted for analysis. **B** PDE10A protein expression appears upregulated in ligated tissue compared to sham at both 4 and 8 hours post-ligation. At 12 and 24 hours, PDE10A expression appears *downregulated* in tied-ligated embryos. Black box indicates bands that show PDE10A protein up-regulation at early timepoints in tied-ligated embryos, compared to sham-ligated embryos. PDE10A protein is recognised at the top band at 95kDa which is expressed in positive control heart tissue. Actin loading controls are below the PDE10A blot. Actin is recognised by a band at 42 kDa. In each group, lysates from 8 embryos were used and experiment performed three times. An unstained Precision Plus Protein Standard ladder was used to identify molecular weights.

This PDE10A protein data reflected the PDE10A mRNA expression profiles observed in the microarray (table 4.4). Having confirmed that PDE10A protein was also upregulated in the area of collateral vessel development 4 hours after ligation, I next wanted to test whether PDE10A protein could be detected in the vessels themselves.

### **5.3 Immunohistochemistry for PDE10A in proximal vitelline and developing collateral vessels**

In the microarray, PDE10A mRNA expression was detected in a heterogeneous sample of extra-embryonic tissue (area of collateral vessel remodelling). I therefore next used immunohistochemistry to attempt to detect expression of PDE10A at a more specific resolution.

I used the same PDE10A antibody as for my Western blot analysis and optimised the concentration for immunofluorescence (section 2.17). PDE10A has not before been investigated in chick in the literature, but in the mouse, expression is highest in the brain and testis (Omori and Kotera, 2007). I therefore first tested the PDE10A antibody in mouse brain tissue sections, over a range of concentrations, to act as a positive control (Appendix, Figure A9). A concentration of 1:500 was found to give optimal labelling on mouse tissue. Recognising that the antibody was not designed against mouse tissue I therefore also tested the antibody on chick brain tissue (Appendix, Figure A10). Sections were taken from chick embryo brain tissue at the same stage as my experimental stage embryos (HH st 17) and tested over the same range of concentrations. In fact, a concentration of 1:250 was found to be optimal for labelling chick tissue (Appendix figure A10).

VE-cadherin was used as a positive control for endothelial cells (following analysis in section 3.6.1, Figures 3.14 -3.16). Tissue incubated with no primary antibody and a secondary antibody alone acted as a negative control to check that the secondary antibody had specifically bound to the primary antibody. Dual labelling of PDE10A and VE-cadherin

was not possible since both primary antibodies were raised against the same species. Adjacent sections were therefore separately labelled to detect PDE10A and VE-cadherin proteins. Serial sections through the area of collateral vessel remodelling were cut to a thickness of 12µm to allow the adjacent cells to align to approximate PDE10A expression and location.

I examined PDE10A protein expression in the area of collateral vessel development 4 hours after ligation (Figure 5.3). I hypothesised that I would detect PDE10A expression in the collateral vessels at early time-points, given the microarray and QRT-PCR validation data. Figure 5.3 shows preliminary evidence of PDE10A protein expression in collateral vessels at 4 hours post-ligation. A punctate expression pattern of PDE10A labelling was detected in regions which expressed VE Cadherin in adjacent sections (Figure 5.4). PDE10A punctate expression patterns have been observed before in striatal neurons (Nishi *et al.*, 2008). I did not examine tissue from sham-ligated tissue as there are very few vessels in this region at the midline, making comparisons to sham-ligated embryos, difficult.

Taken together with my results from the western blotting, my immunohistochemical data suggest that PDE10A protein expression is increased in the area of collateral vessel development, and that this is localised closely to VE-cadherin positive structures, i.e. blood vessels. I cannot conclude from the histology that these blood vessels are collateral vessels, although since sham-ligated vessels possess very few vessels in this area at this timepoint, this does appear likely.

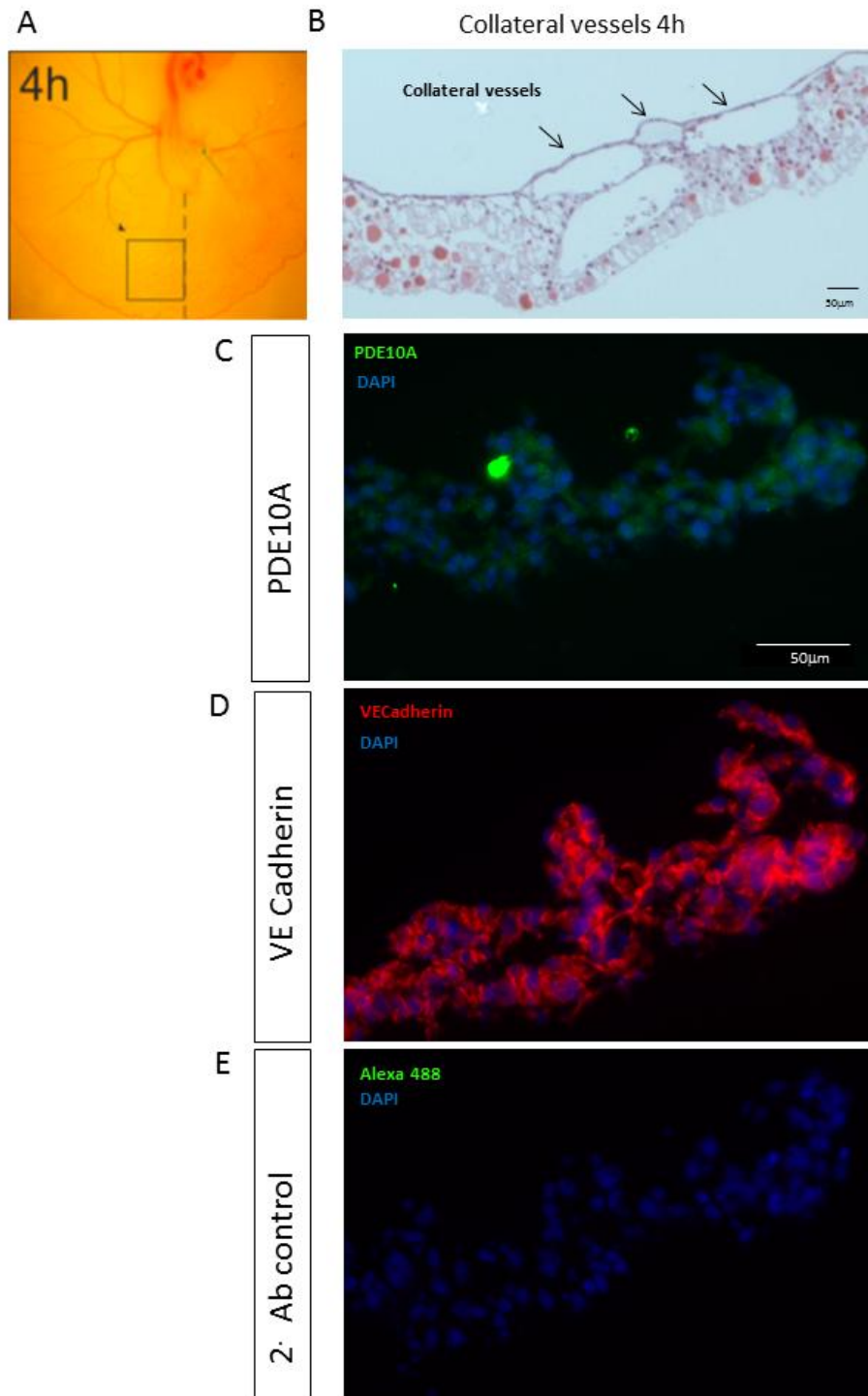


**Figure 5.3 PDE10A can be detected by immunohistochemistry in the collateral vessels 4 hours post tied-ligation**

**A** Representative micrograph of HH st 17 embryo. Boxed region indicates area of tissue dissected for immunohistochemistry. **B** Brightfield image of a cross-section of tissue taken from the boxed area in A. Arrows indicate possible collateral vessels within the tissue. **C** Confocal image of PDE10A immunofluorescent labelling of cross-sectioned tissue containing collateral vessels. **D** shows adjacent section and VE-cadherin labelling. **E** shows adjacent section and secondary antibody only as negative control. All tissues were labelled with DAPI. (n=20 not including those used in optimisation, section 2.17)

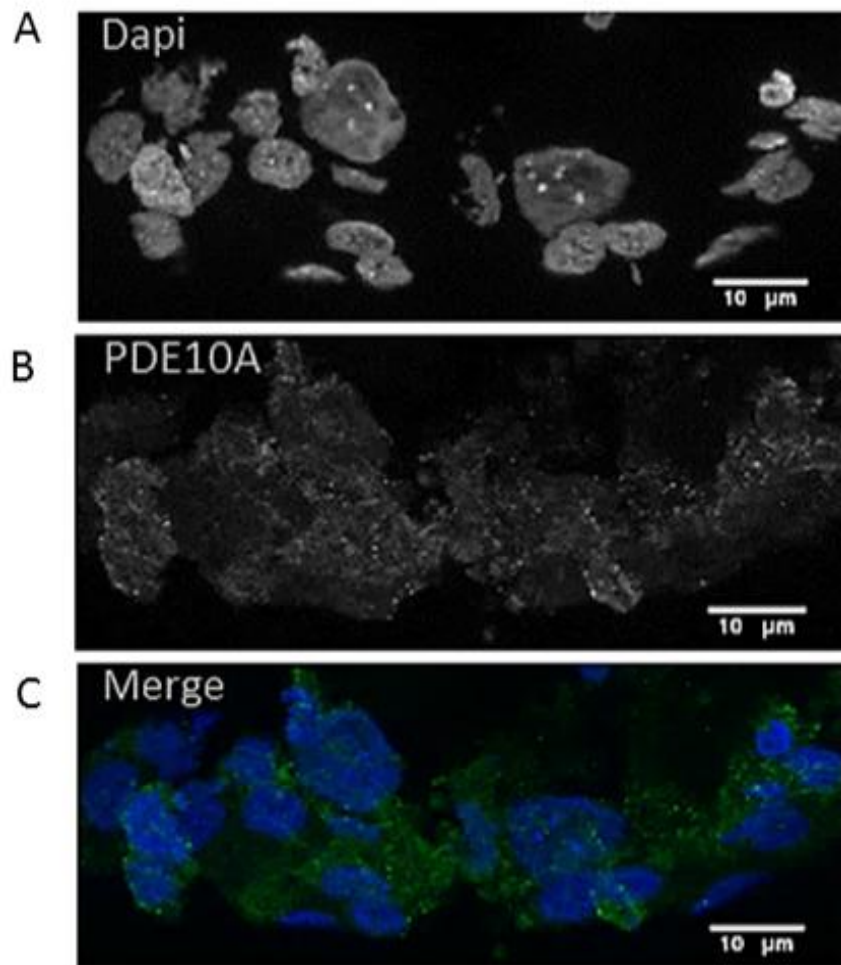


**Figure 5.4 Higher magnification images revealed punctate staining patterns of PDE10A labelling**

**A** High power image of a section through the extra-embryonic tissue in the area of collateral vessel formation showing DAPI labelling. **B** Split channel of the same section showing PDE10A labelling. **C** Merged image showing PDE10A and DAPI labelling of the tissue.

#### **5.4 Investigating the effect of PDE10A inhibition on collateral vessel formation**

I next wanted to test whether PDE10A plays a role collateral vessel formation in the chick embryo. Papaverine hydrochloride is the most potent and widely used PDE10A inhibitor, although it is also able to inhibit other PDEs with lower affinity (Siuciak *et al.*, 2006a). It is used clinically (topically during vascular surgery) as a vasodilator, due to its effects on vascular smooth muscle (Evans *et al.*, 1997, Gherardini *et al.*, 1998).

I hypothesised that papaverine application to the site of flow-induced remodelling would inhibit PDE10A function and thus impair collateral vessel formation. Filter paper discs were a suitable drug delivery mechanism (Section 2.21). For all pharmacological assays, discs were positioned over the midline vitelline veins at the site of collateral vessel development at the anterior and posterior poles of the HH st 17 embryo (Figure 2.5). Drugs were tested on 6 embryos per group with experiments repeated on separate occasions to test reproducibility. Concentrations of papaverine were selected based on previous studies. Tian *et al.* (2011) used papaverine to assess the effect of PDE10A inhibition on pulmonary remodelling in hypertensive rats (as described in section 1.16.1) and used a concentration of 25 $\mu$ M (Tian *et al.*, 2011). I therefore used this as a starting point and tested a range of concentrations from 5-20 $\mu$ M, hypothesising that the chick would tolerate a reduced concentration compared to the mouse.

#### **5.5 The effect of papaverine on normal vitelline vessel development**

I wished to establish the effect of papaverine treatment on normal vessel development to see if it was toxic, or inhibited all vessel formation. I applied papaverine to the proximal vitelline vessels whilst the vasculature was still forming, at an earlier stage (HH st 15) to embryos that underwent ligation in previous studies (HH st 17). Filter paper discs soaked in papaverine or PBS were positioned over the vitelline vessels, lateral to the embryo body.

The vitelline vessels were imaged 24-28 hours following application of papaverine or PBS (Figure 5.5A).

The mean diameter of the control treated vitelline vessels was  $233 \pm 16 \mu\text{m}$ . The mean diameter of vessels treated with  $20 \mu\text{M}$  papaverine was  $302 \mu\text{m} \pm 47$  ( $p$ =non-significant). Heart rate of the embryos was also not affected by papaverine application (Figure 5.5B).

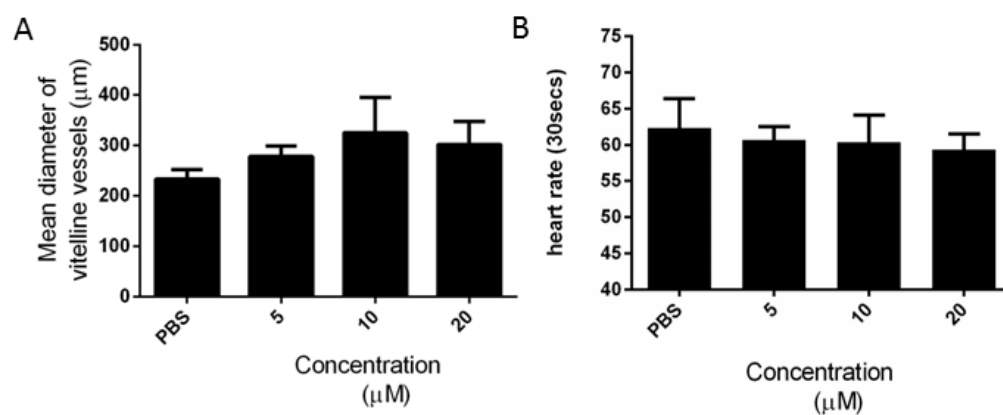


**Figure 5.5 PDE10A inhibition was not toxic to HH st 15 embryos and did not affect the diameter of developing proximal vitelline vessels**

Papaverine was applied to the developing left and right proximal vitelline vessels at HH st 15 for 24h. After 24 hours discs were removed and vitelline vessel diameter quantified. **A** Papaverine did not significantly affect the diameter of vitelline vessels compared to PBS. **B** Papaverine did not adversely affect heart rate of embryos ( $n=12$  per group) 1 way ANOVA with Dunnett's multiple comparisons test.

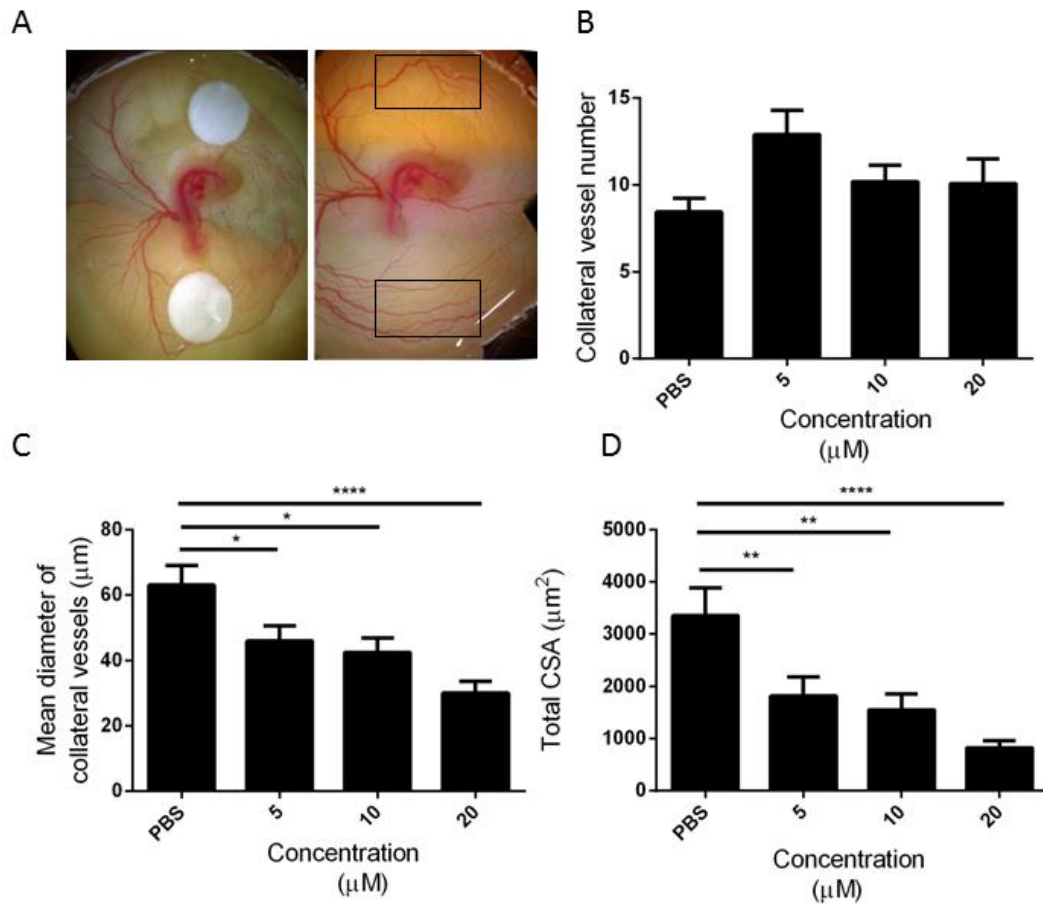
## **5.6 Inhibition of PDE10A reduces collateral vessel diameter but does not affect collateral vessel number**

I next applied filter paper discs of papaverine or PBS to the extra-embryonic tissue at the site of subsequent collateral vessel development (HH st 17, Figure 5.6A) immediately following sham or tied-ligation surgery, for 24 hours (as described in section 2.21). After this time discs were removed and vessels beneath imaged (method explained in section 2.24).

Figure 5.6B shows the number of collateral vessels at the midline 24 hours after ligation in chicks treated with filter paper discs loaded with PBS, 5 $\mu$ M, 10 $\mu$ M, or 20 $\mu$ M papaverine. Although there was a trend to an increase in collateral vessel number in the 5 $\mu$ M treated group, there were no significant differences between any group and PBS.

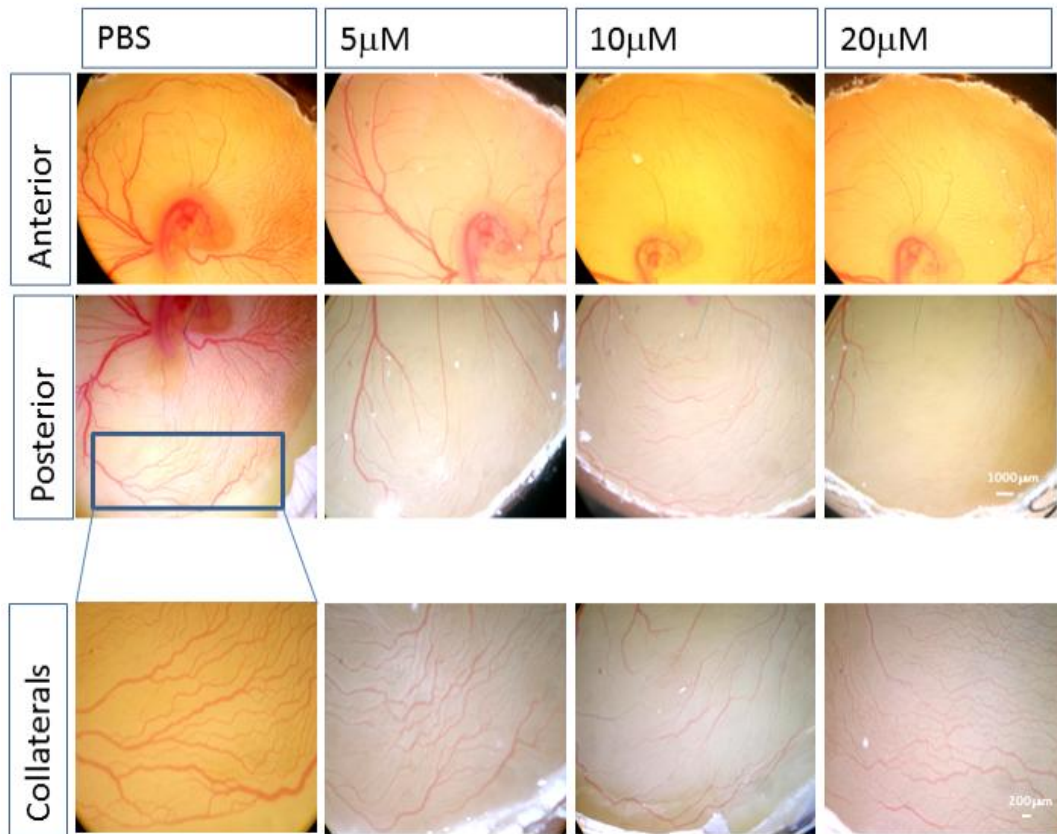
Figure 5.6C shows the diameter of the collateral vessels in the same chicks. I found that papaverine treatment statistically significantly reduced collateral vessel diameter in all concentrations, in a concentration-dependent manner. This led to a similar reduction in total cross sectional area of collateral vessels in papaverine treated embryos (Figure 5.6D).

Figure 5.7 shows representative micrographs of the area of collateral vessel formation following PBS or papaverine treatment, 24 hours post-ligation. In PBS treated chicks, collateral vessels appeared quite large and red, and extend from left to right across the midline. With increasing concentrations of papaverine collateral vessels reduced in size.



**Figure 5.6 PDE10A inhibition significantly impaired collateral vessel formation after 24 hours tied-ligation**

Papaverine was applied at the anterior and posterior poles of HH st17 embryos over the area of collateral vessel formation immediately post tied-ligation. After 24h collateral vessel number and mean diameter were quantified: **A** Representative photomicrographs of the position of the filter paper discs at the poles of the embryo for both papaverine and PBS treated embryos. Black box indicates sites of collaterals **B** Effect of papaverine on collateral vessel number, no significant differences between PBS and any concentration of papaverine **C** Effect of papaverine on collateral vessel diameter **D** Effect of papaverine on total cross-sectional area of collateral vessels after (n=12 per group). 1 way ANOVA with Dunnett's multiple comparisons test. \*=0.05, \*\*=0.001, \*\*\*\*<0.0001



**Figure 5.7 Representative micrographs show that PDE10A inhibition impairs collateral vessel development after 24 hours at the anterior and posterior poles of the embryo**

Embryos received right proximal vitelline vessel tied-ligation and either PBS, 5, 10, 20  $\mu$ M doses of papaverine on filter paper discs at anterior and posterior poles, over the area of collateral vessel formation, for 24h. Representative photomicrographs (as shown here) were analysed to assess the effect of papaverine on collateral vessel formation (described in section 2.24 and Figure 5.6). Increased concentrations of papaverine increasingly impaired collateral vessel formation at both poles of the embryo. When shown at a higher magnification collateral vessels appeared smaller in diameter (as measured in figure 5.6) with increasing concentrations of the drug (5, 10, 20 $\mu$ M), compared to controls (n=12 per group).

The data showed that application of papaverine for 24 hours significantly reduced collateral vessel diameter. However, I had detected upregulation of PDE10A as early as 4 hours after tied-ligation in the region of collateral development. I therefore examined at what stage papaverine could be detected to affect collateral formation. Filter paper discs treated with PBS or 20 $\mu$ M papaverine were applied to the area of collateral vessel remodelling as before (section 5.6) but embryos were imaged every 2 hours after ligation. At each timepoint, discs were removed, a micrograph was taken and fresh discs replaced.

The results, shown in figure 5.8, showed that 20 $\mu$ M papaverine induced a statistically significant reduction in collateral vessel diameter. These data fit with the Western blot and immunohistochemistry results which showed expression of PDE10A protein at early timepoints following ligation. In these regions, application of papaverine reduces vessel diameter. In comparison, the diameter of these vessels was unaffected by papaverine (Figure 5.5).

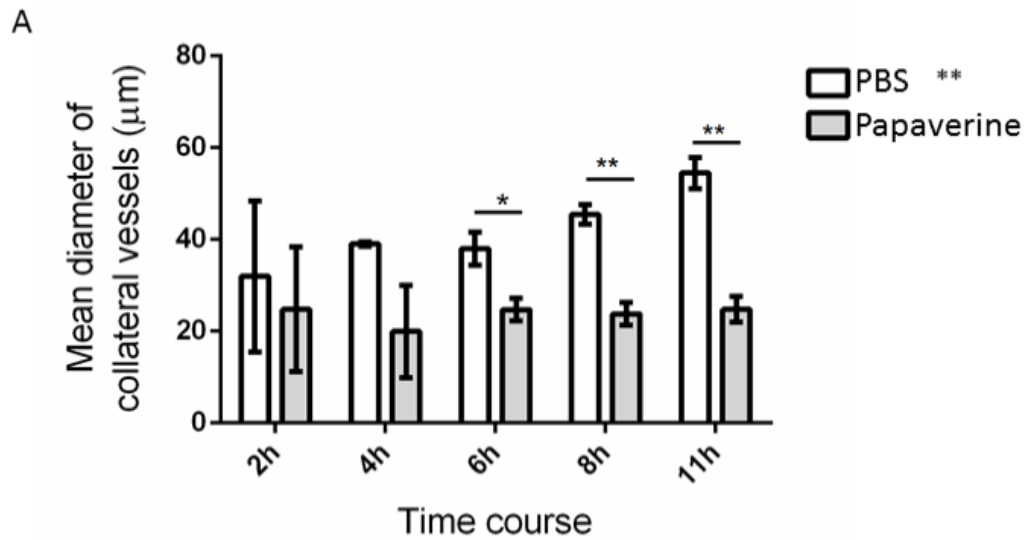


**Figure 5.8 Timecourse analysis of the effect of papaverine treatments showed PDE10A inhibition significantly impaired collateral vessel formation from 6 hours post tied-ligation**

**A** Embryos underwent right proximal vitelline vessel tied-ligation and application of 20µM papaverine or PBS vehicle on filter paper discs at anterior and posterior poles (sites of collateral vessel formation). Serial photomicrographs were performed and collateral vessel diameter quantified. 2way ANOVA showed an overall significant difference between groups over the time-course (\*\* indicates  $p=0.005$ ). Further analysis using an unpaired t-test to compare the means between groups at each timepoint revealed that papaverine significantly impaired collateral vessel formation from 6 hours post tied-ligation. (Student's t-test ; 6h  $p=0.05$ ; 8h  $p=0.005$ ; 11h  $p=0.005$ )( $n=6$  per group).

## 5.7 PKA inhibition rescues the effect of PDE10A inhibition *in vivo*

Rp-8-Br-cAMPS are cAMP analogues (Gjertsen *et al.*, 1995). The molecular structure is modified from the cAMP structure by replacing a hydrogen atom with a bromine atom, and an oxygen atom is modified by sulphur (Gesellchen *et al.*, 2006). Whereas PDE10A hydrolyses cAMP to control cAMP levels, Rp-8-Br-cAMPS competes with cAMP for PKA binding sites and cannot be metabolised by phosphodiesterases (Gjertsen *et al.*, 1995). On the basis that PDE10A and Rp-8-Br-cAMPS act in a similar way – both work to prevent downstream cAMP signalling, I therefore hypothesised that RP-8-Br-cAMPS may rescue the effect of PDE10A antagonism.

Rp-8-Br-cAMPS can penetrate cell membranes when given extra-cellularly and do not degrade during incubation as the structure is hydrolytically stable (Gjertsen *et al.*, 1995). Rp-8-Br-cAMPS are a combination of well-accepted PKA inhibitor and a widely used 8-bromo cAMP. The molecule works by occupying cAMP binding sites preventing PKA activation thus acting as a competitive inhibitor of downstream cAMP/PKA signalling (Dostmann *et al.*, 1990). When PKA is active it is composed of two catalytic subunits bound to a regulatory subunit dimer. With increased levels of cAMP each regulatory subunit binds two cAMP molecules. This causes a conformational change and dissociation of the catalytic subunits. Catalytic subunits can then phosphorylate target molecules (Gesellchen *et al.*, 2006). As cAMP antagonists occupy the cAMP binding site of the regulatory subunit, catalytic subunits cannot dissociate and become active.

Rp-8-Br-cAMPS have been studied in various models in the literature. RP-8-Br-cAMPS have been used at 30µM to investigate the effect on calcium channels in monocytes of a portal vein taken from a rabbit (Ruiz-Velasco *et al.*, 1998). *In vivo* zebrafish studies by a colleague used Rp-8-Br-cAMPS at concentrations of 0.35-1.4mM to study cAMP levels (Nikolay Ogryzko, unpublished data). In rat models Rp-8-Br-cAMPS was used at 100nM to observe

the effect on cAMP signalling via EPAC (Liebenberg *et al.*, 2011). There was little indication of what concentration would be optimal for chick embryo studies. I therefore tested a range of concentrations from 30µM- 500 µM as I expected the vessels in my model to require a higher concentration than that used in cells but less than mammalian or zebrafish studies given the direct application.

### **5.8 Rp-8-Br-cAMPS does not affect normal vessel development, heart rate or collateral vessel development**

As with the papaverine assays I first wanted to assess the toxicity of the drug or any adverse effect on vascular development. I therefore applied a range of concentrations (30µM- 500 µM) on chick embryos whose extra-embryonic vasculature was not yet fully mature and still developing (HH st 15). Filter paper discs soaked in Rp-8-Br-cAMPS were applied to the developing vitelline vessels for 24 hours (Figure 5.9); 30-500µM of Rp-8-Br-cAMPS had no statistically significant effect on the diameter of the vitelline vessels (Controls, 240±10 µm; 50µM Rp-8-Br-cAMPS, 239±26 µm; 1 way ANOVA n.s) These concentrations did not affect heart rate (Figure 5.9B).

I next examined the effect of Rp-8-Br-cAMPS on collateral vessel development in the same assay as described in section 5.6. Figure 5.10A shows that there were no significant differences in number of collateral vessels in Rp-8-Br-cAMPS treated groups compared to controls. Although most concentrations had no effect on collateral vessel diameter, 30µM Rp-8-Br-cAMPS did significantly increase this compared to PBS (Figure 5.10B). However, this was not reproduced in subsequent studies (Figure 5.11), and overall I did not detect an increase in collateral vessel diameter with Rp-8-Br-cAMPS treatment.

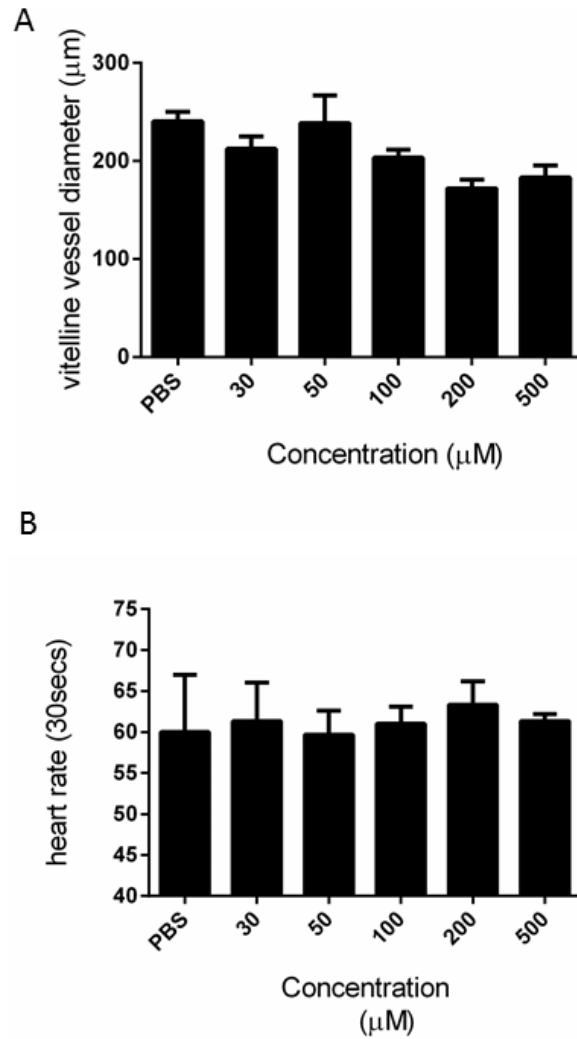


**Figure 5.9 Rp8-Br-cAMP application to the vitelline vessels did not affect vessel diameter or heart rate**

Rp8-Br-cAMP was applied to both (unligated) proximal vitelline vessels at HH st 15 for 24h to observe any adverse effects on the development of the vitelline vasculature. After 24h the discs were removed and the vitelline vessel diameters were quantified. **A** Rp8-Br-cAMP did not significantly affect the diameter of vitelline vessels compared to PBS treated embryos. **B** Rp8-Br-cAMP did not adversely affect heart rate of embryos (n=6 per group). 1 way ANOVA with Dunnett's multiple comparisons test. (n.s)

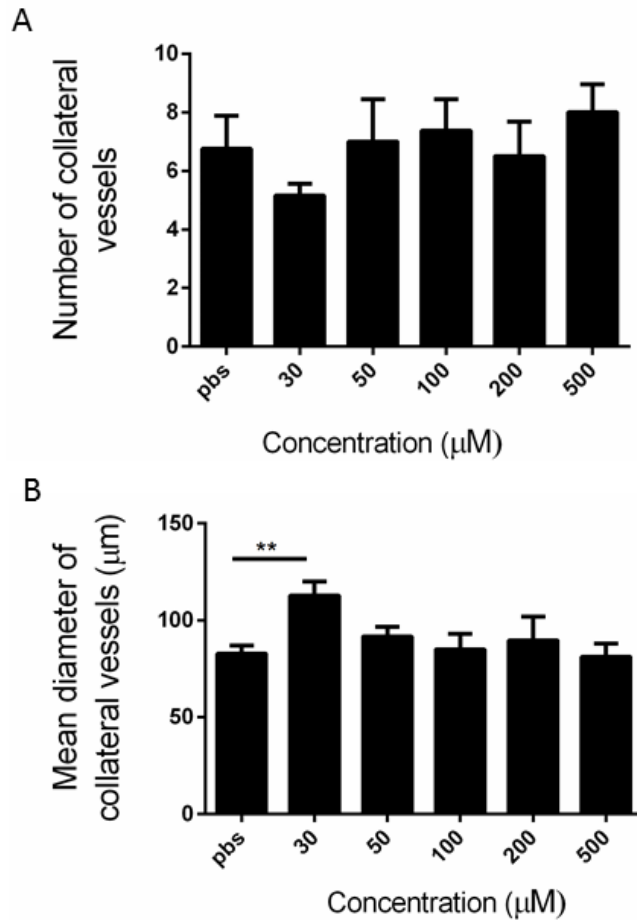


**Figure 5.10** When applied to HH st17 tied-ligated embryos, Rp-8-Br-cAMPS did not affect collateral vessel number, but at 30 $\mu\text{M}$  did increase mean diameter of collateral vessels compared to controls.

**A** Increasing concentrations of Rp-8-Br-cAMPS to the anterior and posterior poles of ligated embryos at the area of collateral vessel formation for 24h did not affect collateral vessel number. **B** The mean diameter of collateral vessels significantly increased, compared to controls at 30 $\mu\text{M}$  Rp-8-Br-cAMPS (n=6 per group). Statistical analysis used 1 way ANOVA and Dunnett's post-test. p=0.005

## **5.9 Rp-8-Br-cAMPS is able to rescue the effect of papaverine on collateral vessel diameter**

I hypothesised that a PKA inhibitor would counteract the effect of PDE10A inhibition and improve the diameter of collateral vessels treated with papaverine. As in figure 5.6, filter paper discs of PBS, 30 $\mu$ M Rp-8-Br-cAMPS, 20 $\mu$ M papaverine, or both were placed at the anterior and posterior poles of the embryo for 24 hours following ligation.

As before, 20 $\mu$ M papaverine had no effect on collateral vessel number but significantly reduced collateral vessel diameter (Figure 5.11). Treatment with 30 $\mu$ M Rp-8-Br-cAMPS had no effect on collateral vessel development, and was unable to rescue the effect of papaverine treatment.

There were many factors which could have prevented a rescue effect, particularly an insufficient concentration of Rp-8-Br-cAMPS. I therefore next tested whether 100 $\mu$ M of Rp-8-Br-cAMPS could rescue the effect of papaverine on collateral development. Repeating the assays with this concentration completely rescued the effect of papaverine on collateral vessel diameter (Figure 5.12B).

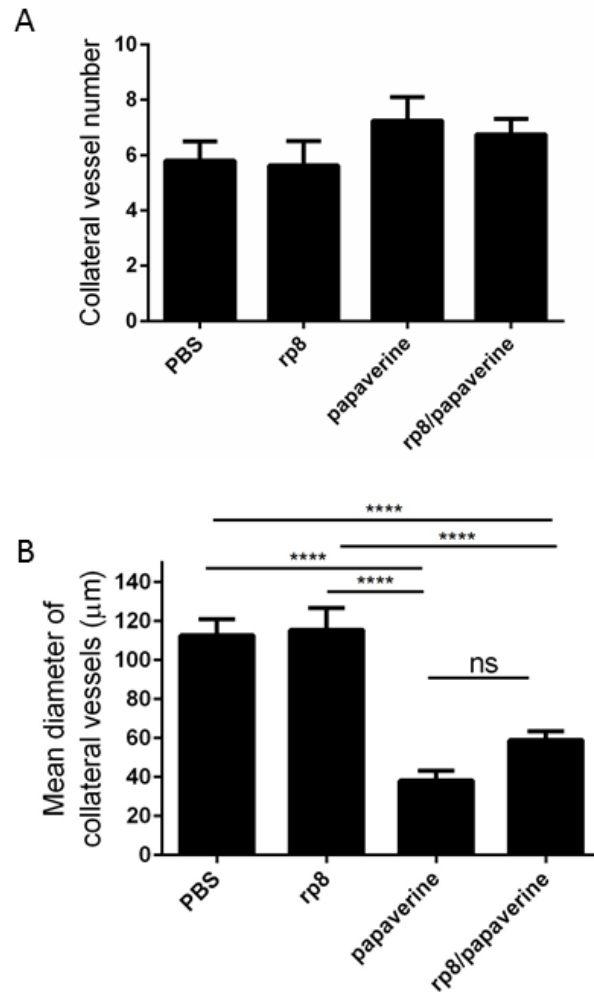


**Figure 5.11** 30μM Rp-8-Br-cAMPS did not affect collateral vessel number, and had no effect on the mean diameter of collateral vessels when co-treated with papaverine for 24 hours post tied-ligation

**A** No significant difference was observed between groups treated with either PBS, Rp-8-Br-cAMPS (30 μM alone), papaverine (20 μM alone) or Rp-8-Br-cAMPS (30 μM) with papaverine (20 μM) (ns) **B** The mean diameter of the collateral vessels of the papaverine treated group and the group co-treated with papaverine and Rp-8-Br-cAMPS were significantly reduced compared to PBS controls and Rp-8-Br-cAMPS (30 μM alone) (n=8 per group). Statistics were performed with 1 way ANOVA and Bonferroni's multiple comparisons post-test. (\*\*\*\* p<0.0001)

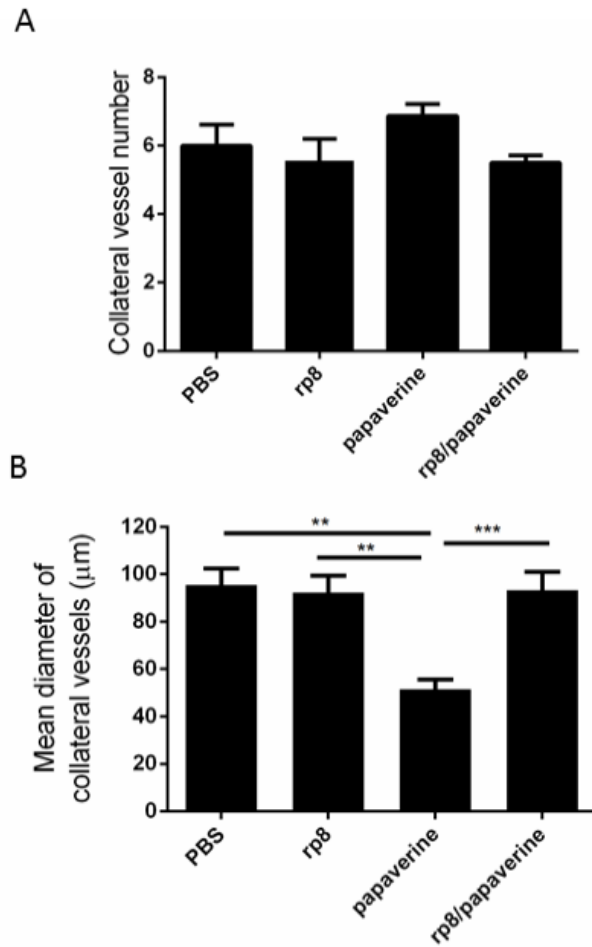


**Figure 5.12 100μM Rp-8-Br-cAMPS did not affect collateral vessel number, but did rescue the mean diameter of collateral vessels when applied to collateral vessels with papaverine for 24 hours post-ligation**

**A** No significant difference was observed between groups treated with either PBS, Rp-8-Br-cAMPS (100 μM alone), papaverine (20 μM alone) or Rp-8-Br-cAMPS (100 μM) with papaverine (20 μM) **B** The mean diameter of the collateral vessels of the papaverine treated group were significantly reduced compared to all other groups after 24h post tied-ligation (n=8 per group). Statistics were performed with 1 way ANOVA and Bonferroni's multiple comparisons post-test. (\*\* p<0.05, \*\*\* p<0.005)

## 5.10 Investigating a functional role for PDE10A in collateral vessel remodelling

I next sought to investigate how PDE10A inhibition impairs collateral vessel formation *in vivo*. A previous investigation of PDE10A inhibition in hypertensive rats showed that papaverine administration induced increased activity of cAMP and phosphorylation of CREB (Tian *et al.*, 2011). One effect of this was reduced remodelling of pulmonary vasculature due to a reduction in proliferation. My previous attempts to assess a role for proliferation in flow-induced vessel remodelling in sham and tied-ligated embryos showed a trend towards an increase in proliferation in the area of flow-induced remodelling 4 hours following ligation (Figure 3.19). Some studies state that proliferation in this extra-embryonic tissue should be minimal during remodelling due to the intussusceptive growth of the vessel network (Buschmann *et al.*, 2010). Other studies of arteriogenesis in mammalian models show that endothelial cell proliferation is required for outward remodelling of the vessel lumen (Scholz *et al.*, 2000, Heil and Schaper, 2004). I examined the effect of PDE10A inhibition on proliferation in the area of collateral vessel remodelling 6 and 8 hours after ligation. These timepoints were selected because in figure 3.19 proliferation at 4 hours showed a trend towards being increased in the ligated embryos. I therefore wanted to test if this trend became significant at later timepoints. Further, in figure 3.7, collateral vessel diameter increased most between 4-12 hours, which could suggest proliferation was occurring or contributing to the outward expansion. My Western blot results (Figure 5.2) also showed up-regulation of PDE10A protein at early timepoints but prominent bands were observed particularly at 8 hours after ligation.

I assessed proliferation using BrdU (Section 2.22). BrdU is technically difficult to administer *in vivo* (Table 2.5). Following ligation, 25 $\mu$ l of 1mM BrdU injected over the vitelline membrane in the area of collateral vessel remodelling. Filter paper discs of 20 $\mu$ M papaverine were then applied to the area of collateral vessel remodelling as before (section 5.6). Tissue was

dissected at 6 and 8 hour timepoints and processed for analysis by immunohistochemistry labelling of the nuclear localised BrdU epitope on cryo-sectioned tissue (section 2.22).

My results showed that papaverine did not significantly affect proliferation in the area of flow-induced remodelling at either 6 hours or 8 hours after tied-ligation. Figure 5.13A showed that at 6 hours post tied-ligation only 1% of cells treated with PBS, compared to 1.5% of cells treated with papaverine were BrdU positive. In Figure 5.13B, at 8 hours post-ligation more cells were labelled by BrdU (4.5%±1 of control treated cells; 5.6%±0.8 of papaverine treated cells). The results suggest that PDE10A inhibition did not affect proliferation during vessel remodelling, although the statistical power of the assay would not be sufficient to detect a small alteration in proliferation. These data suggest collateral vessel remodelling was impaired by PDE10A inhibition due to some other mechanism than proliferation, which was low even in untreated embryos.

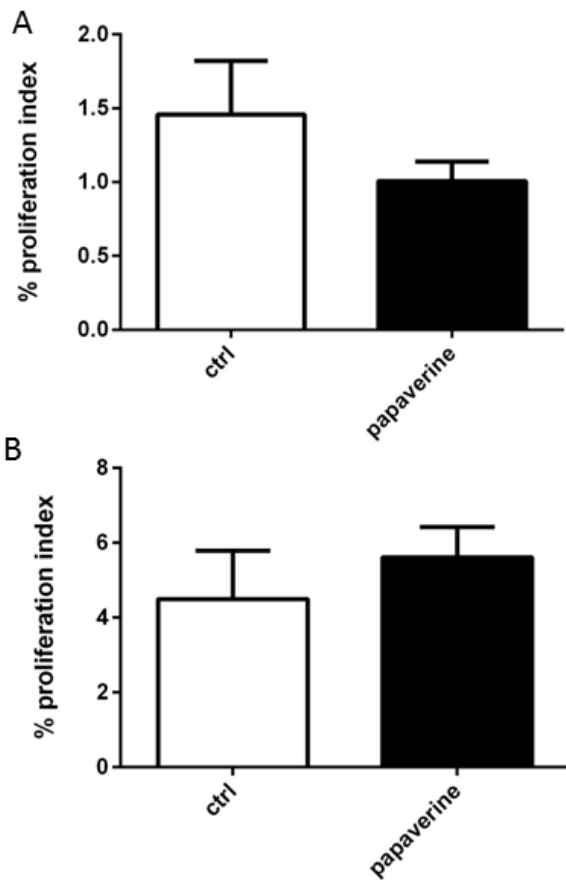


**Figure 5.13 PDE10A inhibition does not affect proliferation in the area of collateral vessel formation at 6 hours and 8 hours post tied-ligation**

Collateral vessels were treated with papaverine and BrdU for 6 or 8 hours *in vivo*, post tied-ligation, then dissected and assayed for proliferation with anti-BrdU and by quantification of proliferation index (positive cell area/DAPI positive area x 100). **A** Papaverine did not significantly alter proliferation in collateral vessels at 6 hours post tied-ligation, compared to controls **B** Papaverine did not significantly affect proliferation *in vivo* at 8 hours compared to control (n=8 per group) (Student's T-test = n.s)

## 5.11 Discussion

In this chapter I attempted to investigate the role of PDE10A in collateral vessel development. I confirmed expression of PDE10A mRNA in human endothelial cells, and that this was increased by exposure to altered flow. I also detected PDE10A protein upregulation in the area of collateral vessel development in the chick. I have shown that pharmacological inhibition of PDE10A impairs collateral vessel formation (in terms of vessel diameter, but not vessel number). The mechanism for the contribution of PDE10A to collateral vessel development remains unclear, and appears not to involve proliferation, but my observation that the effect of PDE10A inhibition can be rescued by Rp-8-Br-cAMP points to an effect that could be mediated by cAMP via effects on PKA.

My first observation in this chapter was that PDE10A was expressed in HUVECs and regulated by altered flow (Figure 5.1). This data supported the suggestion that at least some of the expression changes detected by my microarray were likely to have been induced by the alterations in blood flow induced by vitelline artery ligation. This data could therefore be taken as evidence to support the findings of the microarray. However, the altered flow conditions induced by orbital shaking do not accurately mimic the more complex changes during collateral vessel development. For example, in *in vitro* models such as the cultured HUVECs exposed to orbital flow conditions, complex re-circulation currents occur (Dardik *et al.*, 2005). This may not give a true reflection of flow-related PDE10A expression *in vivo*. Due to the benefits of studying the chick embryo *in vivo*, to investigate an endothelial response to flow (previously discussed in section 3.9), I continued the study of flow-induced PDE10A expression, and its contribution to collateral vessel formation, in my original model.

To determine upregulation of PDE10A protein in my model I used Western blotting (Figure 5.2) and to investigate an endothelial location for PDE10A in collateral vessels I used immunohistochemistry (Figures 5.3-5.4).

I first used Western blot techniques to compare PDE10A expression in the area of collateral vessel formation in sham-ligated and tied-ligated embryos (Figure 5.2). Western blotting also allowed me to semi-quantify changes in PDE10A protein expression over different timepoints. Results showed that PDE10A expression was increased at early timepoints in the tied-ligated embryos compared to the sham-ligated embryos.

On the Western blots, prominent double bands were observed at the 95kDa which corresponds to the molecular weight of PDE10A protein (Fujishige., 1999). The doublet bands could indicate modified PDE10A protein due to phosphorylation, acetylation, methylation or other post-translational events (Seo and Lee., 2004). Phosphorylation of PDE10A by PKA has been shown to alter its cellular location in PDE10A isoforms in the rat (Kotera *et al.*, 2004), indicating that this modification does occur. Double bands could also imply splice variants that share the same epitopes. In the chick there is predicted to be only 1 transcript of PDE10A (Ensembl). A third reason for multiple bands could be due to non-specific binding of the polyclonal antibody. From my results, the positive control (heart tissue), supported that the top band at 95kDa was likely to be PDE10A. Ideally a second antibody (preferably monoclonal) would have allowed confirmation of this result. However, the results of the Western blot data matched the pattern of up-regulation of PDE10A mRNA expression in the microarray (section 4.5) and was consistent with the effects of PDE10A inhibition (Figure 5.8). PDE10A was upregulated in tissue from chicks undergoing collateral vessel development (tied-ligated) compared to the sham-ligated at 4 and 8 hours post-ligation and this appearance was seen on three separate gels, confirming its reproducibility.

I next used immunohistochemistry to attempt to discover if PDE10A protein was expressed in endothelial cells, as the Western blotting data supported, but did not confirm, an endothelial location of flow-regulated PDE10A.

Despite technical challenges, I acquired preliminary immunohistochemical data about PDE10A protein expression in collateral vessels. Although subjective, there appeared to be punctate expression of PDE10A in collateral vessel tissue at 4 hours post-ligation - an expression pattern observed before in mouse striatal tissue (Nishi *et al.*, 2008). This gave me confidence in my results; however, immunohistochemistry was inconclusive in this model at demonstrating exactly which cell type expresses PDE10A during flow-induced remodelling.

In the literature, PDE10A expression has been previously observed in the cardiovascular system. Northern blots revealed PD10A transcripts to be expressed in the heart and aorta in human tissue (Fujishige *et al.*, 1999). Immunohistochemistry has also shown PDE10A expression in pulmonary arteries from human lung tissue (Tian *et al.*, 2011). It has also been shown that PDE10A can be expressed in different cellular compartments such as the nucleus or cytoplasm. This compartmentalisation of PDE10A was identified in a recombinant system which investigated splice variants of PDE10A in an *in vitro* study using COS-7 cells. An expression plasmid containing PKA catalytic subunit was co-transfected with PDE10A plasmids. Subcellular localisation of PDE10A was analysed by immunoblotting. The group found one PDE10A isoform (PDE10A2), was predominantly membrane-bound, but translocated to the cytosol when a particular amino acid was phosphorylated (threonine 16) by protein kinase A (PKA) (Kotera *et al.*, 2004).

My data showed that PDE10A protein is upregulated at early timepoints in tied-ligated embryos in the area of collateral vessel formation. It is likely that the location of PDE10A is endothelial but no solid conclusions can be drawn from the data due to the limitations of

the immunohistochemistry results. However, taking together my microarray, QRT-PCR, Western blot, immunohistochemistry and HUVEC data, PDE10A expression appears to be upregulated in vessels undergoing flow-induced remodelling and that the likeliest source of PDE10A expression is the endothelium.

Having confirmed PDE10A protein expression in the area of collateral vessel formation and upregulation in tissue from chicks undergoing collateral vessel development (tied-ligated) compared with sham-ligated, I next assessed whether PDE10A plays a functional role during collateral development, using a PDE10A inhibitor.

To perform pharmacological assays, I used a simple method of drug delivery by pipetting a set volume of solution onto uniform cut filter paper discs and applied these directly to the vitelline membrane on the surface of the extra-embryonic tissue over the area of interest (collateral vessel remodelling), at both poles of the embryo. Embryos treated with discs of PBS controlled for any adverse reactions due to the filter paper application onto the vitelline membrane surface. This was not observed, further suggesting that for my model filter papers were a useful tool for drug delivery. I used papaverine as the most widely used and most specific PDE10A antagonist available. I chose to use papaverine in a range of 5-20 $\mu$ M.

At a concentration of 20 $\mu$ M, papaverine impaired collateral vessel remodelling. Collateral vessel diameter was significantly reduced in papaverine treated chicks compared to controls after 24 hours (Figure 5.6). No studies have looked at metabolism of papaverine in the chick model, but my results suggested that papaverine was having an effect on the remodelling vessels and was not degrading over time. The published IC<sub>50</sub>s (half maximal inhibitory concentration) against PDE3A and PDE5 suggest that at this concentration there may be effects against these isoforms present in smooth muscle (Ritschel and Hammer, 1977). This was not an issue in my model as at HH st 17, in the chick embryo there is no

smooth muscle present in the extra-embryonic vasculature (Lucitti *et al.*, 2005). Further, evidence to support this comes from the fact that no vasodilation was observed.

My assay was robust, rapid and reproducible despite the difficulty in quantifying diffusion and subsequent dose released from it, but it is important to recognise limitations of this assay.

Papaverine, although widely used as a specific inhibitor of PDE10A, is not selective for PDE10A inhibition only. It is possible some of my results are due to effects on other PDEs. However, the later rescue of the effect of papaverine by Rp-8-Br-cAMPS, coupled with the lack of effect of papaverine on normal vessel development makes it unlikely that papaverine is simply exerting its effect through toxicity or non-specific inhibition.

The kinetics of release of solutions from filter paper *in ovo* is unknown. I attempted to investigate solution diffusion from filter paper to the vitelline membrane by applying food colouring solutions to the filter paper and observing release of the dye after 24 hours (Appendix, Figure A11). The solution did appear to transfer to the vitelline membrane and therefore suggested that liquid diffusion was possible. It would be more sufficient to measure the size of particles in different solutions, and to measure how much solution actually reaches the endothelial cells of the vasculature. Due to the challenges in collecting this information, I was not able to calculate the exact concentration of papaverine which reached the endothelial cells *in vivo*. The highest possible local concentration experienced by the extra-embryonic tissue would be the concentration applied to the filter paper.

Matrigel would be an alternative method of drug delivery which allows slow release of a substance over time (Staton *et al.*, 2004). This would have been useful in my assays, but matrigel contains growth factors and cytokines it contains which may have affected the results and caused an angiogenic response (Staton *et al.*, 2004). Solutions can also be

pipetted onto the surface of the embryo (le Noble *et al.*, 2004), but this does not allow for localised delivery to a targeted area. The filter paper discs, provide a more localised drug delivery to a specified area and have been used in other studies. One such study demonstrated the benefit of using filter paper to focus on an area of vessel distribution after application of a drug (Miller *et al.*, 2004). The group used the discs to target drug delivery of an angiogenesis stimulator (bFGF) to a specified the area on the CAM surface and then used this area to quantify the vascular density beneath the discs (Miller *et al.*, 2004). It is unlikely that topical application alone would have been suitable for my experiments which required localisation of the drug to a targeted area.

I next wished to understand at which point after ligation, PDE10A inhibition began to have an effect on collateral vessel remodelling. Analysis of papaverine inhibition over time identified that the effect of PDE10A inhibition was apparent from 6 hours post-ligation (Figure 5.8). These results showed that PDE10A inhibition caused detectable impairment of collateral vessel diameter at early timepoints following ligation and treatment with papaverine, compared to PBS treated controls. These results were consistent with the Western blot data that suggested PDE10A was upregulated at early timepoints in tied-ligated chicks (Figure 5.2). Since papaverine had no effect on normal vessel development and PBS treated embryos controlled for external influences, the differences between groups observed in this study were likely to be due to the specific effect of the drug.

Vessel measurements were performed as previously described (section 2.24) but for this experiment, vessels were imaged every two hours. This involved removing the embryos from the incubator, therefore exposing the embryos to a reduction in temperature. A cooling effect could have affected development of the embryo slightly and therefore the size of the vessel measured. Cooling of the eggs was unlikely to cause vasoconstriction (as discussed previously chapter 3.2). As the measurements were consistent and all embryos

received the same procedure, I can be confident in my results. To eliminate any concerns in the future, a heated light source to prevent cooling could be used during imaging.

To reduce the risk of evaporation of the drug from the filter paper during imaging of the vessels (which might alter the concentration of the drug), fresh discs were applied to the embryos. There is a possibility that the cumulative effect of replacing discs with fresh drug after each imaging session may have affected the results (i.e. the total dose received might be higher). However, the data was consistent with other experiments and thus supported the hypothesis that papaverine treatment impaired collateral vessel formation from early timepoints, leading to collateral vessels with significantly reduced diameter.

Papaverine inhibition of PDE10A has been shown to increase PKA signalling by elevating levels of cAMP (Giralt *et al.*, 2013). In the Tian study papaverine caused increases in cAMP levels which consequently impaired outward remodelling of pulmonary arteries (Tian *et al.*, 2011). I therefore next investigated if the effect of papaverine inhibition on collateral vessel formation could be rescued with an inhibitor of PKA signalling, which would stop downstream effects of elevated cAMP levels. I used the PKA antagonist, RP-8-Br-cAMPs, which competitively binds to PKA preventing downstream signalling and is more PKA specific than forskolin (Karege *et al.*, 2004). To test this I applied both the PDE10A inhibitor and PKA antagonist to embryos undergoing collateral vessel development after tied-ligation. RP-8B-r-cAMPs successfully rescued the effect of papaverine at 100 $\mu$ M and restored collateral vessel diameter (Figure 5.12). At this dose, Rp-8-Br cAMPs alone did not affect the diameter of collateral vessels. This strongly suggests that papaverine reduces collateral vessel diameter by increasing PKA signalling. This response could lead to changes in gene transcription which may contribute to the impaired collateral vessel growth observed when collateral vessels were treated with papaverine.

In the literature Rp-8-Br-cAMPs have previously been used to rescue the effects of PDE inhibition. A study by Lu *et al.* discovered that a PDE1 inhibitor, zaprinast, inhibited excitation of rat neurons by increasing levels of cAMP and consequent PKA signalling. However, Rp-8-Br-cAMPs prevented downstream effects of zaprinast by inhibiting PKA signalling (Lu *et al.*, 2004). A second study used a PDE inhibitor and Rp-8-Br-cAMPs to investigate immunological disorders related to T lymphocyte function. Mouse T-cells were stimulated with anti-CD3 antibody and Il-12 induced IFN-gamma production was measured. PDE7A was proposed to be involved with regulation of T lymphocyte function as PDE7A inhibition impaired T lymphocyte function. This was further demonstrated to be related to cAMP levels as addition of forskolin (Adenylate cyclase activator) also impaired T-cell function. However, Rp-8-Br-cAMPs reduced the suppressive effect of both the PDE7A inhibitor and Forskolin induced increases in cAMP levels (Kadoshima-Yamaoka *et al.*, 2009).

Image analysis and quantification was conducted in the same way as for previous experiments (as described in section 2.24) and was therefore consistent within these studies. However, the collateral vessel diameters of PBS and papaverine treated collateral vessels were measured to be slightly larger in the rescue assays than in previous experiments (Figure 5.6 Controls:  $63\pm 4$ ; Figure 5.11 Controls,  $113\pm 8\mu\text{m}$ , Figure 5.12, Controls  $95\pm 7\mu\text{m}$ ) (Figure 5.6 papaverine,  $30\pm 3\mu\text{m}$  Figure 5.11 papaverine  $38\pm 4\mu\text{m}$ ; Figure 5.12 papaverine  $51\pm 4\mu\text{m}$ ). This may have been due to the practicalities of the experiment. As described in section 2.21, it took time to operate on each embryo and then to image each individual embryo. It should therefore be taken into consideration that all embryos could not physically be analysed at once and therefore some embryos may have been incubated for slightly longer than others. The group sizes may have needed to be higher to see more consistent results between experiments. Another reason for the slight difference in recorded vessel size could be due to calibration issues which may have occurred from using a different type of camera for the latter experiments. Importantly, the vessel

diameters measured in previous experiments compared with the vessel diameters measured in the rescue experiments, showed a consistently significant difference between papaverine and control treated embryos. Therefore I am confident that my experiments show a rescue of collateral vessel diameter with 100 $\mu$ M Rp-8-Br-cAMPS following papaverine treatment. In summary, papaverine inhibition of PDE10A consistently caused impaired collateral vessel remodelling. Further, regardless of the experimental limitations, inhibition of PKA signalling with Rp-8-Br-cAMPS restored impaired collateral vessel diameter.

Having found some evidence that PDE10A plays a role in collateral vessel remodelling in the chick embryo, I decided to investigate a possible mechanism for this effect. There is little known about how PDE10A is regulated or what its function is. There is also little data available on the vascular effect of PDE10A inhibition. Other than being investigated in the brain, the only study showing a vascular function for PDE10A was published during the course of my own research (Tian *et al.*, 2011). This study showed that PDE10A played a role in regulating proliferation of smooth muscle cells during remodelling of pulmonary vasculature in hypertensive rats (Tian *et al.*, 2011). I had identified only very low levels of proliferation in collateral vessel remodelling at 4 hours post-ligation previously (Figure 3.19). However, taken with the evidence in the literature, it was logical that proliferation may have been prevented by PDE10A inhibition which impaired the size of collateral vessel diameter.

To test whether PDE10A contributed to outward remodelling during collateral vessel formation by influencing proliferation I attempted to determine whether PDE10A inhibition was associated with any alteration in markers of cellular proliferation during collateral vessel development. I tested for BrdU incorporation into the DNA of cells in the area of collateral vessel remodelling following ligation and in the presence of PDE10A inhibitor *in vivo*. I examined 6 and 8 hour

timepoints, post-ligation, as at these early timepoints *in vivo*, PDE10A is highly expressed (Figure 5.2) and papaverine significantly impaired vessel remodelling (Figure 5.6).

My results showed that there was no significant difference in proliferation in the area of vessel remodelling when vessels were treated with papaverine compared to PBS. There was much less proliferation detected at 6 and 8 hours post-ligation, compared to the data from 4 hours after ligation previously studied (Figure 3.19) (4 hours an average of ~10% proliferating cells; 6 hours ~1% proliferating cells; 8 hours ~4% proliferating cells). This result could have been due to the difference in developmental stages between embryos, perhaps the embryo is growing more rapidly at earlier timepoints. Another possibility is that collateral vessel development is associated with a very early increase in proliferation that was not detected by my studies and that had subsided by 4 hours after ligation, although this seems less likely given the progressive increase in collateral vessel diameter for many hours after ligation.

The difference in the levels of proliferation, of cells in the area of collateral vessel remodelling, between experiments (between 4 hours (Figure 3.19) and 6 and 8 hours (Figure 5.13) could be explained by the use of filter paper and the addition of papaverine/PBS solution. This could have affected the results as the discs may have soaked up some of the BrdU which was applied topically to the area prior to adding the discs. This may have impeded the amount/concentration of BrdU which reached the endothelial cells. The BrdU/PBS solution on the discs may have diluted the concentration of BrdU therefore also affecting how much BrdU was incorporated into the DNA. Nevertheless, I was able to detect proliferation in my control (PBS treated) groups; therefore I do not consider these assays to be sufficiently flawed to entirely discount their results.

Finally, it should be noted that PDE10A is a dual PDE; therefore cGMP levels may have also been affected. However, due to the lack of vascular smooth muscle in these vessels at this

stage, it is unlikely that any cGMP mediated vasodilatory responses would have been the cause of reduced collateral diameter (if present it would have led to an increase in diameter). I therefore conclude that I found no evidence to support a role for PDE10A in promoting proliferation during collateral vessel development, and since proliferation seems low even in my earlier studies it seems likely that PDE10A mediates its effects in other ways.

Discovering a single mechanism of action for PDE10A is difficult due to the many different roles of cAMP in mediating many different signalling pathways. For example, in neurons, cAMP levels have been found to regulate growth cone remodelling and axon guidance. cAMP levels in neurons are responsible for a cell's attractive or repulsive response to stimuli by mediating extracellular signals and cytoskeletal interactions (Lohof *et al.*, 1992). In endothelial cells, increased cAMP has been found to affect proliferation, cell cycle progression and migration (Favot *et al.*, 2003).

Since so little is known about PDE10A, speculation about its possible roles requires extrapolation from what is known about other PDE family members. It is worth noting that PDEs of different subtypes are affected and respond differently to inhibition dependent on their vascular location (Netherton and Maurice, 2005). Favot *et al.*, (2003) investigated the effect of inhibiting PDEs to prevent endothelial migration and proliferation response to VEGF in angiogenesis (Favot *et al.*, 2003). The group used a chick CAM assay to inhibit PDE2 and PDE4 in HH st 25 embryos and found that PDE inhibition reduced vessel density and angiogenesis (an effect I did not see in my own studies antagonising PDE10A in earlier stage uninstrumented chicks, Figure 5.5).

Further experiments investigating PDE2,3,4 and 5 inhibition in HUVECs have confirmed that PDE inhibition reduces vascular cell migration during angiogenesis but this was vessel type and PDE type specific (Netherton and Maurice, 2005). This information has clinical

implications as PDE inhibition could potentially therefore prevent VEGF induced angiogenesis in tumours and be used to develop novel anti-cancer therapies.

### **Future Work**

Future work could further investigate the effect of different types of flow on PDE10A expression in cultured flow-sensitised endothelial cells. Although I used HUVECs for my experiments (as these were available) future investigations could use human microvascular endothelial cells (hMVEC) which more accurately represent the microvasculature and could therefore give insights in clinical problems.

Cryosections were used to collect immunohistochemical data; however, tissue processing of the fragile extra-embryonic vessels was difficult and challenging. My attempts to optimise sectioning did not improve the quality of sections taken from tissue. Future work could experiment with different cutting techniques such as vibrotome sectioning.

A second antibody raised in a different species could allow dual labelling with an endothelial marker to confirm PDE10A endothelial expression. Individual collateral vessels could not be isolated from surrounding tissue and other cell types using fine dissection alone and due to these technical challenges, I sought to identify endothelial cells in this heterogeneous tissue. VE-cadherin acted as a marker of endothelial cells with which to co-localise PDE10A expression but could only be performed in adjacent sections due to cross-reactivity of the secondary antibody (Figures 5.3-5.4).

A second antibody would also have confirmed specific PDE10A labelling of collateral vessel tissue as the PDE10A antibody used was not confirmed by the antibody manufacturer to be specific for chick tissue. I checked the amino acid sequence of this antibody by Clustal analysis (Appendix A5) and optimised concentration and blocking steps on tissue known to be positive for PDE10A (Appendix, Figures A6, A7).

To further explore and confirm PDE10A protein expression it would be interesting to perform immunohistochemistry or in situ hybridisation for PDE10A in mammalian models. PDE10A protein studies could be performed on hind-limb ligation models to look for evidence of flow-induced endothelial expression of PDE10A in collateral vessels. PDE10A immunohistochemistry could then also be investigated at other sites of altered blood flow *in vivo*, such as arterial bifurcations, to observe any subtle changes in PDE10A expression which might be due to different types of flow (disturbed/non-disturbed).

To further validate the *in vivo* observations that PDE10A inhibition has most effect at early timepoints following ligation, I could test if papaverine treated embryos could recover their collateral vessel diameter over time. Filter paper discs containing PDE10A inhibitor could be applied to the embryo following ligation but removed at later timepoints, from 12-24 hours. I would hypothesise that this recovery of vessel diameter would be unlikely based on the Western blot results. Downregulation of PDE10A protein was observed in Western blots from 12-24 hours and it is likely that papaverine would have less effect if less PDE10A protein was present, but it would be interesting to confirm this. Filter paper was a cheap and effective drug delivery system for my *in vivo* model, however there are other tools/methods available which might have had advantages. These could be considered for future experiments.

The mechanism of PDE10A in the chick embryo during flow-induced remodelling could be further investigated by testing the role of cAMP in this process and confirming cAMP involvement with a more specific PDE10A inhibitor. A second PDE10A inhibitor such as IBMX (Soderling *et al.*, 1999) could confirm my findings. I attempted to acquire TP-10, a more specific PDE10A inhibitor manufactured by Pfizer, during my studies, but my request to the company was not approved.

Further investigations of PDE10A inhibition on collateral vessel formation could include PIV recordings, to confirm an impairment of collateral vessel diameter and the consequent effect on collateral blood flow.

Changes in gene expression, as a result of any impaired blood flow/consequences of reduced vessel diameter could be investigated by RNA analysis of endothelial cells in the collateral vessels following papaverine treatment. This could be compared to normal collateral vessel gene profiles. To observe any positive effects of enhancing PDE10A on collateral vessel formation an alternative assay could involve application of PDE10A protein to the area of vessel remodelling, following arterial ligation. Conversely, PDE10A gene silencing in the chick model by siRNA or PDE10A knockout mouse models could be used to see if impaired collateral vessel formation resulted from the absence of PDE10A gene expression. PDE10A knockout mouse models already exist and have been generated to investigate the neurological implications of PDE10A expression (Siuciak *et al.*, 2006b).

Finally, as proliferation was not found to be the mechanism by which PDE10A was influencing collateral vessel formation in my model, a migratory mechanism, or other known processes of arteriogenesis in mammalian models, could next be tested.

## Chapter 6

### General discussion

Cardiovascular disease is one of the primary causes of death worldwide (Aschwanden *et al.*, 2014). Negating the need for invasive vascular surgery by developing novel therapeutic agents to promote collateral vessel remodelling would have huge clinical applications. However, clinical trials of agents to promote collateral development have failed to reproduce the promising data from animal models. Understanding more about the process of collateral vessel development and the mechanisms underlying the factors which drive remodelling is vital in advancing this research.

Current mammalian models have provided much knowledge on the subject, yet there are many disadvantages to using these. Mouse, rat and rabbit models have been widely used to investigate collateral formation (Scholz *et al.*, 2000, Herzog *et al.*, 2002, Stabile *et al.*, 2003, Terry *et al.*, 2011) , but the hind-limb model involves invasive surgery under general anaesthesia (Ito *et al.*, 1997a, Herzog *et al.*, 2002). Laser Doppler or angiography are used to quantify blood flow or to visualise collateral vessels (Limbourg *et al.*, 2009) but do not allow for real-time observation of collateral development and are expensive and time-consuming. In the porcine coronary model there are few pre-existing coronary collateral vessels and these do not remodel in response to increased fluid shear stress (Voskuil *et al.*, 2003). Therefore this model does not lend itself well for research in this field. The *gridlock* zebrafish could be used as an alternative to mammalian models of collateral vessel formation. The mutant is a model of aortic occlusion and has been shown to develop collateral vessels in response to aortic occlusion (Gray *et al.*, 2007). However, compared to the chick embryo, the zebrafish has less homology to mammalian genes and pharmacological assays cannot be localised to specific vessels and may lead to off-target

effects. The chick embryo's extra-embryonic network of blood vessels provide insight into flow-induced vessel remodelling which can provide clues about important genes to investigate further in higher models. Although differences in vessel architecture exist between species, the vitelline vessel network of the chick embryo remodels in response to changes in blood flow in a manner that is anatomically similar to its mammalian counterparts, even though the lack of investing pericytes and smooth muscle cells will undoubtedly impact on the ability to compare results between these model species.

The first aim of my project was to assess if the chick embryo could be used as a model of collateral vessel formation, at a time when no such study had been performed. I first established a system to assess collateral vessel formation in the chick embryo. I performed a longitudinal quantification of developing collateral/collateral number and diameter following unilateral vitelline artery ligation. Studies of collateral vessel development in mammalian models, following arterial occlusion, show the process occurs in two distinct phases: an initial increase in collateral vessel number, followed by a "pruning" selection process (Duvall *et al.*, 2004). This selection process allows the more efficient vessels to persist and those carrying less flow to be pruned from the system (Hoefer *et al.*, 2001). My data showed that collateral vessel formation in the chick embryo model also involved an initial expansion of the remodelling vascular network which was refined over time to become more haemodynamically efficient. Although I have not identified the mechanisms driving this selection, its conservation between chick and mammal suggests that studies using the chick model would be likely to contribute to a better understanding of what governs selection of collateral vessels for persistence or regression.

Evidence from mammalian models suggests that therapeutic strategies for alleviating the consequences of arterial occlusive disease should be targeted to improving *arteriogenesis* (collateral vessel development) rather than angiogenesis (as discussed in section 1.8). My

data suggested that the chick embryo remodels collateral vessels from a pre-existing source in a process more akin to arteriogenesis than angiogenesis. Examination of various vascular markers in developing collateral vessels histologically and histochemically showed that flow in these remodelling collateral vessels was capable of regulating gene expression to induce an arterial identity. *In situ* hybridisation data of *nrp1* and *nrp2* markers showed that endothelial cells in remodelling collateral vessels adopted an arterial identity over time as collateral vessel extended into a previous venous territory to deliver arterial blood to an unperfused area. However, in the chick embryo the window of plasticity is brief and once cells become committed to an arterial or venous fate, they are no longer influenced by flow. The ability to induce collaterals to an arterial identity would be optimal for the requirements of carrying large volumes of blood at high pressure and velocity. Placing venous origin vessels in arterial flow conditions (such as coronary artery bypass grafting) this leads to intimal hyperplasia and a significant graft failure rate (Owens., 2010). Thus, understanding how to therapeutically influence endothelial identity, or induce plasticity of arterial/venous marker expression, might be a strategy to promote graft patency as well as promote collateral vessel development.

It can be viewed as either an advantage or a disadvantage to use a model which only gives a read out of the endothelial mechanisms involved in collateral formation depending on the specific question to be addressed. I believe that the chick model may provide some fundamental insights into the endothelial response to changes in flow which will add novel knowledge to the field. In my studies to investigate an endothelial response to changes in flow, the chick model had clear advantages over higher species. However, the collateral vessel architecture of the chick does not match that of mammalian species. Most obvious is the absence of smooth muscle in chick collateral vessels at early developmental stages (Lucitti *et al.*, 2005). For this reason, the chick model alone will never be sufficient for discovering new therapeutic targets to enhance collateral vessel formation in patients with

cardiovascular diseases. However, the chick model does provide an adequate platform from which to identify potential candidate genes or processes to investigate further in higher species and therefore could provide invaluable contributions to the field.

Due to the accessibility of the vitelline vasculature, previous groups have manipulated blood flow to observe morphological patterning and genetic changes following induced vessel occlusion. For example, Buschmann *et al.*, (2010) identified collateral vessels in the chick embryo and used this model to identify a gene which was taken forward into gene knockout studies in mouse models (Buschmann *et al.*, 2010). This gene, originally identified in the collateral vessel of the chick embryo, was found to contribute to collateral vessel remodelling in the mouse, demonstrating the ability of chick studies to identify candidate genes which drive or regulate collateral vessel formation in higher species. However, a microarray analysis of the genes differentially expressed during collateral vessel development in the chick model has not previously been described. The next part of my project was to identify potential candidate genes which may play a role in the remodelling process. My hypothesis was that flow-induced collateral vessel remodelling in my model is associated with a unique transcriptional profile that could be discriminated from the profile of “normal” vascular development that would be taking place in the same region in a developing embryo. I used microarrays to characterise transcriptional changes during different phases of flow-induced vessel remodelling. I used probabilistic data analysis as well as QRTPCR to identify candidate differentially expressed genes which may contribute to collateral development. I focussed on genes which were differentially expressed, above a fold change threshold, in tied-ligated embryos compared to the sham-ligated embryos- which did not develop collateral vessels. The transcriptional profile of the area of flow-induced remodelling showed an active response to changes in flow which reflected the *in vivo* pattern of remodelling and identified a large number of interesting differentially expressed genes.

The gene identified in the Buschmann study (2010) (Gja5) was present in the data from my chick microarray but showed no change in expression over the timepoints or between sham-ligated and tied-ligated models at the timepoints I focussed on. The absence of upregulation of this gene in my model could be explained by the window of time observed. Gja5 was detected in collateral vessels at 20 hours in chick collateral vessels and although the group observed expression of Gja5 at a 4 hour timepoint, this was in the vitelline artery and not the collateral vessels (Buschmann *et al.*, 2010). This study perhaps suggests that a microarray performed at later timepoints on chick collateral vessels may reveal different candidate genes which may be interesting to investigate. One unexpected result was that genes upregulated during arteriogenesis in mammalian models were not differentially expressed in the chick model microarray profiles. Genes found to be upregulated in response to changes in flow both *in vivo* and *in vitro* in previous studies include those involved in proliferation, vascular tone, cytoskeleton and inflammation such as MCP1, VCAM1 and ICAM1 (Ito *et al.*, 1997b, Scholz *et al.*, 2000, McCormick *et al.*, 2001, Pipp *et al.*, 2004) but were unchanged in the chick array. This may be due to the heterogeneity of the tissue analysed (and not specific collateral vessel tissue). Expression of some genes is more dynamic; particularly flow-induced genes which are exquisitely regulated and sensitive. As tissue was taken out of the flow environment in my experiment, this may have led to lost expression of these flow-sensitive genes. This could explain the reason why some of the expression profiles of these genes were not captured by microarray.

Certain transcriptional responses may be universal to endothelial cells exposed to altered flow. Expression of other key genes may differ due to differences in species, windows of expression, environment and flow patterns. For example, Lee *et al.*, (2004) investigated temporal expression of flow-responsive genes in mice following ligation or sham-ligation. The group found early up-regulation of transcription factors and DNA binding proteins, followed by a mid-phase of upregulated inflammatory genes, along with cell cycle genes

and cytoskeletal genes (Lee *et al.*, 2004a). Although MCP1 was upregulated, other adhesion molecule genes which were reported to be expressed in other mammalian species (reviewed by Schaper, 2003) were not observed. It is also noteworthy that *in vitro* studies examining the effect of altered flow on endothelial cells also often identify largely non-overlapping lists of differential gene expression. For example one study conducted by McCormick *et al.*, (2001) looked at the genes that were differentially expressed after HUVECs were exposed to laminar shear stress (25 dynes/cm<sup>2</sup>) for 24 hours (McCormick *et al.*, 2001). Genes encoding cytochromes P450 1A1 and 1A2, glucocorticoid-induced leucine zipper protein, argininosuccinate synthase and human prostaglandin transporter were most significantly altered in gene expression analysis. Most dramatically decreased were MCP1 and ET1 (McCormick *et al.*, 2001). Some genes, such as eNOS, c-jun transcription factor, PDGFA, TGFB, bFGF and ICAM1. MCP1 and ET1 have been shown to be initially upregulated but then significantly downregulated expression over time (Resnick and Gimbrone., 1995).

My data did however identify candidate genes for further study and of these I selected PD10A for functional analysis. Upregulation of RNA transcripts does not confirm a functional role for the protein of the gene; therefore further analysis is required. I began my functional analysis of PDE10A by confirming PDE10A upregulation at the protein level. Temporal and spatial expression of PDE10A protein was identified in the extra-embryonic vitelline vasculature during flow-induced remodelling at early timepoints post-ligation. Pharmacological assays showed that inhibition of PDE10A impaired flow-induced collateral vessel remodelling at early timepoints following vessel ligation. The mechanism whereby PDE10A contributes to flow-induced remodelling remains to be elucidated. However, since these studies confirmed a functional role for PDE10A in collateral development (a role unsuspected by any previous work or known function of PDE10A) it justifies my microarray approach for the relatively unbiased discovery of drivers of collateral vessel development.

Although PDE10A is not well characterised in the literature it is known to hydrolyse both cAMP and cGMP (Beavo., 1995). PDE10A contains two adenylyl cyclases and FhlA (GAF) domains in the N-terminal and a catalytic domain in the C-terminal portions of the molecule (Fujishige *et al.*, 1999, Soderling *et al.*, 1999). Direct activation of PDEs can be achieved by cyclic nucleotide binding to the GAF domain (Gross-Langenhoff *et al.*, 2006). PDE agonists and antagonists can modulate catalytic activity by binding to and stabilising either the 'closed' or 'open' form of GAF domains of PDE proteins. This is likely to be how papaverine inhibits PDE10A function; however I was unable to test an exact mechanism of action. Further, PDE10A function is still not well understood and further investigations are needed to determine whether factors such as phosphorylation or membrane attachment control GAF-dependent regulation of PDE10A catalytic activity (Gross-Langenhoff *et al.*, 2006).

PDE10A acts to regulate cAMP activity. Cyclic nucleotides act as intracellular second messengers to convey and amplify complex signals from outside to inside the cell (Essayan., 2001, Francis *et al.*, 2001) and regulate important mediators of cell signalling such as PKA. Protein kinases are cyclic nucleotide binding proteins consisting of two regulatory and two catalytic subunits (Seino and Shibasaki., 2005). PKA binds two cAMPs to its regulatory subunits which cause a conformational change to release two catalytic subunits. These catalytic subunits catalyse the phosphorylation of proteins such as PDEs (Christina., 2010). Protein kinases activate PDEs by transferring a terminal phosphate group from an ATP molecule to a hydroxyl group on the PDE (Christina., 2010). PDEs in turn inactivate cyclic nucleotides to reduce the cAMP/cGMP signal (Beavo., 1995). I hypothesise that inhibition of PDE10A subsequently increases cAMP levels and ameliorates downstream activation of PKA signalling pathways. PKA has many phosphorylation targets and further studies are required to elucidate what these targets are in case of impairing collateral vessel remodelling when PDE10A is inhibited. Pharmacological assays with a PKA antagonist, Rp-8-

Br-cAMPS, were able to rescue the effect of PDE10A inhibition on collateral vessel remodelling. This result implied that the relationship between PDE10A, PKA and cAMP signalling may be important to collateral vessel formation. A summary of the proposed pathway can be seen in Figure 6.1.

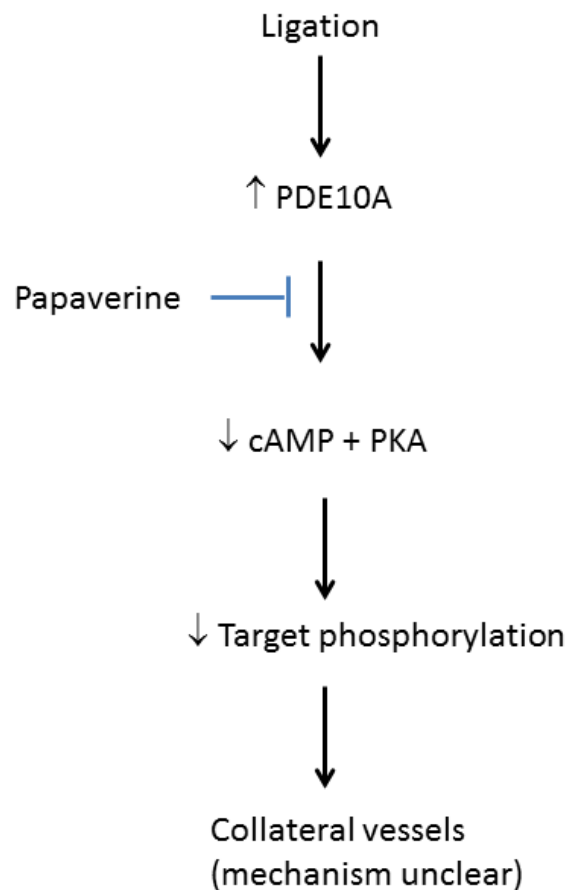


**Figure 6.1 Proposed pathway occurring after proximal vitelline artery ligation in the collateral vessels undergoing flow-induced remodelling**

This schematic proposes the pathway which occurs in the collateral vessels of the chick embryo following vessel ligation. Changes in flow upregulate PDE10A. PDE10A hydrolyses cAMP preventing binding to PKA. This reduced PKA activity reduces phosphorylation of PKA targets. Although the mechanism is unknown, this process allows collateral vessels to develop normally. Papaverine inhibits PDE10A.

Although I did not have time to measure the levels of cAMP to confirm degradation by PDE10A, increased levels of cAMP following PDE10A inhibition by papaverine has been previously documented (Tian *et al.*, 2011). Hypertensive rat models were assessed for a role of PDE10A in pulmonary vascular remodelling. PDE10A mRNA and protein levels were upregulated in the nuclei of remodelling pulmonary vascular smooth muscle. When these rats were infused with papaverine, pulmonary vascular remodelling was impaired. Increased cAMP levels and increased cAMP response binding protein (CREB transcription factor) phosphorylation levels were detected in remodelling pulmonary arterial smooth muscle cells. Papaverine appeared to inhibit proliferation of the vascular smooth muscle cells which prevented normal vessel remodelling in response to hypertension (Tian *et al.*, 2011). The response of PDE10A inhibition in my model did not affect proliferation and was unlikely to influence vessel tone, due to the lack of smooth muscle in the embryo at this stage. Therefore, I speculate that the effect of papaverine may disrupt the regulation of vital signalling pathways or prevent flow-induced changes in gene expression. This might in turn, disrupt downstream processes involved in vessel remodelling, such as inflammation, attraction of monocytes or cell migration.

A PKA mediated effect that reduces collateral vessel formation may explain why PDE10A would be upregulated to regulate PKA signalling. As introduced in section 1.15.2, in the vasculature, cAMP/PKA signalling has been linked to certain activities that would require regulation by PDE10A, to allow an endothelial cell response to changes in flow.

In endothelial cells, PKA signalling has been shown to be involved in activating an arterial fate and arterial gene expression (Chiu and Chien., 2011). Developing collateral vessels have been shown to adopt an arterial fate over time (Figure 3.18). However, it is just as important to inhibit arterial fate of endothelial cells in regressing vessels which are not destined to become collateral vessels. Therefore, it could be hypothesised that PDE10A is

upregulated early on during collateral vessel formation to control cAMP/PKA signalling; thus inhibiting arterial determination of some endothelial cells, enabling the selection process we know to be important to collateral vessel network formation (section 3.3).

cAMP/PKA signalling has also been shown to increase ERK1/2 and MAPK signalling, which leads to actin cytoskeleton rearrangement (Liu *et al.*, 2001). Actin cytoskeletal rearrangement is thought to be involved in an endothelial response to changes in flow (Davies, 1995, Ingber, 2003). This would be expected to occur immediately following altered haemodynamics. Genes involved in actin cytoskeletal rearrangement have indeed been detected *in vivo* (Lee *et al.*, 2004a) and *in vitro* (Peters *et al.*, 2002) at early timepoints. PDE10A could be hypothesised to be upregulated, following ligation, to reduce the increased levels of cAMP/PKA signalling which were initially required during the endothelial response to changes in haemodynamic flow. Other PKA mechanisms which might hinder collateral vessel formation and therefore require an upregulation of PDE10A need to be further investigated. Due to the many targets and different signalling pathways involving PKA this would be difficult to assess.

Given the variety of cAMP target effects, including cell signalling, it may be that PDE10A is involved in mechanotransduction to regulate remodelling vessels. Changes in flow modulate the behaviour and transcriptome of endothelial cells (Peters *et al.*, 2002). Further, it has been proposed that development of normal collateral vessels, induced by changes in flow, may be mediated by signalling pathways such as RAS-ERK and Rho (Eitenmuller *et al.*, 2006). Vossler *et al.*, (1997) showed that agents that increased intracellular cAMP, through PKA, activated MAPK and ERK pathways (Vossler *et al.*, 1997). Or, given PKA involvement in gene transcription, it may be that PDE10A helps to regulate shear responsive genes which may regulate other processes necessary for collateral vessel remodelling. For example in an *in vitro* study a reduction in cAMP decreased PKA activity,

which in turn increased ATF4 DNA binding sites in shear stress induced genes. This increased expression of shear stress responsive genes in endothelial cells exposed to elevated shear stress (White *et al.*, 2011). Future work would include finding a mechanism for PDE10A function in flow-induced vessel remodelling by investigating mechanisms other than proliferation such as endothelial cell migration which is affected by inhibition of other PDEs (Netherton and Maurice, 2005).

Investigations into siRNA knock downs of PDE10A in the chick embryo could reveal a mechanism of action for PDE10A in collateral vessel remodelling. I have previously attempted electroporation to introduce DNA constructs into my vessels of interest. Due to the fragility of the extra-embryonic vasculature at this stage, embryos did not survive this technique. However, I would be keen to see the effect of PDE10A knockdown on the remodelling process, following vessel ligation.

Mouse knockout models of PDE10A have currently, only been used to investigate behaviour and locomotive effects (Siuciak *et al.*, 2006b, Siuciak *et al.*, 2008). Given time and resources it would be interesting to observe the vasculature in the mammalian models and analyse the response to flow-induced vessel remodelling following hind-limb ischaemia.

My results would be greatly strengthened by confirmation using another antagonist. Although the contribution of PDE10A to flow-induced vascular remodelling was supported by rescue experiments, and the control embryos confirmed that there were no off target effects or toxicity, I would have preferred to use an entirely selective inhibitor to rule out any uncertainty. Nevertheless, it is worth noting that the effect of papaverine in mammalian models is to induce vasorelaxation via effects on smooth muscle cells. Therefore my observation that papaverine reduces collateral vessel diameter in the chick (while not affecting vessel size in unligated embryos) underlines the fact that my results

point to a role for phosphodiesterases in collateral vessel formation that is not simply an extension of their role in normal vascular physiology.

I would like to investigate the role of cAMP in more detail. I had previously tried an assay with Forskolin, a compound which increases levels of cAMP, but this was unsuccessful due to the high amounts of DMSO required for the solution on the embryos. Other PKA inhibitors would have also validated a role for cAMP signalling in collateral vessel remodelling and allowed further insight into the pathway and mechanism involved in collateral vessel development.

To further investigate cAMP signalling following ligation, cAMP levels could be measured with an enzyme-linked immuno-absorbent assay (ELISA) on cell lysates. Chromatography analysis could have been performed to validate PDE10A/cAMP binding in my model. Further, it would be interesting to measure the exact amounts of cAMP following PDE10A up-regulation (4 hours post-ligation) and after PDE10A inhibition. This would confirm the action of PDE10A and rule out any contribution of cGMP to the process of remodelling. Increased cAMP/PKA signalling leads to phosphorylation of cAMP dependent substrates (Nishi *et al.*, 2008); Tian *et al.*, (2011) measured this by monitoring CREB phosphorylation following systemic infusion of papaverine into hypertensive rats (Tian *et al.*, 2011). I could have investigated this by checking for phosphorylation using phosphorylation state specific antibodies in the presence and absence of papaverine by Western blot. To determine whether cAMP was regulating shear stress response genes via ATF4 binding sites transcriptomics could be used to look for enriched ATF4 transcription binding sites in flow-induced upregulated genes (White *et al.*, 2011).

A mechanism for the role of PDE10A in collateral development could have been investigated in *in vitro* systems. If PDE10A protein expression was confirmed in flow-treated HUVEC cells, migration assays could be performed to see if PDE10A up-regulation

or inhibition reduces endothelial migration. siRNA could then be applied to cells in culture to observe cell behaviour following PDE10A knock down. Further research could investigate a pharmacological stimulant of collateral vessel formation as opposed to investigating inhibitors which impair the remodelling process. This might reveal results which would be more relevant to developing potential clinical applications.

In conclusion, PDEs are involved in complex pathways, regulating cyclic nucleotide pathways with many variable targets which affect a variety of systems. The function and regulation of cAMP and cGMP pathways in the vascular system depend on location, cellular compartmentalisation, PKA or EPAC activation, signalling cascades and a variety of PDEs. This is therefore a difficult pathway to dissect. My data suggests involvement of PDE10A to the process of flow-induced vessel remodelling, via effects on PKA, however much more evidence and research is required to pinpoint how this enzyme is involved before it becomes therapeutic target with clinical implications.

Should PDE10A be identified as a target for therapeutic development, the focus of the research would be to enhance PDE10A function in people unable to utilise and remodel collateral vessels. PDE inhibitors which impair vessel remodelling could be developed for use in the clinic as anti-cancer therapeutics. For this study the purpose of using a PDE10A inhibitor has been to investigate a role and validate PDE10A expression during collateral vessel remodelling. The chick embryo could also potentially be used as a model to investigate targets to enhance PDE10A function and improve collateral formation.

To conclude, by using global transcriptional profiling in a chick model I have identified PDE10A as a novel regulator of collateral vessel development. The translational potential of this finding remains to be examined.



## References

- International Chicken Genome Sequencing Consortium. 2004. Sequence and comparative analysis of the chicken genome provide unique perspectives on vertebrate evolution. *Nature*, 432, 695-716.
- ARRAS, M., ITO, W. D., SCHOLZ, D., WINKLER, B., SCHAPER, J. & SCHAPER, W. 1998. Monocyte activation in angiogenesis and collateral growth in the rabbit hindlimb. *J Clin Invest*, 101, 40-50.
- ASCHWANDEN, M., PARTOVI, S., JACOBI, B., FERGUS, N., SCHULTE, A., ROBBIN, M., BILECEN, D., STAUB, D. 2014. Assessing the end-organ in peripheral arterial occlusive disease from contrast enhanced ultrasound to blood oxygen level dependent MR imaging. *Cardiovasc Diagn Ther* 4;2 165-72.
- BANAI, S., JAKLITSCH, M. T., SHOU, M., LAZAROUS, D. F., SCHEINOWITZ, M., BIRO, S., EPSTEIN, S. E. & UNGER, E. F. 1994. Angiogenic-induced enhancement of collateral blood flow to ischemic myocardium by vascular endothelial growth factor in dogs. *Circulation*, 89, 2183-9.
- BAUMGARTNER, I., PIECZEK, A., MANOR, O., BLAIR, R., KEARNEY, M., WALSH, K. & ISNER, J. M. 1998. Constitutive expression of phVEGF165 after intramuscular gene transfer promotes collateral vessel development in patients with critical limb ischemia. *Circulation*, 97, 1114-23.
- BEAVO, J. A. 1995. Cyclic nucleotide phosphodiesterases: functional implications of multiple isoforms. *Physiol Rev*, 75, 725-48.
- BENDER, A. T. & BEAVO, J. A. 2006. Cyclic nucleotide phosphodiesterases: molecular regulation to clinical use. *Pharmacol Rev*, 58, 488-520.
- BORGERS, M., SCHAPER, J. & SCHAPER, W. 1971. Localization of specific phosphatase activities in canine coronary blood vessels and heart muscle. *J Histochem Cytochem*, 19, 526-39.
- BRANCOLINI, C. & SCHNEIDER, C. 1994. Phosphorylation of the growth arrest-specific protein Gas2 is coupled to actin rearrangements during G<sub>0</sub>->G<sub>1</sub> transition in NIH 3T3 cells. *J Cell Biol*, 124, 743-56.
- BREIER, G., BLUM, S., PELI, J., GROOT, M., WILD, C., RISAU, W. & REICHMANN, E. 2002. Transforming growth factor-beta and Ras regulate the VEGF/VEGF-receptor system during tumor angiogenesis. *Int J Cancer*, 97, 142-8.
- BROOKS, P. C., MONTGOMERY, A. M. & CHERESH, D. A. 1999. Use of the 10-day-old chick embryo model for studying angiogenesis. *Methods Mol Biol*, 129, 257-69.
- BRUNEAU, B. G., BAO, Z. Z., TANAKA, M., SCHOTT, J. J., IZUMO, S., CEPKO, C. L., SEIDMAN, J. G. & SEIDMAN, C. E. 2000. Cardiac expression of the ventricle-specific homeobox gene *Irx4* is modulated by *Nkx2-5* and *dHand*. *Dev Biol*, 217, 266-77.
- BUCKANOVICH, R. J., SASAROLI, D., O'BRIEN-JENKINS, A., BOTBYL, J., HAMMOND, R., KATSAROS, D., SANDALTZOPOULOS, R., LIOTTA, L. A., GIMOTTY, P. A. & COUKOS, G. 2007. Tumor vascular proteins as biomarkers in ovarian cancer. *J Clin Oncol*, 25, 852-61.
- BUSCHMANN, I., PRIES, A., STYP-REKOWSKA, B., HILLMEISTER, P., LOUFRANI, L., HENRION, D., SHI, Y., DUELSNER, A., HOEFER, I., GATZKE, N., WANG, H., LEHMANN, K., ULM, L., RITTER, Z., HAUFF, P., HLUSHCHUK, R., DJONOV, V., VAN VEEN, T. & LE NOBLE, F. 2010. Pulsatile shear and *Gja5* modulate arterial identity and remodeling events during flow-driven arteriogenesis. *Development*, 137, 2187-96.
- BUSCHMANN, I. & SCHAPER, W. 2000. The pathophysiology of the collateral circulation (arteriogenesis). *J Pathol*, 190, 338-42.
- BUSCHMANN, I. R., VOSKUIL, M., VAN ROYEN, N., HOEFER, I. E., SCHEFFLER, K., GRUNDMANN, S., HENNIG, J., SCHAPER, W., BODE, C. & PIEK, J. J. 2003. Invasive

- and non-invasive evaluation of spontaneous arteriogenesis in a novel porcine model for peripheral arterial obstructive disease. *Atherosclerosis*, 167, 33-43.
- CAI, W. & SCHAPER, W. 2008. Mechanisms of arteriogenesis. *Acta Biochim Biophys Sin (Shanghai)*, 40, 681-92.
- CAI, W. J., KOLTAI, S., KOCSIS, E., SCHOLZ, D., KOSTIN, S., LUO, X., SCHAPER, W. & SCHAPER, J. 2003. Remodeling of the adventitia during coronary arteriogenesis. *Am J Physiol Heart Circ Physiol*, 284, H31-40.
- CAMPBELL, N. E., KELLENBERGER, L., GREENAWAY, J., MOOREHEAD, R. A., LINNERTH-PETRIK, N. M. & PETRIK, J. 2010. Extracellular matrix proteins and tumor angiogenesis. *J Oncol*, 2010, 586905.
- CARMELIET, P. 2000. Mechanisms of angiogenesis and arteriogenesis. *Nat Med*, 6, 389-95.
- CHANG, A. C., JELLINEK, D. A. & REDDEL, R. R. 2003. Mammalian stanniocalcins and cancer. *Endocr Relat Cancer*, 10, 359-73.
- CHIEN, S. 2008. Effects of disturbed flow on endothelial cells. *Ann Biomed Eng*, 36, 554-62.
- CHIU, J. J. & CHIEN, S. 2011. Effects of disturbed flow on vascular endothelium: pathophysiological basis and clinical perspectives. *Physiol Rev*, 91, 327-87.
- CHIU, J. J., CHEN, L. J., LEE, P. L., LEE, L. W., USAMI, S., 2003. Shear stress inhibits adhesion molecule expression in vascular endothelial cells induced by coculture with smooth muscle cells. *Blood*, 1;101(7); 2667-74.
- CHIU, J. J., USAMI, S. & CHIEN, S. 2009. Vascular endothelial responses to altered shear stress: pathologic implications for atherosclerosis. *Ann Med*, 41, 19-28.
- CLAYTON, J. A., CHALOTHORN, D. & FABER, J. E. 2008. Vascular endothelial growth factor-A specifies formation of native collaterals and regulates collateral growth in ischemia. *Circ Res*, 103, 1027-36.
- COOMBER, B. L. & GOTLIEB, A. I. 1990. In vitro endothelial wound repair. Interaction of cell migration and proliferation. *Arteriosclerosis*, 10, 215-22.
- COSKRAN, T. M., MORTON, D., MENNITI, F. S., ADAMOWICZ, W. O., KLEIMAN, R. J., RYAN, A. M., STRICK, C. A., SCHMIDT, C. J. & STEPHENSON, D. T. 2006. Immunohistochemical localization of phosphodiesterase 10A in multiple mammalian species. *J Histochem Cytochem*, 54, 1205-13.
- D'ANGELO, G., LEE, H. & WEINER, R. I. 1997. cAMP-dependent protein kinase inhibits the mitogenic action of vascular endothelial growth factor and fibroblast growth factor in capillary endothelial cells by blocking Raf activation. *J Cell Biochem*, 67, 353-66.
- DALLAS, P. B., GOTTARDO, N. G., FIRTH, M. J., BEESLEY, A. H., HOFFMANN, K., TERRY, P. A., FREITAS, J. R., BOAG, J. M., CUMMINGS, A. J. & KEES, U. R. 2005. Gene expression levels assessed by oligonucleotide microarray analysis and quantitative real-time RT-PCR -- how well do they correlate? *BMC Genomics*, 6, 59.
- DARDIK, A., CHEN, L., FRATTINI, J., ASADA, H., AZIZ, F., KUDO, F. A. & SUMPIO, B. E. 2005a. Differential effects of orbital and laminar shear stress on endothelial cells. *J Vasc Surg*, 41, 869-80.
- DARDIK, A., YAMASHITA, A., AZIZ, F., ASADA, H. & SUMPIO, B. E. 2005b. Shear stress-stimulated endothelial cells induce smooth muscle cell chemotaxis via platelet-derived growth factor-BB and interleukin-1alpha. *J Vasc Surg*, 41, 321-31.
- DAVIES, P. F. 1995. Flow-mediated endothelial mechanotransduction. *Physiological Reviews*, 75, 519-560.
- DAVIES, P. F., REMUZZI, A., GORDON, E. J., DEWEY, C. F., JR. & GIMBRONE, M. A., JR. 1986. Turbulent fluid shear stress induces vascular endothelial cell turnover in vitro. *Proc Natl Acad Sci U S A*, 83, 2114-7.
- DEINDL, E., HOEFER, I. E., FERNANDEZ, B., BARANCIK, M., HEIL, M., STRNISKOVA, M. & SCHAPER, W. 2003. Involvement of the fibroblast growth factor system in adaptive and chemokine-induced arteriogenesis. *Circ Res*, 92, 561-8.

- DEINDL, E. & SCHAPER, W. 2005. The art of arteriogenesis. *Cell Biochem Biophys*, 43, 1-15.
- DEKKER, R. J., BOON, R. A., RONDAIJ, M. G., KRAGT, A., VOLGER, O. L., ELDERKAMP, Y. W., MEIJERS, J. C., VOORBERG, J., PANNEKOEK, H. & HORREVOETS, A. J. 2006. KLF2 provokes a gene expression pattern that establishes functional quiescent differentiation of the endothelium. *Blood*, 107, 4354-63.
- DEKKER, R. J., VAN SOEST, S., FONTIJN, R. D., SALAMANCA, S., DE GROOT, P. G., VANBAVEL, E., PANNEKOEK, H. & HORREVOETS, A. J. 2002. Prolonged fluid shear stress induces a distinct set of endothelial cell genes, most specifically lung Kruppel-like factor (KLF2). *Blood*, 100, 1689-98.
- DERYUGINA, E. I. & QUIGLEY, J. P. 2008. Chick embryo chorioallantoic membrane model systems to study and visualize human tumor cell metastasis. *Histochem Cell Biol*, 130, 1119-30.
- DEWEY, C. F., JR., BUSSOLARI, S. R., GIMBRONE, M. A., JR. & DAVIES, P. F. 1981. The dynamic response of vascular endothelial cells to fluid shear stress. *J Biomech Eng*, 103, 177-85.
- DIAMOND, S. L., SHAREFKIN, J. B., DIEFFENBACH, C., FRASIER-SCOTT, K., MCINTIRE, L. V. & ESKIN, S. G. 1990. Tissue plasminogen activator messenger RNA levels increase in cultured human endothelial cells exposed to laminar shear stress. *J Cell Physiol*, 143, 364-71.
- DJONOV, V., SCHMID, M., TSCHANZ, S. A. & BURRI, P. H. 2000. Intussusceptive angiogenesis: its role in embryonic vascular network formation. *Circ Res*, 86, 286-92.
- DOSTMANN, W. R., TAYLOR, S. S., GENIESER, H. G., JASTORFF, B., DOSKELAND, S. O. & OGREID, D. 1990. Probing the cyclic nucleotide binding sites of cAMP-dependent protein kinases I and II with analogs of adenosine 3',5'-cyclic phosphorothioates. *J Biol Chem*, 265, 10484-91.
- DUGGAN, D. J., BITTNER, M., CHEN, Y., MELTZER, P. & TRENT, J. M. 1999. Expression profiling using cDNA microarrays. *Nat Genet*, 21, 10-4.
- DUVALL, C. L., TAYLOR, W. R., WEISS, D. & GULDBERG, R. E. 2004. Quantitative microcomputed tomography analysis of collateral vessel development after ischemic injury. *Am J Physiol Heart Circ Physiol*, 287, H302-10.
- EGOROVA, A. D., VAN DER HEIDEN, K., VAN DE PAS, S., VENNEMANN, P., POELMA, C., DERUITER, M. C., GOUMANS, M. J., GITTENBERGER-DE GROOT, A. C., TEN DIJKE, P., POELMANN, R. E. & HIERCK, B. P. 2011. Tgfbeta/Alk5 signaling is required for shear stress induced klf2 expression in embryonic endothelial cells. *Dev Dyn*, 240, 1670-80.
- EICHMANN, A., MAKINEN, T. & ALITALO, K. 2005. Neural guidance molecules regulate vascular remodeling and vessel navigation. *Genes Dev*, 19, 1013-21.
- EISEN, M. B., SPELLMAN, P. T., BROWN, P. O. & BOTSTEIN, D. 1998. Cluster analysis and display of genome-wide expression patterns. *Proc Natl Acad Sci U S A*, 95, 14863-8.
- EITENMULLER, I., VOLGER, O., KLUGE, A., TROIDL, K., BARANCIK, M., CAI, W. J., HEIL, M., PIPP, F., FISCHER, S., HORREVOETS, A. J., SCHMITZ-RIXEN, T. & SCHAPER, W. 2006. The range of adaptation by collateral vessels after femoral artery occlusion. *Circ Res*, 99, 656-62.
- EPSTEIN, S. E., FUCHS, S., ZHOU, Y. F., BAFFOUR, R. & KORNOWSKI, R. 2001. Therapeutic interventions for enhancing collateral development by administration of growth factors: basic principles, early results and potential hazards. *Cardiovasc Res*, 49, 532-42.
- ESSAYAN, D. M. 2001. Cyclic nucleotide phosphodiesterases. *J Allergy Clin Immunol*, 108, 671-80.

- EVANS, G. R., GHERARDINI, G., GURLEK, A., LANGSTEIN, H., JOLY, G. A., CROMEENS, D. M., SUKUMARAN, A. V., WILLIAMS, J., KILBOURN, R. G., WANG, B. & LUNDEBERG, T. 1997. Drug-induced vasodilation in an in vitro and in vivo study: the effects of nicardipine, papaverine, and lidocaine on the rabbit carotid artery. *Plast Reconstr Surg*, 100, 1475-81.
- FAVOT, L., KERAUIS, T., HOLL, V., LE BEC, A. & LUGNIER, C. 2003. VEGF-induced HUVEC migration and proliferation are decreased by PDE2 and PDE4 inhibitors. *Thromb Haemost*, 90, 334-43.
- FLAMME, I. 1989. Is extraembryonic angiogenesis in the chick embryo controlled by the endoderm? A morphology study. *Anat Embryol (Berl)*, 180, 259-72.
- FRANCIS, S. H., TURKO, I. V. & CORBIN, J. D. 2001. Cyclic nucleotide phosphodiesterases: relating structure and function. *Prog Nucleic Acid Res Mol Biol*, 65, 1-52.
- FUJISHIGE, K., KOTERA, J., MICHIBATA, H., YUASA, K., TAKEBAYASHI, S., OKUMURA, K. & OMORI, K. 1999. Cloning and characterization of a novel human phosphodiesterase that hydrolyzes both cAMP and cGMP (PDE10A). *J Biol Chem*, 274, 18438-45.
- FUNG, E. & HELISCH, A. 2012. Macrophages in collateral arteriogenesis. *Front Physiol*, 3, 353.
- FUSTER, V., STEIN, B., AMBROSE, J. A., BADIMON, L., BADIMON, J. J. & CHESEBRO, J. H. 1990. Atherosclerotic plaque rupture and thrombosis. Evolving concepts. *Circulation*, 82, 1147-59.
- GARCIA-CARDENA, G. & GIMBRONE, M. A., JR. 2006. Biomechanical modulation of endothelial phenotype: implications for health and disease. *Handb Exp Pharmacol*, 79-95.
- GERHARDT, H., GOLDING, M., FRUTTIGER, M., RUHRBERG, C., LUNDKVIST, A., ABRAMSSON, A., JELTSCH, M., MITCHELL, C., ALITALO, K., SHIMA, D. & BETSHOLTZ, C. 2003. VEGF guides angiogenic sprouting utilizing endothelial tip cell filopodia. *J Cell Biol*, 161, 1163-77.
- GESELLCHEN, F., PRINZ, A., ZIMMERMANN, B. & HERBERG, F. W. 2006. Quantification of cAMP antagonist action in vitro and in living cells. *Eur J Cell Biol*, 85, 663-72.
- GHERARDINI, G., GURLEK, A., CROMEENS, D., JOLY, G. A., WANG, B. G. & EVANS, G. R. 1998. Drug-induced vasodilation: in vitro and in vivo study on the effects of lidocaine and papaverine on rabbit carotid artery. *Microsurgery*, 18, 90-6.
- GIMBRONE, M. A., JR., RESNICK, N., NAGEL, T., KHACHIGIAN, L. M., COLLINS, T. & TOPPER, J. N. 1997. Hemodynamics, endothelial gene expression, and atherogenesis. *Ann N Y Acad Sci*, 811, 1-10; discussion 10-1.
- GIRALT, A., SAAVEDRA, A., CARRETON, O., ARUMI, H., TYEBJI, S., ALBERCH, J. & PEREZ-NAVARRO, E. 2013. PDE10 inhibition increases GluA1 and CREB phosphorylation and improves spatial and recognition memories in a Huntington's disease mouse model. *Hippocampus*, 23, 684-95.
- GJERTSEN, B. T., MELLGREN, G., OTTEN, A., MARONDE, E., GENIESER, H. G., JASTORFF, B., VINTERMYR, O. K., MCKNIGHT, G. S. & DOSKELAND, S. O. 1995. Novel (Rp)-cAMPS analogs as tools for inhibition of cAMP-kinase in cell culture. Basal cAMP-kinase activity modulates interleukin-1 beta action. *J Biol Chem*, 270, 20599-607.
- GLAGOV, S., WEISENBERG, E., ZARINS, C. K., STANKUNAVICIUS, R. & KOLETTIS, G. J. 1987. Compensatory enlargement of human atherosclerotic coronary arteries. *N Engl J Med*, 316, 1371-5.
- GONZALEZ-CRUSSI, F. 1971. Vasculogenesis in the chick embryo. An ultrastructural study. *Am J Anat*, 130, 441-60.
- GRAY, C., PACKHAM, I. M., WURMSER, F., EASTLEY, N. C., HELLEWELL, P. G., INGHAM, P. W., CROSSMAN, D. C. & CHICO, T. J. 2007. Ischemia is not required for arteriogenesis in zebrafish embryos. *Arterioscler Thromb Vasc Biol*, 27, 2135-41.

- GROENENDIJK, B. C., HIERCK, B. P., GITTENBERGER-DE GROOT, A. C. & POELMANN, R. E. 2004. Development-related changes in the expression of shear stress responsive genes KLF-2, ET-1, and NOS-3 in the developing cardiovascular system of chicken embryos. *Dev Dyn*, 230, 57-68.
- GROENENDIJK, B. C., HIERCK, B. P., VROLIJK, J., BAIKER, M., POURQUIE, M. J., GITTENBERGER-DE GROOT, A. C. & POELMANN, R. E. 2005. Changes in shear stress-related gene expression after experimentally altered venous return in the chicken embryo. *Circ Res*, 96, 1291-8.
- GROSS-LANGENHOFF, M., HOFBAUER, K., WEBER, J., SCHULTZ, A. & SCHULTZ, J. E. 2006. cAMP is a ligand for the tandem GAF domain of human phosphodiesterase 10 and cGMP for the tandem GAF domain of phosphodiesterase 11. *J Biol Chem*, 281, 2841-6.
- GRUNDMANN, S., HOEFER, I., ULUSANS, S., BODE, C., OESTERLE, S., TIJSSEN, J. G., PIEK, J. J., BUSCHMANN, I. & VAN ROYEN, N. 2006. Granulocyte-macrophage colony-stimulating factor stimulates arteriogenesis in a pig model of peripheral artery disease using clinically applicable infusion pumps. *J Vasc Surg*, 43, 1263-9.
- HADJIGHASSEM, M. R., AUSTIN, M. C., SZEWCZYK, B., DAIGLE, M., STOCKMEIER, C. A. & ALBERT, P. R. 2009. Human Freud-2/CC2D1B: a novel repressor of postsynaptic serotonin-1A receptor expression. *Biol Psychiatry*, 66, 214-22.
- HAEFLIGER, J. A., NICOD, P. & MEDA, P. 2004. Contribution of connexins to the function of the vascular wall. *Cardiovasc Res*, 62, 345-56.
- HAMBURGER, V., AND HAMILTON, H 1951. A series of normal stages in the development of the chick embryo. *Journal of Morphology*, 88, 49-92.
- HAMBURGER, V., HAMILTON, H.L. 1992. A Series of Normal Stages in the Development of the Chick Embryo. *Developmental Dynamics*, 195, 231-272.
- HATCHER, C. J. & BASSON, C. T. 2009. Specification of the cardiac conduction system by transcription factors. *Circ Res*, 105, 620-30.
- HAYASHI, S., MORISHITA, R., MATSUSHITA, H., NAKAGAMI, H., TANIYAMA, Y., NAKAMURA, T., AOKI, M., YAMAMOTO, K., HIGAKI, J. & OGIHARA, T. 2000. Cyclic AMP inhibited proliferation of human aortic vascular smooth muscle cells, accompanied by induction of p53 and p21. *Hypertension*, 35, 237-43.
- HEBB, A. L., ROBERTSON, H. A. & DENO VAN-WRIGHT, E. M. 2004. Striatal phosphodiesterase mRNA and protein levels are reduced in Huntington's disease transgenic mice prior to the onset of motor symptoms. *Neuroscience*, 123, 967-81.
- HEIL, M., EITENMULLER, I., SCHMITZ-RIXEN, T. & SCHAPER, W. 2006. Arteriogenesis versus angiogenesis: similarities and differences. *J Cell Mol Med*, 10, 45-55.
- HEIL, M. & SCHAPER, W. 2004. Influence of mechanical, cellular, and molecular factors on collateral artery growth (arteriogenesis). *Circ Res*, 95, 449-58.
- HEIL, M. & SCHAPER, W. 2005. Cellular mechanisms of arteriogenesis. *EXS*, 181-91.
- HEIL, M. & SCHAPER, W. 2007. Insights into pathways of arteriogenesis. *Curr Pharm Biotechnol*, 8, 35-42.
- HELDERMAN, F., SEGERS, D., DE CROM, R., HIERCK, B. P., POELMANN, R. E., EVANS, P. C. & KRAMS, R. 2007. Effect of shear stress on vascular inflammation and plaque development. *Curr Opin Lipidol*, 18, 527-33.
- HELISCH, A. & SCHAPER, W. 2003. Arteriogenesis: the development and growth of collateral arteries. *Microcirculation*, 10, 83-97.
- HELLSTROM, M., PHNG, L. K., HOFMANN, J. J., WALLGARD, E., COULTAS, L., LINDBLOM, P., ALVA, J., NILSSON, A. K., KARLSSON, L., GAIANO, N., YOON, K., ROSSANT, J., IRUELA-ARISPE, M. L., KALEN, M., GERHARDT, H. & BETSHOLTZ, C. 2007. Dll4 signalling through Notch1 regulates formation of tip cells during angiogenesis. *Nature*, 445, 776-80.

- HELMKE, B. P. & DAVIES, P. F. 2002. The cytoskeleton under external fluid mechanical forces: hemodynamic forces acting on the endothelium. *Ann Biomed Eng*, 30, 284-96.
- HERSHEY, J. C., BASKIN, E. P., GLASS, J. D., HARTMAN, H. A., GILBERTO, D. B., ROGERS, I. T. & COOK, J. J. 2001. Revascularization in the rabbit hindlimb: dissociation between capillary sprouting and arteriogenesis. *Cardiovasc Res*, 49, 618-25.
- HERZOG, S., SAGER, H., KHMELEVSKI, E., DEYLIG, A. & ITO, W. D. 2002. Collateral arteries grow from preexisting anastomoses in the rat hindlimb. *Am J Physiol Heart Circ Physiol*, 283, H2012-20.
- HIERCK, B. P., VAN DER HEIDEN, K., ALKEMADE, F. E., VAN DE PAS, S., VAN THIENEN, J. V., GROENENDIJK, B. C., BAX, W. H., VAN DER LAARSE, A., DERUITER, M. C., HORREVOETS, A. J. & POELMANN, R. E. 2008. Primary cilia sensitize endothelial cells for fluid shear stress. *Dev Dyn*, 237, 725-35.
- HIROHATA, S., WANG, L. W., MIYAGI, M., YAN, L., SELDIN, M. F., KEENE, D. R., CRABB, J. W. & APTE, S. S. 2002. Punctin, a novel ADAMTS-like molecule, ADAMTSL-1, in extracellular matrix. *J Biol Chem*, 277, 12182-9.
- HOEFER, I. E., VAN ROYEN, N., BUSCHMANN, I. R., PIEK, J. J. & SCHAPER, W. 2001. Time course of arteriogenesis following femoral artery occlusion in the rabbit. *Cardiovasc Res*, 49, 609-17.
- HOEFER, I. E., VAN ROYEN, N., RECTENWALD, J. E., DEINDL, E., HUA, J., JOST, M., GRUNDMANN, S., VOSKUIL, M., OZAKI, C. K., PIEK, J. J. & BUSCHMANN, I. R. 2004. Arteriogenesis proceeds via ICAM-1/Mac-1-mediated mechanisms. *Circ Res*, 94, 1179-85.
- HUGHES, A. F. 1935. Studies on the Area Vasculosa of the Embryo Chick: I. The First Differentiation of the Vitelline Artery. *J Anat*, 70, 76-122 5.
- HUGHES, A. F. 1937. Studies on the Area Vasculosa of the Embryo Chick: II. The Influence of the Circulation on the Diameter of the Vessels. *J Anat*, 72, 1-17.
- ILICH, N., HOLLENBERG, N. K., WILLIAMS, D. H. & ABRAMS, H. L. 1979. Time course of increased collateral arterial and venous endothelial cell turnover after renal artery stenosis in the rat. *Circ Res*, 45, 579-82.
- INGBER, D. E. 2003. Tensegrity II. How structural networks influence cellular information processing networks. *J Cell Sci*, 116, 1397-408.
- ITO, W. D., ARRAS, M., SCHOLZ, D., WINKLER, B., HTUN, P. & SCHAPER, W. 1997a. Angiogenesis but not collateral growth is associated with ischemia after femoral artery occlusion. *Am J Physiol*, 273, H1255-65.
- ITO, W. D., ARRAS, M., WINKLER, B., SCHOLZ, D., SCHAPER, J. & SCHAPER, W. 1997b. Monocyte chemotactic protein-1 increases collateral and peripheral conductance after femoral artery occlusion. *Circ Res*, 80, 829-37.
- JACKSON, C. J. & NGUYEN, M. 1997. Human microvascular endothelial cells differ from macrovascular endothelial cells in their expression of matrix metalloproteinases. *Int J Biochem Cell Biol*, 29, 1167-77.
- JAYAPAL, M. & MELENDEZ, A. J. 2006. DNA microarray technology for target identification and validation. *Clin Exp Pharmacol Physiol*, 33, 496-503.
- JAYE, M., MCCONATHY, E., DROHAN, W., TONG, B., DEUEL, T. & MACIAG, T. 1985. Modulation of the sis gene transcript during endothelial cell differentiation in vitro. *Science*, 228, 882-5.
- JELKMANN, W. 2001. Pitfalls in the measurement of circulating vascular endothelial growth factor. *Clin Chem*, 47, 617-23.
- JILANI, S. M., MURPHY, T. J., THAI, S. N., EICHMANN, A., ALVA, J. A. & IRUELA-ARISPE, M. L. 2003. Selective binding of lectins to embryonic chicken vasculature. *J Histochem Cytochem*, 51, 597-604.

- JONES, E. A., LE NOBLE, F. & EICHMANN, A. 2006. What determines blood vessel structure? Genetic prespecification vs. hemodynamics. *Physiology (Bethesda)*, 21, 388-95.
- JONSSON-RYLANDER, A. C., NILSSON, T., FRITSCHÉ-DANIELSON, R., HAMMARSTRÖM, A., BEHRENDT, M., ANDERSSON, J. O., LINDGREN, K., ANDERSSON, A. K., WALLBRANDT, P., ROSENGREN, B., BRODIN, P., THELIN, A., WESTIN, A., HURT-CAMEJO, E. & LEE-SOGAARD, C. H. 2005. Role of ADAMTS-1 in atherosclerosis: remodeling of carotid artery, immunohistochemistry, and proteolysis of versican. *Arterioscler Thromb Vasc Biol*, 25, 180-5.
- KADOSHIMA-YAMAOKA, K., MURAKAWA, M., GOTO, M., TANAKA, Y., INOUE, H., MURAFUJI, H., NAGAHIRA, A., HAYASHI, Y., NAGAHIRA, K., MIURA, K., NAKATSUKA, T., CHAMOTO, K., FUKUDA, Y. & NISHIMURA, T. 2009. ASB16165, a novel inhibitor for phosphodiesterase 7A (PDE7A), suppresses IL-12-induced IFN-gamma production by mouse activated T lymphocytes. *Immunol Lett*, 122, 193-7.
- KAREGE, F., SCHWALD, M. & EL KOUAISSI, R. 2004. Drug-induced decrease of protein kinase a activity reveals alteration in BDNF expression of bipolar affective disorder. *Neuropsychopharmacology*, 29, 805-12.
- KERR, M. K., MARTIN, M. & CHURCHILL, G. A. 2000. Analysis of variance for gene expression microarray data. *J Comput Biol*, 7, 819-37.
- KHACHIGIAN, L. M., ANDERSON, K. R., HALNÓN, N. J., GIMBRONE, M. A., JR., RESNICK, N. & COLLINS, T. 1997. Egr-1 is activated in endothelial cells exposed to fluid shear stress and interacts with a novel shear-stress-response element in the PDGF A-chain promoter. *Arterioscler Thromb Vasc Biol*, 17, 2280-6.
- KLEMM, D. J., WATSON, P. A., FRID, M. G., DEMPSEY, E. C., SCHAACK, J., COLTON, L. A., NESTEROVA, A., STENMARK, K. R. & REUSCH, J. E. 2001. cAMP response element-binding protein content is a molecular determinant of smooth muscle cell proliferation and migration. *J Biol Chem*, 276, 46132-41.
- KOLKER, E., MAKAROVA, K. S., SHABALINA, S., PICONE, A. F., PURVINE, S., HOLZMAN, T., CHERNY, T., ARMBRUSTER, D., MUNSON, R. S., JR., KOLESOV, G., FRISHMAN, D. & GALPERIN, M. Y. 2004. Identification and functional analysis of 'hypothetical' genes expressed in *Haemophilus influenzae*. *Nucleic Acids Res*, 32, 2353-61.
- KONDO, K., UMEMURA, K., MIYAJI, M. & NAKASHIMA, M. 1999. Milrinone, a phosphodiesterase inhibitor, suppresses intimal thickening after photochemically induced endothelial injury in the mouse femoral artery. *Atherosclerosis*, 142, 133-8.
- KLOOSTERMAN, A., HIERCK, B., POELMA, C., WESTERWEEL, J., 2014. Quantification of blood flow and topology in developing vascular networks. *PLoS One*, 13;9.
- KOTERA, J., SASAKI, T., KOBAYASHI, T., FUJISHIGE, K., YAMASHITA, Y. & OMORI, K. 2004. Subcellular localization of cyclic nucleotide phosphodiesterase type 10A variants, and alteration of the localization by cAMP-dependent protein kinase-dependent phosphorylation. *J Biol Chem*, 279, 4366-75.
- KU, D. N., GIDDENS, D. P., ZARINS, C. K. & GLAGOV, S. 1985. Pulsatile flow and atherosclerosis in the human carotid bifurcation. Positive correlation between plaque location and low oscillating shear stress. *Arteriosclerosis*, 5, 293-302.
- KUGLER, C. F. & RUDOFISKY, G. 2003. The challenges of treating peripheral arterial disease. *Vasc Med*, 8, 109-14.
- LAN, Q., MERCURIUS, K. O. & DAVIES, P. F. 1994. Stimulation of transcription factors NF kappa B and AP1 in endothelial cells subjected to shear stress. *Biochem Biophys Res Commun*, 201, 950-6.
- LANAHAN, A., ZHANG, X., FANTIN, A., ZHUANG, Z., RIVERA-MOLINA, F., SPEICHLINGER, K., PRAHST, C., ZHANG, J., WANG, Y., DAVIS, G., TOOMRE, D., RUHRBERG, C. & SIMONS, M. 2013. The neuropilin 1 cytoplasmic domain is required for VEGF-A-dependent arteriogenesis. *Dev Cell*, 25, 156-68.

- LAWSON, N. D., SCHEER, N., PHAM, V. N., KIM, C. H., CHITNIS, A. B., CAMPOS-ORTEGA, J. A. & WEINSTEIN, B. M. 2001. Notch signaling is required for arterial-venous differentiation during embryonic vascular development. *Development*, 128, 3675-83.
- LAWSON, N. D. & WEINSTEIN, B. M. 2002. In vivo imaging of embryonic vascular development using transgenic zebrafish. *Dev Biol*, 248, 307-18.
- LE NOBLE, F., MOYON, D., PARDANAUD, L., YUAN, L., DJONOV, V., MATTHIJSEN, R., BREANT, C., FLEURY, V. & EICHMANN, A. 2004. Flow regulates arterial-venous differentiation in the chick embryo yolk sac. *Development*, 131, 361-75.
- LEE, C. W., STABILE, E., KINNAIRD, T., SHOU, M., DEVANEY, J. M., EPSTEIN, S. E. & BURNETT, M. S. 2004a. Temporal patterns of gene expression after acute Hindlimb ischemia in mice - Insights into the genomic program for collateral vessel development. *J Am Coll Cardiol*, 43, 474-482.
- LEE, C. W., STABILE, E., KINNAIRD, T., SHOU, M., DEVANEY, J. M., EPSTEIN, S. E. & BURNETT, M. S. 2004b. Temporal patterns of gene expression after acute hindlimb ischemia in mice: insights into the genomic program for collateral vessel development. *J Am Coll Cardiol*, 43, 474-82.
- LEE, J. C., KIM, D. C., GEE, M. S., SAUNDERS, H. M., SEHGAL, C. M., FELDMAN, M. D., ROSS, S. R. & LEE, W. M. 2002. Interleukin-12 inhibits angiogenesis and growth of transplanted but not in situ mouse mammary tumor virus-induced mammary carcinomas. *Cancer Res*, 62, 747-55.
- LEE, J. Y., JI, H. S. & LEE, S. J. 2007. Micro-PIV measurements of blood flow in extraembryonic blood vessels of chicken embryos. *Physiol Meas*, 28, 1149-62.
- LEE, J. Y. & LEE, S. J. 2010. Hemodynamics of the omphalo-mesenteric arteries in stage 18 chicken embryos and "flow-structure" relations for the microcirculation. *Microvasc Res*, 80, 402-11.
- LEE, M.-L. T. 2004. *Analysis of microarray gene expression data*, Boston, Kluwer Academic.
- LIBBY, P., GENG, Y. J., AIKAWA, M., SCHOENBECK, U., MACH, F., CLINTON, S. K., SUKHOVA, G. K. & LEE, R. T. 1996. Macrophages and atherosclerotic plaque stability. *Curr Opin Lipidol*, 7, 330-5.
- LIEBENBERG, N., MULLER, H. K., FISCHER, C. W., HARVEY, B. H., BRINK, C. B., ELFVING, B. & WEGENER, G. 2011. An inhibitor of cAMP-dependent protein kinase induces behavioural and neurological antidepressant-like effects in rats. *Neurosci Lett*, 498, 158-61.
- LIMBOURG, A., KORFF, T., NAPP, L. C., SCHAPER, W., DREXLER, H. & LIMBOURG, F. P. 2009. Evaluation of postnatal arteriogenesis and angiogenesis in a mouse model of hind-limb ischemia. *Nat Protoc*, 4, 1737-46.
- LIU, F., VERIN, A. D., BORBIEV, T. & GARCIA, J. G. 2001. Role of cAMP-dependent protein kinase A activity in endothelial cell cytoskeleton rearrangement. *Am J Physiol Lung Cell Mol Physiol*, 280, L1309-17.
- LIU, X., MILO, M., LAWRENCE, N. D. & RATTRAY, M. 2005. A tractable probabilistic model for Affymetrix probe-level analysis across multiple chips. *Bioinformatics*, 21, 3637-44.
- LOHOF, A. M., QUILLAN, M., DAN, Y. & POO, M. M. 1992. Asymmetric modulation of cytosolic cAMP activity induces growth cone turning. *J Neurosci*, 12, 1253-61.
- LU, Y., LI, Y., HERIN, G. A., AIZENMAN, E., EPSTEIN, P. M. & ROSENBERG, P. A. 2004. Elevation of intracellular cAMP evokes activity-dependent release of adenosine in cultured rat forebrain neurons. *Eur J Neurosci*, 19, 2669-81.
- LUCITTI, J. L., TOBITA, K. & KELLER, B. B. 2005. Arterial hemodynamics and mechanical properties after circulatory intervention in the chick embryo. *J Exp Biol*, 208, 1877-85.

- LUGNIER, C. 2006. Cyclic nucleotide phosphodiesterase (PDE) superfamily: a new target for the development of specific therapeutic agents. *Pharmacol Ther*, 109, 366-98.
- LYSSENKO, N. N., HANNA-ROSE, W. & SCHLEGEL, R. A. 2007. Cognate putative nuclear localization signal effects strong nuclear localization of a GFP reporter and facilitates gene expression studies in *Caenorhabditis elegans*. *Biotechniques*, 43, 596, 598, 560.
- MAHONEY, Z. X., SAMMUT, B., XAVIER, R. J., CUNNINGHAM, J., GO, G., BRIM, K. L., STAPPENBECK, T. S., MINER, J. H. & SWAT, W. 2006. Discs-large homolog 1 regulates smooth muscle orientation in the mouse ureter. *Proc Natl Acad Sci U S A*, 103, 19872-7.
- MANN, G. E., YUDILEVICH, D. L. & SOBREVIA, L. 2003. Regulation of amino acid and glucose transporters in endothelial and smooth muscle cells. *Physiol Rev*, 83, 183-252.
- MATSUMOTO, T., KOBAYASHI, T. & KAMATA, K. 2003. Phosphodiesterases in the vascular system. *J Smooth Muscle Res*, 39, 67-86.
- MATSUSAKA, S. & WAKABAYASHI, I. 2005. 5-Hydroxytryptamine as a potent migration enhancer of human aortic endothelial cells. *FEBS Lett*, 579, 6721-5.
- MAY, S. R., STEWART, N. J., CHANG, W. & PETERSON, A. S. 2004. A Titin mutation defines roles for circulation in endothelial morphogenesis. *Dev Biol*, 270, 31-46.
- MCCORMICK, S. M., ESKIN, S. G., MCINTIRE, L. V., TENG, C. L., LU, C. M., RUSSELL, C. G. & CHITTUR, K. K. 2001. DNA microarray reveals changes in gene expression of shear stressed human umbilical vein endothelial cells. *Proc Natl Acad Sci U S A*, 98, 8955-60.
- MILLER, W. J., KAYTON, M. L., PATTON, A., O'CONNOR, S., HE, M., VU, H., BAIBAKOV, G., LORANG, D., KNEZEVIC, V., KOHN, E., ALEXANDER, H. R., STIRLING, D., PAYVANDI, F., MULLER, G. W. & LIBUTTI, S. K. 2004. A novel technique for quantifying changes in vascular density, endothelial cell proliferation and protein expression in response to modulators of angiogenesis using the chick chorioallantoic membrane (CAM) assay. *J Transl Med*, 2, 4.
- MILO, M., FAZELI, A., NIRANJAN, M. & LAWRENCE, N. D. 2003. A probabilistic model for the extraction of expression levels from oligonucleotide arrays. *Biochem Soc Trans*, 31, 1510-2.
- MIYAKAWA, A. A., DE LOURDES JUNQUEIRA, M. & KRIEGER, J. E. 2004. Identification of two novel shear stress responsive elements in rat angiotensin I converting enzyme promoter. *Physiol Genomics*, 17, 107-13.
- MOREY, J. S., RYAN, J. C. & VAN DOLAH, F. M. 2006. Microarray validation: factors influencing correlation between oligonucleotide microarrays and real-time PCR. *Biol Proced Online*, 8, 175-93.
- MORITA, K., SASAKI, H., FUJIMOTO, K., FURUSE, M. & TSUKITA, S. 1999. Claudin-11/OSP-based tight junctions of myelin sheaths in brain and Sertoli cells in testis. *J Cell Biol*, 145, 579-88.
- MOYON, D., PARDANAUD, L., YUAN, L., BREANT, C. & EICHMANN, A. 2001. Plasticity of endothelial cells during arterial-venous differentiation in the avian embryo. *Development*, 128, 3359-70.
- MURLEY, R. 1984. John Hunter, velvet and vascular surgery. *Ann R Coll Surg Engl*, 66, 214-8.
- NAKAZAWA, M., CLARK, E. B., HU, N. & WISPE, J. 1985. Effect of environmental hypothermia on vitelline artery blood pressure and vascular resistance in the stage 18, 21, and 24 chick embryo. *Pediatr Res*, 19, 651-4.
- NETHERTON, S. J. & MAURICE, D. H. 2005. Vascular endothelial cell cyclic nucleotide phosphodiesterases and regulated cell migration: implications in angiogenesis. *Mol Pharmacol*, 67, 263-72.

- NGUYEN, T. H., EICHMANN, A., LE NOBLE, F. & FLEURY, V. 2006. Dynamics of vascular branching morphogenesis: the effect of blood and tissue flow. *Phys Rev E Stat Nonlin Soft Matter Phys*, 73, 061907.
- NIMMAGADDA, S., GEETHA-LOGANATHAN, P., PROLS, F., SCAAL, M., CHRIST, B. & HUANG, R. 2007. Expression pattern of Dll4 during chick embryogenesis. *Histochem Cell Biol*, 128, 147-52.
- NISHI, A., KUROIWA, M., MILLER, D. B., O'CALLAGHAN, J. P., BATEUP, H. S., SHUTO, T., SOTOGAKU, N., FUKUDA, T., HEINTZ, N., GREENGARD, P. & SNYDER, G. L. 2008. Distinct roles of PDE4 and PDE10A in the regulation of cAMP/PKA signaling in the striatum. *J Neurosci*, 28, 10460-71.
- NISSEN, S. E., NICHOLLS, S. J., SIPAHI, I., LIBBY, P., RAICHLLEN, J. S., BALLANTYNE, C. M., DAVIGNON, J., ERBEL, R., FRUCHART, J. C., TARDIF, J. C., SCHOENHAGEN, P., CROWE, T., CAIN, V., WOLSKI, K., GOORMASTIC, M. & TUZCU, E. M. 2006. Effect of very high-intensity statin therapy on regression of coronary atherosclerosis: the ASTEROID trial. *JAMA*, 295, 1556-65.
- NOLAN, T., HANDS, R. E. & BUSTIN, S. A. 2006. Quantification of mRNA using real-time RT-PCR. *Nat Protoc*, 1, 1559-82.
- O'DONOVAN, M. C., CRADDOCK, N., NORTON, N., WILLIAMS, H., PEIRCE, T., MOSKVINA, V., NIKOLOV, I., HAMSHERE, M., CARROLL, L., GEORGIEVA, L., DWYER, S., HOLMANS, P., MARCHINI, J. L., SPENCER, C. C., HOWIE, B., LEUNG, H. T., HARTMANN, A. M., MOLLER, H. J., MORRIS, D. W., SHI, Y., FENG, G., HOFFMANN, P., PROPPING, P., VASILESCU, C., MAIER, W., RIETSCHER, M., ZAMMIT, S., SCHUMACHER, J., QUINN, E. M., SCHULZE, T. G., WILLIAMS, N. M., GIEGLING, I., IWATA, N., IKEDA, M., DARVASI, A., SHIFMAN, S., HE, L., DUAN, J., SANDERS, A. R., LEVINSON, D. F., GEJMAN, P. V., CICHON, S., NOTHEN, M. M., GILL, M., CORVIN, A., RUJESCU, D., KIROV, G., OWEN, M. J., BUCCOLA, N. G., MOWRY, B. J., FREEDMAN, R., AMIN, F., BLACK, D. W., SILVERMAN, J. M., BYERLEY, W. F. & CLONINGER, C. R. 2008. Identification of loci associated with schizophrenia by genome-wide association and follow-up. *Nat Genet*, 40, 1053-5.
- ODORI, T., PASKINS-HURLBURT, A. & HOLLENBERG, N. K. 1983. Increase in collateral arterial endothelial cell proliferation induced by captopril after renal artery stenosis in the rat. *Hypertension*, 5, 307-11.
- OMORI, K. & KOTERA, J. 2007. Overview of PDEs and their regulation. *Circ Res*, 100, 309-27.
- OTHMAN-HASSAN, K., PATEL, K., PAPOUTSI, M., RODRIGUEZ-NIEDENFUHR, M., CHRIST, B. & WILTING, J. 2001. Arterial identity of endothelial cells is controlled by local cues. *Dev Biol*, 237, 398-409.
- PACKHAM, I. M., GRAY, C., HEATH, P. R., HELLEWELL, P. G., INGHAM, P. W., CROSSMAN, D. C., MILO, M. & CHICO, T. J. 2009. Microarray profiling reveals CXCR4a is downregulated by blood flow in vivo and mediates collateral formation in zebrafish embryos. *Physiol Genomics*, 38, 319-27.
- PARTRIDGE, J., CARLSEN, H., ENESA, K., CHAUDHURY, H., ZAKKAR, M., LUONG, L., KINDERLERER, A., JOHNS, M., BLOMHOFF, R., MASON, J. C., HASKARD, D. O. & EVANS, P. C. 2007. Laminar shear stress acts as a switch to regulate divergent functions of NF-kappaB in endothelial cells. *FASEB J*, 21, 3553-61.
- PATAN, S., HAENNI, B. & BURRI, P. H. 1993. Evidence for intussusceptive capillary growth in the chicken chorio-allantoic membrane (CAM). *Anat Embryol (Berl)*, 187, 121-30.
- PEARSON, R. D., LIU, X., SANGUINETTI, G., MILO, M., LAWRENCE, N. D. & RATTRAY, M. 2009. puma: a Bioconductor package for propagating uncertainty in microarray analysis. *BMC Bioinformatics*, 10, 211.

- PETERS, D. G., ZHANG, X. C., BENOS, P. V., HEIDRICH-O'HARE, E. & FERRELL, R. E. 2002. Genomic analysis of immediate/early response to shear stress in human coronary artery endothelial cells. *Physiol Genomics*, 12, 25-33.
- PIPP, F., BOEHM, S., CAI, W. J., ADILI, F., ZIEGLER, B., KARANOVIC, G., RITTER, R., BALZER, J., SCHELER, C., SCHAPER, W. & SCHMITZ-RIXEN, T. 2004. Elevated fluid shear stress enhances postocclusive collateral artery growth and gene expression in the pig hind limb. *Arterioscler Thromb Vasc Biol*, 24, 1664-8.
- POELMA, C., KLOOSTERMAN, A., HIERCK, B. P. & WESTERWEEL, J. 2012. Accurate blood flow measurements: are artificial tracers necessary? *PLoS One*, 7, e45247.
- POELMA, C., VAN DER HEIDEN, K., HIERCK, B. P., POELMANN, R. E. & WESTERWEEL, J. 2010. Measurements of the wall shear stress distribution in the outflow tract of an embryonic chicken heart. *J R Soc Interface*, 7, 91-103.
- POLSON, J. B. & STRADA, S. J. 1996. Cyclic nucleotide phosphodiesterases and vascular smooth muscle. *Annu Rev Pharmacol Toxicol*, 36, 403-27.
- PORTER, S., CLARK, I. M., KEVORKIAN, L. & EDWARDS, D. R. 2005. The ADAMTS metalloproteinases. *Biochem J*, 386, 15-27.
- POURATI, I., KIMMELSTIEL, C., RAND, W. & KARAS, R. H. 2003. Statin use is associated with enhanced collateralization of severely diseased coronary arteries. *Am Heart J*, 146, 876-81.
- R.T. CHRISTINA, C. D., EUGENIA DUMITRESCU, ALINA NETOTEA, A.GURBAN 2010. Pharmacologic activity of phosphodiesterases and their inhibitors. *Lucrari Stiintifice Medicina Veterinara Vol. XLIII*.
- RAJEEVAN, M. S., VERNON, S. D., TAYSAVANG, N. & UNGER, E. R. 2001. Validation of array-based gene expression profiles by real-time (kinetic) RT-PCR. *J Mol Diagn*, 3, 26-31.
- RESNICK, N., COLLINS, T., ATKINSON, W., BONTHRON, D. T., DEWEY, C. F., JR. & GIMBRON, M. A., JR. 1993. Platelet-derived growth factor B chain promoter contains a cis-acting fluid shear-stress-responsive element. *Proc Natl Acad Sci U S A*, 90, 7908.
- RESNICK, N. & GIMBRONE, M. A., JR. 1995. Hemodynamic forces are complex regulators of endothelial gene expression. *FASEB J*, 9, 874-82.
- RIBATTI, D., GUALANDRIS, A., BASTAKI, M., VACCA, A., IURLARO, M., RONCALI, L. & PRESTA, M. 1997. New model for the study of angiogenesis and antiangiogenesis in the chick embryo chorioallantoic membrane: the gelatin sponge/chorioallantoic membrane assay. *J Vasc Res*, 34, 455-63.
- RISAU, W. 1997. Mechanisms of angiogenesis. *Nature*, 386, 671-4.
- RISAU, W. & FLAMME, I. 1995. Vasculogenesis. *Annu Rev Cell Dev Biol*, 11, 73-91.
- RITSCHEL, W. A. & HAMMER, G. V. 1977. Pharmacokinetics of papaverine in man. *Int J Clin Pharmacol Biopharm*, 15, 227-8.
- RODEFER, J. S., MURPHY, E. R. & BAXTER, M. G. 2005. PDE10A inhibition reverses subchronic PCP-induced deficits in attentional set-shifting in rats. *Eur J Neurosci*, 21, 1070-6.
- RUIJTENBEEK, K., LE NOBLE, F. A., JANSSEN, G. M., KESSELS, C. G., FAZZI, G. E., BLANCO, C. E. & DE MEY, J. G. 2000. Chronic hypoxia stimulates periarterial sympathetic nerve development in chicken embryo. *Circulation*, 102, 2892-7.
- RUIZ-VELASCO, V., ZHONG, J., HUME, J. R. & KEEF, K. D. 1998. Modulation of Ca<sup>2+</sup> channels by cyclic nucleotide cross activation of opposing protein kinases in rabbit portal vein. *Circ Res*, 82, 557-65.
- SAADI, I., ALKURAYA, F. S., GISSELBRECHT, S. S., GOESSLING, W., CAVALLESCO, R., TURBEDOAN, A., PETRIN, A. L., HARRIS, J., SIDDIQUI, U., GRIX, A. W., JR., HOVE, H. D., LEBOULCH, P., GLOVER, T. W., MORTON, C. C., RICHERI-COSTA, A., MURRAY, J. C., ERICKSON, R. P. & MAAS, R. L. 2011. Deficiency of the cytoskeletal protein SPECC1L leads to oblique facial clefting. *Am J Hum Genet*, 89, 44-55.

- SABURI, S., HESTER, I., FISCHER, E., PONTOGLIO, M., EREMINA, V., GESSLER, M., QUAGGIN, S. E., HARRISON, R., MOUNT, R. & MCNEILL, H. 2008. Loss of Fat4 disrupts PCP signaling and oriented cell division and leads to cystic kidney disease. *Nat Genet*, 40, 1010-5.
- SCHAPER, W. 1971. Pathophysiology of coronary circulation. *Prog Cardiovasc Dis*, 14, 275-96.
- SCHAPER, W., DE BRABANDER, M. & LEWI, P. 1971. DNA synthesis and mitoses in coronary collateral vessels of the dog. *Circ Res*, 28, 671-9.
- SCHAPER, W. & ITO, W. D. 1996. Molecular mechanisms of coronary collateral vessel growth. *Circ Res*, 79, 911-9.
- SCHAPER, W. & PASYK, S. 1976. Influence of collateral flow on the ischemic tolerance of the heart following acute and subacute coronary occlusion. *Circulation*, 53, 157-62.
- SCHAPER, W. & SCHOLZ, D. 2003. Factors regulating arteriogenesis. *Arterioscler Thromb Vasc Biol*, 23, 1143-51.
- SCHAPER, W., SHARMA, H. S., QUINKLER, W., MARKERT, T., WUNSCH, M. & SCHAPER, J. 1990. Molecular biologic concepts of coronary anastomoses. *J Am Coll Cardiol*, 15, 513-8.
- SCHIERLING, W., TROIDL, K., TROIDL, C., SCHMITZ-RIXEN, T., SCHAPER, W. & EITENMULLER, I. K. 2009. The role of angiogenic growth factors in arteriogenesis. *J Vasc Res*, 46, 365-74.
- SCHOLZ, D., CAI, W. J. & SCHAPER, W. 2001. Arteriogenesis, a new concept of vascular adaptation in occlusive disease. *Angiogenesis*, 4, 247-57.
- SCHOLZ, D., ITO, W., FLEMING, I., DEINDL, E., SAUER, A., WIESNET, M., BUSSE, R., SCHAPER, J. & SCHAPER, W. 2000. Ultrastructure and molecular histology of rabbit hind-limb collateral artery growth (arteriogenesis). *Virchows Arch*, 436, 257-70.
- SCHOLZ, D., ZIEGELHOEFFER, T., HELISCH, A., WAGNER, S., FRIEDRICH, C., PODZUWEIT, T. & SCHAPER, W. 2002. Contribution of arteriogenesis and angiogenesis to postocclusive hindlimb perfusion in mice. *J Mol Cell Cardiol*, 34, 775-87.
- SEILER, C., POHL, T., WUSTMANN, K., HUTTER, D., NICOLET, P. A., WINDECKER, S., EBERLI, F. R. & MEIER, B. 2001. Promotion of collateral growth by granulocyte-macrophage colony-stimulating factor in patients with coronary artery disease: a randomized, double-blind, placebo-controlled study. *Circulation*, 104, 2012-7.
- SEINO, S. & SHIBASAKI, T. 2005. PKA-dependent and PKA-independent pathways for cAMP-regulated exocytosis. *Physiol Rev*, 85, 1303-42.
- SEO, J., LEE, K., 2004, Post translational modifications and their biological functions: Proteomic analysis and systematic approaches. *Journal of biochemistry and molecular biology* 35-44.
- SHYY, Y. J., HSIEH, H. J., USAMI, S. & CHIEN, S. 1994. Fluid shear stress induces a biphasic response of human monocyte chemotactic protein 1 gene expression in vascular endothelium. *Proc Natl Acad Sci U S A*, 91, 4678-82.
- SIUCIAK, J. A., CHAPIN, D. S., HARMS, J. F., LEBEL, L. A., MCCARTHY, S. A., CHAMBERS, L., SHRIKHANDE, A., WONG, S., MENNITI, F. S. & SCHMIDT, C. J. 2006a. Inhibition of the striatum-enriched phosphodiesterase PDE10A: a novel approach to the treatment of psychosis. *Neuropharmacology*, 51, 386-96.
- SIUCIAK, J. A., MCCARTHY, S. A., CHAPIN, D. S., FUJIWARA, R. A., JAMES, L. C., WILLIAMS, R. D., STOCK, J. L., MCNEISH, J. D., STRICK, C. A., MENNITI, F. S. & SCHMIDT, C. J. 2006b. Genetic deletion of the striatum-enriched phosphodiesterase PDE10A: evidence for altered striatal function. *Neuropharmacology*, 51, 374-85.
- SIUCIAK, J. A., MCCARTHY, S. A., CHAPIN, D. S., MARTIN, A. N., HARMS, J. F. & SCHMIDT, C. J. 2008. Behavioral characterization of mice deficient in the phosphodiesterase-10A

- (PDE10A) enzyme on a C57/Bl6N congenic background. *Neuropharmacology*, 54, 417-27.
- SODERLING, S. H., BAYUGA, S. J. & BEAVO, J. A. 1999. Isolation and characterization of a dual-substrate phosphodiesterase gene family: PDE10A. *Proc Natl Acad Sci U S A*, 96, 7071-6.
- SODERLING, S. H. & BEAVO, J. A. 2000. Regulation of cAMP and cGMP signaling: new phosphodiesterases and new functions. *Curr Opin Cell Biol*, 12, 174-9.
- STABILE, E., BURNETT, M. S., WATKINS, C., KINNAIRD, T., BACHIS, A., LA SALA, A., MILLER, J. M., SHOU, M., EPSTEIN, S. E. & FUCHS, S. 2003. Impaired arteriogenic response to acute hindlimb ischemia in CD4-knockout mice. *Circulation*, 108, 205-10.
- STATON, C. A., STRIBBLING, S. M., TAZZYMAN, S., HUGHES, R., BROWN, N. J. & LEWIS, C. E. 2004. Current methods for assaying angiogenesis in vitro and in vivo. *Int J Exp Pathol*, 85, 233-48.
- TABER, L. A., NG, S., QUESNEL, A. M., WHATMAN, J. & CARMEN, C. J. 2001. Investigating Murray's law in the chick embryo. *J Biomech*, 34, 121-4.
- TAKESHIMA, H., KOMAZAKI, S., NISHI, M., IINO, M. & KANGAWA, K. 2000. Junctophilins: a novel family of junctional membrane complex proteins. *Mol Cell*, 6, 11-22.
- TAN, Z. P., HUANG, C., XU, Z. B., YANG, J. F. & YANG, Y. F. 2012. Novel ZFPM2/FOG2 variants in patients with double outlet right ventricle. *Clin Genet*, 82, 466-71.
- TANIGUCHI, K., TAKEYA, R., SUETSUGU, S., KAN, O. M., NARUSAWA, M., SHIOSE, A., TOMINAGA, R. & SUMIMOTO, H. 2009. Mammalian formin fhod3 regulates actin assembly and sarcomere organization in striated muscles. *J Biol Chem*, 284, 29873-81.
- TERRY, T., CHEN, Z., DIXON, R. A., VANDERSLICE, P., ZOLDHELYI, P., WILLERSON, J. T. & LIU, Q. 2011. CD34(+)/M-cadherin(+) bone marrow progenitor cells promote arteriogenesis in ischemic hindlimbs of ApoE(-)/(-) mice. *PLoS One*, 6, e20673.
- THOMA, R. 1893. Untersuchungen u"ber die Histogenese und Histomechanik des Gefa"ßsystems.
- TIAN, X., VROOM, C., GHOFrani, H. A., WEISSMANN, N., BIENIEK, E., GRIMMINGER, F., SEEGER, W., SCHERMULY, R. T. & PULLAMSETTI, S. S. 2011. Phosphodiesterase 10A upregulation contributes to pulmonary vascular remodeling. *PLoS One*, 6, e18136.
- TOPPER, J. N. & GIMBRONE, M. A., JR. 1999. Blood flow and vascular gene expression: fluid shear stress as a modulator of endothelial phenotype. *Mol Med Today*, 5, 40-6.
- UNGER, E. F., BANAI, S., SHOU, M., LAZAROUS, D. F., JAKLITSCH, M. T., SCHEINOWITZ, M., CORREA, R., KLINGBEIL, C. & EPSTEIN, S. E. 1994. Basic fibroblast growth factor enhances myocardial collateral flow in a canine model. *Am J Physiol*, 266, H1588-95.
- VAN DEN WIJNGAARD, J. P., SCHULTEN, H., VAN HORSSSEN, P., TER WEE, R. D., SIEBES, M., POST, M. J. & SPAAN, J. A. 2011. Porcine coronary collateral formation in the absence of a pressure gradient remote of the ischemic border zone. *Am J Physiol Heart Circ Physiol*, 300, H1930-7.
- VAN DER WAL, A. C., BECKER, A. E., VAN DER LOOS, C. M. & DAS, P. K. 1994. Site of intimal rupture or erosion of thrombosed coronary atherosclerotic plaques is characterized by an inflammatory process irrespective of the dominant plaque morphology. *Circulation*, 89, 36-44.
- VAN ROYEN, N., PIEK, J. J., BUSCHMANN, I., HOEFER, I., VOSKUIL, M. & SCHAPER, W. 2001. Stimulation of arteriogenesis; a new concept for the treatment of arterial occlusive disease. *Cardiovasc Res*, 49, 543-53.
- VAUGHAN, C. J., GOTTO, A. M., JR. & BASSON, C. T. 2000. The evolving role of statins in the management of atherosclerosis. *J Am Coll Cardiol*, 35, 1-10.

- VENNEMANN, P., KIGER, K. T., LINDKEN, R., GROENENDIJK, B. C., STEKELENBURG-DE VOS, S., TEN HAGEN, T. L., URSEM, N. T., POELMANN, R. E., WESTERWEEL, J. & HIERCK, B. P. 2006. In vivo micro particle image velocimetry measurements of blood-plasma in the embryonic avian heart. *J Biomech*, 39, 1191-200.
- VOSKUIL, M., VAN ROYEN, N., HOEFER, I. E., SEIDLER, R., GUTH, B. D., BODE, C., SCHAPER, W., PIEK, J. J. & BUSCHMANN, I. R. 2003. Modulation of collateral artery growth in a porcine hindlimb ligation model using MCP-1. *Am J Physiol Heart Circ Physiol*, 284, H1422-8.
- VOSSLER, M. R., YAO, H., YORK, R. D., PAN, M. G., RIM, C. S. & STORK, P. J. 1997. cAMP activates MAP kinase and Elk-1 through a B-Raf- and Rap1-dependent pathway. *Cell*, 89, 73-82.
- WAGNER, C. 2008. Function of connexins in the renal circulation. *Kidney Int*, 73, 547-55.
- WALLIS, J. W., AERTS, J., GROENEN, M. A., CROOIJMANS, R. P., LAYMAN, D., GRAVES, T. A., SCHEER, D. E., KREMITZKI, C., FEDELE, M. J., MUDD, N. K., CARDENAS, M., HIGGINBOTHAM, J., CARTER, J., MCGRANE, R., GAIGE, T., MEAD, K., WALKER, J., ALBRACHT, D., DAVITO, J., YANG, S. P., LEONG, S., CHINWALLA, A., SEKHON, M., WYLIE, K., DODGSON, J., ROMANOV, M. N., CHENG, H., DE JONG, P. J., OSOEGAWA, K., NEFEDOV, M., ZHANG, H., MCPHERSON, J. D., KRZYWINSKI, M., SCHEIN, J., HILLIER, L., MARDIS, E. R., WILSON, R. K. & WARREN, W. C. 2004. A physical map of the chicken genome. *Nature*, 432, 761-4.
- WEINBAUM, S., TARBELL, J. M. & DAMIANO, E. R. 2007. The structure and function of the endothelial glycocalyx layer. *Annu Rev Biomed Eng*, 9, 121-67.
- WHITE, F. C., CARROLL, S. M., MAGNET, A. & BLOOR, C. M. 1992. Coronary collateral development in swine after coronary artery occlusion. *Circ Res*, 71, 1490-500.
- WHITE, S. J., HAYES, E. M., LEHOUX, S., JEREMY, J. Y., HORREVOETS, A. J. & NEWBY, A. C. 2011. Characterization of the differential response of endothelial cells exposed to normal and elevated laminar shear stress. *J Cell Physiol*, 226, 2841-8.
- WINSAUER, G. & DE MARTIN, R. 2007. Resolution of inflammation: intracellular feedback loops in the endothelium. *Thromb Haemost*, 97, 364-9.
- WOLF, C., CAI, W. J., VOSSCHULTE, R., KOLTAI, S., MOUSAVIPOUR, D., SCHOLZ, D., AFSAH-HEDJRI, A., SCHAPER, W. & SCHAPER, J. 1998. Vascular remodeling and altered protein expression during growth of coronary collateral arteries. *J Mol Cell Cardiol*, 30, 2291-305.
- WU, S., WU, X., ZHU, W., CAI, W. J., SCHAPER, J. & SCHAPER, W. 2010. Immunohistochemical study of the growth factors, aFGF, bFGF, PDGF-AB, VEGF-A and its receptor (Flk-1) during arteriogenesis. *Mol Cell Biochem*, 343, 223-9.
- XIAO, L., KOOPMANN, T. T., ORDOG, B., POSTEMA, P. G., VERKERK, A. O., IYER, V., SAMPSON, K. J., BOINK, G. J., MAMARBACHI, M. A., VARRO, A., JORDAENS, L., RES, J., KASS, R. S., WILDE, A. A., BEZZINA, C. R. & NATTEL, S. 2013. Unique cardiac Purkinje fiber transient outward current beta-subunit composition: a potential molecular link to idiopathic ventricular fibrillation. *Circ Res*, 112, 1310-22.
- ZIPPIN, J. H., CHEN, Y., NAHIRNEY, P., KAMENETSKY, M., WUTTKE, M. S., FISCHMAN, D. A., LEVIN, L. R. & BUCK, J. 2003. Compartmentalization of bicarbonate-sensitive adenylyl cyclase in distinct signaling microdomains. *FASEB J*, 17, 82-4.



## Appendix

### Chapter 3

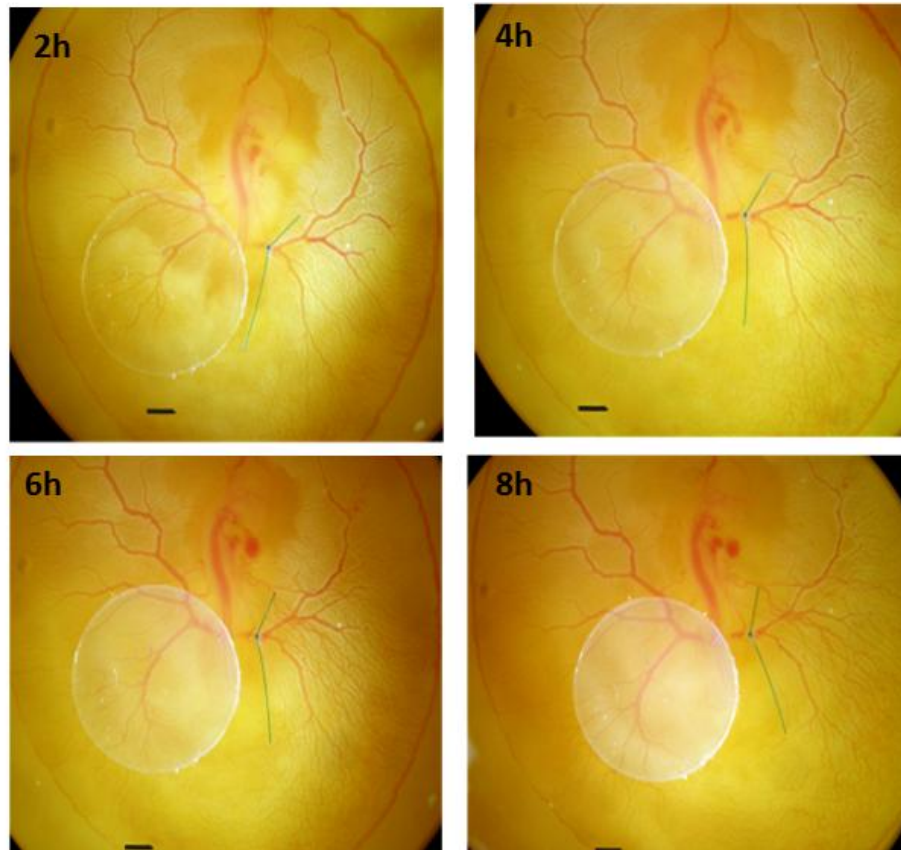


**Figure A1. Following tied-ligation, over an 8h timecourse collateral vessels could be seen to develop from a pre-existing distal branch of the unligated left vitelline artery.**

Following right proximal vitelline artery tied-ligation, a plastic disc was placed over the left vitelline artery to follow one field of view over time. The panels show micrographs from one representative chick embryo from T0 post tied-ligation to 8 hours. Scale bar = 1000µm

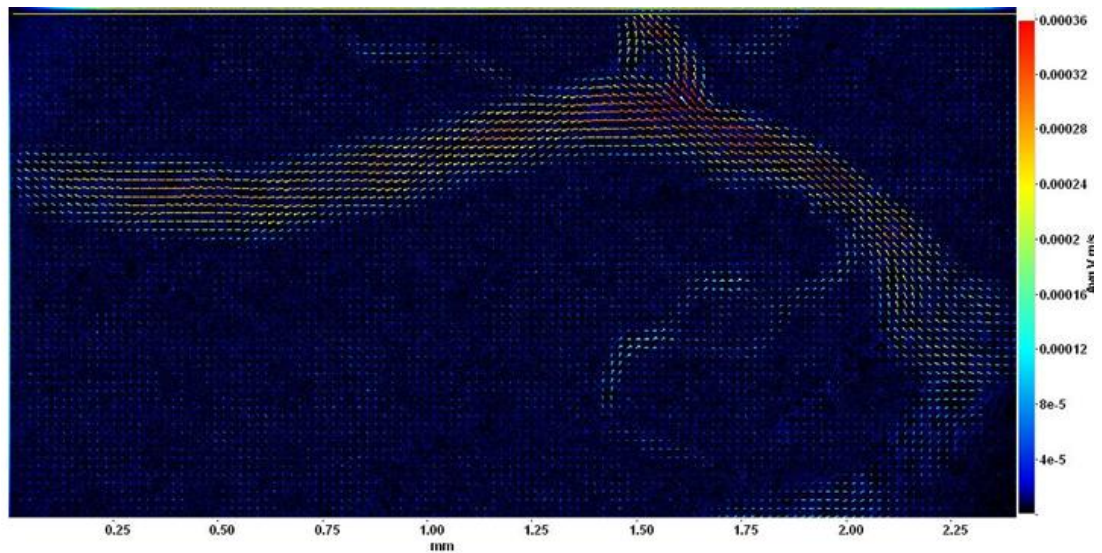


**Figure A2. A representative PIV image of the blood velocity in the left proximal vitelline vessel of a HHst 17 chick embryo**

The heatmap on the side of the image shows average velocity of the vectors recorded in the vessel. The highest velocity is indicated by red vectors.

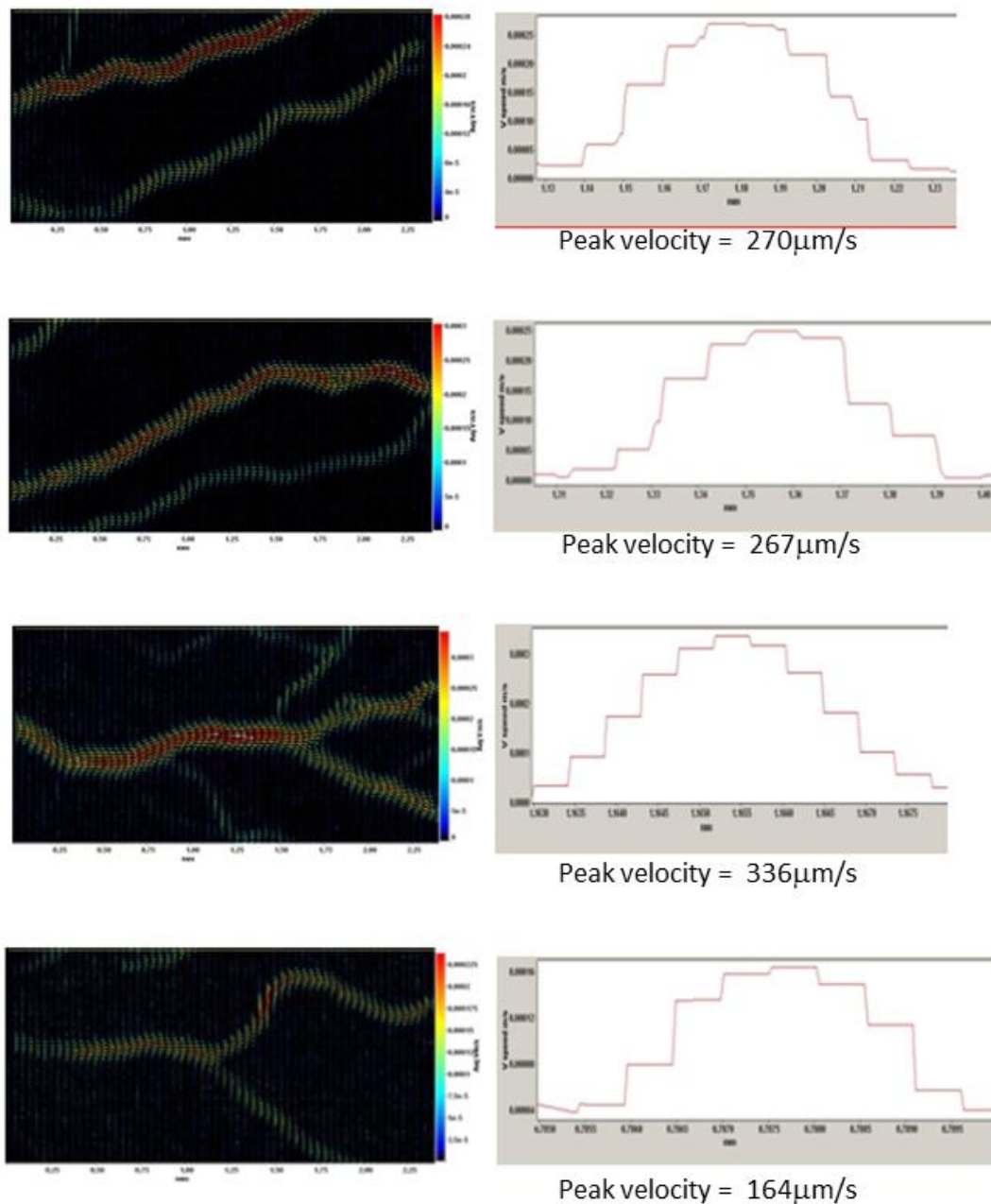


**Figure A3. The parabolic curves to show the blood flow was fastest at the centre of the vessel in collateral vessels recorded at 24h using PIV**

For vessels recorded at 24 hours LaVision processing software also produced parabolic curves from the data which showed blood velocity was highest at the centre of the vessel. Each of the vessels shown in the panels on the left are individual collateral vessels from one chick embryo (Figure 3.12). The corresponding parabolic flow data is shown in the graphs on the right.

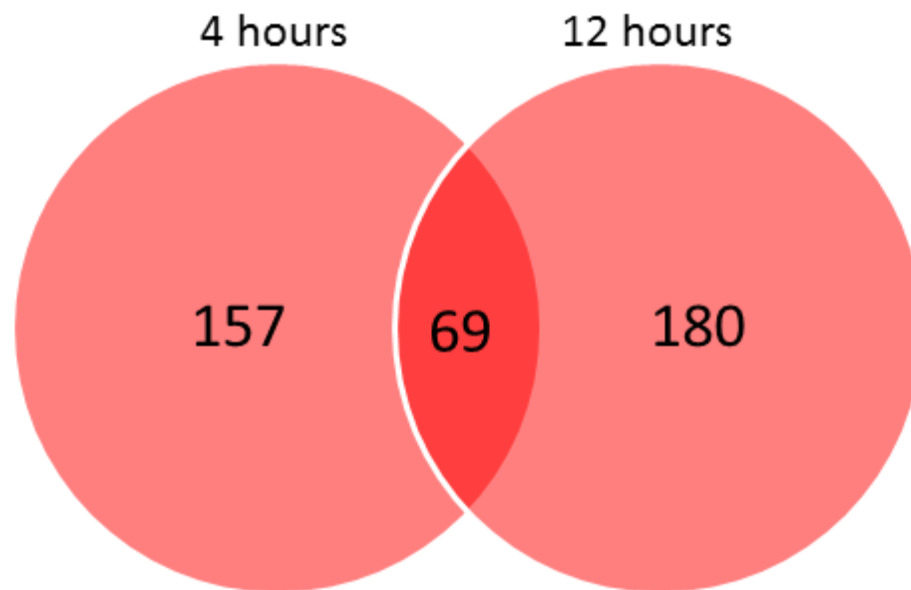


**Figure A4. Venn diagram showing number of differentially expressed genes at 4 hours and 12 hours post-sham-ligation, compared to the baseline measurement.**

The circle on the left represents the number of differentially expressed genes at 4 hours post-sham surgery compared to baseline (HH st17). The circle on the right represents the number of differentially expressed genes 12 hours post sham-ligation compared to baseline. The overlapping section of the circles represents 69 genes which are differentially expressed at both timepoints compared to baseline.

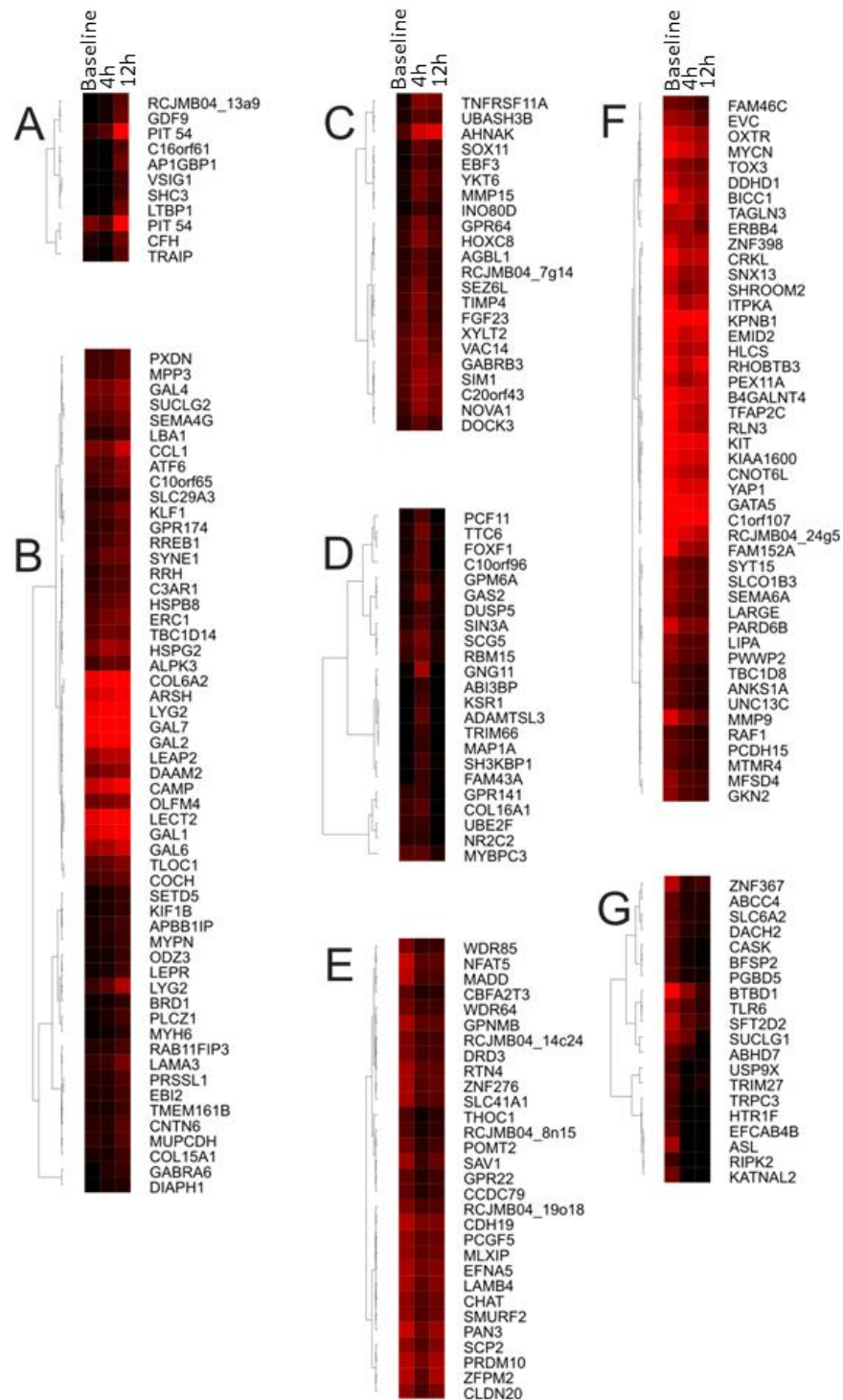


**Figure A5. Hierarchically clustered heatmaps of the fold changes of the differentially expressed genes during normal development**

Shows normalised expression over time. Black indicates no expression, intensity of red is proportional to expression level. The tree has been separated out into nodes (A-G). Each represents a cluster of genes with similar expression profiles. The tree map to the left of each coloured node represents the relatedness of genes in each node.

**Table A1. The shared differentially expressed genes which were expressed in both tied-ligated (L) and sham-ligated (sh) models (taken from the heatmap data)**

gene symbol	gene name	Node (sh)	T0	4h sh	12h sh	Node (L)	4h sh	4h L	12h sh	12h L
CHAT	choline acetyl transferase	E	up	down	up	A	down	no change	down	down
SUCLG1	succinate co-A ligase	B	down	down	up	A	down	down	down	down
MMP9	matrix metalloproteinase	F	up	down	down	B	down	down	down	up
EVC	Ellis van creveld syndrome	F	up	up	down	B	no change	no change	down	no change
MADD	Map kinase activating death domain	E	up	down	down	B	down	down	down	no change
ZNF367	zinc finger protein	G	up	down	down	B	down	down	down	no change
TBC1D8	TBC1 domain	F	down	down	down	B	down	down	down	no change
NOVA1	neuro-oncological ventral antigen	C	down	up	down	B	no change	no change	no change	up
NR2C2	nuclear receptor family	D	down	down	down	B	no change	down	down	up
COL16A1	collagen 16 A 1	D	down	up	down	C	up	no change	down	down
SIN3A	transcription regulator	D	down	up	down	C	up	down	down	no change
FGF23	fibroblast growth factor	C	down	up	down	C	up	no change	no change	no change
MAP1A	microtubule associated protein	D	down	up	down	C	up	no change	no change	no change
TTC6	tetratricopeptide	D	down	up	down	C	up	no change	no change	no change
SIM1	single minded homolog 1	C	down	up	down	C	up	up	up	up
MMP15	matrix metalloproteinase	C	down	up	down	C	up	no change	up	up
TRIM66	tripartite motif	D	down	up	down	C	up	no change	no change	up
TIMP4	TIMP metalloproteinase inhibitor	C	down	up	down	C	up	no change	no change	up
EBF3	early b cell factor 3	C	down	up	down	C	up	no change	up	no change
SYNE1	spectrin repeat containing nuclear envelope	B	down	up	up	D	no change	up	no change	down
KLF1	kruppel like factor 1	B	down	up	up	E	up	up	up	up
LEPR	leptin receptor	B	down	down	up	E	no change	up	up	up
MYPN	myopalladin	B	down	down	down	E	up	no change	up	no change
GPR174	g protein coupled receptor 4	B	down	down	up	E	no change	up	up	no change
ERC1	elks/rab 6 interacting protein	B	down	up	up	E	up	no change	up	up
MPP3	membrane protein palmitoylated	B	down	down	down	E	no change	down	up	no change
TRAF1	TRAF interacting protein	A	down	down	up	E	down	down	up	no change
CFH	complement factor H	A	down	down	up	E	down	down	up	no change
LYG2	lysozyme g like 2	B	down	up	up	F	up	no change	up	up
SETD5	set domain containing 5	B	down	down	down	F	up	no change	up	up
UBASH3B	ubiquitin and SH3 domain containing	C	down	up	down	F	up	up	up	up
ADAMTSL3	ADAMTS like 3	D	down	up	down	F	up	no change	no change	up
KSR1	kinase suppressor of ras1	D	down	up	down	F	up	no change	no change	up

**Table A2. The gene functions of the shared differentially expressed genes which were expressed in both tied-ligated (L) and sham-ligated (sh) models (as in Table A1)**

gene symbol	gene name	function
CHAT	choline acetyl transferase	catalyzes the biosynthesis of the neurotransmitter acetylcholine.
SUCLG1	succinate co-A ligase	catalyzes the conversion of succinyl CoA and ADP or GDP to succinate and ATP or GTP
MMP9	matrix metalloproteinase	involved in the breakdown of extracellular matrix
EVC	Ellis van creveld syndrome	positive mediator of Hedgehog signaling
MADD	Map kinase activating death domain	Plays a significant role in regulating cell proliferation, survival and death
ZNF367	zinc finger protein	DNA binding transcription factor activity
TBC1D8	TBC1 domain	May act as a GTPase-activating protein for Rab family protein
NOVA1	neuro-oncological ventral antigen	mRNA binding and RNA binding
NR2C2	nuclear receptor family	repressor or activator of transcription
COL16A1	collagen 16 A 1	Involved in mediating cell attachment and inducing integrin-mediated cellular reactions
SIN3A	transcription regulator	cell attachment and inducing integrin-mediated cellular reactions,
FGF23	fibroblast growth factor	Regulator of phosphate homeostasis
MAP1A	microtubule associated protein	involved in microtubule assembly
TTC6	tetratricopeptide	?
SIM1	single minded homolog 1	DNA binding transcription factor activity
MMP15	matrix metalloproteinase	involved in the breakdown of extracellular matrix
TRIM66	tripartite motif	transcription repressor
TIMP4	TIMP metalloproteinase inhibitor	inhibitor of metalloproteinases and ECM breakdown
EBF3	early b cell factor 3	Transcriptional activator
SYNE1	spectrin repeat containing nuclear envelope	subcellular spatial organization
KLF1	kruppel like factor 1	Transcription regulator of erythrocyte development
LEPR	leptin receptor	mediates signaling through JAK2/STAT3
MYPN	myopalladin	Component of the sarcomere that tethers together muscle
GPR174	g protein coupled receptor 4	Putative receptor for purines coupled to G-proteins
ERC1	elks/rab 6 interacting protein	organization of the cytomatrix at the nerve terminals
MPP3	membrane protein palmitoylated	MAGUKs interact with the cytoskeleton and regulate cell proliferation
TRAF1	TRAF interacting protein	Inhibits activation of NF-kappa-B mediated by TNF
CFH	complement factor H	regulation of complement activation
LYG2	lysozyme g like 2	lysozymal activity
SETD5	set domain containing 5	?
UBASH3B	ubiquitin and SH3 domain containing	accumulation of activated target receptors on cell surface
ADAMTSL3	ADAMTS like 3	metalloproteinase activity
KSR1	kinase supressor of ras1	MEK and RAF phosphorylation

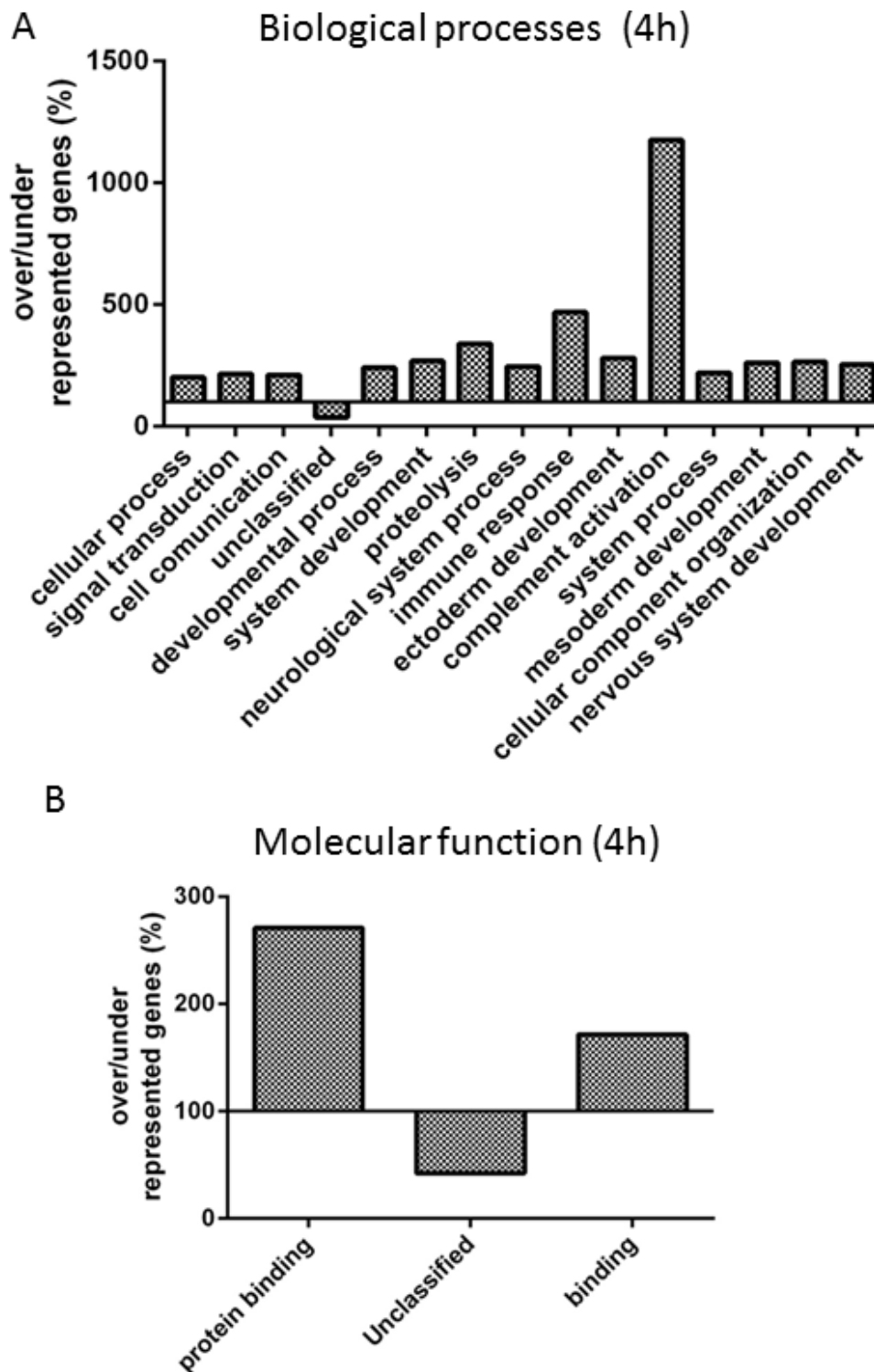


**Figure A6.** Gene ontology was used to cluster differentially expressed genes by biological processes and molecular function from the data analysed at 4 hours after tied-ligation

**A** Biological processes which were statistically significantly over/under represented at 4h. Complement activation was most highly over-represented. **B** Molecular functions which were statistically over/under represented at 4h, included protein binding. 100% indicates the same number as expected by chance.  $P < 0.05$

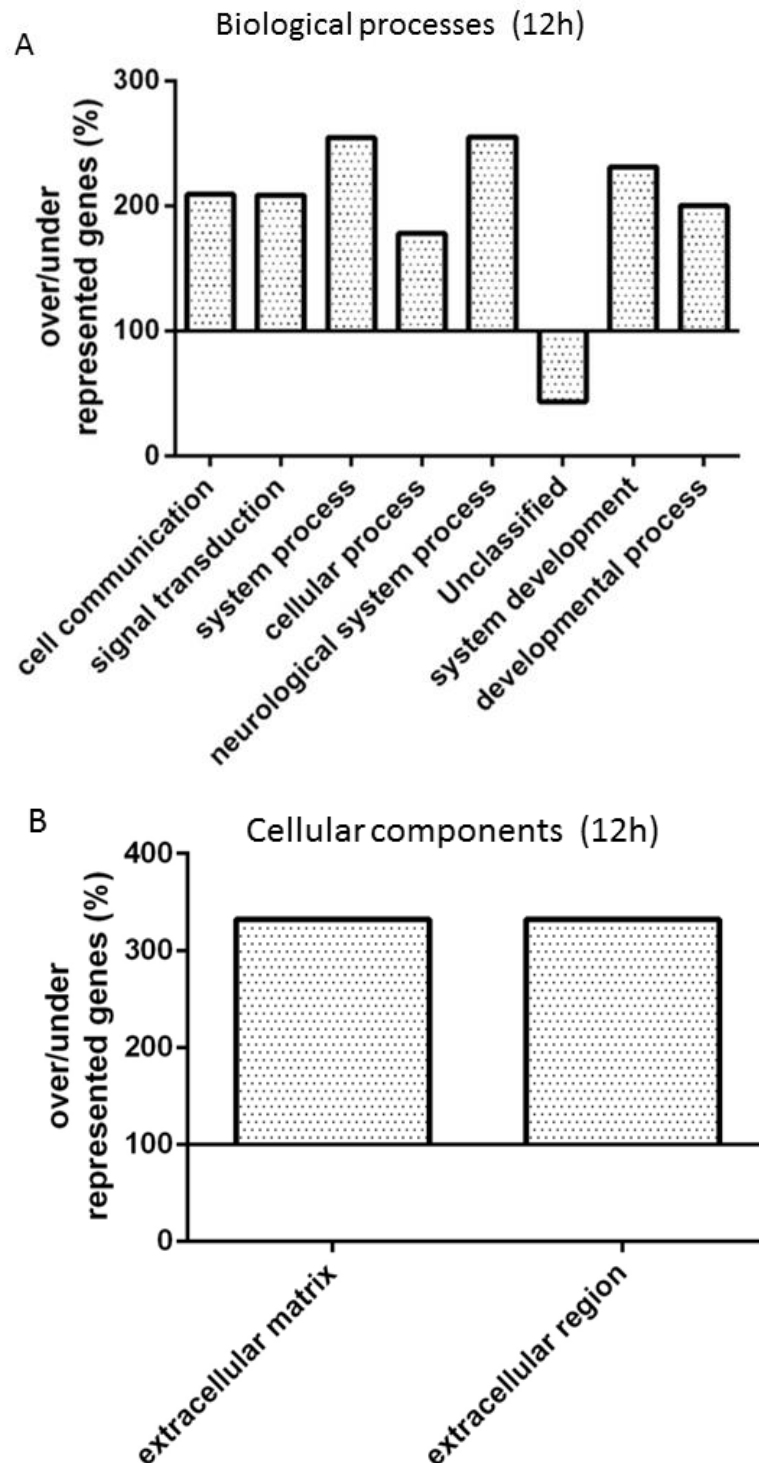


**Figure A7. Gene ontology was used to cluster differentially expressed genes by biological processes and cellular components from the data analysed at 12 hours after tied-ligation**

**A** Gene ontology showed the biological processes statistically significantly over/under represented at 12h based on the number of differentially expressed genes observed, compared to the number of genes expected in that process in the chicken genome. **B** Cellular components which were over-represented at 12h post tied-ligation included components involved with the extracellular matrix and extracellular region. 100% indicates the same number as expected by chance.  $P < 0.05$



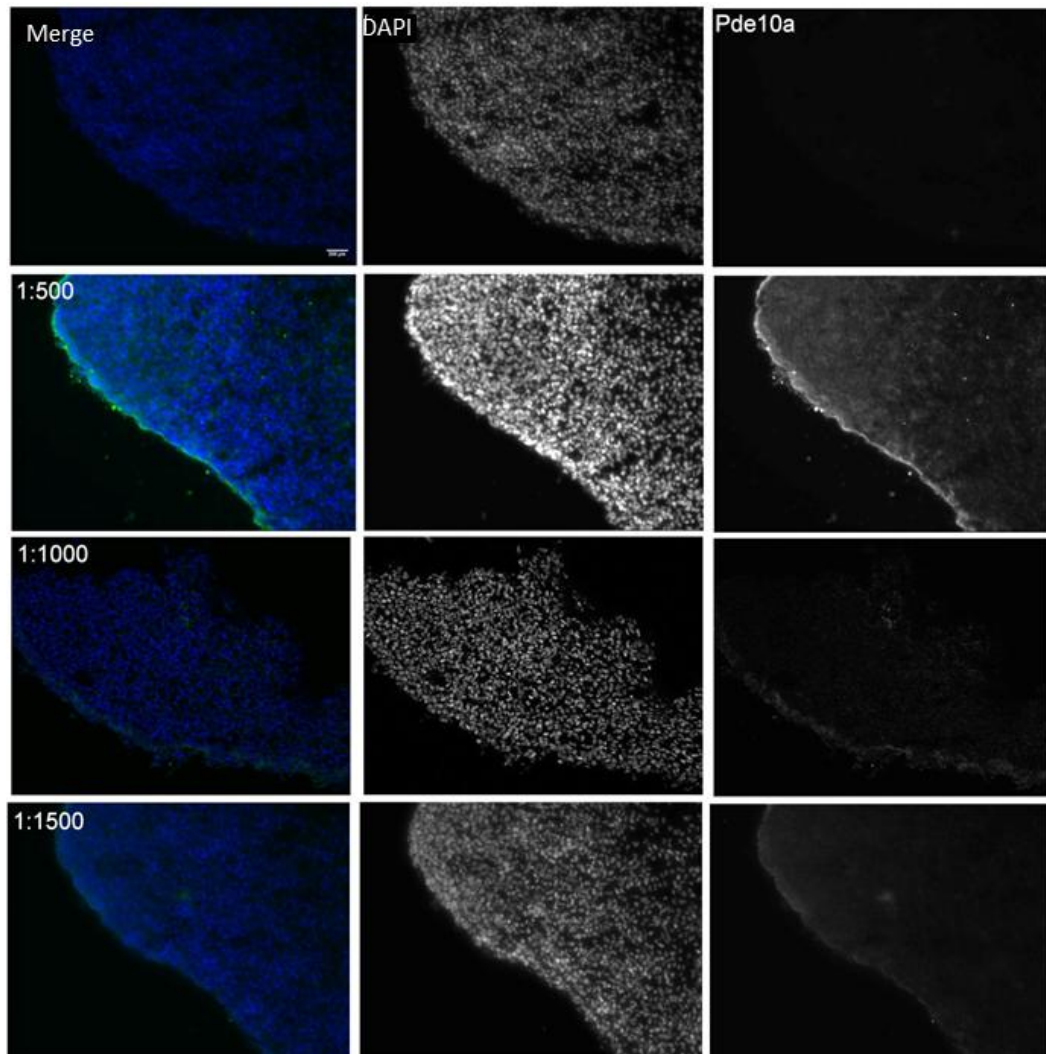


**Figure A9. PDE10A immunohistochemistry of a transverse section through embryonic mouse brain tissue**

Mouse brain tissue aimed to serve as a positive control. The panels show representative examples of a panel of different concentrations tested. The first panel shows the merged labelling patterns of DAPI (blue) and PDE10A (green). These images could then be split into separate colour channels to view the individual staining patterns. Representative image from 3 embryos.

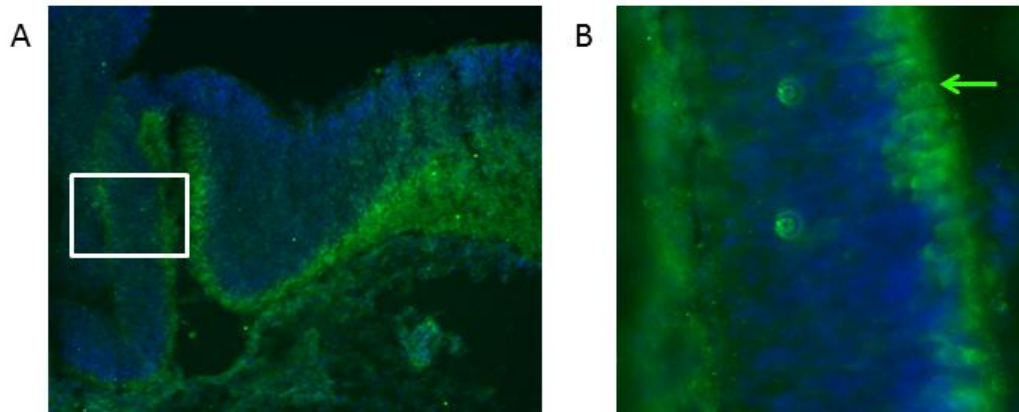


**Figure A10. PDE10A immunohistochemistry of a transverse section through chick embryo brain tissue (HH st 17)**

Chick brain tissue aimed to serve as a positive control. The white box shows the magnified region in B. The green arrow indicates positive PDE10A labelling in neurons positive for PDE10A. DAPI labelling of cell nuclei is indicated by blue stain. Representative image from 6 embryos.



**Figure A11. Dye assays showed diffusion from the filter paper to the vitelline membrane**

Food dye solution was able to freely diffuse from the filter paper placed over the left vitelline artery. 24h after the disc was removed the food dye had transferred to the area of the disc, suggesting that at least this solution was able to leave the filter paper.